Identification and characterization of the grapevine flagelline eceptor (VvFLS2) and search for the receptor to chito oligosaccharides in grapevine

Lucie Trdá

UNIVERSITÉ DE BOURGOGNE
UFR Sciences Vie Terre Environnement
Ecole Doctorale n° 554 "Environnements-Santé"

UMR 1347 Agroécologie - Pôle Interactions Plantes Micro-organismes
Université de Bourgogne, INRA, CNRS ERL 6300, Agrosup, Dijon, France

THÈSE

Pour obtenir le grade de
Docteur de l'Université de Bourgogne
Sciences de la Vie, spécialité Biochimie, Biologie Cellulaire et Moléculaire

par

Lucie TRDÁ

Identification et caractérisation du récepteur à la flagelline (VvFLS2) et recherche du récepteur aux chito-oligosaccharides chez la vigne

Soutenue le 26 juin 2014 devant le jury composé de:

B. DUMAS, Directeur de Recherche, CNRS Toulouse	Rapporteur
F. BRUNNER, Research Group Leader, ZMBP, Universität Tübingen	Rapporteur
F. BAILLIEUL, Professeur, Université de Reims	Rapporteur
C. ZIPFEL, Professeur, East Anglia University, Norwich	Examinateur
B. POINSSOT, Maître de Conférences, Université de Bourgogne	Co-encadrant de thèse
X. DAIRE, Ingénieur de Recherche, INRA Dijon	Directeur de thèse
D. WENDEHENNE, Professeur, Université de Bourgogne	Président de jury

Abstract

Pattern-recognition receptors (PRRs) play a key role in plant immunity by assuring recognition of microbe-associated molecular patterns (MAMPs), signature of microbial presence. MAMP perception constitutes the first layer of pathogen detection and activates defense mechanisms that aim to block the intruder.

This study brings an insight into how grapevine (*Vitis vinifera*) perceives two MAMPs: the flagellin-derived flg22 peptide and chitin, which are conserved motifs occurring over the whole bacterial and fungal classes, respectively. This study analyzed MAMP-triggered early signaling events, defense gene expression and also the efficiency of elicited defense against gray mold and downy mildew diseases. These two MAMPs are active in grapevine suggesting that perception systems exist. So far, no PRR is known for this crop.

Given the availability of grapevine genome, we could identify *in silico* putative grapevine receptors (VvFLS2, VvCERK1-3 and VvCEBiP1-2) that might function as PRRs for flg22 and chitin, respectively. Their functional characterization was firstly achieved by complementation assays in the corresponding *A. thaliana* mutants and, secondly, by a gene silencing strategy in grapevine.

Our results permitted the identification of VvFLS2, the *V. vinifera* receptor for the bacterial flagellin. The function of VvFLS2 was demonstrated by restoring the flg22 responsiveness in the Arabidopsis *fls2* null mutant. Thus, our work provides the first description of an active grapevine PRR-MAMP pair. We further compared VvFLS2 and the Arabidopsis receptor, AtFLS2, in their capability to perceive flagellin-derived flg22 epitopes from endophytic or pathogenic bacteria. Our data clearly show that VvFLS2 differentially recognizes flg22 from different bacteria and suggest that flagellin from the beneficial plant growth-promoting rhizobacteria (PGPR) *Burkholderia phytofirmans* has evolved to evade grapevine immune recognition system. We also obtained preliminary data on chitin sensing system in grapevine and show that VvCERK3 might be a functional ortholog of AtCERK1 by partly restoring the oxidative burst triggered by chitin in the Arabidopsis *cerk1-2* mutant.

Key words: grapevine, immunity, MAMP, receptors, PRR, FLS2, flg22, CERK1, chitin, *Vitis vinifera*

Résumé

Les récepteurs PRR (Pattern-recognition receptors) jouent un rôle clé dans l'immunité des plantes en assurant la reconnaissance d'éliciteurs, des motifs moléculaires associés aux microorganismes (MAMP) qui témoigne de leur présence microbienne. La perception de ces MAMPs constitue le premier système de détection d'agents potentiellement pathogène, et déclenche des mécanismes de défense qui ont pour but de bloquer leur développement.

Cette étude met en lumière comment la vigne (*Vitis vinifera*) perçoit deux MAMPs : le peptide flg22 dérivé de la flagelline et la chitine, des motifs conservés existant dans la plupart des espèces bactériennes et fongiques, respectivement. Cette étude analyse les événements précoces de signalisation, l'expression de gènes de défense activés par ces MAMPs et l'efficacité de la résistance induite contre les agents de la pourriture grise et du mildiou de la vigne. Si nos résultats suggèrent que des systèmes de perception pour ces deux MAMPs existent chez la vigne, aucun récepteur PRR n'est actuellement connu pour cette plante cultivée.

La disponibilité du génome de la vigne nous a permis d'identifier *in silico* des récepteurs putatifs (VvFLS2, VvCERK1-3 et VvCEBiP1-2) pouvant fonctionner comme PRR respectif de flg22 et de chitine. Leur analyse fonctionnelle a été réalisée d'une part par complémentation des mutants correspondants d'Arabidopsis et, d'autre part, par une stratégie d'extinction de gène chez la vigne.

Nos résultats ont permis d'identifier VvFLS2, le récepteur de la vigne à la flagelline bactérienne. La fonction de VvFLS2 a été démontrée en restaurant la réponse à flg22 du mutant *fls2* d'Arabidopsis. Ainsi, nos travaux sont les premiers à décrire un couple PRR-MAMP actif chez la vigne. Nous avons également comparé les capacités de perception de VvFLS2 et du récepteur d'Arabidopsis, AtFLS2, envers des épitopes flg22 provenant de bactéries endophytes ou pathogènes. Nos données montrent clairement que VvFLS2 reconnait différemment les peptides flg22 des différentes bactéries et suggèrent que la flagelline de la bactérie bénéfique *Burkholderia phytofirmans* a évolué pour échapper au système de reconnaissance immunitaire de la vigne. Nous avons également obtenu des données préliminaires concernant le système de perception de la chitine chez la vigne et montré que VvCERK3 pourrait être un orthologue fonctionnel d'AtCERK1 en restaurant partiellement le burst oxydatif induit par la chitine dans le mutant *cerk1-2* d'Arabidopsis.

Mots-clés : vigne, immunité, éliciteurs, récepteurs, PRR, FLS2, flg22, CERK1, chitine, *Vitis vinifera.*

Table of contents

Acknowledgements

Je tiens tout d'abord à remercier Messieurs **Bernard Dumas** et **Frédéric Brunner** ainsi que Madame **Fabienne Baillieul** pour avoir accepté d'examiner ce travail. J'adresse également mes remerciement a **Cyril Zipfel** et **David Wendehenne** pour participer à mon jury de thèse.

Je tiens tout également à remercier les différents financeurs de mon allocation de recherche : le **Bureau Interprofessionnel des Vins de Bourgogne** (**BIVB**) et le **Conseil Régional de Bourgogne**, qui m'a permis de réaliser cette thèse ; ainsi que **Vivienne Gianinazzi-Pearson** et **David Wendehenne** de m'avoir acceuillie dans ancienne l'UMR Plante Microbe Environnement, au sein de l'ex-OP2.

Merci à **David**, **Benoit, Valérie** et **Nathalie** de m'avoir inspiré aux cours en mon Master1 et de m'avoir fait abandonner les souris pour aller vers les plantes. Je ne regrette pas une seule seconde!

Merci, **Ben**, de m'avoir acceptée pour le Master et pour diriger cette thèse. Merci pour tes conseils, ta confiance dans mes travaux et pour la bonne autonomie que tu m'as laissée. Un grand merci également pour les portes que tu m'as ouvertes, notamment, les collaborations et les enseignements. Un grand merci aussi pour m'avoir permis de finir la rédaction en Tchéquie... Merci **Marie-Claire** de m'avoir « secourue » avec les lignées transgéniques, ta bonne humeur et tous tes conseils pratiques. Merci à vous deux pour les coups de main donnés aux manips, et de prendre le relais pour continuer le projet! Merci **Xavier** de m'avoir accepté pour cette thèse et de s'être intéressé au sujet, même si c'est éloigné de la résistance induite;-)

Car la thèse (surtout la mienne), c'est aussi un travail d'équipe, je remercie donc tous les gens qui ont contribué à ce projet, notamment: Many thanks to **Freddy**, **Cyril** and **Lena Stransfeld** for the nice long-term collaboration, advices, discussions and the complemented lines. Thanks for the **ERA-PG project** and the great meetings held every year. Merci à la **plateforme transformation de la vigne** à Colmar pour avoir généré des lignées transgéniques, à **Jérôme Collemare** pour la microscopie sur le *N. benthamiana* et enfin à **Olivier Fernandez** et **Stephan Dorey** pour cette étroite collaboration dynamique et fructueuse, qui m'a passionnée et inspirée.

Merci à tous les membres et ex-membres de l'ex-OP2, pour les conseils, l'inspirations, les discussions et surtout pour les lab-cleaning! Merci à **Marielle**, **Sophie**, **Annick** (Merci la championne des MAPK pour s'être cassé les dents avec moi!), **Camille** (Merci pour la qPCR!),

Emilie, **Ian**, **Franck**, **Christelle** et **Malik** pour avoir bossé ensemble sur la vigne. Thanks **Jani** for explaining me the biomol stuff.

Merci à **Stephane**, **Olivier**, **Sylvain**, **Hoai-Nam** pour votre bonne humeur constante. Une dédicace spéciale pour les deux premiers et leur « Conneries » (là, il faut mettre une Majuscule !), mais aussi pour leur investissement dans l'organisation du labo. Merci aussi pour la bonne ambiance du « labo prot »: n'est-ce pas **Vincent**, **Pauline**, **Angélique ?** Merci à **Leo**, **Jean-Luc**, **Nassima**, **Marine**, **Virginie**, **Marie-Lara**, **Ian** ainsi que **Soukayna, Soumaira**, **Hamid**, **Herbert**, **Franck**, **Ivan et Tomasso** pour les sympathiques moments passés ensemble.

Ma chère **Agnès**, un grand merci pour les cellules toujours impec, pour ton soutien, ton amour, ta force, ton cœur grand ouvert que ce soit pour l'écoute ou pour une rigolade... Bref, merci pour tout.

Merci **Florence**, miss unfatigable, pour ton rire, ton énergie, ton soutien, nos escapades au ski ou à pied et d'avoir partagé un midi à se donner des coups de pied. Merci **Iulia**, pour ton courage, ta folie et tes rêves. Merci **Arnaud** pour ton grand soutien, ta sincérité et ton mythique « Si je peux me permettre... ». Merci à l'équipe ski/volley ADAS sans oublier **David** et **Nico** pour les super tournois de volley et les championnats de ski, les fou-rires, et les médailles gagnées. « Say what, say Captain! » Merci Nico pour les cours de self-défense.

Merci aussi à toutes les personnes avec qui je pouvais partager le grand plaisir d'être dehors. Merci aux **CAFistes Dijonnais** pour la bonne ambiance, les encadrants pour leur investissement et leur générosité à partager, de m'avoir fait goûter à la montagne et à la Dent Blanche! Des mercis spéciaux à **Thibaud** (pour un accueil chaleureux), **Jeremy**, **Laure**, **Pascal**, **Thomas**, pour les aventures et fatigues partagées et bien sûr merci à **Florian**, toujours motivé! Merci **Cha-chou** pour ton esprit ouvert, ta gentillesse, ta folie et de m'avoir inclus dans tes cercles, à **Magda** pour ton amitié, les retours nocturnes après la grimpette, le barbecue et les soirées Péniche. Merci **Jean-Luc** pour la grimpette, la philosophie et la guitare! Pour le regard illuminé, pour parler de tout et de rien, ainsi que pour ta motivation infinie pour grimper dehors, même si sa caille.

Merci aux membres de la chorale **Solfamis** pour les mardis enchantés et les concerts réussis. Merci à **Mommo**, **Thibaud** (le papa, quoi) et **Magda** pour la collocation! **Anna**, thanks for that long friendship and staying in touch.

Merci à **Dr. Richard**, pour l'optimisme, la bonne humeur et pour m'avoir ouvert les yeux.

Merci **Aymeric** pour cette longue amitié, de croire en moi et de cultiver le barbare musical que je suis « Tu ne connais Daft Punk, quoi?! »

Díky českým přivandrovalcům do Dijonu (**Katce**, **Hance**, **Pavle**, **Romanovi** a **Martinovi**) za smích, kafíčkové dýchánky, kantýnové diskuze a všeobecnou veselost a zpestření v labu. Díky, **Dášo**, **Štěpáne, Tomáši** za kamarádství na dálku. **Michale**, tobě díky za víru, obětavost, ochotu a bezmezné nadšení pro cestování.

Redakci R&R za ten pěkný časopis, za to, že otravovaly s deadlinama a za prostor na zvířátkovou seberealizaci. 30 článků za 3 roky!

Velké díky **Lence Burketové** za důvěru, toleranci a trpělivost! Dík patří také babinci z labu 321 za adopci, zejména pak **Mirce**, **Martinovi:-)**, **Monice** a **Hance**.

Díky **rodičům**, **bráškovi** a **babičce** za podporu, starost a péči.

List of abbreviations

aa	amino acid
At	*Arabidopsis thaliana*
	Agrobacterium tumefaciens
ABA	abscisic acid
ATP	adenosine triphosphate
Avr	avirulence
Bc	*Botrytis cinerea*
Bp	*Burkholderia phytofirmans*
bp	base pair
BAK1	BRI1-associated kinase 1
BIK	Botrytis-induced kinase 1
BKK1	BAK1-like 1
BLAST	basic local alignment search tool
BR	brassinosteroid
BRI1	brassinosteroid insensitive 1
BSA	bovine serum albumin
CEBiP	chitin elicitor-binding protein
CERK1	chitin elicitor receptor kinase 1
CBB	Coomassie brilliant blue
CcdB	control of cell death B
cDNA	complementary DNA
Col-0	Columbia-0
CDPK	calcium-dependent protein kinase
CDS	coding DNA sequence
Cf	*Cladosporium fulvum*
CFU	colony-forming unit
COS	chitooligosaccharide
CRIBI	Centro di Ricerca Interdipartimentale per le Biotecnologie Innovative
Da	dalton
DAMP	damage-associated molecular pattern
DNA	deoxyribonucleic acid
DNase	deoxyribonuclease
DP	degree of polymerization
dpi	days post infection
dpt	days post transformation
DTT	dithiothreitol
ECL	enhanced chemiluminescence
EDTA	ethylene diamine tetraacetic acid
EF-Tu	elongation factor thermo unstable
EFR	EF-Tu receptor
EF1-α, γ	elongation factor 1 α , γ
EGF	epidermal growth factor
EGTA	ethylene glycol tetraacetic acid
EIN(1/3)	ethylene-insensitive (1/3)
Eix	ethylene-inducing xylanase
ELISA	enzyme-linked immunosorbent assay
EC	embryogenic calli
ER	endoplasmic reticulum
pERK1/2	phosphorylated extracellular regulated protein kinase 1/2
ET	ethylene
ETI	effector-triggered immunity
ETS	effector-triggered susceptibility
FliC	flagellin (protein/gene)
FLS2	flagellin sensing 2
FWC	fresh weight of cells

GFP	green fluorescent protein
GlcN	glucosamine
GlcNAc	N-Acetylated glucosamine
GPI	glycosylphosphatidylinositol
GUS	β-glucuronidase
HEPES	(4-(2-hydroxyethyl)-1-piperazineethanesulfonic acid)
hpt	hours post treatment
HR	hypersensitive response
IgG	immunoglobulin G
INRA	Institut National de la Recherche Agronomique (National Institute for Agricultural Research)
INSEE	Institut National de la Statistique et des Études Économiques (National Institute for Statistics and Economic Studies)
JA	jasmonic acid
KAPP	kinase-associated protein phosphatase
KLH	keyhole limpet hemocyanin
Lam	laminarin
LB	Luria-Bertani broth
Le	*Lycopersicum esculentum* (newly *Solanum lycopersicum*)
LexA	lambda excision A
LG	Le-Gascuel
Lj	*Lotus japonicus*
LOX	lipoxygenases
LPS	lipopolysaccharide
LRR	leucine-rich repeat
LRRNT	N-terminal of LRR ectodomain
LysM	lysin motif
LYK	LysM-RLK
LYP	LysM-RLP
MAMP	microbe-associated molecular pattern
MAPK	mitogen-activated protein kinase
MES	2-(N-morpholino)ethanesulfonic acid
miRNA	micro RNA
M-MLV	Moloney Murine Leukemia Virus
MS	Murashige & Skoog
Mt	*Medicago truncatula*
MUSCLE	multiple sequence comparison by log- expectation
Myc	mycorrhiza
NAA	1-Naphthaleneacetic acid
NADPH	nicotinamide adenine dinucleotide phosphate
NCBI	National center for biotechnology information
NF	nodulation factor
NF-κB	nuclear factor κB
NFP	Nod-factor perception
NFR	Nod factor receptor
NO	nitric oxide
Nod	nodulation
NPK	nitrogen, phosphorous and potassium
nt	nucleotide
dNTP	deoxyribonucleotide triphosphate
OG	oligogalacturonides

OIV	L'Organisation Internationale de la Vigne et du Vin (International Organisation of Vine and Wine)
Os	*Oryza sativa*
qPCR	quantitative polymerase chain reaction
PAL	phenylalanine ammonia lyase
PAMP	pathogen-associated molecular pattern
PBL	PBS1-like
PBS	phosphate buffered saline
PBS1	avrPphB Susceptible 1
Pcal	*Pseudomonas cannabina* pv *alisalensis*
PCR	polymerase chain reaction
qPCR	quantitative PCR
Pep	peptide
PEPR	Pep(1) receptor
Pfu	*Pyrococcus furiosus*
PGN	peptidoglycan
PGPR	plant growth promoting rhizobacteria
PMSF	phenylmethylsulfonyl fluoride
PR	pathogenesis-related
PROPEP	protein precursor of AtPeps
PRR	pattern recognition receptor
PS3	sulfated laminarin
Pto	*Pseudomonas syringae* pv *tomato*
PUB	plant U-box
Pv	*Plasmopara viticola*
R	Resistance
RbohD	respiratory burst oxidase homolog D
RC DC	reducing and detergent compatible
RH	relative hygrometry
RLK	receptor-like kinase
RLP	receptor-like protein
RLU	relative luminescence unit
RNA	ribonucleic acid
RNAi	RNA interference
ROS	reactive oxygen species
RT-PCR	reverse transcription PCR
SA	salicylic acid
SAIL	the *Syngenta Arabidopsis insertion library*
SDS	sodium dodecyl sulfate
SDS-PAGE	SDS polyacrylamide gel electrophoresis
SERK	somatic embryo receptor kinase
seWT	somatic embryogenesis wild type
Sl	*Solanum lycopersicum* (*Lycopersicum esculentum*)
SNP	single nucleotide polymorphism
60SRP	60S ribosomal protein
STS	stilbene synthase
T1/2/3	transformant generation 1/2/3
Taq	*Thermus aquaticus*
T-DNA	transfer DNA
TBS	Tris-buffered saline
TF	transcription factor
TLR	Toll-like receptor
TNF	tumor necrosis factor
TTSS	type III secretion system
U	unit
UDP	uridine diphosphate
UniProt	universal protein resource
UTR	untranslated region
VST	*Vitis* stilbene synthase

Vv	*Vitis vinifera*
v/v	volume/volume
WAK1	Wall-associated kinase 1
WP	Woody Plant medium
WT	wild-type
w/v	weight/volume
Xc	*Xanthomonas campestris*
Xcc	*Xanthomonas campestris* pv *campestris*
(CaMV)35S	Cauliflower Mosaic Virus 35S
α-	anti-
αs-	antisense-

List of Annexes

INTRODUCTION

I. General introduction

1 Socio-economical context

The modern agriculture has massively intensified over the past 70 years, which was enabled by adoption of high-yielding crop varieties, intense agricultural practices using frequent fertilization and irrigation together with the pesticide use. As the global population expands, this intensification meets the requirements for increased food supply. However, it also causes severe environmental problems, such as the deteriorated soil quality and the release of toxic compounds.

Domestication and breeding of plant varieties for yield and fruit quality brings a negative effect on disease resistance. Nowadays, most of the crops are susceptible to numerous diseases, caused by different microorganisms (pathogens). Diseases decrease crop yield and the food quality and toxins released by some microorganisms may be present in the harvest. In the past, plant diseases were responsible for severe economical and nourishment crises and are currently, to blame for a loss of approximately 14% of the worldwide crop production (Agrios, 2005). To date, an intensive use of numerous phytochemical pesticides is required to ensure a satisfactory yield and the quality of the harvest. However, pesticides cause harmful effects on crops, on the environment, the health of farmers and consumers. As a side-effect, they select resistant pathogen strains. All these reasons call for alternative and sustainable disease management.

Viticulture is an important agricultural and economical sector of many countries. In 2011 world vineyards reached a total area surface of 7,585 million hectares (OIV report 2012, http://www.oiv.int/oiv/info/enstatsro). European vineyards represented 38% of this surface, but produced 65% of the total wine production. France belongs to the main five wine producers, competing mostly with Italy and Spain for the 1st place (OIV report 2012). In 2012, French wines contributed by 19% to the world wine production. This production also represented more than 15% of the total national value of the agricultural products sold in 2012 (INSEE, http://www.franceagrimer.fr).

The cultivated grapevine (*Vitis Vinifera*) is susceptible to many diseases. Roots, leaves, wood or grapes can be infected by different microorganisms, such as oomycetes (downy mildew), fungi (gray mold, powdery mildew, anthracnose, black rot, esca), bacteria (crown gall, Pierce's disease, bacterial necrosis) or phytoplasms (flavescence dorée). Diseases of grapevine plants affect yield, wine taste and quality. Viticulture is an important consumer of pesticides. For illustration, French viticulture consumes 20% of all the pesticides used in France, although vineyards constitute only 3.2% of cultivated land (Viniflhor, 2005). In average, 15 preventive or curative

fungicide treatments are applied in vineyards every year (Delaunois *et al.*, 2014). In 2010, only 2.1% of the overall grape production area in European Union was of organic origin bypassing the pesticide use (http://www.eubusiness.com/topics/food/organic-wine/). Current European and French regulation aims to reduce the use of pesticides in agriculture by 50% and to ban the most harmful ones by 2018 (REACH & Ecophyto 2018, set in 2008). Viticulture is among the first to comply with this target and to adopt alternative strategies.

Among these alternatives are organic and integrated farming practices, the biological control, the use of resistant hybrids or transgenic crops. However, genetic improvement based on the assisted crossing or transgenesis is not allowed for French grapevines with an AOC (Appellation d'origine contrôlée) seal. Another alternative consists in stimulating of the plant immune system with elicitors, natural molecules that mimic pathogen attack, or by living organisms.

In our laboratory, we study the mechanisms of elicitor-induced resistance in grapevine. This implies a detailed knowledge on the biotic interaction of grapevine with its pathogens, but also on mechanisms of elicitor perception and triggered defense responses. My work focused on the perception of several microbial elicitors in grapevine and aimed to identify the corresponding receptors.

2 Plant immunity

All plants are steadily subject to an environment rich in potentially harmful (pathogenic) microbes, such as bacteria, fungi, oomycetes or viruses. Microbes (either pathogenic or symbiotic) infect plants to pump nutrients for their growth and development. Nevertheless, plants are resistant to most microbes due to an efficient immune system, combining constitutive and inducible defense responses.

The constitutive defenses are formed by physical and chemical barriers, such as cuticle, cell walls, and antimicrobial phytoanticipins. The second defense line is inducible by the detection of microbial presence. Immune receptors detect a variety of molecules recognized as "non-host" or "danger" signals and switch on, on their turn, complex system of defense tools but also attacking weapons. These molecule signals are therefore called elicitors, as they elicit host responses (Jones and Dangl, 2006). Mechanisms of these immune responses are similar to the innate immunity described in animals. This is an ancient, broad-spectrum defense strategy with germ-line encoded components. Unlike jawed vertebrate animals, plants lack the adaptive immunity capable of the specific antibody production. On the other hand, all plant cells (not only specialized immune cells) can activate innate immune system in an autonomous manner (Jones and Dangl, 2006).

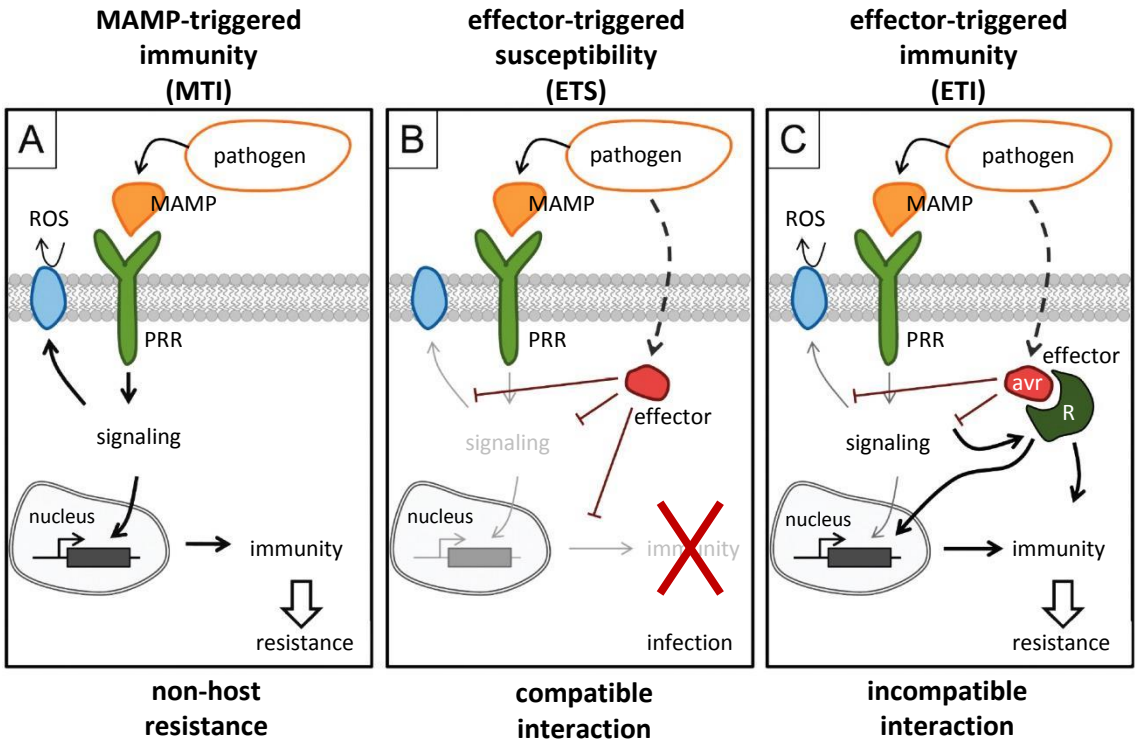

Figure 1. Simplified model of the plant immune system

A. Upon infection, pathogens/microbes are source of microbe-associated molecular patterns (MAMPs). Plants sense these motifs by pattern recognition receptors (PRRs) localized at the cell surface and activates its immune responses, such as reactive oxygen species (ROS) production and defense gene activation. This first defense is referred to as MAMP-triggered immunity (MTI). **B.** Microbial effectors are secreted into the plant cell cytoplasm and disrupt immune signaling at multiple levels leading to disease susceptibility and infection: this is the effector-triggered susceptibility (ETS). **C.** Plants sense these effectors (avirulence products, avr) by cytoplasmic R proteins leading to the activation of immune responses and immunity, which is referred to as effector-triggered immunity (ETI). Adapted from Gamm (2011).

The main and evolutionary older layer of this inducible immunity is based on the external recognition of conserved microbial signatures called microbe/pathogen-associated molecular patterns (MAMPs/PAMPs) that are generated during microbial attack. The early external recognition is also achieved with the host-derived damage-associated molecular patterns (DAMPs) produced as a consequence of enzymatic microbial activities and toxins (Boller and Felix, 2009; Dodds and Rathjen, 2010; Monaghan and Zipfel, 2012). MAMPs and DAMPs are recognized by the plasma-membrane localized pattern recognition receptors (PRRs) and induce a broad variety of defense responses commonly referred to as MAMP-triggered immunity (MTI; Fig. 1A). This layer is also referred as PAMP- or Pattern-triggered immunity (PTI) or even basal immunity.

However successful pathogens can secrete effectors, pathovar-specific microbial molecules that are delivered into host cells to suppress or interfere with MTI responses, resulting in facilitated host colonization and effector-triggered susceptibility (ETS; Fig. 1B). In an ongoing arms-race between the host and attacking microorganism, another more specialized layer of microbial detection evolved more recently, termed effector-triggered immunity (ETI, Fig. 1C). In ETI, host-specific intracellular receptors known as resistance (R) proteins detect the presence or activities of effectors. Host can sense effector activity by monitoring perturbations in a few key cellular processes. As the number of pathogen effectors is virtually unlimited, this indirect detection allows minimizing the array of sensing receptors. As the effector recognition reduces the pathogen virulence, effectors are also referred to as avirulence (Avr) products (Jones and Dangl, 2006). The bases for formulating the ETI model were already set in 1942 by Flor proposing the gene-for-gene resistance. According to this concept, the resistance or the disease outcome is controlled by corresponding gene pairs, encoding the R and Avr proteins in the plant or the pathogen, respectively. Upon the co-evolution of a host with its pathogen, the ETI can be broken by new effector(s) leading again to susceptibility (ETS; Fig. 1B). The co-evolution of host immunity along with pathogen's effectors can be suitably illustrated by the zig-zag model (Jones and Dangl, 2006).

Interactions between plants and pathogenic microbes can be classified according to the mechanisms of the "molecular dialog" and the disease outcome. A non-host interaction is established between a plant and a non-adapted pathogen that lacks specialized effectors to disrupt immunity of a given plant. In this case, MTI responses are sufficient to block pathogen and result in a lack of disease (Fig. 1A). We speak about the incompatible interaction, when a specific pathovar overcoming MTI attempts to infect a plant that recognizes its effector(s). The resulting ETI leads to a resistance (Fig. 1C). In contrast, the compatible interaction occurs when the effective ETI is missing or was overcome by novel effectors, finally leading to disease (Fig. 1B).

MAMP	Active motif	Microorganism
Activator of XA21 (Ax21)	axyS22 (sulfated peptide)	Bacteria (*Xanthomonas* spp.)
β-glucans	tetraglucosyl glucitol, branched hepta-β-glucoside, linear oligo-β-glucosides	Fungi (*Pyricularia oryzae*), Oomycetes (*Phytophthora* spp.), Brown algae
Cerebrosides	sphingoid	Fungi *(Magnaporthe* spp.)
Cellulose-binding elicitor lectin (CBEL)	not defined	Oomycetes (*Phytophthora* spp.)
Chitin/Chitosan	$(GlcNAc)_n$ / $(GlcN)_n$	All fungi
Cold shock protein	N-terminal peptide	Bacteria Gram -; +
Elicitins	not defined	Oomycetes (*Phytophthora* spp., *Pythium* spp.)
Elongation factor (EF-Tu)	N-terminal peptide elf18	Bacteria Gram -
Ergosterol	not defined	All fungi
Flagellin	N-terminal peptide flg22	Bacteria Gram -
Harpin (HrpZ)	not defined	Bacteria Gram - (*Pseudomonas* spp., *Erwinia*)
Invertase	N-mannosylated peptide	Yeast
LPS	LipidA lipooligosacharide	Bacteria Gram - (*Xanthomonas* spp., *Pseudomonas* spp., *Burkholderia* spp.)
Necrosis-inducing protein	not defined	Bacteria (*Bacillus* spp.), Fungi (*Fusarium* spp., *Verticillium* spp.), Oomycetes (*Phytophthora* spp., *Pythium* spp.)
Peptidoglycan (PGN)	muropeptides	Bacteria Gram - ; +
Siderophores		*Pseudomonas fluorescens*
Sulfated fucans	Oligomer	Brown algae
Transglutaminase (TGase)	peptide pep-13	Oomycetes (*Phytophthora* spp.)
Xylanase (EIX)	pentapeptide	Fungi (*Trichoderma* spp.)
DAMP		
Systemin	not defined	protein (defense)
PROPEPs	Peps	precursor protein
Oligogalacturonides	oligomer	plant cell wall (pectins)
Cutin	dodecane-1-ol	plant cuticle
Cellodextrins	oligomer	plant cell wall (cellulose)

Table 1. Summary of selected MAMPs and DAMPs recognized by plants.
Adapted from Postel and Kemmerling (2009) and Newman *et al*. (2013).

2.1 MAMP-triggered immunity

2.1.1 MAMPs

It is believed that during plant-microorganism interactions, MAMPs are the first non-host molecules that plant senses. By MAMPs we understand molecular structures or parts of structures that are essential for the overall fitness of microbes. It is therefore difficult for a microbe to modify or loose these motifs and as a consequence, MAMPs are conserved among microbes, pathogenic or not. Diverse MAMPs have been already described (Table 1; Postel and Kemmerling, 2009; Newman *et al.*, 2013); they can be (glyco)proteins, carbohydrates or lipids.

The most extensively studied MAMPs are the bacterial flagellin, the elongation factor Tu (EF-Tu) and the fungal chitin. The protein flagellin, the main building block of bacterial flagella, and its minimal motif flg22 is a potent plant elicitor recognized by many plant species (Felix *et al.*, 1999). EF-Tu is the most abundant bacterial protein playing a crucial role in protein biosynthesis. EF-Tu and its minimal epitope elf18 are active at subnanomolar concentrations but responses are restricted uniquely to Arabidopsis and the *Brassicaceae* family (Kunze *et al.*, 2004). Chitin, a homopolymer of N-acetylglucosamine (GlcNAc), is the major component of fungal cell walls. Other identified MAMPs include i) harpin proteins, cold-shock proteins, lipopolysaccharides (LPS), peptidoglycans (PGN), Ax21 protein and rhamnolipids, derived from bacteria, ii) xylanase, ergosterol and different glycans, derived from fungi, or iii) transglutaminases, β-glucans and fucanes derived from oomycetes or evolutionary close brown algae (Table 1). Calcium-dependent cell wall transglutaminases of the *Phytophthora* spp. are recognized *via* the conserved epitope pep-13 and elicit defense responses in parsley and potato (Brunner *et al.*, 2002). Beta-1,3-glucans are found as the main cell wall components of oomycetes. Laminarin, a ß-1,3-linked glucan of the brown algae *Laminaria digitata*, induces defense responses in tobacco, Arabidopsis or grapevine (Klarzynski *et al.*, 2000; Aziz *et al.*, 2003; Menard *et al.*, 2004). MAMPs can be components of distinct microbial structures, such as organs of motility (flagellin) or cell walls (LPS, PGN, chitin or β-glucans). They can be also cytoplasmic (EF-Tu, cold-shock proteins) or secreted by microbes (Ax21, xylanase; Boller and Felix, 2009).

MAMPs were initially considered as invariant, but recent works show that MAMPs evolve more than expected (Cai *et al.*, 2011; McCann *et al.*, 2012). Although MAMPs are under a strong negative selection to preserve function required for the microbial fitness, they are also under strong positive selection exerted by host PRRs. It was observed that the immunogenic epitopes elf18 and flg22 diversified between different bacteria species and strains (Sun *et al.*, 2006; Cai *et al.*, 2011) with a higher rate than the non-immunogenic protein parts (McCann *et al.*, 2012).

MAMPs can be also required for microbial virulence, which was considered for a long time as an exclusive effector characteristic (Boller and Felix, 2009; Thomma *et al.*, 2011). Moreover, while many described MAMPs are widely distributed among the whole microorganism

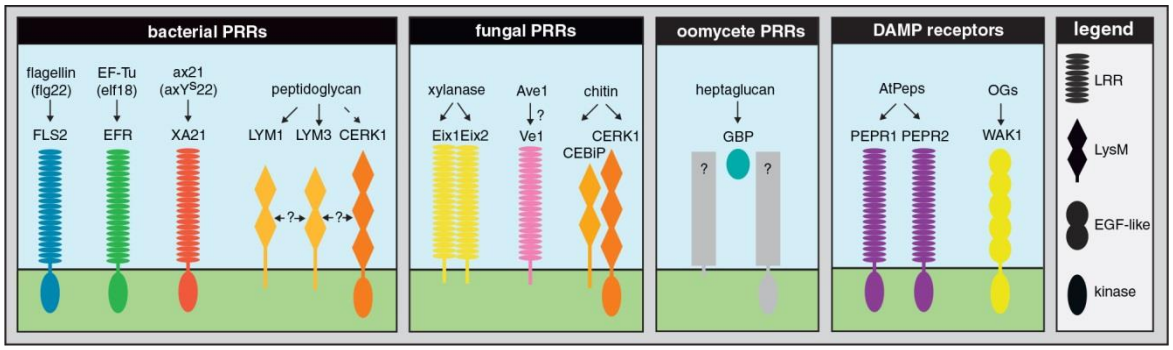

Figure 2. Summary of selected plant pattern recognition receptors (PRRs) with their ligands. PRRs for peptidic PAMPs of bacterial origin are LRR-RLKs: FLS2 recognizing flagellin (or the active epitope flg22) identified in Arabidopsis, tomato, *N. benthamiana* and rice, EFR recognizing the elongation factor Tu (or the active epitope elf18) in *Brassicaceae* and XA21 recognizing the type-I secreted quorum sensing peptide Ax21 in rice. LysM RLPs LYM1 and LYM3 are the receptors for bacterial peptidoglycan (PGN) with CERK1 as a co-receptor. Tomato LRR-RLPs Eix1 and Eix2 recognize a fungal PAMP xylanase. Tomato LRR-RLP Ve1 recognizes Ave1 ligand from a fungus *Verticillium*. In rice, the LysM RLP CEBiP binds chitin and interacts with the LysM RLK (LYK) CERK1 to initiate signaling. In Arabidopsis, CERK1 is the major chitin-binding protein and possibly interacts with other LYKs. In legumes, an extracellular β-glucan-binding protein (GBP) binds *Phytophthora* heptaglucan. Concerning damage-associated molecular patterns (DAMPs), the LRR-RLKs PEPR1 and PEPR2 bind endogenous AtPeps, and the RLK WAK1, containing an EGF-like domain, is a receptor for cell wall-derived oligogalacturonides (OG). From Monaghan and Zipfel (2012).

classes of bacteria, fungi or oomycetes (called also general elicitors), others are conserved only within smaller taxonomic units (orders, families or genera), such as pep-13 or Ax21 (Boller and Felix, 2009). The border between MAMP and effector classification seems thus less clear (Thomma *et al.*, 2011).

Besides MAMPs, plants sense DAMPs, the endogenous elicitors (Table 1). The examples of DAMPs are fragments of plant cell walls, such as oligogalacturonides (OG) and cutin monomers released by the hydrolysis of pectin and cuticle, respectively. Other examples are short peptides, the 18-amino acid long systemin or the 23-amino acid long Pep1. Both originate from precursor proteins, prosystemin and PROPEP, that are expressed upon wounding and pathogen attack (Boller and Felix, 2009).

2.1.2 PRRs, receptors to MAMPs and DAMPs

During the last decade, a considerable progress in the identification of novel plant PRRs has been achieved. Known plant PRRs are Receptor-Like Kinases (RLKs) or Receptor-Like Proteins (RLPs), which are localized at the plasma membrane and possess extracellular domain for ligand recognition (Fig. 2). The RLKs are transmembrane proteins and contain a cytosolic serine/threonine kinase domain. The catalytic loop of most of plant PRR kinases contains the sequence CD or GD instead of the most frequent RD. These non-RD kinases are rarely present in other immune receptors and may be a hallmark of both plant and animal PRRs (Dardick and Ronald, 2006). RLPs can be either glycosylphosphatidylinositol (GPI)-anchored or membranous proteins lacking a kinase domain.

Based on the analysis of the Arabidopsis genome, the array of putative PRRs encoded in plants is much higher than in mammals. In total, the Arabidopsis genome carries 417 RLKs with an obvious receptor configuration and 57 RLPs (Shiu and Bleecker, 2003). RLKs and RLPs encoded by plant genomes can be classified into 14 classes according to the type of the extracellular domain. The major PRR types carry leucine rich repeats (LRR) or lysine motifs (LysM), while others can carry C-type lectin or EGF-like ectodomain (Shiu and Bleecker, 2003). These domains confer distinct ligand specificities.

2.1.2.1 Leucine rich repeat (LRR) receptors

Around half of Arabidopsis RLKs (~200) falls into the class of LRR-RLKs that can be grouped into 13 subfamilies (I to XIII) (Shiu and Bleecker, 2003). It seems that LRR-RLKs are involved in defense-related responses and in growth and developmental processes. In plants, the LRR domain recognizes proteinaceous microbial ligands (Boller and Felix, 2009; Monaghan and Zipfel, 2012) and is formed by LRR repeats that each comprises 23-25 residues and matches the consensus sequence IPxxLxxLxx L**xx**L**x**L**xx**NxL$^{T}/_{S}$Gx (Mueller *et al.*, 2012). Based on crystallographic studies on animal and plant LRR-RLKs (She *et al.*, 2011; Lu and Sun, 2012; Sun

et al., 2013), LRR domain assembles into a horseshoe-shaped solenoid. Leucines form the backbone of LRR repeat and can be substituted by other hydrophobic residues. The ligand binds on the concave surface of the horseshoe, where variable residues (**x**) can be solvent-exposed and thus participate in ligand binding and specificity (Lu and Sun, 2012; Mueller *et al.*, 2012).

Among the best characterized plant PRRs is the flagellin/flg22 receptor FLAGELLIN SENSING 2 (FLS2), a LRR-RLK conserved in many plant species (Fig. 2; Gomez-Gomez and Boller, 2000; Hann and Rathjen, 2007; Robatzek *et al.*, 2007; Takai *et al.*, 2008). The structurally related LRR-RLK XII Elongation factor-Tu receptor (EFR) recognizes the bacterial EF-Tu/elf18 in the *Brassicaceae* (Zipfel *et al.*, 2006). Another LRR-RLK XA21 confers recognition of the type-I secreted bacterial protein Ax21 conserved among *Xanthomonas* spp. and involved in the bacterial quorum sensing (Lee *et al.*, 2009). The LRR-RLP type PRRs include the tomato (*Solanum lycopersicum*) Eix1 and Eix2, which bind ethylene-inducing xylanases derived from fungi (Ron and Avni, 2004), and the tomato receptor Ve1, which recognizes the protein Ave1 derived from the *Verticillium* fungi (de Jonge *et al.*, 2012). The recently described LRR-RLP AtRLP30 functions as a receptor for a proteinaceous elicitor SCFE1 purified from the axenic culture filtrate of *Sclerotinia sclerotiorum* (Zhang *et al.*, 2013). Another LRR-RLP Responsiveness to Botrytis Polygalacturonase 1 (RBPG1; AtRLP42), recognizes fungal endopolygalacturonases from the necrotroph *Botrytis cinerea* or the saprotroph *Aspergillus niger* (Zhang *et al.*, 2014).

LRR-RLKs possess a similar architecture to animal Toll-like receptors (TLRs) that are important innate immune PRRs. TLRs contain a cytoplasmic tyrosine kinase domain of Toll/interleukin-1 receptor (TIR) type. Each TLR can recognize very distinct ligands lacking structural similarity by employing different sets of LRRs. Upon ligand perception, TLRs form homodimers, which are crucial for signaling. Different TLRs can even assemble to heterodimers to recognize certain MAMPs, such as lipopeptides (Pasare and Medzhitov, 2004). This high versatility is yet unknown for plant LRR-RLKs.

2.1.2.2 Lysin motif (LysM) receptors

Plant LysM-PRRs contain ectodomains built from one to three lysin motifs. LysM is a sequence of ~40 amino acids in length, found in most organisms. Lysin motifs can be assembled into a LysM domain interspaced by short peptides with Cys x Cys (CxC) motifs. The latter might be implicated in keeping the spatial conformation of ectodomain *via* formation of cysteine disulfide bridge (Radutoiu *et al.*, 2003). LysM-proteins were initially described in bacteria as hydrolases modifying bacterial cell wall. In plants, LysM RLKs and RLPs recognize GlcNAc-containing glycans and aminosugars present on microbial surface, such as fungal chitin and bacterial PGN, or lipochitooligosaccharides secreted by beneficial microorganisms (reviewed in Gust *et al.*, 2012).

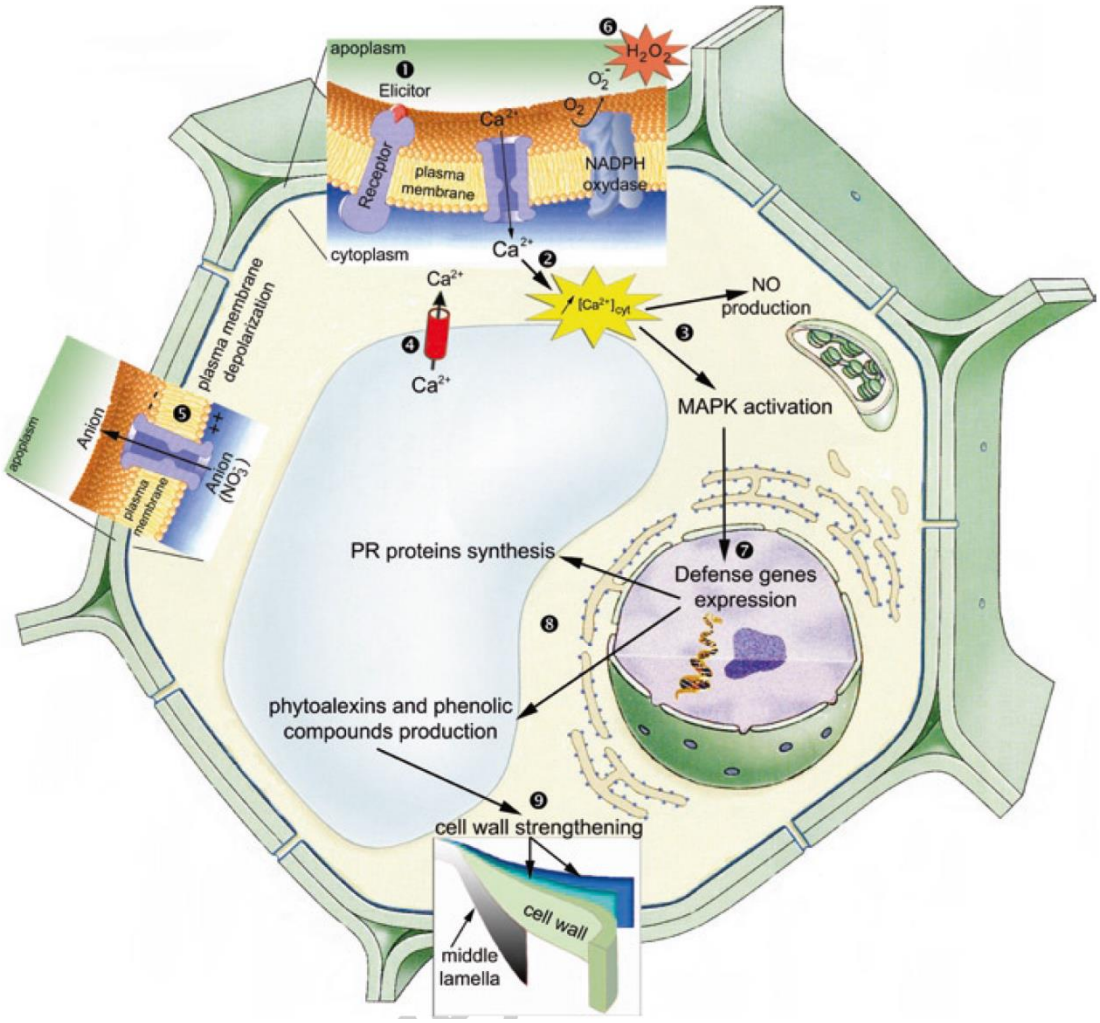

Figure 3. Scheme of defense events triggered by MAMPs in plant cells.
The perception of MAMP/elicitor (1) induces a cascade of events including a calcium influx (2), leading to an increase in the cytoplasmic calcium concentration $[Ca^{2+}]_{cyt}$ that further activates MAPKs and CDPKs and nitric oxide (NO) production (3). NO participates in triggering the calcium efflux from intracellular store pools (4), anion efflux (5) and ROS production (6). This signal amplification leads to the activation of defense genes (7), production of defense metabolites such as PR proteins, callose, phytoalexins and other phenolic compounds (8) and cell wall reinforcement (9). From Adrian *et al.* (2012).

Plant LysM RLKs or RLPs assure a highly specific recognition of their corresponding ligands, although the latter possess a similar structure (Petutschnig *et al.*, 2010; Gust *et al.*, 2012). Fungal chitin is recognized by the LysM-RLP Chitin elicitor-binding protein (CEBiP) in rice (Kaku *et al.*, 2006) and the LysM-RLK Chitin elicitor receptor kinase 1 (CERK1) in *A. thaliana* (Fig. 2; Miya *et al.*, 2007). CERK1 together with LysM-RLPs LYM1 and LYM3 mediate PGN perception in Arabidopsis (Willmann *et al.*, 2011).

Also several PRRs for DAMPs have been identified (Fig. 2). The Arabidopsis LRR-RLKs PEPR1 and PEPR2 recognize AtPep peptides, including AtPep1 (Yamaguchi *et al.*, 2006; Krol *et al.*, 2010). Another PRR, Wall-Associated Kinase 1 (WAK1), perceives OG released from defected plant cell walls (Brutus *et al.*, 2010).

2.1.3 PRR-mediated signaling and defense

From what we know, PRRs are often associated with other RLKs or RLPs to form molecular complexes. This can improve the ligand recognition, signal transduction or perform a regulatory role (Monaghan and Zipfel, 2012). Notably RLP receptors interact with RLKs for signal transduction. The recognition of MAMPs/DAMPs leads to the activation of the PRR kinase domain, which initiates phosphorylation events on signaling components. Once activated, these proteins elicit a complex cascade of signaling events, including ion fluxes leading to plasma membrane depolarization, production of reactive oxygen species (ROS) and nitric oxide (NO) and activation of Mitogen-Activated and Calcium-Dependent Protein Kinases (MAPKs and CDPKs, Fig. 3; Boller and Felix, 2009; Boudsocq *et al.*, 2010). These signaling events lead to the activation of transcription factors (TFs) and massive transcriptional reprogramming related to defense (Boller and Felix, 2009). Recently, a novel model for PRR function was described (Park and Ronald, 2012). Upon ligand recognition, the rice PRR XA21 is cleaved to release an intracellular kinase domain that is translocated into the nucleus, where it interacts with a repressor of defense genes (Park and Ronald, 2012).

Defense gene activation leads to the accumulation of different enzymes or metabolites. Among them are frequently found: i) the pathogenesis-related (PR) proteins including hydrolytic enzymes (β-1,3-glucanases and chitinases), which degrade microbial cell walls, cationic defensins disrupting pathogen membrane, peroxidases, proteinase inhibitors or lipid-transfer proteins; ii) compounds with an antimicrobial activity such as phytoalexins, iii) lignin and callose that are deposited to cell wall assuring its strengthening (Fig. 3). Other key stones of MTI are iv) production of ROS with direct antimicrobial effect, or v) stomatal closure (Jones and Dangl, 2006; Melotto *et al.*, 2006; Boller and Felix, 2009).

PRR	Plant	Pathogen	Reference
Loss-of-function			
FLS2	Arabidopsis	*Pseudomonas syringae* pv *tomato DC3000*	Zipfel *et al.*, 2004; Heese *et al.*, 2007; Xiang *et al.*, 2008
	N. benthamiana	*Pseudomonas syringae* (multiple compatible and incompatible strains)	Hann *et al.*, 2007
EFR	Arabidopsis	*Agrobacterium tumefaciens*	Zipfel et *al.*, 2006
CERK1	Arabidopsis	*Alternaria brassicicola* (incompatible interaction)	Miya *et al.*, 2007; Wan *et al.*, 2008; Wan *et al.*, 2012
	Arabidopsis	*Erysiphe cichoracearum*	Miya *et al.*, 2007
	Arabidopsis	*Pseudomonas syringae* pv *tomato DC3000*	Gimenez-Ibanez *et al.*, 2009; Wan *et al.*, 2012
CERK1	wheat	*Mycosphaerella graminicola* (non pathogenic)	Lee *et al.*, 2014
LYM1, LYM3	Arabidopsis	*Pseudomonas syringae* pv *tomato* DC3000	Willmann *et al.*, 2011
LYK4	Arabidopsis	*Alternaria brassicicola*	Wan *et al.*, 2012
		Pseudomonas syringae pv *tomato DC3000*	Wan *et al.*, 2012
CEBiP	rice	*Magnaporthe oryzae* (rather incompatible strain and weakly virulent)	Kishimoto *et al.*, 2010; Kouzai *et al.*, 2014
CEBiP	wheat	*Mycosphaerella graminicola* (non pathogenic)	Lee *et al.*, 2014
LYP4, LYP6	rice	*Magnaporthe oryzaecola, Xanthomonas oryzae* pv *oryzae*	Liu *et al.*, 2012a
RLP30	Arabidopsis	*Sclerotinia sclerotiorum, Botrytis cinerea*	Zhang *et al.*, 2013
Transfer			
XA21	rice => rice	*Xanthomonas oryzae* pv *oryzae* (multiple pathogen isolates)	Wang *et al.*, 1996; Lee *et al.*, 2009
	rice => *Citrus sinensis*	*Xanthomonas axonopodis* pv *citri*	Mendes *et al.*, 2010
EFR	Arabidopsis = > *N. benthamiana*	*Pseudomonas syringae* pv *syringae* (B728a)	Lacombe *et al.*, 2010
		Pseudomonas syringae pv *tabaci* (11528)	Lacombe *et al.*, 2010
		Agrobacterium tumefaciens (a virulent tumorigenic strain)	Lacombe *et al.*, 2010
	Arabidopsis => tomato	*Ralstonia solanacearum*	Lacombe *et al.*, 2010
		Xanthomonas perforans (*X. axonopodis* pv *Vesicatoria*)	Lacombe *et al.*, 2010
Ve1	tomato= > Arabidopsis	*Verticillium dahliae* , *Verticillium albo-atrum*	Fradin *et al.*, 2011

Table 2. Involvement of PRRs in disease resistance. List of principal works.
Loss of function studies have shown an increased susceptibility to the indicated pathogen, whereas the transfer studies have lead to an enhanced resistance against the mentioned microbe.

The MAMP perception also triggers the production of phytohormones, such as salicylic acid (SA), jasmonic acid (JA), ethylene (ET) and abscisic acid (ABA; Glazebrook, 2005). The interplay and fine tuning between these hormones and others, such as auxins, brassinosteroids (BR) or giberellins, coordinates activation of these above mentioned defenses and allow directing immune responses against the specific intruder. Many of the defense responses strictly depend on these phytohormones (Glazebrook, 2005; Robert-Seilaniantz *et al.*, 2011). However, successful pathogens are able to manipulate the plant hormonal balance to their own profit (Gohre *et al.*, 2008; Shan *et al.*, 2008; Gimenez-Ibanez *et al.*, 2009; Tsuda *et al.*, 2009). It was also reported that MTI can be sometimes associated with a localized programmed cell death (Hann and Rathjen, 2007), termed hypersensitive response (HR), which is more likely to be a hallmark of ETI. MTI can also trigger a systemic signal leading to resistance induction in distant non-challenged tissues, called systemic acquired resistance (SAR; Jones and Dangl, 2006). Triggered immunity aims to prevent further microbial entry, disintegrate the microbial protective cell wall, delay its maturation or prevent its reproduction.

It has been proposed that DAMP signaling mediated by the family of small AtPep peptides may amplify immune responses induced by MAMPs and compensate for eventual hormonal perturbation caused by effectors (Tintor *et al.*, 2013; Ross *et al.*, 2014).

2.1.4 PRR-mediated disease resistance

Different works highlight the importance of PRR-mediated MTI in plant disease resistance (Table 2; reviewed in Monaghan and Zipfel, 2012). Loss of a given PRR can lead to enhanced susceptibility to infections. The mutation/silencing of FLS2 in both *A. thaliana* and *N. benthamiana* led to enhanced susceptibility to a range of pathogenic and non-pathogenic bacteria (Zipfel *et al.*, 2004; Hann and Rathjen, 2007). The mutation in RLP30 caused the hypersusceptibility to *S. sclerotiorum*, *B. cinerea* or *Hyaloperonospora arabidopsidis* (Zhang *et al.*, 2013).

On the other hand, the PRR transfer is able to confer resistance (Table 2). The expression of the LRR-RLK AtEFR in *N. benthamiana* or tomato, plants normally blind to elf18, induced elf18-triggered defense responses and increased resistance to bacterial pathogens (Zipfel *et al.*, 2006; Lacombe *et al.*, 2010). Among others, *N. benthamiana* AtEFR$^+$ plants were highly resistant to *P. syringae* pv *tabaci* or a virulent tumorigenic *Agrobacterium tumefaciens* strain (Lacombe *et al.*, 2010). Tomato AtEFR$^+$ also drastically reduced wilting symptoms induced by *Ralstonia solanacearum*, an important agriculturally relevant pathogen (Lacombe *et al.*, 2010). The transfer of the tomato LRR-RLP Ve1 to Arabidopsis conferred the resistance to vascular wilts caused by several strains of fungi *Verticillium dahliae* and *V. albo-atrum* (Fradin *et al.*, 2011). The rice LRR-RLK XA21 is another receptor mediating robust resistance to multiple *Xanthomonas oryzae* pv

oryzae (bacterial leaf blight) isolates (Wang *et al.*, 1996). Interaction of XA21 with its ligand leads to HR and effective immunity in rice cells (Lee *et al.*, 2009). Transfer of XA21 receptor from rice into orange (*Citrus sinensis*) led to increased resistance against *X. axonopodis* pv *citri* causing citrus canker, showing that the PRR transfer from monocots to dicots can be successful (Mendes *et al.*, 2010). The expression of chimeric receptors combining the transmembrane and kinase domain of XA21 and the chitin-binding ectodomain of OsCEBiP in rice could initiate HR response to chitin and decreased rice susceptibility to the fungus *Magnaporthe oryzae* (Kishimoto *et al.*, 2010). Studies using chimeric PRRs have shown that it is entirely the kinase domain which dictates the type of immune responses (Brutus *et al.*, 2010; Kishimoto *et al.*, 2010).

Although many studies show that PRRs are key for plant immunity, not all of the PRRs studied so far seem to contribute similarly to the plant resistance. Upon plant-pathogen interactions, the importance of a given PRR depends on the abundance of its cognate MAMP, the rapidity/efficiency of the immune activation after ligand binding and last, but not least, on the set of pathogen effectors or toxins that can affect the immune signaling.

2.2 Effector-triggered immunity

2.2.1 Effectors target MTI

Bacteria, fungi, oomycetes can all secrete effectors in order to perturb MTI signaling. Bacterial effectors secreted through the Type III secretion system (TTSS) are the best studied. Their activity may be as various as a protease, kinase, phosphatase or E3 ubiquitin ligase. Effectors can directly target PRRs, co-receptor RLKs or important signaling components such as the MAPK cascade. Some virulent pathogens sometimes employ toxins that cause perturbations in hormonal pathways, leading to decreased MTI (Gohre *et al.*, 2008; Shan *et al.*, 2008; Gimenez-Ibanez *et al.*, 2009; Tsuda *et al.*, 2009).

2.2.2 ETI responses

Effectors are recognized by cytoplasmic R-proteins that contain a nucleotide binding domain (NB) and a LRR domain; they are referred to as NB-LRR proteins. Effector mediated immunity (ETI) leads to partly overlapping, if not the same, signaling and responses as MTI. However, ETI is more rapid and stronger in intensity and also includes the HR. HR occurs locally to the pathogen presence and is highly effective in preventing further microbial spread. R protein-mediated resistance was exploited in traditional breeding and transgenic crops; however, pathogens can overcome ETI by mutating or losing their effectors (Jones and Dangl, 2006; Tsuda and Katagiri, 2010).

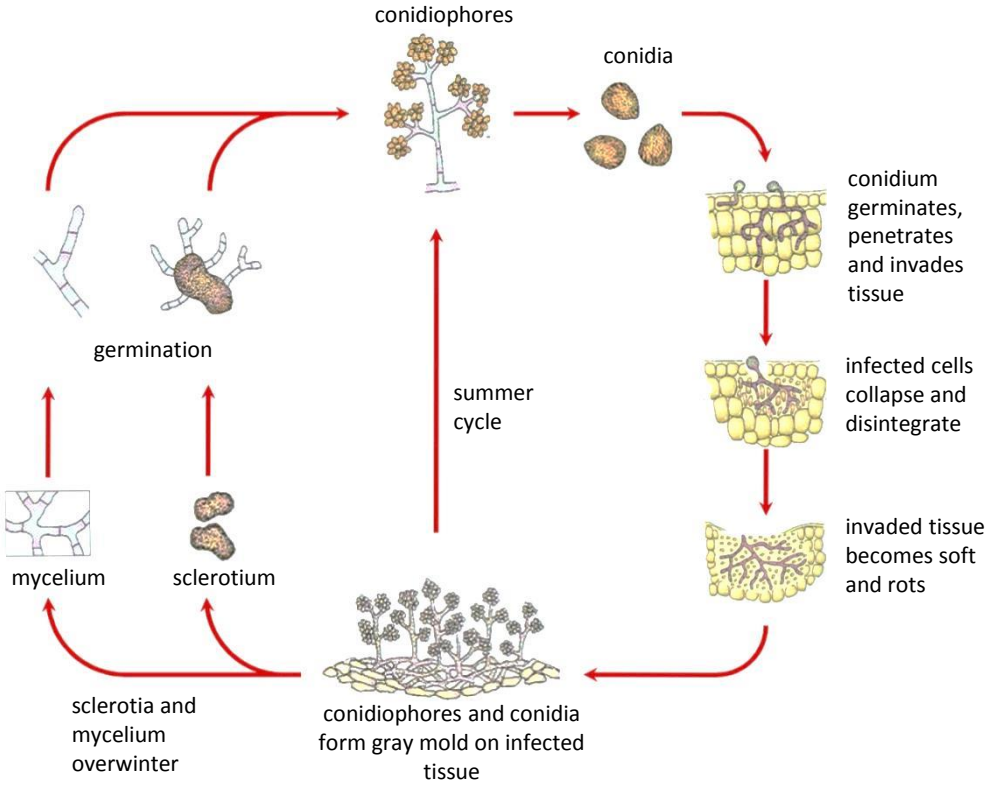

Figure 4. Life cycle of *Botrytis cinerea*, the causal agent of gray mold. Adapted from Agrios (2005) and Gauthier (2009).

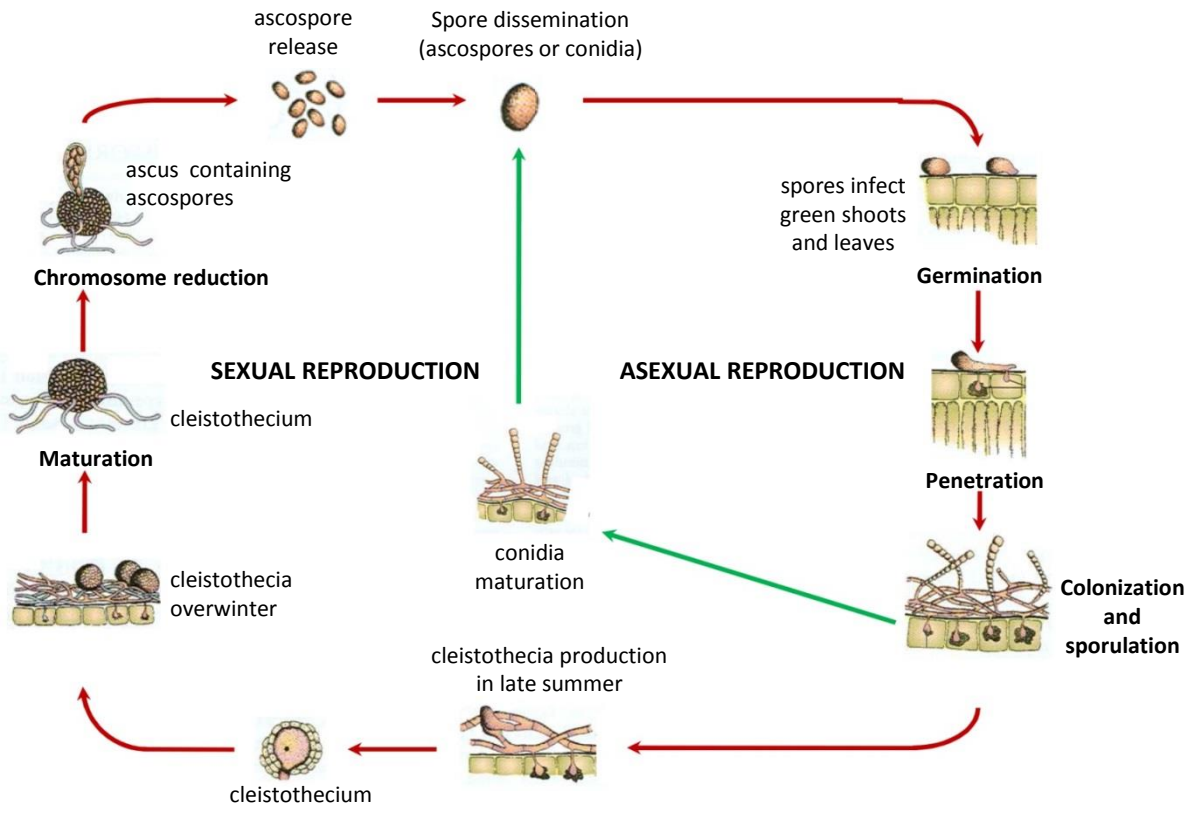

Figure 5. Life cycle of *Erysiphe necator*, the causal agent of powdery mildew. Adapted from Agrios (2005) and Gauthier (2009).

3 Grapevine: its biotic interactions and immunity

In its environment, cultivated grapevine (*V. vinifera*) interacts with many microorganisms. Some of them are pathogenic, colonize grapevine and cause infections, other are mutualists, such as mycorrhiza fungi or plant growth promoting rhizobacteria (PGPR), which can improve the plant physiology.

3.1 Biotic interactions

3.1.1 Fungi

***Botrytis cinerea*: Gray mold (bunch rot)**

B. cinerea, a necrotrophic fungus from the family of *Sclerotiniaceae*, infects more than 235 species including grapevine. Mature berries are highly susceptible, although infections may occur also on young leaves and inflorescences. *B. cinerea* overwinters as a mycelium or a sclerotium (a resistant compact mass of mycelium) in berry or leaf litter (Fig. 4). In spring, both can germinate and emerging conidiophores produce conidia, a source of primary infections. Conidia are dispersed by wind or rain, penetrate in wounded tissues or tissues with a high sugar content, eventually causing necrosis. New conidiophores can emerge from necrosed tissues and thus multiple infection cycles may follow during the spring/summer season (Fig. 4; Elmer and Michailides, 2007).

***Erysiphe necator*: Powdery mildew**

Erysiphe necator (*Uncinula necator*) is a fungus of *Ascomycetes* and an obligate biotroph developing on green tissues of grapevine, including leaves, inflorescences and young berries. In spring, the primary inoculum consists of mature ascospores that are spread by wind and germinate on the leaf surface (Fig. 5). Fungus penetrates the cuticle by a specialized structure, the appressorium, then forms haustoria for the nutrient intake. Conidiophores, visible as white spots, appear on the upper leaf surface under humid conditions and are a source of secondary infections. *E. necator* overwinters as cleistothecium formes in the infected tissues at the end of the season (Agrios, 2005).

***Plasmopara viticola*: Downy mildew**

P. viticola is an oomycete of the order of *Peronosporales* and a strict biotroph, infecting specifically *V. vinifera* species of all known cultivars. Similarly to the powdery mildew fungus, *P. viticola* infects all green parts of grapevine. In spring, oospores that overwintered in leaf litter and soil of vineyards germinate and macrosporangia are produced, eventually leading to zoospore release. Zoospores are splashed by rain and infect plants through stomata (Fig. 6). Mycelium then extensively colonizes mesophyll and after 7-10 days, “oil spots” are formed on the upper leaf part.

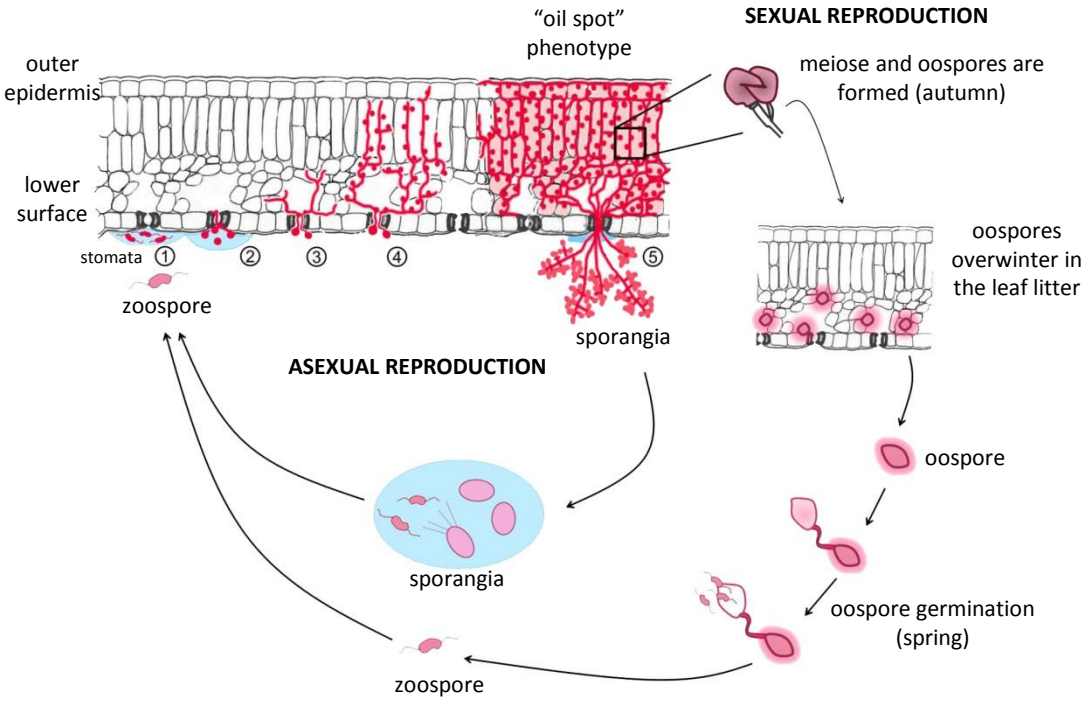

Figure 6. Life cycle of *Plasmopara viticola*, the causal agent of downy mildew. Zoospores swim in the water film until they reach stomata (1), where they encyst and form a germ tube and an infection vesicle in the substomatal cavity (2). Mycelium penetrates host tissues (3) and forms haustoria, specialized structures for nutrient uptake (4). After tissue colonization, new sporangiophores emerge (5) and release sporangia that can serve as a secondary inoculum. In autumn, oospores are formed in the infected tissues and overwinter in the leaf litter. In spring, oospore germination generates a primary inoculum. Adapted from Gamm (2011).

Bacterium species	Disease	Country	References
Pathogens			
Agrobacterium vitis	crown gall	worldwide	Burr and Otten, 1999
Agrobacterium tumefaciens			Szegedi *et al.,* 2005
Xanthomonas campestris pv *viticola*	bacterial canker	Brazil, India	Neto *et al.,* 2011
Xylella fastidiosa subsp. *fastidiosa*	Pierce's disease	American continent	Nunney *et al.,* 2010
Xylophilus ampelinus	bacterial blight	Australia	Dreo *et al.*, 2007
Pseudomonas syringae pv *syringae*	bacterial inflorescence rot	Australia, Argentina	Whitelaw-Weckert *et al.,* 2011
Endophytes			
Pseudomonas fluorescens			West *et al.,* 2010
Pseudomonas syringae sp.			
Burkholderia phytofirmans			Compant *et al.,* 2005b
Epiphytes			
Pseudomonas aeruginosa			West *et al.,* 2010
Pseudomonas putida			

Table 3. Bacterial pathogens, endophytes and epiphytes of grapevine.
Selection of endophytes and epiphytes with regard to presented work.

With humid conditions, white sporulation (or down) formed by emerging sporangiophores appears on the lower leaf surface and new secondary infections occur. Many cycles of infections can follow in spring and summer. Finally, the infected tissue dry and eventually drop (Agrios, 2005; Gessler *et al.*, 2011)

In contrast to *V. vinifera*, American *Vitis* species such as *V. riparia*, *V. rupestris* and *V. labrusca* or *Muscadinia rotundifolia* (from a distinct genus of the *Vitaceae* family) are resistant to downy mildew (Bellin *et al.*, 2009).

3.1.2 Bacteria

Grapevine interacts with many bacteria (Table 3). Bacterial infections are not so frequent in European vineyards, but represent an important threat elsewhere. The major bacterial disease is crown gall, caused by *Agrobacterium vitis*, and occasionally by *A. tumefaciens* (Burr and Otten, 1999; Szegedi et *al.*, 2005). The agrobacteria infect roots and the wood bases at the sites of injury. *Agrobacterium* perceives plant phenolic compounds, attaches to cells and transfer the T-DNA into the plant cell causing an overgrowth, visible as crown galls (Burr and Otten, 1999).

Other pathogenic bacteria are *Xanthomonas campestris* pv *viticola* (bacterial canker) or *Xylella fastidiosa* subsp. *fastidiosa* (Pierce's disease) infecting xylem vessels from xylem-feeding insects (Nunney *et al.*, 2010). Grapevine is also associated with many *Pseudomonas* spp., including pathogenic, endophytic and epiphytic strains (Table 3). *Pseudomonas aeruginosa*, an opportunistic pathogen of animals and plants (Rahme *et al.*, 1997), was found as a grapevine epiphyte (West *et al.*, 2010).

***Burkholderia phytofirmans*: a grapevine-associated PGPR**

PGPR are soilborne bacteria that form non-symbiotic beneficial association with their host plants. PGPR grow endophytically inside roots and upper plant parts and provide beneficial effects such as enhanced plant growth and induced systemic resistance (ISR) to biotic and abiotic stresses (Ait Barka *et al.*, 2000; Compant *et al.*, 2005a; Lugtenberg and Kamilova, 2009). The genus *Burkholderia* (β-proteobacteria) contains over 30 species including plant growth-promoting bacteria (*B. phytofirmans*, *B. cepacia*, *B. vietnamiensis*), plant pathogens (*B. caryophylli*, *B. plantarii*, *B. glumae*, *B. andropogonis*) and even animal/human pathogens (*B. mallei*, *B. pseudomallei*).

B. phytofirmans strain PsJN is notably an endophytic PGPR of grapevine (*V. vinifera*; Sessitsch *et al.*, 2005; Lo Piccolo *et al.*, 2010), but also of potato, tomato and sugarbeet (Mitter *et al.*, 2013). Recently, *B. phytofirmans* has also been shown to colonize Arabidopsis and to promote its growth (Zuniga *et al.*, 2013). In grapevine, *B. phytofirmans* closely attaches to the rhizodermal cell walls, extensively colonizes root surface and penetrates the root internal tissues to further

Molecule	**Origin**	**Cultivar (*V. vinifera*)**
α-1,4-oligogalacturonides (OG)	plant pectins	Gamay
glucan	*Botrytis cinerea*	Optima
endopolygalacturonase BcPG1	*Botrytis cinerea*	Gamay
β-1,3-glucans (laminarin)	*Laminaria digitata* (brown algae)	Gamay, Chardonnay
chitosan	crustaceans	Chardonnay
β-1,4-glucans (cellodextrins)	cellulose hydrolysis	Gamay, Chardonnay
rhamnolipids	*Pseudomonas aeruginosa*, *Burkholderia plantarii*	Gamay, Chardonnay
ergosterol	fungi	Ugni blanc
flg22	*Pseudomonas aeruginosa*	Pinot Noir, *V. rupestris*
harpin	bacteria	Pinot Noir, *V. rupestris*
oligandrin (elicitin)	*Pythium oligandrum* (oomycete)	Pinot Noir
yeast extract	*Saccharomyces cerevisiae*	Pinot Noir

Table 4. Selection of MAMPs inducing defense responses in grapevine.
Adapted from Delaunois *et al.* (2014).

spread into aerial parts of the plant such as stems and leaves *via* xylem vessels (Compant *et al.*, 2005b). By altering grapevine metabolism, *B. phytofirmans* confers better tolerance to *B. cinerea* infection and to cold stress (Ait Barka *et al.*, 2000; Ait Barka *et al.*, 2006; Fernandez *et al.*, 2012; Theocharis *et al.*, 2012). In grapevine cells, *B. phytofirmans* triggers a transient extracellular alkalinization, the production of SA and defense-related transcripts, suggesting that it is perceived by *V. vinifera* potentially *via* MAMP detection (Bordiec *et al.*, 2011).

3.2 Grapevine MAMP-triggered immunity

Grapevine recognizes a variety of MAMPs including the *B. cinerea* endopolygalacturonase 1 (BcPG1; Poinssot *et al.*, 2003), the linear β-1,3-glucan laminarin extracted from the brown algae *Laminaria digitata* (Aziz *et al.*, 2003), a deacetylated derivative of chitin, chitosan (Trotel-Aziz *et al.*, 2006), OG (Dubreuil-Maurizi *et al.*, 2010), flg22 (Chang and Nick, 2012) and others (Table 4). Some were shown effective to induce disease resistance when applied on plants (reviewed in Delaunois *et al.*, 2014).

MAMPs elicit signaling and defense responses in grapevine (Aziz *et al.*, 2003; Vandelle *et al.*, 2006) including events strongly reminiscent to defense in other plant species (Jones and Dangl, 2006; Boller and Felix, 2009). Using the pharmacological approach the link between the single signaling events has been shown with the proteinaceous elicitor BcPG1 (Vandelle *et al.*, 2006). BcPG1 triggers a calcium influx leading to a rise in free cytosolic Ca^{2+} concentration, which further triggers NO production. In a back loop, NO induces the calcium efflux from intracellular store pools (Vandelle *et al.*, 2006), in agreement with what was observed in tobacco signaling (Lamotte *et al.*, 2006). This amplification of Ca^{2+} signal activates the ROS production and is required for the expression of grapevine defense genes and the production of phytoalexins. Interestingly, BcPG1-triggered activation of two grapevine MAPKs is independent of the Ca^{2+} - NO - ROS pathway (Vandelle *et al.*, 2006). Therefore, as observed in other species (Garcia-Brugger *et al.*, 2006), the signaling events are not arranged in a simple linear pathway but rather in a complex signaling branched network.

Some defense genes are known in grapevine, mainly encoding enzymes involved in the phenylpropanoid pathway such as the phenylalanine ammonia lyase (*PAL*) leading to the production of i) phytoalexins *via* the stilbene synthase (*VST* or *STS*), ii) flavonoids *via* the chalcone synthase (*CHS*), iii) lignins *via* the coumarate 3-hydroxylase (*C3H*). Other defense-associated genes encode lipoxygenases (*9-LOX* and *13-LOX*) involved in the synthesis of oxylipins and JA, respectively, chitinases (*PR3, PR4, PR8, PR11*), glucanase (*PR2*), protease inhibitor (*PR6/PIN*) or polygalacturonase inhibiting protein (*PGIP*) (Adrian *et al.,* 2012; Delaunois *et al.*, 2014). For example chitinases are induced by MAMPs or upon infection with *P. viticola*, *B. cinerea* or *E. necator* (Busam *et al.*, 1997; Derkel *et al.*, 1999; Jacobs *et al.*, 1999).

Grapevine is very rich in content of phenolics, such as stilbenes (and flavonoids). These compounds also accumulate following MAMP detection but also abiotic stresses such as UV light or ozone. They protect against numerous herbivores and pathogens (Aziz *et al.,* 2003; Poinssot *et al.,* 2003; Adrian *et al.,* 2012; Delaunois *et al.*, 2014). The main grapevine stilbenes are resveratrol and its derivatives viniferins and pterostilbenes, the latter two providing the highest antifungal activity (Jeandet *et al.*, 2002; Pezet *et al.*, 2004). The overexpression of stilbene synthase in grapevine confers the resistance against *B. cinerea* (Coutos-Thevenot *et al.*, 2001).

Many works studied the resistance mechanisms against *P. viticola*. A comparative study between

the resistant *V. riparia* and a susceptible *V. vinifera* species showed that the "resistance state" results from a more rapid and stronger induction of defense gene expression, especially those genes encoding PR-proteins such as PR1 (unknown function), PR3, PR4 (chitinases), PR9 (peroxydase) or the phytoalexin-related STS (Polesani *et al.*, 2010). Resistant species also contain a higher basal level of phenolics (Kortekamp, 2006). The sulfated laminarin (PS3)-induced protection in grapevine against *P. viticola* was associated with potentiated ROS production at the site of infection, defense gene expression, callose and phenol depositions and a HR-like cell death (Trouvelot *et al.*, 2008). A number of studies have shown that both SA and JA are implicated in the resistance against *P. viticola* (Trouvelot *et al.*, 2008; Polesani *et al.*, 2010; Gauthier *et al.*, 2014).

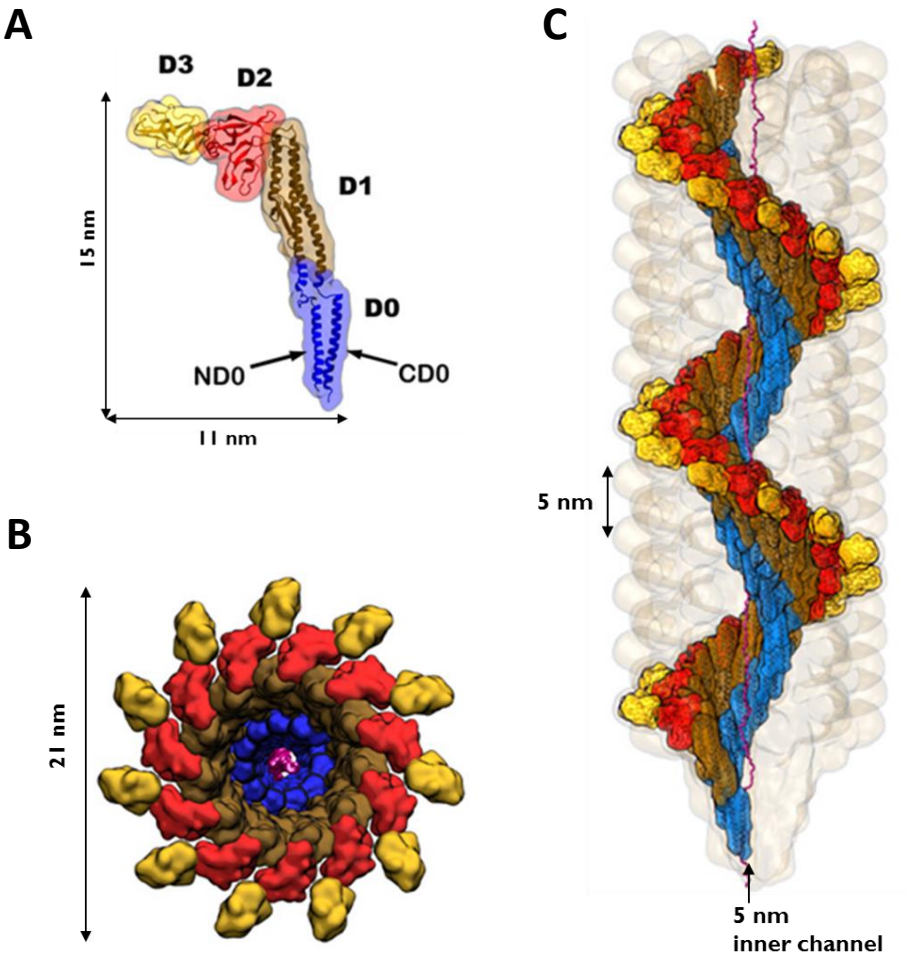

Figure 7. Schematic structure of flagellin and the flagellar filament.
The filament is formed by the helical arrangement of flagellin monomers along its axis. **A.** The folded flagellin monomer (494 amino acids) consists of four domains: D0 (1-55, 451-494, blue), D1 (56-176, 402-450, brown), D2 (177-189, 284-401, red) and D3 (190-283, yellow). **B.** View along the filament axis. Each helix turn is constituted by 11 flagellin monomers. D0 and D1 domains are stacked to form the filament core, whereas domains D2 and D3 are surface exposed and protrude from the filament. **C.** Tubular filament structure, an assembly of 11 intertwined flagellin protofilaments. Here, the side-view on one flagellin helical protofilament is presented. Adapted from Tanner *et al.* (2011).

II. Flagellin-triggered immunity

1 Bacterial flagellum and flagellin

In bacteria world, motility is important to react to environmental cues such as nutrient availability, abiotic factors or for the competitivity in habitation of ecological niches. For most "swimming" bacteria, the locomotion is driven by flagellum. Bacteria can possess only a single flagellum, a tuft of flagella or multiple flagella randomly distributed over the entire bacterium surface. For many bacteria, flagellum is required for pathogenicity. Indeed, the loss of motility decreases severly the frequency of host-pathogen interactions (Macnab, 1999). Mammalian pathogens often require flagella for adhesion to the mucus or epithelial cell surface, invasion and colonization into mucus tissues (Ramos *et al.*, 2004). For beneficial bacteria, such as symbiotic *Rhizobia*, full motile flagellum is required for competition in nodule formation in host legume rhizosphere (Ames and Bergman, 1981).

The eubacterial flagellum is a complex surface organelle. The model of its structure is derived from numerous studies on *Escherichia coli* or *Salmonella enterica* species. Flagellum comprises three main parts: the basal body, the hook and the filament. The basal body is formed by membrane-associated proteins of rod and rings that together work as a platform for motor and an apparatus for exporting proteins. The motor uses the ion gradient across the plasma membrane to generate flagellum rotation. The hook, a flexible joint, links the basal body and the filament. The filament is a long, thin helical structure up to 15 µm long. The filament is built up from 20.000 – 30.000 identical units of a single structural protein flagellin (FliC) which makes it the most abundant flagellar protein (Macnab, 2003).

Flagellar assembly is a highly ordered process and require about 50 genes. Among them, 20-30 genes encode structural proteins of flagellum; the others are involved in regulation or chemosensory mechanisms. Flagellar proteins, including flagellin, are synthetized inside the cell, then exported *via* the export apparatus at the cell surface or outside (Macnab, 1999; Ramos *et al.*, 2004).

Flagellin and its structure are crucial for a proper flagellum function. The molecule of flagellin is highly conserved in its N-terminal and C-terminal parts, forming conserved domains D0 and D1 (Fig. 7A). These domains build the filament core and are required for flagellin polymerization and filament function (Macnab, 2003). The central part of flagellin (D2 and D3 domains) can vary in length and sequence or be absent according to bacterial species (Hayashi *et al.*, 2001) and was described to be responsible for flagellin adhesive properties (Ramos *et al.*, 2004). Flagellin assembles into a hollow cylindrical structure, with 11 flagellin monomers per turn (Fig. 7B). Quaternary interactions between flagellin monomers lead to a subtle break of symmetry

underlying the helical shape of filament. The tubular filament can be also considered as composed of 11 intertwined protofilaments (Fig. 7C; Arkhipov *et al.*, 2006). The flagellar helical shape, similar to propeller-like screw, enables transmission of flagellum rotatory motion into pushing motion for bacterial motility.

2 Flagellin: a general elicitor of MTI

Flagellin is a molecule wide-spread over different eubacteria classes. Flagellin is recognized by the innate immune system of plants and animals, where it activates defense against bacteria (Boller and Felix, 2009). For plants, it is one of the best studied MAMPs. Both plants and animals possess a highly sensitive and selective perception system detecting flagellin (Felix *et al.*, 1999; Hayashi *et al.*, 2001). Although perceived *via* distinct epitope/receptor couple, both plant and animal species detect a key region, which is required for the assembly of flagellin monomers into protofilaments and flagellar motility (Yonekura *et al.*, 2003). Therefore, this region is conserved and unlikely to mutate. As these regions are buried within the flagellum structure and are surface inaccessible, only a state of monomeric flagellin possesses eliciting activity (Hayashi *et al.*, 2001). Flagellin monomers can be also released into environment due to inefficient filament capping, during flagellum construction or flagellum break that can be spontaneous or regulated by bacterial or host factors such as proteases. Flagellin monomers can be also found in a detritus of a bacterial colony (Ramos *et al.*, 2004).

2.1 flg22/FLS2 perception system in plants

Plants detect flagellin in its conserved N-terminal D0 domain *via* a 22 residue-long epitope (Felix *et al.*, 1999). Flg22 peptide spaning the recognized epitope is highly eliciting in many plant species even at nanomolar concentrations (Felix *et al.*, 1999). The plant PRR responsible for flagellin perception and binding flg22 is FLAGELLIN SENSING 2 (FLS2) (Gomez-Gomez and Boller, 2000; Chinchilla *et al.*, 2006), an LRR-RLK of the family XII (Shiu and Bleecker, 2003). FLS2 was first identified in *Arabidopsis thaliana* (Gomez-Gomez and Boller, 2000), but functional FLS2 orthologs have since been identified in tomato (LeFLS2; Robatzek *et al.*, 2007), *Nicotiana benthamiana* (NbFLS2; Hann and Rathjen, 2007) and rice (OsFLS2; Takai *et al.*, 2008). The synthetic peptide flg22 QRLSTGSRINSAKDDAAGLQIA, based on the flagellin sequence of *P. aeruginosa* strain PAK (Felix *et al.*, 1999), is a commonly used epitope substituting the effect of flagellin in Arabidopsis (Sun *et al.*, 2006) and became a tool to decipher the flg22/FLS2 binding and signaling. Flg22- and flagellin-induced responses were abolished in Arabidopsis mutant *fls2* indicating that FLS2 is a unique flagellin-perceiving receptor in Arabidopsis (Gomez-Gomez and Boller, 2000; Zipfel *et al.*, 2004).

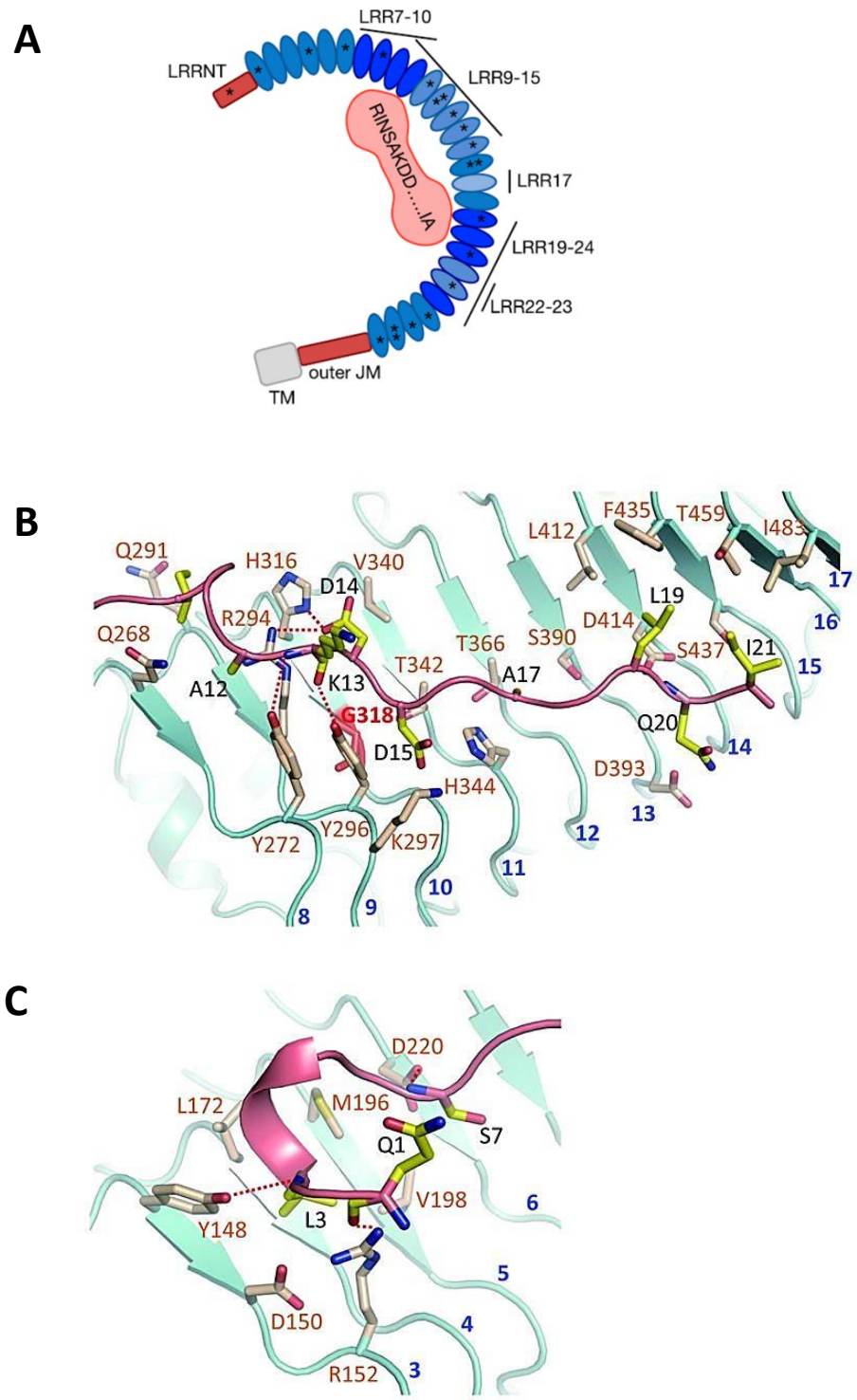

Figure 8. Mechanism of flg22 recognition by FLS2.
A. Schema of flg22 binding to the FLS2 LRR ectodomain (FLS2LRR). Indicated are LRR important for flg22 binding and signal transduction. Asterisks indicate predicted N-glycosylation motifs. From Robatzek and Wirthmueller (2012). **B.** Interaction of the core and the C-terminal side (residues 8 to 21) of flg22 with FLS2LRR. The FLS2LRR residues Y272 and Y296 interact with K13 of flg22; residues R294 and H316 interact with D14 of flg22. **C.** Interaction of the N-terminal portion (residues 1 to 7) of flg22 with FLS2LRR *via* Y148 and R152. The side chains of FLS2LRR and flg22 are labeled in cream white and yellow, respectively. From Sun *et al*. (2013). A: Ala, C:Cys, D:Asp, E:Glu, F:Phe, G:Gly, H:His, I:Ile, K:Lys, L:Leu, M:Met, N:Asn, P:Pro, Q:Gln, R:Arg, S:Ser, T:Thr, V:Val, W:Trp, Y:Tyr.

2.1.1 Ligand binding

The LRR ectodomain of FLS2 is formed by 28 LRRs that directly bind flg22 in an equimolar ratio (Bauer *et al.*, 2001; Chinchilla *et al.*, 2006). Many studies identified LRRs critical for FLS2 signaling. According to the resulting model, the flg22 core sequence RINSAKDD (flg22 aa 8-15) binds to LRRs 7-10 with a high affinity, then the flg22 C-terminus is recognized by LRRs 19-24 leading to changes in FLS2 conformation and activation of the intracellular signaling (Fig. 8A; Meindl *et al.*, 2000; Mueller *et al.*, 2012). The LRRs 10, 17, 9-15, 22-23 were also shown to be critical for FLS2 signaling in other studies (reviewed in Robatzek and Wirthmueller, 2012). FLS2 form a receptor complex with the shorter LRR-RLK BRI1-associated kinase (BAK1; also named somatic embryo receptor kinase 3, SERK3; Chinchilla *et al.*, 2007). Recently, the crystal structure of FLS2 and BAK1 ectodomains complexed with flg22 was solved (Sun *et al.*, 2013). This revealed that the FLS2 LRRs 8-11 form two positively charged pockets as an interface for binding of two aspartates D14 and D15 in the flg22 core (Fig. 8B; Sun *et al.*, 2013); which fits well with previous studies. It was also shown that the N-terminal part of flg22 (aa 1-7) is recognized by the FLS2 LRRs 2-6 (Fig. 8C), while the C-terminal part of flg22 is perceived by LRRs 13-17 (Fig. 8B). The FLS2 LRRs 18-26 are involved in the interaction with LRRs of BAK1 (Sun *et al.*, 2013). BAK1 recognizes the C-terminus of flg22 acting as a flg22 co-receptor (Sun *et al.*, 2013). This model applies for Arabidopsis, however differences may exist for other FLS2 orthologs as ligand specificities and receptor activations are distinct (Chinchilla *et al.*, 2006; Mueller *et al.*, 2012).

2.1.2 Downstream signaling

In the absence of flg22, FLS2 forms a constitutive complex with the inactive receptor-like cytoplasmic kinases Botrytis-Induced kinase 1 (BIK1) and avrPphB Susceptible PBS1-like (PBLs) that are positive regulators of most FLS2-mediated MTI downstream responses (Fig. 9; Lu *et al.*, 2010; Zhang *et al.*, 2010). Within seconds of flg22 binding, FLS2 associates with BAK1 and eventually other SERKs, such as BKK1/SERK4, are recruited to FLS2 complex leading to rapid phosphorylations (Chinchilla *et al.*, 2007; Heese *et al.*, 2007). BAK1 directly phosphorylates BIK1 that is immediately released from FLS2-BAK1 complex and activates MTI signaling (Fig. 9; Lu *et al.*, 2010). FLS2 was also shown to form FLS2-FLS2 dimers, but its role in flg22 binding and FLS2 activation is not yet clear (Sun *et al.*, 2012).

Flg22-induced early signaling include plasma membrane depolarization associated with changes in ion fluxes and extracellular alkalinization, ROS production (Felix *et al.*, 1999), MAPK and CDPK activation (Asai *et al.*, 2002; Ichimura *et al.*, 2006; Boudsocq *et al.*, 2010) that lead to transcription of defense-related genes through WRKY TFs WRKY22/29 and WRKY25/33 (reviewed in Segonzac and Zipfel, 2011). The defense program includes upregulation of PR genes,

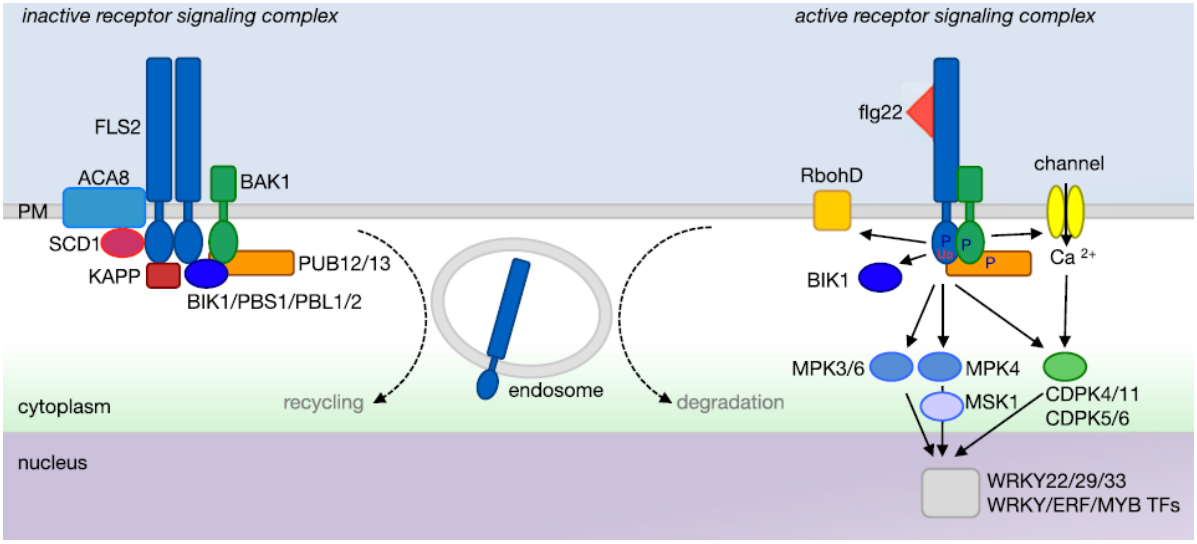

Figure 9. Schema of flg22-FLS2 signaling pathway in Arabidopsis.
In the absence of ligand, FLS2 can form homodimeric complexes and interact with proteins SCD1 and receptor-like cytoplasmic kinases (RLCK) BIK1 and PBLs. Nonactivated FLS2 is constitutively recycled between the plasma membrane (PM) and endosomes. Upon flg22 binding, FLS2 associates almost instantaneously with BAK1 to form FLS2-BAK1-BIK1 complex. Rapidly, multiple phosphorylation events occur on RLK kinase domains. BAK1 directly phosphorylates BIK1 that is immediately released from FLS2-BAK1 complex and activates Ca^{2+} channels, RbohD NADPH oxidase to generate oxidative burst, downstream MAPK cascade (MPK 3/6, MPK4, MSK1) and Ca^{2+} dependent protein kinases (CDPKs 4/11 and 5/6) that are involved in the activation of transcription factors (TFs) and the consequent induction of defense gene expression. Activated FLS2 is then internalized into endosomes and degraded. The FLS2 pathway is negatively regulated by phosphatases (KAPP) and ubiquitin ligases (PUB12/13). From Robatzek and Wirthmueller (2012). PM: plasma membrane, ACA8: Arabidopsis-autoinhibited Ca^{2+}-ATPase, PBS1: AvrPphB Susceptible 1, SCD1: stomatal cytokinesis-defective 1

callose deposition, increased ET and SA production and stomatal closure to prevent bacteria entry (Felix *et al.*, 1999; Gomez-Gomez *et al.*, 1999; Zipfel *et al.*, 2004; Melotto *et al.*, 2006). Evidence was brought that early flagellin signaling is split in two separate branches: one leading to MAP kinase activation and the other to CDPK-mediated ROS production (Fig. 9; Boudsocq *et al.*, 2010; Segonzac *et al.*, 2011; Xin *et al.*, 2012). Another hallmark of flg22-triggered responses is the Arabidopsis seedling growth inhibition (Gomez-Gomez *et al.*, 1999). FLS2 pathways seem to be conserved between plant species as demonstrated by the successful transfer of the FLS2 receptor from tomato or rice to Arabidopsis or from tomato to *N. benthamiana* (Robatzek *et al.,* 2007; Takai *et al.*, 2008; Mueller *et al.*, 2012).

2.1.3 FLS2/flg22 signaling regulation

The FLS2 signaling is regulated at several levels. i) The *FLS2* transcription is under the direct control of EIN3 and EIL1, two ethylene-dependent TFs (Boutrot *et al.*, 2010). As FLS2 triggers ET production, the FLS2 signaling itself autoregulates *FLS2* transcription *via* a positive feedback loop (Boutrot *et al.*, 2010). The level of *FLS2* transcript impacts heavily the intensity of flg22 responses (Gomez-Gomez and Boller, 2000; Vetter *et al.*, 2012). ii) The FLS2 kinase domain associates with the protein phosphatase KAPP (kinase-associated protein phosphatase), which prevents flg22 binding and keeps FLS2 signaling switched off (Fig. 9; Gomez-Gomez *et al.*, 2001). Then, once activated, the intensity of flg22/FLS2 signaling is kept in check by negative regulation executed by different mechanisms; iii) plant U-box E3 ligases PUB12 and PUB13 ubiquitinate activated FLS2, which, in turn, triggers FLS2 degradation and attenuates immunity (Lu *et al.*, 2011); iv) FLS2 is also regulated by subcellular compartmentalization. Activated FLS2 that binds flg22 undergoes internalization (Fig. 9) and is degraded afterwards (Robatzek *et al.*, 2006; Beck *et al.*, 2012). In contrast, non-activated FLS2 is constitutively recycled between the plasma membrane and endosomal compartments (Beck *et al.*, 2012).

2.1.4 FLS2 protein structure

FLS2 contains the serine/threonine kinase of the non-RD type that harbors Cys-Asp in the catalytic activation loop. The kinase activity was shown crucial to mediate flg22 signaling (Bauer *et al.*, 2001; Gomez-Gomez *et al.,* 2001). A kinase dead mutation *fls2-17* (G1064R) not only abolished flg22 responsiveness but also flg22 binding and the level of FLS2 protein, indicating that kinase activity may be required for FLS2 turnover (Gomez-Gomez *et al.,* 2001; Robatzek *et al.*, 2006). Mutations in serine/threonine residues at potential phosphorylation sites in the kinase domain or the juxtamembrane regions affected flg22 responses (Robatzek *et al.*, 2006).

As observed from the electrophoretic mobility, the native FLS2 is a glycosylated protein (Chinchilla *et al.*, 2006; Haweker *et al.*, 2010). Twenty N-linked glycosylation sites with NxS/T

motifs are predicted in its LRR domain and one in C-terminal region of the LRR domain (LRRCT, Fig. 8A; Haweker *et al.*, 2010). The N-glycosylation takes place in the endoplasmic reticulum (ER) and was shown to be required for correct protein folding of different receptors (Sun *et al.*, 2012). It is also critical for the functionality of receptors EFR (Nekrasov *et al.*, 2009; Sun *et al.*, 2012) or the R-protein Cf-9 (van der Hoorn *et al.*, 2005); however, N-glycosylation contributes only weakly if at all to the FLS2 function (Sun *et al.*, 2012).

The conserved cysteine pair (C61 and C68) in the LRRNT of FLS2 also appears to be required for the FLS2 quality control (Sun *et al.*, 2012). Mutation of Cys led to the retention of FLS2 in ER, dramatically decreased FLS2 abundance and affected flg22 signaling (Sun *et al.*, 2012).

2.1.5 Crosstalk with brassinosteroid signaling and other MAMP signaling pathways

BAK1, the regulator of FLS2-mediated responses, form receptor complexes with several other LRR-PRRs, such as EFR, Ve1, XA21, but not chitin receptors, and is required for triggering the downstream signaling cascade (Fradin *et al.*, 2011; Roux *et al.*, 2011; Park *et al.*, 2013). BAK1 is also critical for the restriction of bacterial and oomycete infections (Heese *et al.*, 2007; Roux *et al.*, 2011). Furthermore, BAK1 is involved in the brassinosteroid (BR) signaling (Li *et al.*, 2002). BR promotes cell elongation and division, stimulates flowering. BR is recognized by the LRR-RLK Brassinosteroid Insensitive 1 (BRI1; He *et al.*, 2000), which forms a ligand-dependent heterodimer with BAK1 (Li *et al.*, 2002) leading to the activation of BIK1 (Lin *et al.*, 2013). It was shown that the BR-mediated growth inhibits innate immune signaling initiated by flg22, EF-Tu or chitin, but independently and downstream from BAK1 (Albrecht *et al.*, 2012). It seems that the cross-regulation is finely tuned at the level of BIK1, the chief kinase executing activation of signaling initiated by distinct MAMPs but also by BR (Lin *et al.*, 2013). This kinase undergoes different phosphorylation events specific to the given receptor complex upstream (Lin *et al.*, 2013).

2.1.6 FLS2 polymorphism: ligand specificities

Plant species are generally sensitive to flg22 (Felix *et al.*, 1999; Albert *et al.*, 2010), although with species-characteristic traits that can differ in sensitivity to flg22-derived peptide variants (Felix *et al.*, 1999; Bauer *et al.*, 2001; Robatzek *et al.*, 2007). Most of the structure-function studies investigating principles underlying differences in flg22 sensitivity were carried out in Arabidopsis and tomato. One of the first observations was that the perception system in tomato is more efficient and recognizes smaller parts of flg22 peptide than Arabidopsis (Felix *et al.*, 1999; Meindl *et al.*, 2000). Flg15, the shorter flg22 epitope variant lacking the first 7 N-terminal amino

acid residues, is still highly active in tomato and *N. benthamiana* but it is about a 100 fold and 30 fold less active agonist in Arabidopsis and tobacco, respectively (Felix *et al.*, 1999; Bauer *et al.*, 2001; Robatzek *et al.*, 2007). Overexpression of AtFLS2 in tomato cells led to the gain of Arabidopsis-type flg22 perception showing that ligand specificities can be transferred only with FLS2 receptor (Chinchilla *et al.*, 2006). It was shown, that this diversity in flg22 perception is caused by the allelic diversity of FLS2, and more precisely of the LRR ectodomain (Dunning *et al.*, 2007; Mueller *et al.*, 2012). It appears that LeFLS2 possesses LRRs 7-10 with higher affinity to flg22 core sequence than AtFLS2 (Mueller *et al.*, 2012), which could explain why tomato does not require the N-ter of flg22 for FLS2 activation. Several studies also indicated that upon flg22 perception in tomato, the ligand is irreversibly "locked" in the LeFLS2 binding site (Meindl *et al.*, 2000; Chinchilla *et al.*, 2006). In contrast, stimulation of AtFLS2 with flg22 exhibits a weaker ligand affinity and receptor locking leading to the reversibility of flg22 binding (Bauer *et al.*, 2001; Chinchilla *et al.*, 2006). Therefore, tomato FLS2 is more tolerant to variations in the C_{ter} of flg22, whereas its mutations are critical for flg22 agonist activity in AtFLS2 (Mueller *et al.*, 2012).

The allelic variations of FLS2 between cultivars/ecotypes also include wild-type null mutations. For example, Arabidopsis ecotypes Wassilewskija (Ws-0) and Cape Verde Islands (Cvi-0) express a non-functional C-terminally truncated version of AtFLS2 (Dunning *et al.*, 2007).

In rice, flg22 acts as a relatively weak MAMP. Neither flg22, neither flagellin of *P. syringae* pv *tabaci* triggered a detectable alcalinization in rice cell suspensions (Felix *et al.*, 1999). Since, Takai and colleagues reported flg22 responsiveness in rice; however the classical flg22 (from *P. aeruginosa*) and flg22 derived from the incompatible strain *Pseudomonas avenae* induced only weak immune responses compared to the effect of purified full-length flagellin from *P. avenae* (Takai *et al.*, 2008). The low sensitivity of rice to flg22 might also be due to low levels of the OsFLS2 protein. Indeed, a higher sensitivity to flg22 was acquired when OsFLS2 was stably overexpressed in rice cells (Takai *et al.*, 2008).

2.2 Extra-flg22 flagellin recognition

2.2.1 flgII-28: a novel flagellin epitope for plants?

Recently, an additional perception system for flagellin was described in tomato (Cai *et al.*, 2011; Clarke *et al.*, 2013). Besides flg22, tomato can also recognize flagellin *via* the flgII-28 epitope. FlgII-28 lies in a close proximity of the flg22 epitope within the N-terminal D1 domain of flagellin (codons 84-111), partly overlapping with the epitope recognized by animals (§2.3). FlgII-28 peptides derived from *P. syringae* pv *tomato* (*Pto*) strains are biologically active only in a number of Solanaceae species, such as cultivated and wild tomato (*S. lycopersicum* and *S. peruvianum*), potato (*S. tuberosum*) and pepper (*Capsicum annuum*), but not in *N. benthamiana*,

tobacco or Arabidopsis (Clarke *et al.*, 2013). FlgII-28 epitopes are conserved within *P. syringae* pathovars but not in all phytopathogens.

For a given *Pto* strain, the eliciting activity of derived flgII-28 and flg22 peptides appears to be similar (Clarke *et al.*, 2013). However, the biologic importance of flgII-28 perception is not known. In tomato, Felix and colleagues showed that flg15-Δ5, the flg22 binding site antagonist, completely blocked the eliciting activity of the purified flagellin or boiled extracts of *Pto*, but also of other bacteria (Felix *et al.,* 1999). The receptor to flgII-28 is yet unknown. The FLS2 heterologous expression in Arabidopsis and silencing experiments in tomato showed that LeFLS2 is not the receptor required for the flgII-28-triggered responses (Clarke *et al.*, 2013).

2.2.2 Flagellin glycosylation

Flagellins of some bacteria (*P. aeruginosa* and *syringae*, *Campylobacter jejuni* or *Helicobacter pylori*) are glycosylated. Glycosylation stabilizes the filament structure and lubricates the flagellum rotation (Taguchi *et al.*, 2008). The glycan moieties are O-linked to the flagellin protein *via* Ser or Thr residues (Takeuchi *et al.*, 2003; Taguchi *et al.*, 2008). The pattern and the role of glycosylation in the flagellum function depend on the bacterial strain.

It was shown that plants can detect glycosylated patterns on flagellin. Purified flagellins of *P. syringae* pv *glycinea* and *tomato* (*Pto*) triggered HR on non-host tobacco plants, while flagellin of pathogenic *P. syringae* pv *tabaci* did not cause HR on tobacco, its natural host (Taguchi *et al.*, 2003). Similarly in rice, flagellin from a rice-incompatible strain of *P. avenae* induced immune responses, including cell death, while the flagellin from the compatible strain was not recognized (Che *et al.*, 2000; Takai *et al.*, 2008). This differential eliciting activity was not due to the flg22 recognition, as the protein sequences were totally identical (Taguchi *et al.*, 2003; Takai *et al.*, 2008). Glycosylation appears to be the reason of this different recognition. Mutants of *P. syringae* pv *glycinea* (pathogenic on soybean) with non-glycosylated or weakly glycosylated flagellins were altered in the host specificity and could infect tobacco, naturally a non-host plant (Takeuchi *et al.*, 2003).

2.3 Flagellin/TLR5 perception in animals

Flagellin acts as an important MAMP in animal innate immunity, particularly for human epithelial cells (Zeng *et al.*, 2003). Flagellin is recognized and directly bound by the LRR-RLK Toll-Like Receptor 5 (TLR5; Hayashi *et al.*, 2001; Smith *et al.*, 2003; Yoon *et al.*, 2012). The recognition site lies mainly in the N-terminal D1 domain (Andersen-Nissen *et al.*, 2005; Yoon *et al.*, 2012). Two TLR5 receptors bind two flagellin molecules, forming a 2:2 complex (Yoon *et al.*, 2012). Also the C-terminal D1 domain as well as D2 and D3 domains of flagellin were shown to contribute to its recognition by TLR5 (Smith *et al.*, 2003). The D0 domain contributes to the

activation of TLR5 signaling (Yoon *et al.*, 2012). It thus seems that a specific flagellin conformation is required for proper TLR5 signaling (Smith *et al.*, 2003).

TLR5 dimerization induces a TLR-specific activation of the adaptor Myeloid Differentiation Factor 88 (MyD88; Hayashi *et al.*, 2001). Also a signaling complex composed of the Interleukin-1 Receptor-Associated Kinase 1 (IRAK1), the TNF Receptor Associated Factor (TRAF6) and the IκB kinase (IKK) is required for the activation of the proinflammatory transcription factor Nuclear Factor (NF)-κB. Activated immune responses consist of production of proinflammatory cytokines, antimicrobial compounds, recruitment of phagocyting cells at sites of injury and triggering an adaptive immunity (Hayashi *et al.*, 2001; Pasare and Medzhitov, 2004). Species-specific differences in flagellin recognition were observed between human and mouse (Hayashi *et al.*, 2001). TLR5 polymorphism in humans correlates with the susceptibility to *Legionella pneumophila* infection (Hawn *et al.*, 2003).

Flagellin can be also recognized intracellulary. In macrophages, flagellin is sensed by the inflammasome, a large cytoplasmic inflammatory complex, assembled by the Nucleotide-binding Oligomerization Domain (NOD)-like receptor protein NLRC4 (Zhao *et al.*, 2011).

While most bacteria express only one form of flagellin (*fliC*, monophasic), some animal associated-bacterial strains, such as some serovars of *Salmonella enterica*, possess extra structural genes for flagellin (*fljB*/*fljA* or *flpA*) and can alternate expression of two (biphasic) or rarely three (triphasic) forms of flagellins. This switch is termed as a phase variation and can contribute to bacterial virulence (Ikeda *et al.*, 2001).

3 The flagellin perception upon plant-bacteria interaction

3.1 Evasion of flagellin-mediated immunity

As flagellin immunogenicity betrays bacteria aiming to colonize plant tissues, different strategies have been evolved to avoid this detection.

Effectors can suppress FLS2 signaling

FLS2 signaling can be targeted by bacterial effectors. *P. syringae* secretes effectors AvrPto and AvrPtoB that target directly the FLS2 protein. In Arabidopsis, the E3 ubiquitin ligase AvrPtoB ubiquitinylates the FLS2 kinase domain as a strategy for FLS2 degradation and elimination from the cell surface (Gohre *et al.*, 2008). Also, AvrPto binds the kinase of AtFLS2 or LeFLS2, inhibiting activation of downstream MTI (Xiang *et al.*, 2008). The effector HopQ1 secreted by *Pto* was shown to decrease the FLS2 expression (Hann *et al.*, 2013). Other effectors can target the central kinase BAK1 or attack components downstream of PRRs, including the MAPK cascade (Zhang et *al.,* 2007; Shan *et al.*, 2008).

Mutations in the *fliC* gene

To reduce or completely evade MTI, some pathogens evolved mutations in *fliC,* at the sites recognized by host immune systems. The single nucleotide polymorphism (SNP) standing for the recent adaptations of the pathogen can be identified by sequencing strains and isolates within a given pathovar (Cai *et al.*, 2011). Such a study on different *Pto* strains revealed SNPs within the flg22 epitop of the *fliC* gene (Cai *et al.*, 2011). Compared to the ancestral allele, the evolutionary novel *flg22* allelles triggered weaker MTI in tomato and potato but the difference in eliciting activity of alleles was highly dependent on host species (Cai *et al.*, 2011; Clarke *et al.*, 2013). Similarly, SNPs were also found within the newly discovered flgII-28 epitop (Cai *et al.*, 2011). Over the last thirty years, the ancestral *flgII-28* allele almost completely disappeared from the worldwide population of *Pto* and was replaced by a novel less eliciting variant (Cai *et al.*, 2011). Interestingly, the genetic diversity in *Pto* strains and isolates show rather higher frequency of mutations in flgII-28 than in flg22 (Cai *et al.*, 2011). From the evolutionary point of view, it seems that flagellin-triggered host immunity is disturbing even for highly virulent pathogens such as *Pto*.

Mutation within the flg22 epitope can even lead to complete MTI evasion. For pathogens, such as *X. campestris* pv *campestris* (*Xcc*), co-evolving with *Brassicaceae*, a single amino acid polymorphism in flg22 (D14G) can completely abolish the Xcc flagellin eliciting activity, as observed in Arabidopsis (Sun *et al.*, 2006). *Pseudomonas cannabina* pv *alisalensis* (*Pcal*) ES4326 also possesses a divergent flg22 epitope. The flg22 peptide derived from *Pcal* not only lacks eliciting activity in Arabidopsis or tomato, but may act as an antagonist of FLS2 signaling in tomato. Pretreatment with flg22-ES4326 led to increased *Pto* growth in tomato (Clarke *et al.*, 2013).

The flg22 epitopes derived from *A. tumefaciens*, *Sinorhizobium meliloti* and *R. solanacearum* flagellins are highly divergent and are not recognized by Arabidopsis and tomato (Felix *et al.*, 1999; Bauer *et al.*, 2001; Pfund *et al.*, 2004). The flagellin of *S. meliloti* is also not recognized in the host legume *Lotus japonicus* (Lopez-Gomez *et al.*, 2012). Both *A. tumefaciens* and *S. meliloti* flagellins possess compensatory mutations to preserve motility (Andersen-Nissen *et al.*, 2005), as flagellum act as a virulence factor for both bacteria.

Concerning human immunity, ε-proteobacteria including the important pathogens *H. pylori* or *C. jejuni* evade TLR5 recognition by mutating the entire flagellin recognition site (Andersen-Nissen *et al.*, 2005).

Reduced flagellin content and flagella shedding

Bacterial motility is important primarily at early stages of infection. At later stages, bacteria colonizing plants or animals may lose motility and shed or degrade their flagella (Drake and Montie, 1988; Hatterman and Ries, 1989). Bacteria can regulate their flagellin biosynthesis in response to different environmental conditions and the localization within the host tissue (Ramos

et al., 2004). Bacteria can even block the flagellin immunogenicity; they produce proteases that specifically cut monomeric flagellin to release inactive peptides into the environment (Bardoel *et al.*, 2011).

3.2 The role of FLS2-mediated sensing

The significance of flagellin perception for the plant immunity was mainly studied in Arabidopsis upon infection with *P. syringae* (notably *Pto*) and *Xcc.* The knowledge of flagellin involvement in the interactions with plant-associated beneficial bacteria is scarce.

Pseudomonas syringae* pv *tomato

Pto causes bacterial speck of tomato, a worldwide economically important disease. *Pto* is a foliar pathogen colonizing mesophyll cells after the entry through stomata or wounds. The *Pto* pathogenicity relies on TTSS-delivered effectors and toxins, such as coronatine, disrupting the hormonal balance (Zeng and He, 2010). *Pto* can also infect Arabidopsis, although it does not naturally infect *Brassicaceae.*

The FLS2-mediated sensing of flagellin is an important security point to detect and control invasion of *Pto* DC3000 in Arabidopsis leaves (Zipfel *et al.*, 2004; Zhang *et al.*, 2007; Xiang et al., 2008; Clay *et al.*, 2009; Zeng and He; 2010) and *N. benthamiana* (Kvitko *et al.*, 2009), where the loss of FLS2 causes enhanced bacterial growth. Similarly, *NbFLS2* silencing led to enhanced growth of non-pathogenic, non-host strains of *Pto* and even the compatible virulent strain of *Pta* (Hann and Rathjen, 2007). Several studies have shown that the enhanced susceptibility of the *fls2* mutant towards *Pto* was observed when plants were infected by inoculum spray or dipping, but not with apoplast-infiltrated inoculum, suggesting that flagellin perception restricts bacterial invasion at an early step but does not play a major role in post-entry defenses in the apoplast (Zipfel *et al.*, 2004; Zeng and He, 2010). In Arabidopsis, FLS2 was shown to play an essential role in mediating the stomatal closure during the initial *Pto* DC3000 invasion through stomata (Zeng and He, 2010). Likewise, the pretreatment with flg22 was effective to restrict *Pto* infection (Zipfel *et al.*, 2004; Sun *et al.,* 2006). However, we have to keep in mind that flg22 is not the only active MAMP in crude bacterial extracts of *Pto* (Zipfel *et al.*, 2004).

Xanthomonas campestris* pv *campestris

Xcc causes black rot, the most important bacterial disease of *Brassicaceae*/crucifers, including Arabidopsis. *Xcc* is a vascular pathogen; thus it enters the plant *via* the hydathodes, specialized pores at leaf margins, enabling a direct access to xylem and a systemic host infection.

It was shown that for *Xcc*, the increase in strain virulence correlates with the loss of eliciting activity of crude extracts or purified flagellins. Pretreatment of Arabidopsis leaves with purified eliciting flagellins of *Xcc* constrained growth of both *Pto* and *Xcc* pathogens (Sun *et al.*,

2006). However flagellin turned out not to be the main eliciting determinant of *Xcc* (Sun *et al.*, 2006). Moreover, possessing an eliciting flagellin did not limit the virulent isogenic *Xcc* strain in growth on Arabidopsis leaves, both in leaf mesophyll and hydathode/vascular colonization assays (Sun *et al.*, 2006). This suggests that *Xcc* might interfere with flagellin signaling by complementary inhibitory tools.

Sinorhizobium meliloti

Rhizobia are soil plant beneficial bacteria that colonize roots of legumes (*Fabaceae*) and form root nodules, where they fix nitrogen. During the establishment of beneficial associations, microbes are initially recognized as invaders by the host immunity. At later stages of the interaction, microbes modulate and minimize plant immune responses to allow tissue colonization (Zamioudis and Pieterse, 2012).

Defenses triggered by flg22 from *P. aeruginosa* delayed nodule organogenesis in the early symbiotic establishment between *L. japonicus* and *S. meliloti* (Lopez-Gomez *et al.*, 2012). However, no effect of flg22 was observed once the symbiosis was established, probably because of secreted MTI-suppressing factors (Lopez-Gomez *et al.*, 2012; Zamioudis and Pieterse, 2012). Interestingly, the *LjFLS2* expression was down-regulated in nodules (Lopez-Gomez *et al.*, 2012), eventhough the flagellin of *S. meliloti* is not immunogenic.

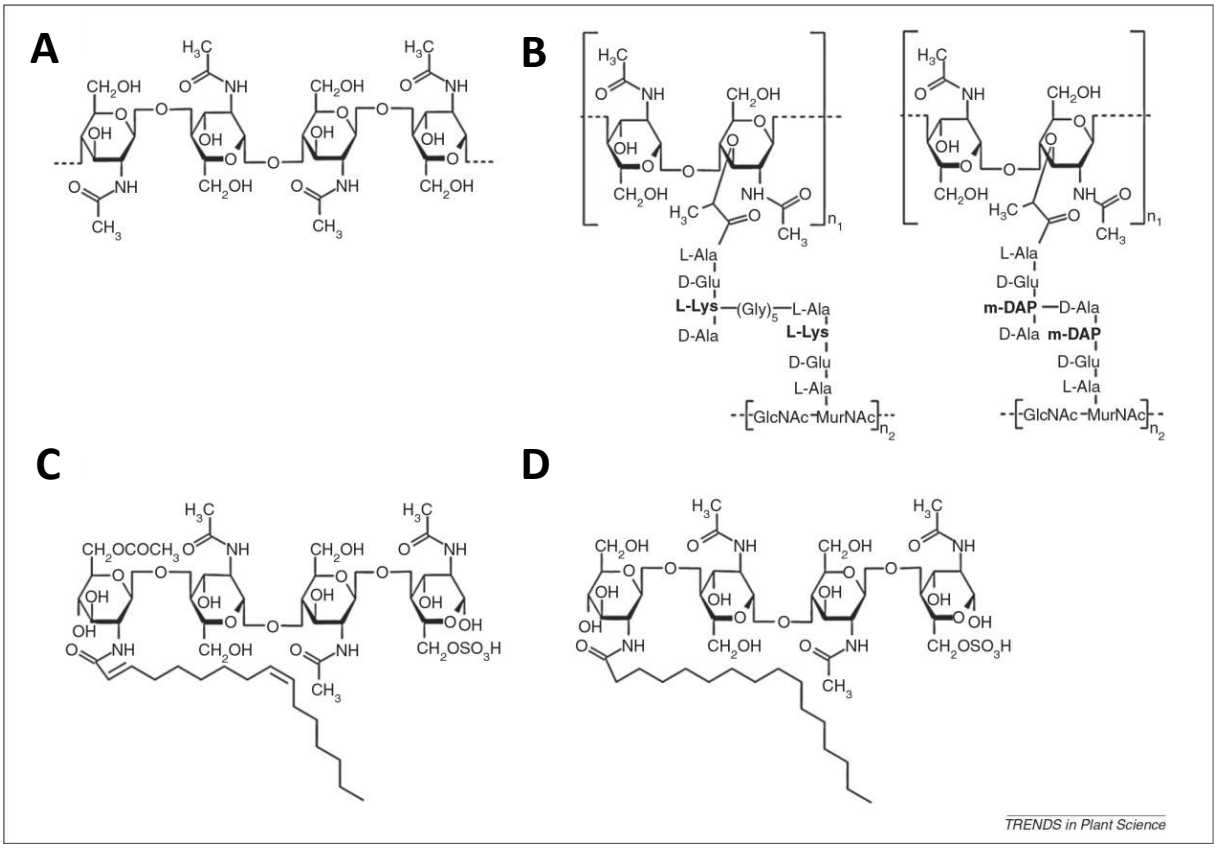

Figure 10. Structure of N-acetylglucosamine (GlcNAc)-containing ligands recognized by plant lysin motif (LysM) proteins.

A. Chitin, which is a GlcNAc homopolymeric chain. **B.** Peptidoglycan (PGN), which contains heteropolymeric chains of GlcNAc and N-Acetylmuramic acid crosslinked with a short peptide. The diaminopimelic acid (DAP)-type PGN is mainly found in Gram-negative bacteria, whereas the Lys-type PGN is mainly found in Gram-positive bacteria. **C.** Nod factors, in which three to five GlcNAc residues are N-linked to an acyl chain. As an example, the major Nod factor of *Sinorhizobium meliloti* is shown. **D.** Myc factors, in which up to five GlcNAc residues carry acyl and sulfate attachments. As an example, a Myc factor from *Glomus intraradices* is shown. From Gust *et al.* (2012).

III. Chitin-triggered immunity

1 Microbial GlcNAc-containing ligands

Many distinct microbial patterns are composed from N-acetylglucosamine (GlcNAc) units, including fungal chitin (Fig. 10 A) or bacterial peptidoglycan (Fig. 10 B) present in microbial cell walls, but also lipochitooligosaccharidic nodulation (Nod) or mycorrhizal (Myc) factors (Fig. 10 C, D) secreted by rhizobia and arbuscular mycorrhiza fungi of the *Glomeromycota* phylum, respectively.

Plants can specifically recognize these motifs by distinct LysM-containing receptor systems (Fig. 11). The chitin and PGN perception (Fig. 11 C, D) will be further presented in detail (§3.1-2 and §3.3). For the perception of lipochitooligosaccharides, we note several basic findings. Nod factors (NFs) are recognized by the legume *L. japonicus* LysM-RLKs NF Receptor 1 (LjNFR1) and LjNFR5 and their functional orthologs are found in *Medicago truncatula* (MtNFP and MtLYK3) or *Pisum sativum* (PsSym37, PsSym10, Fig. 11 A; reviewed in Gust *et al.*, 2012). Less is known about the perception of Myc factors. Nod Factor Perception (PaNFP), a LysM-RLK structurally similar to LjNFR5 and MtNFP5, recognizes Myc factors in *Parasponia andersonii*, the non-legume host (Fig. 11 B; reviewed in Gust *et al.*, 2012). Recognition of microbial Nod and Myc factors by host plants is required for the symbiosis establishment (Geurts *et al.*, 2005; Gust *et al.*, 2012).

2 Chitin, a structural component of fungal cell walls

Chitin, a linear polymer of β-1,4-linked GlcNAc (Fig. 10A), is the second most ubiquitous natural polysaccharide, after cellulose. Chitin is a major component of fungal cell walls, it is also present in the cuticle of non-vertebrates such crustacean shells, insect exoskeletons, in eggs of parasitic nematodes, protists, algae (Bueter *et al.*, 2013). Naturally occurring chitin is not a pure homopolymer, but it is rather a heteropolymer with varying percentage of deacetylated chitin (GlcN) (Merzendorfer, 2011). Chitosan, the deacetylated derivative of chitin produced by chitin deacetylases, is also naturally occurring polysaccharide, albeit less common. Chitosan can be notably found in some fungal species such as *Cryptococcus*. While chitin is neutral, chitosan is cationically charged (Merzendorfer, 2011; Bueter *et al.*, 2013).

Cell walls of filamentous fungi contain up to 20% of chitin that is mainly occurring in the inner cell wall, close to the plasma membrane. Chitin forms a network made of rigid structural fibrils that each contains around twenty tightly packed chitin chains. Chitin fibers are cross-linked with glucans for the cell wall reinforcement. Chitin biosynthesis from glucose requires at least 8

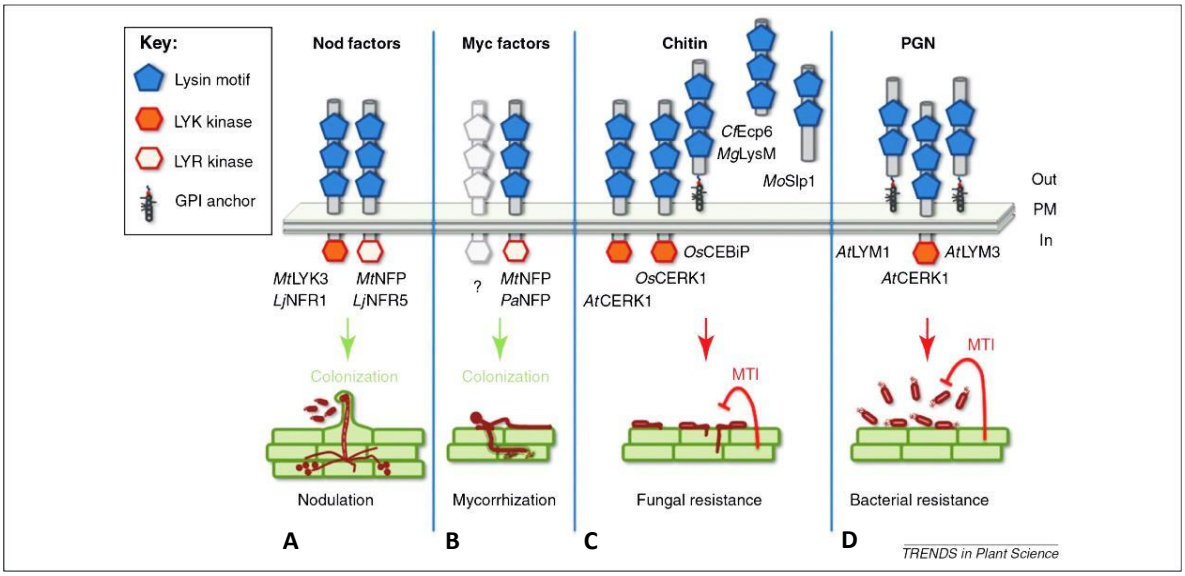

Figure 11. Plant LysM receptors.
Plant LysM receptors mediating perception of N-Acetylglucosamine (GlcNAc)-containing ligands are involved in the establishment of symbiotic interaction with rhizobacteria or mycorrhization or in the defense against both bacteria and fungi. **A.** Nodulation factors (NFs) from rhizobacteria are recognized by NF receptors (NFRs) leading to colonization and formation of a legume-specific root nodule. **B.** In arbuscular mycorrhiza, mycorrhization factors (MFs) are sensed by MF receptors leading to fungal penetration and establishment of arbuscules for nutrient exchange. **C., D**. Upon fungal or bacterial infection, chitin and peptidoglycan (PGN) are sensed by LysM-PRRs that initiate defense responses aiming to prevent further microbial spread. LysM-containing effectors (Ecp6, Slp1) compete with the chitin binding. From Gust *et al.* (2012). CERK1: chitin elicitor receptor kinase 1, CEBiP: chitin elicitor binding protein, GPI: glycosylphosphatidylinositol, LYK: LysM-RLK, LYR: nonactive LysM-RLK, NFP: Nod factor perception, PM: plasma membrane

enzymes. As the last step, chitin synthase polymerizes cytoplasmic stores of UDP-GlcNAc to make chitin chains that are secreted through plasma membrane into the extracellular space. There, chitin is finally organized into fibrils and deposited mainly at growth sites, such as hyphal tips. The chitin synthesis is tightly controlled at multiple levels during growth and development. For example, cell walls of spores contain lower amounts of chitin than hyphae. Both bacteria and fungi possess chitinases to degrade GlcNAc/GlcN, which allows the degradation of exogenous chitin but also the cell wall remodeling during autolysis of old hyphae (Merzendorfer, 2011; Hartl *et al.*, 2012). Chitinases cleave chitin polymers into chitooligosaccharides (COSs) of the minimal length $(GlcNAc)_2$, which can be further hydrolyzed by *N*-acetylglucosaminidases (Hartl *et al.*, 2012).

3 Chitin: elicitor of MTI in plants

Chitin is a main molecular pattern for most of fungi and it acts as a MAMP both in plants and animals. In plants, chitin elicits a variety of defense responses including the activation of the phenylpropanoid pathway or production of PR proteins such as peroxidases, chitinases or thaumatin-like proteins (Kaku *et al.*, 2006; Miya *et al.*, 2007; Boller and Felix, 2009). However, its eliciting capacity is highly dependent on the oligomer size. In general, the highest activity was reported for heptamers and octamers and little or no activity for shorter COSs (Hamel and Beaudoin, 2010).

While the mechanism of FLS2-mediated flagellin perception system is conserved in different plant species (Takai *et al.*, 2008; Boller and Felix, 2009), chitin recognition differs between rice, the monocot model, and the dicot model Arabidopsis. In rice, the crucial PRR mediating chitin binding is Chitin Elicitor-Binding Protein (CEBiP; Kaku *et al.*, 2006), whereas in Arabidopsis it is Chitin Elicitor Receptor Kinase1 (CERK1; Miya *et al.*, 2007).

3.1 OsCEBiP/OsCERK1 perception system in rice

Receptors

The mechanisms underlying the chitin perception and signaling were extensively studied in rice. CEBiP was the first plant chitin receptor discovered as a high-affinity binding protein from the plasma membrane of rice cells (Kaku *et al.*, 2006). OsCEBiP, a LysM-RLP with three LysM in the extracelular domain, is the major chitin-binding protein in rice (Kaku *et al.*, 2006; Hayafune *et al.*, 2014). The third LysM (LysM0) domain in the N-terminal part of OsCEBiP was reported only recently (Hayafune *et al.*, 2014). Biochemical and computational studies have shown that the central LysM (LysM1) and notably the I122 is required for chitin binding mediated *via* N-acetyl groups (Fig. 12A; Hayafune *et al.*, 2014). OsCEBiP exhibits high affinity for chitooligomers containing at least 7 GlcNAc residues (Hayafune *et al.*, 2014). Upon chitin binding, two OsCEBiP

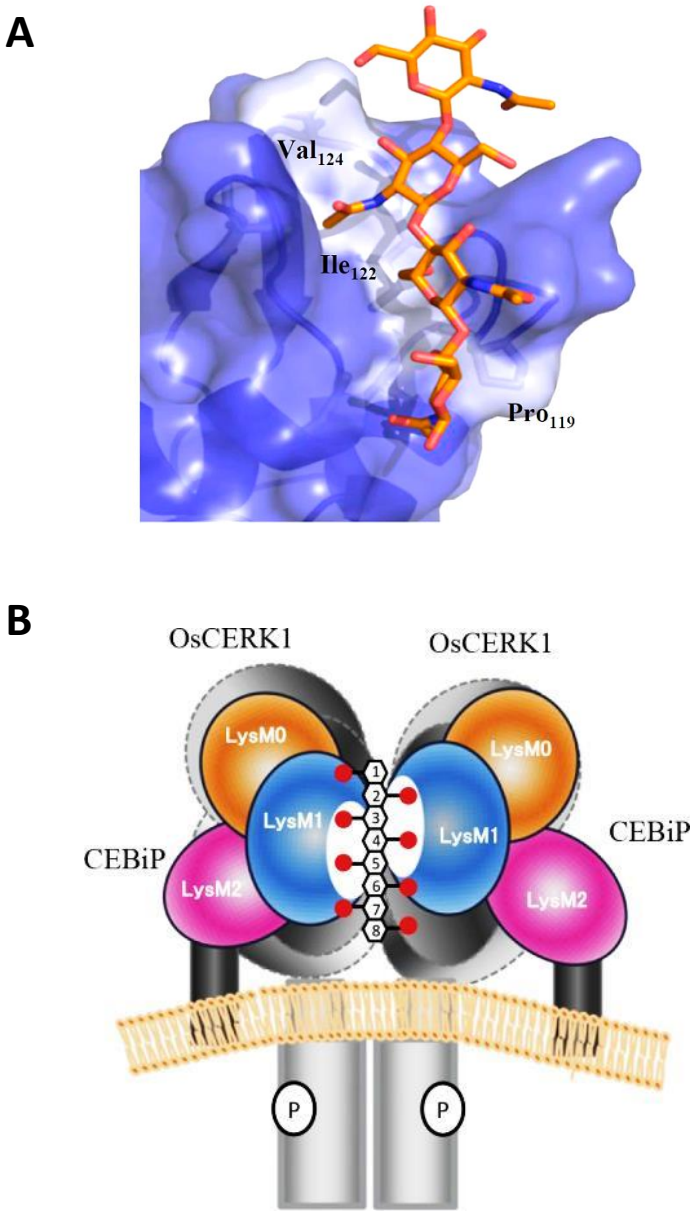

Figure 12. Model of the chitin perception system in rice constituted of CEBiP and OsCERK1. **A.** Modeling of binding of chitin oligomers to the central LysM1 domain of CEBiP containing the key I122 residue. **B.** Model of the activation of CEBiP-OsCERK1 complex by binding the $(GlcNAc)_8$ ligand. The receptor complex is activated in a sandwich-like manner. Upon ligand binding, CEBiP and OsCERK1 form heterodimers with two CEBiP receptors simoultaneously binding to the $(GlcNAc)_8$ chain *via* the LysM1 domain. From Hayafune *et al.* (2014).

receptors form dimers enclosing the chitin chain in a sandwich-like manner (Fig. 12B; Hayafune *et al.*, 2014). Plants silenced for *OsCEBiP* totally failed to respond to chitin (Kaku *et al.*, 2006; Kouzai *et al.*, 2014). OsCEBiP is a specific chitin receptor, as its gene knock down affected response to chitin, but not to PGN nor LPS (Kouzai *et al.*, 2014). It was also reported that the dimerization and chitin-induced ROS production was inhibited by $(GlcN\beta1,4GlcNAc)_4$, which is N-acetylated only on one side of the molecule (Hayafune *et al.*, 2014).

During chitin perception, OsCEBiP cooperates with OsCERK1, the closest homolog of AtCERK1 in rice, on the chitin perception (Shimizu *et al.*, 2010; Hayafune *et al.*, 2014). While OsCEBiP lacks an intracellular kinase domain, OsCERK1 is a LysM-RLK with a functional kinase capable of signaling initiation (Shimizu *et al.*, 2010). The ectodomain of OsCERK1 possesses one LysM domain but cannot bind chitin directly (Shimizu *et al.*, 2010). OsCERK1 is a less abundant membranous protein than OsCEBiP (Shimizu *et al.*, 2010). RNAi lines for *OsCERK1* were affected in chitin responses including the reduction by 90% in chitin-induced transcriptome (Shimizu *et al.*, 2010). OsCEBiP and OsCERK1 form transient hetero-dimers in chitin-treated rice cells (Fig. 12B; Shimizu *et al.*, 2010; Hayafune *et al.*, 2014). Therefore in rice, the receptor system for chitin signaling is built of two-components, OsCEBiP and OsCERK1, that are both required: the first one for chitin binding, the second for initiation of the signal transduction.

In wheat, another monocot crop, homologs of CERK1 and CEBiP are both required for chitin-induced defenses (Lee *et al.*, 2014), suggesting conserved CEBiP/CERK1 perception in monocots.

OsCERK1-mediated signaling

Recently, a considerable progress in unraveling the chitin signaling in rice has been made, notably by Japanese research teams (reviewed in Kawano and Shimamoto, 2013). After formation of the OsCEBiP/OsCERK1 complex, the OsCERK1 kinase rapidly activates the GDP/GTP Exchange Factor for OsRac1 (OsRacGEF1) by direct phosphorylation. OsRacGEF1 then directly activates a small GTPase OsRac1 (Akamatsu *et al.*, 2013) that initiates cellular signaling, including a MAPK cascade (OsMKK6, OsMPK1/3/6), which leads to phytoalexin and lignin biosynthesis (Kawano and Shimamoto, 2013). Genes encoding OsRacGEF1 and OsRac1 were previously shown to be involved in rice disease resistance against the rice blast fungus *M. oryzae* (Ono *et al.*, 2001; Suharsono *et al.*, 2002). Phosphorylation of MAPKs in rice seems to be crucial for biosynthesis of phytoalexins that are highly effective in defense against *M. oryzae* (Kishi-Kaboshi *et al.*, 2010).

Chitin downstream signaling also requires a receptor-like cytoplasmic kinase OsRLCK186 that is recruited to the plasma membrane and phosphorylated by OsCERK1 (Yamaguchi *et al.*, 2013). Similarly to OsRac1, the activated OsRLCK186 also triggers the MAPK cascade (Yamaguchi *et al.*, 2013). One of the effectors from *Xanthomonas oryzae* pv *oryzae*, Xoo1488,

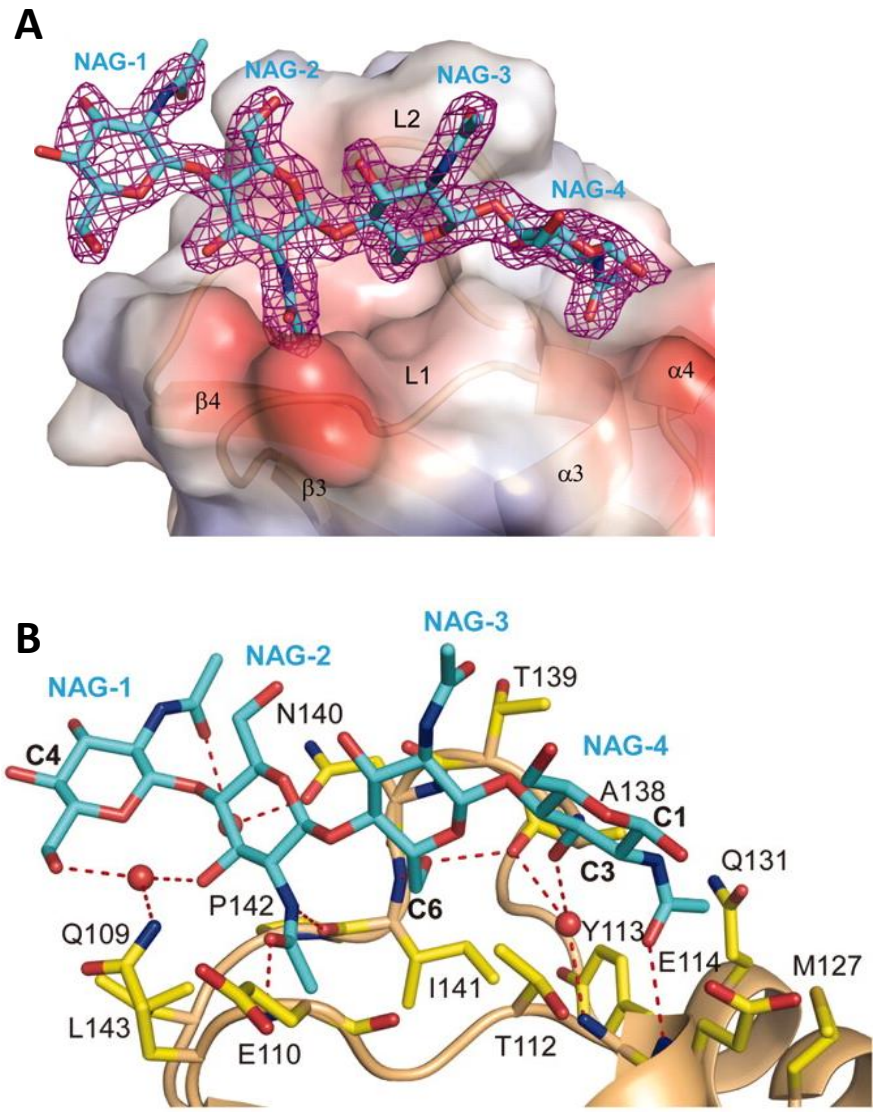

Figure 13. Mechanism of chitin oligomer recognition by CERK1 in Arabidopsis.
A crystal structure of CERK1 ectodomains complexed with chitin pentamer was solved. **A.** Four N-Acetylglucosamine residues (NAG 1-4) bind to a shallow groove on lysin motif 2 (LysM2) domain of CERK1 ectodomain. White, blue and red indicate neutral, positive and negative surfaces, respectively. **B.** Detailed interaction between chitin and the LysM2 domain of CERK1. The side chains of AtCERK1 are shown in yellow. Dashed lines and red spheres represent bonds and water molecules, respectively. C1, C3, C4 and C6 indicate carbon atoms in the chitin oligomer. D, Asp; E, Glu; G, Gly; I, Ile; L, Leu; M, Met; Q, Gln; N, Asn; R, Arg; P, Pro; T, Thr; Y, Tyr. From Liu *et al.* (2012b).

targets OsRLCK186 leading to suppression of chitin-induced responses and eventually increased susceptibility to the pathogen (Yamaguchi *et al.*, 2013). The *Xoo1488* expression in rice also abolished the PGN-induced responses, suggesting that the OsRLCK186-mediated signaling downstream of chitin and PGN perception are common (Yamaguchi *et al.*, 2013).

3.2 CERK1: perception system in Arabidopsis

In *Arabidopsis thaliana*, CERK1 is the key chitin binding and signaling component (Miya *et al.*, 2007; Wan *et al.*, 2008; Petutschnig *et al.*, 2010). AtCERK1 is a LysM-RLK with three LysM domains in the extracellular part of the protein. The knockout mutant *cerk1* lost its capacity to respond to chitin as neither oxidative burst, nor chitin-responsive genes were induced (Miya *et al.*, 2007; Wan *et al.*, 2008). AtCERK1 binds chitin directly without any requirement for interacting proteins and initiates signaling *via* its cytoplasmic Ser/Thr kinase domain (Miya *et al.*, 2007; Wan *et al.*, 2008; Iizasa *et al.*, 2010; Petutschnig *et al.*, 2010). Recognition of chitin by AtCERK1 is independent of BAK1 (Gimenez-Ibanez *et al.,* 2009)

Different studies have shown that AtCERK1 protein binds to $(GlcNAc)_5$ and longer COSs (Petutschnig *et al.*, 2010; Liu *et al.*, 2012b), with the highest affinity observed for the polymeric chitin (Iizasa *et al.*, 2010; Petutschnig *et al.*, 2010). The minimum $(GlcNAc)_5$ is required to induce AtCERK1 phosphorylation *in vitro* (Petutschnig *et al.*, 2010).

Since, a deeper insight into the chitin binding and the mode of AtCERK1 activation was brought in a recent study of Liu *et al.* (2012b) that solved the crystal structure of AtCERK1 ectodomain complexed with chito-pentamer $(GlcNAc)_5$. This study revealed that the three LysMs of AtCERK1 ectodomain are tightly packed in a globular structure forming a groove for GlcNAc anchoring and that the amino acid residues within the central LysM2 interact with three GlcNAc units (Fig. 13A; Liu *et al.*, 2012b). The N-acetyl moities play a key role in this interaction, as glutamic acid residues E110 and E114 of AtCERK1 engage hydrogen bonds with GlcNAc carbonyl oxygens and I141 binds to amide nitrogen of GlcNAc (Fig. 13B; Liu *et al.*, 2012b). Previously, it has been shown that all three LysMs are required for chitin binding, suggesting that ectodomain conformation might be required for optimal ligand fixation (Petutschnig *et al.*, 2010). The CxC motifs in inter-LysM spacers together with the N-terminal two cysteine residues form three pairs of disulfide bridges (Radutoiu *et al.*, 2003; Liu *et al.*, 2012b).

Liu *et al.* also showed that $(GlcNAc)_8$ induced AtCERK1 ectodomain dimerization, which was required for downstream signaling. Shorter COSs such as $(GlcNAc)_5$ were unable to induce dimerization of AtCERK1 ectodomain *in vitro* and inhibited $(GlcNAc)_8$-induced signaling (Liu *et al.*, 2012b). Authors also hypothesized that the clustering of two or more AtCERK1 proteins around a chitin chain of a sufficient length is required for signaling (Liu *et al.*, 2012b), possibly

explaining the higher affinity of AtCERK1 for polymeric chitin (Iizasa *et al.*, 2010; Petutschnig *et al.*, 2010).

3.2.1 AtLYM2-mediated chitin perception independently of AtCERK1

An intriguing question was whether a CEBiP-type receptor also takes part in the chitin perception in Arabidopsis. The closest OsCEBiP homolog, AtLYM2, is not required for chitin-triggered defense, as the *lym2* mutant was not affected in chitin responses (Wan *et al.*, 2012). Yet, AtLYM2 is biochemically functional as a chitin-binding protein in Arabidopsis (Shinya *et al.*, 2012), similarly to OsCEBiP in rice (Kaku *et al.*, 2006).

But seek and you will find. Recently it was shown that AtLYM2 is involved in chitin-induced plasmodesmata closure, independently of AtCERK1 (Faulkner *et al.*, 2013). This suggests two chitin perception systems in Arabidopsis, one which is AtCERK1-mediated, the other AtLYM2-mediated. The LYM2 also contributes to the *B. cinerea* disease resistance (Faulkner *et al.*, 2013). This regulation of plasmodesmata molecular flux seems therefore important in the chitin-triggered immunity.

3.3 Tight regulation of chitin and PGN perception

More and more evidence show that PRRs are in complex receptor associations to perceive MAMPs. Sensing ligands of distinct origins is linked and tightly regulated by common perception components. It seems now evident that chitin and PGN sensing shares co-receptors which are independent of signaling to LPS or flg22.

Arabidopsis

Apart from chitin recognition, CERK1 is also required for perception of peptidoglycan (PGN) (Gimenez-Ibanez *et al.*, 2009; Willmann *et al.*, 2011). PGN consists of heteropolymeric chains of GlcNAc and N-Acetylmuramic acid (MurNAc) crosslinked with a short peptide. PGN is structurally related to chitin and present in bacterial cell walls (Fig. 10B; Gust *et al.*, 2012). Loss of AtCERK1 caused increased susceptibility to bacterial infection caused by *Pseudomonas syringae* pv *tomato* DC3000 in Arabidopsis (Gimenez-Ibanez *et al.*, 2009). The AtCERK1 protein is also a target of the bacterial AvrPtoB effector that ubiquitinates the CERK1 kinase domain and targets it for degradation (Gimenez-Ibanez *et al.*, 2009). AtCERK1 cooperates with two LysM-RLPs, AtLYM1 and AtLYM3, that are glycosylphosphatidylinositol (GPI)-anchored proteins (Fig. 11D). AtLYM1 and AtLYM3 directly bind PGN (Willmann *et al.*, 2011), whereas AtCERK1 cannot (Petutschnig *et al.*, 2010; Willmann *et al.*, 2011). It was reported that AtLYM1 and AtLYM3 are not involved in chitin response (Wan *et al.*, 2012) and even the triple mutant *lym1*/*lym2*/*lym3* was not affected in the expression levels of chitin-responsive genes (Wan *et al.*, 2012).

In Arabidopsis, CERK1 has a dual perception role, mediating responses either to fungi (*via* chitin) or bacteria (*via* PGN). Similarly to BAK1 regulator for LRR-mediated MTI, CERK1 may function as a regulatory RLK for BAK1-independent LysM-mediated MTI.

Rice

Similarly, rice seems to engage overlapping perception components for chitin and PGN sensing as PGN pretreatment of rice cells attenuated the response to chitin and *vice versa* (Liu *et al.*, 2012a). Liu *et al.* (2012) also showed that the rice homologs of AtLYM1 and AtLYM3 (OsLYP4 and OsLYP6) also bind PGN and function as PGN receptors (Liu *et al.*, 2012a). Interestingly, OsLYP4 and OsLYP6 also bind chitin and are required for the chitin response (Liu *et al.*, 2012a). Silencing of OsLYP4 or OsLYP6 also led to compromised resistance to *X. oryzae* and *M. oryzae* infections (Liu *et al.*, 2012a). The role of OsCERK1 in PGN sensing in rice is still not clear.

3.4 Role of other LysM-RLKs (LYKs) in Arabidopis

The Arabidopsis genome encodes a total of five LysM kinases (AtLYK1-5) including CERK1/LYK1. It was suggested that AtLYK4, another LysM kinase (LYK), has an auxiliary role in chitin signaling (Wan *et al.*, 2012) and might form a receptor complex with AtCERK1 in Arabidopsis. AtLYK4 is induced by chitin treatment (Wan *et al.*, 2008) and can be pulled down from an Arabidopsis extract by chitin magnetic beads (Petutschnig *et al.*, 2010) suggesting chitin binding capacity. The Arabidopsis mutant *lyk4* was slightly reduced in Ca^{2+} signaling and induction of chitin-responsive genes (Wan *et al.*, 2012). The other three AtLYK proteins (AtLYK2, 3 and 5) are not required for chitin responses (Wan *et al.*, 2012). Nevertheless, AtLYK3 has been recently shown to act as a negative regulator of basal defense gene expression and resistance to fungal and bacterial infections in Arabidopsis. Indeed, *lyk3* mutants exhibited an enhanced disease resistance to *B. cinerea* and *Pectobacterium carotovorum* (Paparella *et al.*, 2014). Actually, AtLYK3 is required for ABA signaling, therefore assuring the crosstalk between immune responses and ABA (Paparella *et al.*, 2014). The roles of the other two LysM-RLK, AtLYK2 and AtLYK5 remain unknown.

3.5 Chitosan perception

Chitosan, a chitin derivative, is also a potent elicitor of plant immunity (Aziz *et al.*, 2006; Trotel-Aziz *et al.*, 2006; Povero *et al.*, 2011). For example in grapevine, chitosan elicits phytoalexins, chitinase and glucanase activities leading to resistance against *B. cinerea* and *P. viticola* (Aziz *et al.*, 2006; Trotel-Aziz *et al.*, 2006). AtCERK1 can weakly bind the partially deacetylated chitosan whereas it possesses no affinity for fully deacetylated chitooligomers

(Petutschnig *et al.*, 2010). Therefore, according to Petutschnig *et al.* (2010), the acetylation status of GlcNAc is crucial for CERK1 binding. Chitosan heptaose and octaose did not elicit ROS burst and cell death in rice, suggesting that also rice requires acetylated ligands for immune activation (Kaku *et al.*, 2006; Kishimoto *et al.*, 2010). The Arabidopsis c*erk1* null mutant lost its responsiveness to the partially deacetylated chitosan, as demonstrated by ROS burst and MAP kinase assays (Petutschnig *et al.*, 2010). In disagreement with these data, another study reported that the partially deacetylated chitosan induces an AtCERK1-independent defense signaling (Povero *et al.*, 2011). Therefore a discrepancy exists about the chitosan perception. The character of chitosan (degree of polymerization or acetylation) varies among different studies, which was shown as an important factor to affect chitosan activity (Iriti and Faoro, 2009). It is also speculated that chitosan may be active due to its positive charges which can interact with the negatively charged phospholipids, instead of a receptor-specific interaction (Bueter *et al.*, 2013).

3.6 Chitin perception by animals

Chitin is known to elicit proinflammatory responses in mammals (Lee *et al.*, 2008). However, studies on mechanisms underlying chitin perception in mammals are rather scarse, possibly because fungi are mainly plant pathogens. Three innate immune receptors, Toll-like receptor (TLR) 2, Dectin-1, and the mannose receptor, have been reported to mediate chitin recognition (Bueter *et al.*, 2013). The LRR-RLK Toll-like receptor 2 (TLR2) contributes to the chitin sensing by keratinocytes or macrophages (Lee *et al.*, 2008; Koller *et al.*, 2011). It was proposed that depending on their size, chitin fragments were recognized by distinct receptors leading to distinct immune response. While long chitin fragments were inert, the smaller ones induced proinflammatory cytokines with the smallest causing an anti-inflammatory response (Lee *et al.*, 2008).

Also chitosan activates animal immune system. In humans, chitosan is used as an adjuvant in vaccines to induce a robust antibody production and T-cell responses (Bueter *et al.*, 2013).

4 Role of chitin perception in plant immunity

Different studies show the importance of chitin perception in plant immunity to fungal infections. The Arabidopsis c*erk1* mutant displayed a partly impaired resistance during the interaction with an incompatible fungus *Alternaria brassicicola* and with a compatible fungus *Erysiphe cichoracearum* (Miya *et al.*, 2007; Wan *et al.*, 2008). However, the involvement of CERK1 in disease resistance is dependent on the type of fungi (Miya *et al.*, 2007). Also the knock down of *OsCEBiP* gene caused increased susceptibility to a weakly virulent strain of the rice blast fungus (*M. oryzae*; Kishimoto *et al.*, 2010; Kouzai *et al.*, 2014). HvCEBiP, the closest OsCEBiP orthologue in barley, is slightly involved in the resistance during the interaction with the

compatible fungus *M. oryzae* (Tanaka *et al.*, 2010). However, its involvement in chitin recognition has not been reported.

Fungi have developed different strategies to avoid chitin recognition and prevent antifungal responses. One frequent strategy is the secretion of LysM-containing effectors (Fig. 11C). *M. oryzae* secretes a LysM Protein (Slp1) that accumulates in the apoplastic space of rice tissues (Mentlak *et al.*, 2012). Slp1 sequesters chitooligosaccharides by direct binding to avoid host recognition (Mentlak *et al.*, 2012). *Cladosporium fulvum* secretes another LysM effector (Ecp6) that binds chitooligosacharides released from invading hyphae (de Jonge *et al.*, 2010). The fungal wheat pathogen *Mycosphaerella graminicola* evades chitin-initiated immunity by the means of Ecp6 homolog (Lee *et al.*, 2014). The effector Avr4 of *C. fulvum* inhibits the activation of chitin-mediated immunity by binding to chitin in fungal cell walls, thus preventing degradation by host chitinases (van Esse *et al.*, 2007). Homologs of Avr4 was also identified in other pathogenic fungi of the *Dothideomycete* class, including *Mycosphaerella fijiensis*, the pathogen of banana (Stergiopoulos *et al.*, 2010).

Some fungi, including *M. oryzae*, *Cochliobolus miyabeanus* and *Rhizoctonia solani*, mask cell wall surface with α-1,3-glucans, non-degradable by plants. This camouflage occurs specifically during plant invasion, as was shown in rice (Fujikawa *et al.*, 2012). It was reported that pathogens require production of these LysM proteins or the synthesis of α-1,3-glucans for their full pathogenicity (Fujikawa *et al.*, 2012; Mentlak *et al.*, 2012; Lee *et al.*, 2014).

Treatment with chitin reduced the susceptibility of rice to *M. oryzae* (Tanabe *et al.*, 2006). While the effect of chitin treatment on resistance remains rather mild, chitosan induces a strong resistance to fungal pathogens, in different plant species including grapevine (Benhamou *et al.*, 1994; El Ghaouth *et al.*, 1994; Trotel-Aziz *et al.*, 2006). However, besides its elicitor activity, chitosan possesses also antifungal properties by inhibiting mycelial growth and spore germination of various fungi (Benhamou *et al.*, 1994; El Ghaouth *et al.*, 1994; Trotel-Aziz *et al.*, 2006). A direct antifungal effect was not reported for chitin.

AIMS OF WORK

Although a dozen of MAMPs are known to elicit defense responses in grapevine, nothing is known about their perception systems. No PRRs have been identified in this crop. Nowadays, the recent sequencing of the grapevine genome (Jaillon *et al.*, 2007; Velasco *et al.*, 2007) facilitates the identification of candidate genes encoding putative receptors.

In this context, my study focused on MAMP perception, as a key part of MTI, in grapevine (*Vitis vinifera*). My thesis work has been performed in the frame of the European project "PRR-CROP" (ERA-NET Plant Genomics) coordinated by Dr. C. Zipfel. This collaborative project aimed to identify PRRs of important crops (barley, wheat, grapevine) and novel MAMPs from agriculturally important pathogens.

The main objectives were:

i) to assess the activity of typical MAMPs (such as flg22, elf18, pep-13, chitin and chitosan) in grapevine,

ii) to identify the putative cognate receptors for active MAMPs by an orthology based approach,

iii) to investigate their function by functional complementation in Arabidopsis mutants and reverse genetics in grapevine,

iv) to characterize the MAMP/PRR perception systems in grapevine (ligand specificities, expression profiles of receptors), and

iv) to investigate the role of a given perception system in the dialog with an encountered microorganism, *i.e.* its involvement in grapevine disease resistance.

The receptor identification work was done in collaboration with Drs. Freddy Boutrot, Lena Stransfeld and Cyril Zipfel from The Sainsbury Laboratory (Norwich, United Kingdom) that carried out the Arabidopsis transformations and mutant selection. The work on the interaction between grapevine/Arabidopsis - Burkholderia phytofirmans *was done in collaboration with Drs. Stephan Dorey and Olivier Fernandez from the University of Reims Champagne-Ardenne (Laboratoire Stress, Défenses et Reproduction des Plantes, Reims, France).*

MATERIALS AND METHODS

1 Materials

1.1 Grapevine materials

1.1.1 Cell suspensions

Grapevine cells (*Vitis vinifera* cv Gamay) were cultivated in Nitsch-Nitsch medium (Nitsch and Nitsch, 1969); 20 g l^{-1} sucrose, pH 5.5, Annex 1) on a rotary shaker (120 rpm) at 25°C and under continuous light (50 µmol m^{-2} s^{-1}). Cell suspension was subcultured every 7 days by transferring 30 ml of cell suspension into 70 ml of culture medium. Transformed grapevine cells (*V. vinifera* cv Gamay) expressing apoaequorin (pBIN19 *p35S::apoaequorin*) in the cytosol (Vandelle *et al.*, 2006) were cultivated in the same conditions except that the Nitsch-Nitsch medium was supplemented with 100 mg l^{-1} paromomycin. For all experiments, 7-day old cultures were diluted twice with new medium 24 h prior to use.

1.1.2 *In vitro* plantlets

Wild-type and transgenic grapevine *in vitro* plantlets (*Vitis vinifera* cv Pinot Noir PN40024) were micropropagated by nodal explants grown on McCown Woody Plant (WP) agar medium (Duchefa M0219; 15 g l^{-1} sucrose, 7 g l^{-1} agar, pH 6.2) in a climatic chamber at 25°C/22°C (day/night) under fluorescent light (125 µmol m^{-2} s^{-1}) with a photoperiod 16 h of light. Explants were first grown in Petri dishes (93 x 21 mm, Greiner) sealed with Parafilm on WP medium supplemented with charcoal 3 g l^{-1} and 6.5 g l^{-1} bactoagar (Difco). After 2 months, plantlet apexes were cut and transferred into tubes (25 x 150 mm, diameter x height) containing 15 ml of WP medium. The first transfer in a Petri dish improved the explants' vigour and the subsequent growth of the *in vitro* plantlets. Two month-old plantlets were used for generation of new explants or for experiments. The middle three leaves (non-senescent and adult) were used for bioassays.

In vitro plantlets (*V. vinifera* cv Chardonnay) were grown in the Murashige & Skoog (MS) agar medium (30 g l^{-1} sucrose, 8 g l^{-1} agar, pH 5.9) at 26 °C with a photoperiod of 16 h of light.

1.1.3 Plants

Grapevine (*V. vinifera* cv Marselan) herbaceous cuttings were grown in individual pots (7 x 7 x 8 cm) containing a mixture of peat and perlite (4/1, v/v) in a greenhouse. Growth conditions were 25 ± 4°C and 18 ± 7 °C (day and night, respectively), 16 h light period (artificial illumination was supplemented when the natural light was less than 200 µmol m^2 s^{-1}), hygrometry 50 ±10%. Plants were watered with a fertilizing solution (0.25% Topfert2 solution NPK 10-10-10 +

oligonutrients, Plantin, France). Plants were grown until they developed 6 – 8 leaves. The second and third youngest adult leaves from each plant were used for experiments.

1.2 Arabidopsis materials

1.2.1 Cell suspensions

Arabidopsis thaliana cells from ecotype Columbia (Col-0) were kindly provided by Pr. Jean-Pierre Métraux (University of Fribourg, Switzerland). Arabidopsis cells were cultivated in the same conditions as grapevine cells except that suspensions were subcultured every 7 days by transferring 5 ml of cell suspension into 100 ml of fresh liquid Linsmaier and Skoog medium (Duchefa L0230, 30 g l^{-1} sucrose, 0.5 mg l^{-1} NAA, 50 µg l^{-1} kinetin, pH 5.5). Eight-day old cell suspensions were used for experiments.

1.2.2 Plants

Arabidopsis (*A. thaliana*) plants from wild-type (WT) Col-0, mutants *fls2c* (SAIL_691C4, Basta resistance, T-DNA insertion in the FLS2 promoter; Zipfel *et al.*, 2004) and *cerk1-2* (GABI-Kat_096F09, sulfadiazine resistance, T-DNA knock-out mutant; Gimenez-Ibanez *et al.*, 2009), or transgenic lines *fls2/p35S::VvFLS2-GFP*, *cerk1-2/p35S::VvCERK1-GFP, cerk1-2/pLexA35S::VvCERKs-GFP* and *pPR1::GUS* were grown in Jiffy-7 peat pellets (Jiffy) in a controlled growth chamber under a 10/14 h day/night cycle at 20/18°C (70% relative humidity) with a light intensity of 175 µmol m^{-2} s^{-1} .

For the *in vitro* culture, Arabidopsis plants were grown on solid or in liquid half MS medium (Duchefa M0222; 5 g l^{-1} sucrose). Seedlings were grown at 22°C with a 16 h photoperiod at a light intensity of 100 µmol m^{-2} s^{-1}. *A. thaliana* seeds were sterilized by treating them for 1 min in a mix of 95% ethanol and 2% commercial bleach (9/1; v/v), supplemented with 0.01% Tween 20, followed by three quick washes with 99% ethanol and drying under the hood.

1.3 Microorganisms

1.3.1 Botrytis cinerea

Botrytis cinerea, strain B05.10, was cultivated at 20°C on malt-yeast agar medium (15 g l^{-1} malt extract, 5 g l^{-1} glucose, 1 g l^{-1} tryptone, 1g l^{-1} casein, 1 g l^{-1} yeast extract, 0.2 g l^{-1} RNA, 15 g l^{-1} agar). Conidia (5 x 10^4) were plated on an agar medium in Petri dishes that was kept for 5 days in the dark for mycelium development, then 5 days under 16 h photoperiod of near-UV light to induce sporulation. Conidia were collected with water, filtered through glass-wool to remove mycelia, counted and kept at 4°C prior to infection assays.

1.3.2 Plasmopara viticola

A *Plasmopara viticola* isolate collected in Burgundy in 2001 was maintained by successive infections on susceptible grapevine plants (*V. vinifera* cv Marselan) grown in greenhouse. To obtain sporangia, plants presenting "oil spot" symptoms (6-7 days) were placed in the dark overnight at 100% relative humidity. Sporangia were collected from the lower side of a sporulating leaf by using a brush, then suspended in distilled water to obtain a 1.10^4 sporangia ml^{-1} suspension for *P. viticola* subculture or experiments. Sporangia were used immediately for infection assays.

1.3.3 Burkholderia phytofirmans

B. phytofirmans strain PsJN expressing GFP (Sessitsch *et al.*, 2005) was grown in King's B liquid medium at 20°C and 150 rpm for 48 h. The inoculum of *B. phytofirmans strain* PsJN was produced as described by Theocharis *et al.* (2012). Briefly, bacteria were collected by centrifugation (3 000 g for 15 min), washed twice with phosphate buffered saline (PBS; 10 mM, pH 6.5) and suspended in PBS. The bacterial density was estimated by spectrophotometry (600 nm) and adjusted to 3×10^8 CFU ml^{-1} with PBS.

1.4 Elicitors

1.4.1 Peptides

Sequences of the flagellin-derived flg22 peptides from *P. aeruginosa* strain PAK (QRLSTGSRINSAKDDAAGLQIA), *X. campestris* pv *campestris* strain 305 (QRLSSGLRINSAKDDAAGLAIS), *B. phytofirmans* strain PsJN (TRLSSGKRINSAADDAAGLAIS) and *A. tumefaciens* strain C58C1 (ARVSSGLRVGDASDNAAYWSIA) were retrieved from UniProt database, purchased from Proteogenix (purity superior to 95%) and kindly provided by Drs. C. Zipfel and S. Dorey. Peptides elf18 (SKEKFERTKPHVNVGTIG) from *E. coli* and pep-13 (VWNQPVRGFKVYE) from *P. sojae* (Brunner *et al.*, 2002) were obtained from Drs. C. Zipfel and F. Brunner, respectively. Peptides were dissolved in sterile ultra-pure water, prepared as 1 mM and 100 µM aliquots and stored at - 20°C.

1.4.2 Oligosaccharides

The crab shell chitin NA-COS-Y (Lloyd *et al.*, 2014), obtained from Yaizu Suisankagaku Industry CO (Yaizu, Japan), was kindly provided by Dr. Chris Ridout. Chitin was dissolved in sterile ultra-pure water and prepared as 100 g l^{-1} aliquots. Chitosan polymer (≥75% deacetylated form of chitin; mean degree of polymerization (DP) > 500) was purchased from Sigma and

purified according to (Bhaskara *et al.*, 1998). Purified chitosan was dissolved in 50 mM HCl, pH was adjusted to 5.6 and aliquots of 1 g l^{-1} were prepared. Laminarin (Lam; β-1,3-glucan with a mean DP of 25-30), its shorter version (DP of 13), sulfated laminarin (PS3, degree of sulfation of 2.4) and oligogalacturonides (OG, mean DP of 9-20) were provided by Goëmar Laboratories. Laminarin in all forms and OG were dissolved in sterile ultrapure water (25 g l^{-1}). Aliquots were stored at -20°C.

1.4.3 Elicitor doses

For cell suspension treatments, 1 µM flg22, 1 g l^{-1} laminarin, 1 g l^{-1} chitin or 25 mg l^{-1} chitosan were applied, if not otherwise mentioned. For screening of MAMP responses in transgenic lines of *in vitro* plantlets, 500 nM flg22, 1 g l^{-1} chitin or 0.5 g l^{-1} OG were used. For protection assays performed on leaf discs from grapevine plants grown in the greenhouse (§ 2.6), the elicitor concentrations were 10 µM for flg22, 2.5 g l^{-1} for Lam and PS3, 1 g l^{-1} for chitin and 150 mg l^{-1} for chitosan. For these resistance tests, elicitors were dissolved in an appropriate surfactant (confidential) at 0.1% (v/v).

2 Methods

2.1 MAMP responsiveness in cells and *in vitro* plantlets

2.1.1 Cell culture equilibration for early signaling bioassays

To measure early signaling events, such as ROS production, variations in cytosolic Ca^{2+} concentrations ($[Ca^{2+}]_{cyt}$) and MAPK phosphorylation, cells were collected and washed three times with M10 buffer (175 mM mannitol, 0.5 mM $CaCl_2$, 0.5 mM K_2SO_4, 10 mM MES, pH 5.3) and suspended at 0.1 g fresh weight of cells (FWC).ml^{-1} in M10 buffer. For measurement of H_2O_2 production or MAPK phosphorylation, cells were equilibrated 1h (130 rpm, 25°C) before elicitor treatments. For $[Ca^{2+}]_{cyt}$ variations, washed cells were processed as described elsewhere (§ 2.1.3).

Arabidopsis Col-0 cells were washed with M10 pH 6.2, equilibrated 1h (130 rpm, 25°C) and used for measurements of H_2O_2 production.

2.1.2 Luminol-based oxidative burst analysis

After equilibration, cells were treated with elicitors or a control treatment. At a given time point post treatment, 250-µL cell aliquots were mixed with 300 µL of H50 buffer (50 mM HEPES, 175 mM mannitol, 10 mM $CaCl_2$, 0.5 mM K_2SO_4, pH 8.5) and 50µL of 0.3 mM luminol. Luminescence, expressed in relative luminescence units (RLU), was integrated over 10s by a luminometer (Lumat LB9507, Berthold Technologies) and was converted into nmol H_2O_2.g^{-1}

FWC, using a standard calibration curve obtained by addition of H_2O_2 in grapevine cell suspension aliquots. For dose response, oxidative burst was measured at 15 min post treatment or at maximal response. Oxidative burst in Arabidopsis cell suspensions was monitored using the same protocol as for grapevine.

The ROS production in Arabidopsis leaf discs was measured in two discs per plant from at least 6 plants. Leaf discs (4 mm diameter) were cut and floated on 100 µl ultrapure water in a 96-well plate overnight in darkness at room temperature. Then 16 h later, water was replaced with 100 µl of the reaction/elicitation mixture (60 µM luminol, 1 U horse radish peroxidase, elicitor) and the luminescence (RLU) was recorded every 90 s (integration over 1 s) and until 60 min, using a microplate luminescence reader (Mithras LB 940, Berthold Technologies).

For grapevine, at least 12 discs (4 mm diameter) from 3 leaves of 2 plants were vacuum-infiltrated with water and floated on 100 µl water in a 96-well plate overnight in darkness at room temperature. Then 16 h later, water was replaced with 100 µl of the reaction mix (60 µM luminol and 10 U horse radish peroxidase in H50 buffer, pH 8.5) and luminescence was counted as described for Arabidopsis leaf discs. Once ROS levels decreased to the basal level ≤ 80 RLU (~5 min), elicitor or water was added in each well and the luminescence was recorded every 90s and during a 60 min period.

2.1.3 Analysis of free cytosolic calcium concentration variation

Apoaequorin-expressing grapevine cells were suspended in M10 buffer (§2.1.1) and further incubated for 4h with 3 µM coelenterazine (130 rpm, 25°C, at dark) to perform the *in vivo* aequorin reconstitution before the elicitor treatments. Then, 250 µl cell aliquots were treated with elicitors and the emitted bioluminescence was recorded as RLU s^{-1} for 30 min using a luminometer. Remaining aequorin was discharged by automatic injection of 300 µl of lysis buffer containing an excess of Ca^{2+} (2M $CaCl_2$ in 20% ethanol (v/v)) and luminescence was recorded for another 5 min until values were within 1% of the highest discharge value. RLU values were converted into Ca^{2+} concentrations using the calibration equation $p([Ca^{2+}]_{cyt}) = 0.332588\ (-\log k) + 5.5593$, described in detail by Rentel and Knight (2004), where k is the luminescence counts per second/total luminescence counts remaining (Ranf *et al.*, 2008).

2.1.4 MAPK bioassay

Grapevine cells were first equilibrated (§2.1.1), then treated with elicitors or a control treatment. Aliquots of 1.5 ml were harvested at 0, 5, 10, 15, 30 and 60 min post treatment by filtration on GF/A filters, frozen in liquid N_2 and kept at -80°C prior to perform the protein extraction (§2.2.1) and MAPK detection (§2.2.4).

Leaves of *in vitro* grapevine plantlets were first vacuum-infiltrated with water then floated on water (lower leaf surface facing the solution) during 2 h before adding elicitor solutions. Treated leaves were collected into liquid N_2 at 15 min post treatment and kept at -80°C prior to perform the protein extraction (§2.2.2) and MAPK detection (§2.2.4).

2.1.5 Defense gene induction assay

For defense gene expression kinetics on grapevine cell suspensions, the cell culture density was adjusted to 0.1 g FWC ml^{-1} with sterile Nitsch-Nitsch medium 16 h prior to experiment. Otherwise, they were maintained under their culture conditions (25°C, continuous light, 120 rpm). Cells were then treated with elicitors or a control treatment and sampled under sterile conditions. Aliquots of 1 ml were harvested at indicated time points into liquid N_2.

Leaves of *in vitro* grapevine plantlets were floated on elicitor solutions with the lower leaf surface facing treatment in the growth climatic chamber (25°C). After 6 h of treatment, leaves were harvested into liquid N_2. For the basal level of *VvPRR* transcripts, leaves from 2-month old plantlets were frozen.

All harvested tissues were kept at -80°C prior to RNA extraction (§2.2.7) and qPCR (§2.2.8).

2.1.6 Cell death quantification

Cells were cultured in their culture medium as described for defense gene induction assays (§2.1.5). Cell viability was quantified by neutral red staining as a vital dye. Neutral red stains vacuoles of living cells, while those of dead cells are colourless (Naton *et al.*, 1996). After 24 h of treatment, 500 µl of cell aliquot (~ 50 mg cells) was washed twice with H50 buffer (§2.1.2, pH 7.5) and colored by 0.01 % neutral red (w/v). The viability was blindly evaluated on at least 500 cells per sample. The incubation of cells 3 min at 95°C served as a positive control of cell death.

2.2 Biochemistry, molecular biology and bioinformatics

2.2.1 Total protein extraction from grapevine cells and Arabidopsis

Samples of grapevine cells were ground in a mortar. Total proteins were extracted by adding 250 µl of the protein extraction buffer (50 mM HEPES-KOH pH 7.5; 10 mM EGTA, 10 mM EDTA, 1 mM Na_3VO_4, 50 mM β-glycerol phosphate, 10 mM NaF, 1 mM PMSF, 5 mM DTT, 5 µg ml^{-1} leupeptin, 5 µg ml^{-1} antipain) to 100 mg of ground frozen powder. After centrifugation (15 min, 10 000 g, 4°C), proteins in the supernatant were quantified by spectrophotometry with the Bradford's method (Bradford, 1976) using bovine serum albumin (BSA) as standard. Samples were stocked in Laemmli sample buffer (Laemmli, 1970) heated at

95ºC for 5 min prior to electrophoresis. Total proteins from Arabidopsis leaves were extracted with the same method.

2.2.2 Total protein extraction from *in vitro* grapevine plantlets

One hundred mg of fine powder obtained by grinding leaves in mortar were mixed with 250 µl of the mixture TRI Reagent® (SIGMA) and after 3 min 25 µl of 1-Bromo-3-Chloropropane (BCP; Tri Reagent/BCP : 10/1, v/v) was added. Samples were incubated 5 min at room temperature and centrifuged (15 min, 12 000 g, 4°C). The supernatants were discarded and pellets were mixed by inversion with 75 µl ethanol and let 3 min at room temperature. Samples were centrifuged (5 min, 2 000 g, 4°C) and proteins were concentrated by acetone precipitation (supernatant/glacial acetone: 1/9, v/v) for at least 1 hour at -20°C. The resulting pellet was homogenized in a modified Laemmli buffer (0.125 mM Tris-HCl pH 6.8, 2 % SDS, 5 % β-mercaptoethanol) without glycerol and bromophenol blue. Extracted proteins were quantified using the reducing agent and detergent compatible protein assay kit (RC DC™, Bio-Rad) with BSA as the standard. Glycerol (10%) and bromophenol blue (0.01%, w/v) were added to samples, which were then heated 5 min at 95°C prior to SDS-PAGE.

2.2.3 Protein extraction enriched in membrane fraction

To detect the membrane-associated proteins in Arabidopsis leaves, protein extracts were prepared as mentioned above (§ 2.2.1) until the centrifugation step (15 min, 10 000 g, 4°C). Hereafter, supernatants were processed differently. To obtain a fraction enriched in the membranous proteins, recovered supernatants were further centrifuged (40 min, 100 000 g, 4°C). The resulting supernatants were discarded and the pellet was suspended in a volume of Laemmli buffer allowing a 50 fold concentration of the extract. Samples were not boiled to preserve solubilisation of membranous proteins.

2.2.4 Detection of phosphorylated MAPK by Western blotting

Twenty µg of total proteins and molecular mass standards (All Blue Standards; Biorad) were separated by 10% SDS-PAGE and transferred to a 0.45 µm nitrocellulose membrane (Hybond C, Amersham) by semi-dry electroblotting using a buffer containing 48 mM Tris–HCl, 39 mM glycine, 0.0375% SDS (w/v) and 20% methanol (v/v). The membrane was saturated overnight at 4°C in TBS buffer (10 mM Tris–HCl pH 7.5, 150 mM NaCl) supplemented with 0.1% Tween 20 and 1% BSA. Phosphorylated MAPKs were detected with a primary antibody raised against a phospho-Thr202/Tyr204 peptide of human phosphorylated extracellular regulated protein kinase 1/2 (α-pERK1/2, Cell Signaling) that was co-incubated with the membrane for 1 h at 1/5 000 dilution in TBS buffer + 0.1% (v/v) Tween 20. For the secondary detection, membrane was

incubated 1 h with a goat anti-rabbit IgG horseradish peroxidase conjugate (Bio-Rad) at 1/100 000 dilution in TBS buffer + 0.1% (v/v) Tween 20. The final detection was performed with the ECL detection kit (Western Lightning Plus; PerkinElmer). Transfer quality and/or homogenous loading were checked by Ponceau red staining of membranes (0.1% Ponceau S (w/v) and 5.0% acetic acid (v/v) in water) or by colloidal Coomassie brilliant blue (CBB) staining (34% methanol (v/v), 17% ammonium sulphate (w/v), 0.5% acetic acid (v/v), 0.1% Coomassie Brilliant Blue G-250 (w/v)) of a parallel SDS-PAGE gel.

2.2.5 Detection of GFP and VvFLS2 by Western blotting

The GFP and VvFLS2 proteins were detected by Western blotting on protein extracts from Arabidopsis leaves. Twenty µg of total proteins (§2.2.1) or the microsomal fraction obtained from 400 µg of total proteins (§2.2.3) were subjected to 8% SDS-PAGE and thereafter transferred and treated as previously described for Western blotting of phosphorylated MAPKs (§2.2.4). After saturation with BSA, the membrane was incubated 1 h with an anti-GFP primary antibody (Genetex, GTX30738; diluted 1/10 000) raised against all variants of *Aequoria victoria* GFP or with the anti-VvFLS2 antibody, both from rabbit, in dilutions from 1/1 000 to 1/10 000.

2.2.6 Generation of VvFLS2 antibody and dot-blot specificity test

A rabbit polyclonal antibody against VvFLS2 (*anti*-VvFLS2) was purchased from Proteogenix. Two rabbits were immunized with the synthetized peptide KTVENPEPEYASALT conjugated to keyhole limpet hemocyanin (KLH) carrier protein, antibody titres were determined in each rabbit serum with ELISA tests. The antibodies were antigen affinity purified and solubilized in PBS buffer pH 7.4 with 0.02% NaN_3 (w/v).

For the *anti*-VvFLS2 antibody dot-blot immuno-analysis, dots comprising of 0.2 µg of Cys-KTVENPEPEYASALT immunogenic antigen or 0.23 µg flg22 (used as a negative control) were spotted directly onto the nitrocellulose membrane and were allowed to dry. The membrane was incubated with anti-VvFLS2 antibody in dilutions from 1/1 000 to 1/128 000.

2.2.7 Isolation of total RNA

Total RNA was isolated either from 100 mg of ground grapevine cells by adding 1 ml of Trizol® (Invitrogen) or from 100 mg of ground *in vitro* plantlet leaves by using the Spectrum™ Plant Total RNA Kit (Sigma). Both isolations were carried out according to the manufacturer's instructions. Purity of RNA samples was determined by measuring the absorbance ratio 260/280 nm with the NanoDrop 2000 spectrophotometer (Thermo Scientific). RNA quality was visualized by electrophoresis in 1% agarose gel.

Gene	Accession # (GenBank)	Sequences (5' => 3')	Amplicon size (pb)	Efficiency (%)	Tm (°C)	References
VvFLS2	XM_002272283.1	CCAATCATGTCATATCGGTCTCG GTTGGAACTCAAGTCTAGAACCTG	107	91.6 ± 1.5	81.6 ± 0.2	
VvCERK1	XM_002270951.1	TGGCTTTGTTCGAGGATGTG CGAGTGGGTAGTTATCTTCAAGC	92	92.7 ± 1.4	81.5 ± 0.3	
VvCERK2	XM_002264291.1	GACTTGTTGCTTTGTTTGAGGA GTAGTCATCTCCAAGCCTCTG	91	85.2 ± 8.9	79.2 ± 0.1	
VvCERK3	XM_002264252.1	GGCAATGACTACCCACTTGAC TTAGTGCGACAACTACTGACTG	111	94.6 ± 1.8	82.6 ± 0.4	
VvCEBiP1	XM_002278724.1	ATGGAATGTGGGAGTAGTGG TGTGAAGATTGTTTGGTTGGTG	104	94.4 ± 1.7	80.6 ± 0.1	
VvCEBiP2	XM_002278706.1	GATCGGTCTACAAGTCTGGAG CGGAAATTTGCTCATACACTGAC	174	90.6 ± 2.4	80.5 ± 0.2	
EF1α	XM_002284888.1	GAACTGGGTGCTTGATAGGC AACCAAAATATCCGGAGTAAAAGA	150	88.6 ± 2.3	82.6 ± 0.2	Dubreuil-Maurizi *et al.,* 2010; Bordiec *et al.,* 2011
EF1γ	XM_003633372.1	GAAGGTTGACCTCTCGGATG AGAGCCTCTCCCTCAAAAGG	84	94.7 ± 1.8	81.4 ± 0.3	Dufour *et al.,* 2013
60SRP	XM_002270599.1	ATCTACCTCAAGCTCCTAGTC CAATCTTGTCCTCCTTTCCT	165	ND	ND	Gamm *et al.,* 2011
PR6 (PIN)	XM_002284411.1	AGTTCAGGGAGAGGTTGCTG CGTCGACCCAAACACGGACCCTAGTGC	131	85.8 ± 1.7	81.0 ± 0.3	Trouvelot *et al.,* 2008; Aziz *et al.,* 2003
PR3-4c (Chit4c)	XM_002275480.1	GCAACCGATGTTGACATATCA CGTCGCCCTAGCAAGTGAG	223	90.6 ± 1.7	83.6 ± 0.3	Aziz *et al.,* 2003
LOXC	XM_002280615.1	CTGGGTGGCTTCTGCTCTC GCATGAATCTGCGGCTTATC	98	90.4 ± 0.9	84.4 ± 0.1	Dubreuil-Maurizi *et al.,* 2010; Aziz *et al.,* 2003
RBOHD	XM_002268568.1	CACCACCATGCTTCAGTCCCTCCAT AGCGATCTTCTTGAAGACTTGTCGCC	115	90.8 ± 1.0	84.4 ± 0.2	Dubreuil-Maurizi *et al.,* 2010; Aziz *et al.,* 2003
ACCS	XM_002278453.2	ACGCTGCCACCGTCTTCAGC GCTCGACATCTTGCGGCCGAT	190	92.0 ± 0.7	83.0 ± 0.2	
PAL	XM_002268220.1	AGTCTCCATGGACAACACCCG TGCTCAGCACTTTCGACATGG	237	91.1 ± 0.9	83.6 ± 0.1	Dubreuil-Maurizi *et al.,* 2010; Aziz *et al.,* 2003
STS1.2	XM_002265193.1	AGGAAGCAGCATTGAAGGCTC TGCACCAGGCATTTCTACACC	102	91.2 ± 1.8	81.1 ± 0.3	Trouvelot *et al.,* 2008
PR1-2	XM_002274239.1	GCGTGGGTGGGGAATGCCGA GATGTTGTCCCTGATAGTTGCC	143	91.3 ± 0.9	85.2 ± 0.2	
PR2-1 (Gluc)	XM_002277133.1	ATGCTGGGTGTCCCAAACTCG CAGAACAAACTGCGCAAACCGT	180	88.2 ± 1.0	86.1 ± 0.2	Aziz *et al.,* 2003
17.3	XM_002283642.1	GTACCATCAGACCACCCATAAGTAGTG AGACCAACGGCAAATCAAGTG	91	ND	ND	
VvFLS2-like	GSVIVT01021409001*	GTCGTGTCATGTCAATTATAC TTATTTCTGTACCCTGTGAAGAC	394	85.4 ± 3.8	82.4 ± 0.1	

Table 5. Primers used for qPCR quantification.

Amplicon melting temperatures (Tm) were analysed by the LightCycler 480. The mean PCR efficiency was calculated by the LinRegPCR program (version 2012.3). For Tm and PCR efficiency data are presented as means ± SD. * Sequence was retrieved from Genoscope (http://www.genoscope.cns.fr/externe/GenomeBrowser/Vitis/), ND=Not Determined

2.2.8 cDNA synthesis and quantitative real-time PCR (qPCR)

One µg of RNA treated with DNase I (Sigma-Aldrich) was reverse-transcribed using 100 U of SuperScript™ III Reverse Transcriptase kit (Invitrogen) and 2.5 µM 20-mer oligo dTs in a 10-µl reaction following the instructions of manufacturer. Quantitative polymerase chain reactions (qPCR) were carried out in technical triplicates in 384-well plates (5 µl per well) with GoTaq qPCR Master Mix 2x (Promega), 500 nM primers and 1:50 dilution of cDNA using a cycler platform LightCycler 480 (Roche Applied Science). Used primers are listed in Table 5. PCR conditions were as follows: 95°C / 10 min (initial denaturation); 40 cycles of 95°C / 45 s (denaturation); 60°C / 45 s (annealing); 72°C / 30 s (elongation). After amplification, a melting curve program was performed in each assay to ensure the production of a single amplicon. Using the LinRegPCR program (version 2012.3; Ruijter *et al.*, 2009), the mean PCR efficiencies were determined per each primer pair and were used to calculate a starting relative quantity of template (N_0) per sample. The N_0 values of a target gene were normalized with N_0 values of two reference genes encoding the elongation factor 1α and γ (EF1α, Dubreuil-Maurizi *et al.*, 2010 and EF1γ; Dufour *et al.*, 2013) giving the gene expression ratio (Ruijter *et al.*, 2009). Gene induction between control and treated sample was determined by comparison of normalized relative template quantity of target genes versus control samples.

$$Fold\ change\ of\ gene\ induction = \frac{\left(\frac{N_0^{Target}}{N_0^{Ref}}\right)^{Treated}}{\left(\frac{N_0^{Target}}{N_0^{Ref}}\right)^{Control}}$$

The conditions for cDNA synthesis and the qPCR analyses realized in the frame of collaboration with the University of Reims were different. The cDNAs were synthesized from 150 ng of RNA using M-MLV reverse transcriptase (Invitrogen) following the manufacturer's protocol. qPCR reactions were carried out in technical duplicates in 96-well plates. Each reaction of 15 µl volume contained SYBR Green I mix (PE Biosystems, Foster City, CA, USA), 280 nM primers and a 1:30 diluted cDNA. PCR conditions were as follows: 95ºC / 15 s (denaturation); 40 cycles of 60ºC / 1 min (annealing/elongation), using a GeneAmp 5700 sequence Detection System (Applied Biosystems). Transcript level was calculated using the comparative ΔΔCt method (Livak and Schmittgen, 2001) with the EF1α (Dubreuil-Maurizi *et al.*, 2010) and 60S ribosomal protein L 18 (60SRP; Gamm *et al.*, 2011) reference genes for normalization.

2.2.9 Bioinformatics

Orthologous proteins were searched with BLASTp algorithm available at NCBI (NCBI http://www.ncbi.nlm.nih.gov/), CRIBI (http://genomes.cribi.unipd.it/grape/), and Genoscope.fr

Gene		Construct type	Sequences (5' => 3')		T_A (°C)	Size / (Position)[b] (bp)
Name	Accession # (GenBank)		Forward	Reverse		
VvFLS2	XM_002272283.1	fl	CACCATGGTGTCTGAAAGAGTCAGTTTAATCC	**GGC**TGATGATGATGGTAATGGAGG	55	3516
		αs	CACCTCTGTACCTCGATGACAATGC	AGCCGAGAAAGACGAGCCATG	55	210 / +1602
VvFLS2-like	GSVIVT01021409001[a]	fl	CACCATGGAGCCCAGAAGTGTTGGTTTAAC	**GGC**GGCCAGTTTAAGGACCTCTTCCAA	62	ND (~3312)
VvCERK1	XM_002270951.1	fl	CACCATGAAACAGAAGGTGGGTTTAGGG	**GGC**CCTTCCAGACATTAGATTGACGAGG	55	1845
		αs		GGTGGTGTGATTGCTGGCATA	55	684 / +1
VvCERK2	XM_002264291.1	fl	CACCATGGTCATTTCATCAAACAGCAGGAACGC	**GGC**CCTTCCTGACATTAGATTCATCAGAGCC	55	1878
		αs		GGGCATTTTCGAACCTCACTACTGAG	55	378 / +1
VvCERK3	XM_002264252.1	fl	CACCATGTTGGTTTTTAGAATCTCAAGG	**GGC**TCTTCCTGACATCAGATTCACTAGAGC	55	1869
		αs	CACCATGTTAGTGTTTTCTGTGTTGATATTTCTC	TCCCCTTCTCCTGCAGTTGCA	55	235 / +34
VvCEBiP1	XM_002278724.1	fl	CACCATGCTAACGTGCACACCGGTGG	GGCCATAGCACTTAGGCTATATTCAGGC	55	ND (~1056)
		αs	CACCATGCTAACGTGCACACCGGTGG	TCGAGGCCGGGAGGGAGTTG	55	317 / -100

Table 6. Primers used for cloning of putative *VvPRR* genes

For full-length (fl) cloning, forward primers possess 5‘ overhang CACC (underlined) for directional cloning into pENTR/D-TOPO (Invitrogen) and the stop codon in reverse primers is replaced by Ala (GCC, bold). T_A : Annealing temperature in PCR. [a]) Sequence was retrieved from Genoscope (http://www.genoscope.cns.fr/externe/GenomeBrowser/Vitis/), [b]) The localization of the 5‘ end of the antisense (αs) fragment with regard to the start of translation (+1).

(http://www.genoscope.cns.fr/externe/GenomeBrowser/Vitis/, Vitis 12x) that all provide different genome annotations based on two grapevine genome sequencing projects (Jaillon *et al.*, 2007 and Velasco *et al.*, 2007). Multiple protein alignments were done with T-Coffee (http://tcoffee.crg.cat/apps/tcoffee/) or ClustalW2 (http://www.ebi.ac.uk/Tools/services/web_clustalw2/) and visualized with Boxshade (http://www.ch.embnet.org/software/BOX_form.html). Annotation of protein structure was performed with SMART (http://smart.embl-heidelberg.de/). Prediction of subcellular localization was done with Predotar (http://expasy.org/tools/). The exon-intron structure of genes was visualized with the software on http://wormweb.org/exonintron.

For phylogenetic analyses, protein sequences were aligned with MUSCLE program implemented in www.phylogeny.fr (Dereeper *et al.*, 2008). The Maximum-likelihood phylogenetic tree was generated with SeaView version 4 software (Gouy *et al.*, 2010) using LG substitution model and bootstrapping with 1000 replications. The tree was displayed with MEGA 5.2.2 software (Tamura *et al.*, 2011). Sequences of other Arabidopsis RLKs, such as EF-TU RECEPTOR (AtEFR; Kunze *et al.*, 2004) and Wall-associated kinase 1 (WAK1; Brutus *et al.*, 2010) were used as outgroups.

2.2.10 General cloning technics

Escherichia coli strain TOP10 (Invitrogen) or K12 (*ccdB* resistant variant) were used for multiplication of the different original or recombined vectors. Transformation of chemically competent bacteria was carried out by heat shock (4°C / 30 min, 42°C / 1 min, 4°C / 2 min). Bacteria were cultivated in liquid LB medium (10 g l^{-1} tryptone, 10 g l^{-1} NaCl, 5 g l^{-1} Yeast Extract) at 37°C and 200 rpm, and plated on LB agar medium with selection antibiotic. Transformant screening was carried out by PCR on colonies. Each of at least 10 independent colonies was suspended in 50 µl of water in a sterile manner. PCR was done with 5 µl of the bacterial suspension, 200 µM dNTPs, 200 nM forward and reverse primers and 0.0375 µl of GoTaq DNA polymerase (Promega) in a reaction volume of 15 µl. Plasmids were purified with the Pure Yield Plasmid™ Mini Prep System kit (Promega) from 2 ml of an overnight culture and eluted with 50 µl of water. Restriction endonuclease digest was performed on 600 ng of plasmid with restriction endonucleases (Promega or Fermentas) during 2 h at 37°C and visualized on 1% agarose gel with DNA ladders (New England BioLabs).

2.2.11 Cloning of GFP-tagged or antisense VvPRRs by Gateway® technology

Full-length or antisense (*αs*) fragments of candidate *VvPRR* genes were amplified by PCR from cDNA obtained from elicited grapevine cells (*V. vinifera* cv Gamay) by using a proof-reading *Pfu* DNA polymerase (Finnzymes) and gene specific primers (Table 6). For full-length cloning,

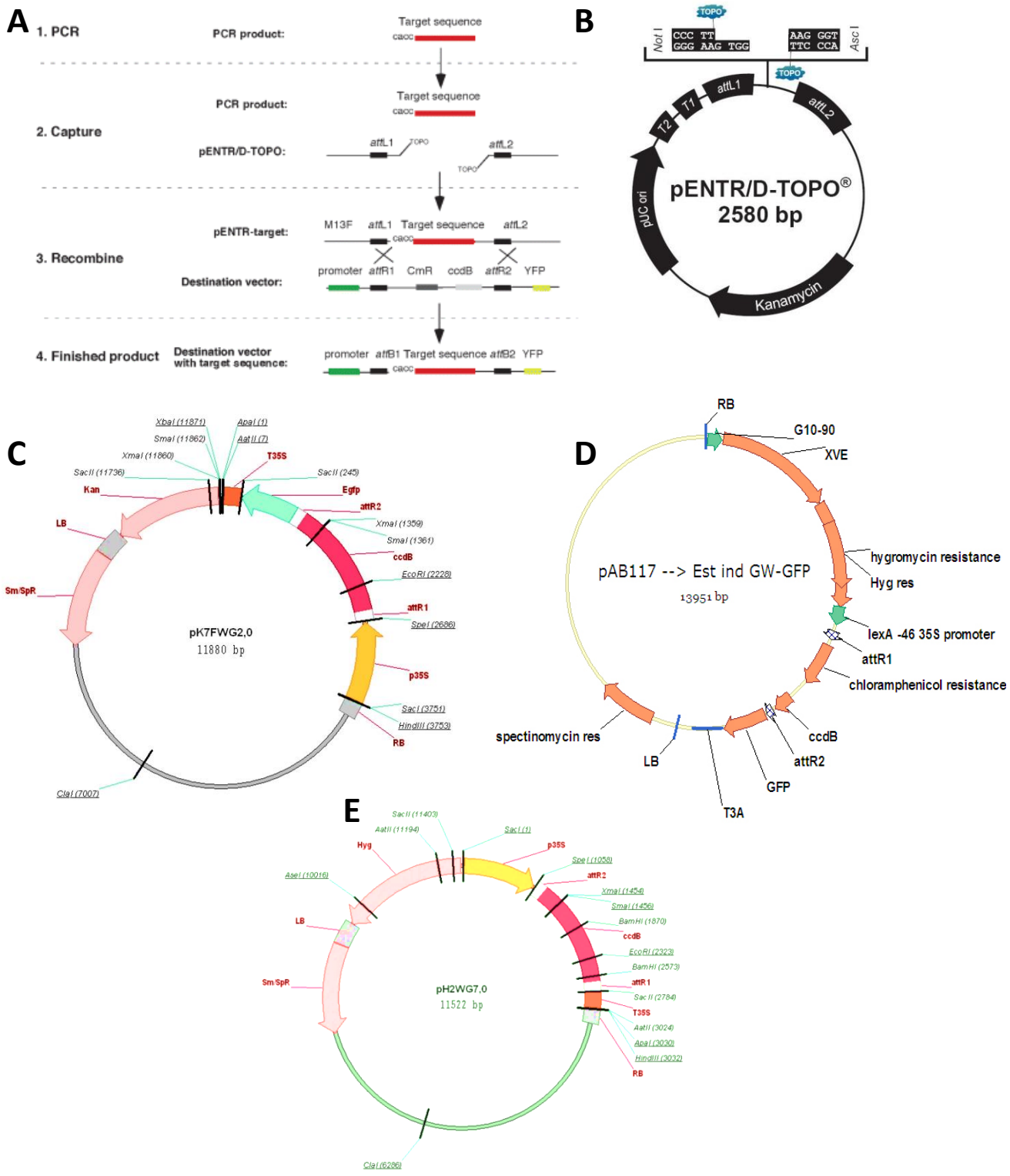

Figure 14. Gateway®-based functional genomics strategy and maps of the vectors used.
A. 1) A cDNA is PCR-amplified using a forward primer that has the sequence CACC for directional cloning into the pENTR/D-TOPO vector. 2) A topoisomerase catalyzes ligation between PCR products and the pENTR/D-TOPO vector. 3) Using the LR clonase enzyme, the target sequence is recombined into a destination vector of choice between *att*L and *att*R sites. 4) A *ccdB* gene, located between the *att*R sites of the destination vector, is lethal to most strains of *Escherichia coli*. As a result, only those *E. coli* transformed with plasmids having undergone successful recombination events survive. **B.** Map of the pENTR/D-TOPO entry vector used. **C., D., E.** Maps of the destination vectors used for the functional complementation of the Arabidopsis mutants using a constitutive (**C.**) or inducible (**D.**) over-expression in the sense orientation with a fused GFP or for the silencing strategy using a constitutive over-expression in the antisense orientation (**E.**). Sm/Sp R: Streptomycin/Spectinomycin resistance, Kan: kanamycin resistance, Hyg: hygromycin resistance, LB: left border, RB: right border, P35S or lexA: constitutive or inducible promoter, T35S or T3A: terminator, *ccdB*: lethal gene, attR and attL: sites used for the Gateway recombination, XVE : engineered estradiol receptor, GFP: green fluorescent protein.

primers were designed to replace the stop codon by the Ala codon (GCC nucleotides). Products were separated on 0.8% agarose gel, stained by Blue Nil (20 mg l^{-1} in water) and a single PCR product of the expected size was excised. A gel-purified (Wizard® SV Gel and PCR Clean-Up System, Promega) PCR product was first directionally subcloned (Fig. 14A) into the entry vector pENTR™/D-TOPO® vector (Fig. 14B; kanamycin resistance, Invitrogen), then inserted into Gateway expression vectors (Table 7) by using Gateway LR Clonase™ II enzyme mix (Invitrogen).

The full-length CDS of *VvFLS2* was cloned into pK7FWG2 (Karimi *et al.*, 2002; kanamycin resistance) for *p35S::VvFLS2-GFP* expression (Fig. 14C). The three full-length coding sequences of *VvCERK1*, *VvCERK*2 and *VvCERK3* were cloned into pK7FWG2 (kanamycin resistance) to obtain a constitutive overexpression construct (*p35S::VvCERK1/2/3-GFP*) or in pABindGFP (Bleckmann *et al.*, 2010; hygromycin resistance, Fig. 14D) for a β-estradiol inducible gene expression (*pLexA35S::VvCERK1/2/3-GFP*).

Fragments of ~200-700 bp from each of candidate *VvPRR* genes were cloned into pH2WG7 (Karimi *et al.*, 2002; Fig. 14E, hygromycin resistance) in the antisense orientation (*p35S::αsVvFLS2, p35S::αsVvCERK1, p35S::αsVvCERK2, p35S::αsVvCERK3 and p35S::αsVvCEBiP1*). All constructs were verified by sequencing (GATC Biotech) with primers listed in Table 8.

2.3 Plant transformation

2.3.1 Grapevine transformation and plantlet generation *via* somatic embryogenesis

The *Agrobacterium*-mediated transformation of embryogenic calli from *V. vinifera* (cv Pinot Noir PN40024) and plantlet regeneration *via* somatic embryogenesis were performed by the grapevine transformation platform, INRA Colmar (Jean Masson, Mireille Perrin, Carine Schmitt). Briefly, embryogenic calli (EC) initiated from anther filaments (Perrin *et al.*, 2004; Fig. 15A-C) were transformed by *A. tumefaciens* (strain C58pMP90) harboring the antisense constructs (pH2WG7 *p35S::αsVvPRR*) for silencing. In parallel, a transformation with GFP (pBI121 *p35S::m-gfp5-ER,* referred as *p35S::GFP*) and a mock-transformation with water were performed. These EC were further grown on medium supplemented with 100 mg l^{-1} cefotaxim to remove the remaining Agrobacteria, according to (Perrin *et al.*, 2004). Selection of the transformants was initiated 28 days after transformation by transferring EC on growth medium supplemented with 25 mg l^{-1} hygromycin (pH2WG7 constructs), 25 mg l^{-1} kanamycin (pBI121 construct) or without antibiotics for the mock-transformation (somatic embryogenesis wild-type, hereafter referred as seWT). The hygromycin/kanamycin-resistant EC issued from independent transformation events appeared after 60 days (Fig. 15D) and were subcultured every 21 days on new selection media. Different calli lines were tested for αs*VvPRR* transgene expression by RT-PCR using primers

Vector name	Promoter / Expression	Insert Orientation	Protein Tag	Resistance		References
				plants	bacteria	
pK7FWG2	35S / constitutive	5'=>3' (OE)	C_{ter}-GFP	Kan	Sp/Sm	Karimi *et al.*, 2002
pH2WG7	35S / constitutive	3'=>5' (antisense)	---	Hyg	Sp/Sm	Karimi *et al.*, 2002
pABindGFP	lexA-46 35S / estradiol-inducible	5'=>3' (OE)	C_{ter}-GFP	Hyg	Sp	Bleckmann *et al.*, 2010

Table 7. List of Gateway-type expression vectors.
OE: overexpression, Kan: kanamycin, Hyg: hygromycin, Sp: spectinomycin, Sm: streptomycin. Vector maps are shown in Figure 14.

Name	Sequence (5' => 3')	Target	Purpose
M13 F	GTAAAACGACGGCCAG	pENTR/D-TOPO	Insert localization, orientation and sequencing
M13 R	CAGGAAACAGCTATGAC		
OE1 L (P35S)	TCATTTCATTTGGAGAGGACTCCG	pK7FWG2, pH2WG7	
GFP R	GTGGTGCAGATGAACTTCAGG	pK7FWG2	
OE1 R (T35S)	TGCTCAACACATGAGCGAAA	pH2WG7, (pK7FWG2)	
lexA_35S_F	GCCATGTAATATGCTCGACTCTAG	pABindGFP	
GFP_pABind_R	GGTAGTTTTCCAGTAGTGCAA		
FLS2 seqF1	CCAGAGATCGGGAACTTATCG	*VvFLS2*	Insert sequencing
FLS2 seqF2	AGTTCTGAAACCAGGCATTG		
FLS2 seqR1	TCTCTCCAATAAAGTCCACC		
CERK1 seqF1	GATTAGCAGGTGGTGTGATT	*VvCERK1*	
CERK2 seqMid1R	AGGAACCCTCGACACAATATC	*VvCERK2*	
CERK3 seqF1	AACCCTGGAGTTGATTTCAG	*VvCERK3*	
CERK3 seqF2	TTACTATGCGGAGCTGCAAG		

Table 8. Primers used for insert sequencing.

specific to the 3' end of the 35S promoter (OE1L, Table 8) and to the 5' end of the αs*VvPRR* (forward primer for each of αs*VvPRR* fragments). *In vitro* plantlets were generated from 10 different transgenic EC lines (Fig. 15E) per construct *via* the somatic embryogenesis (Perrin *et al.*, 2001; Perrin *et al.*, 2004; Fig. 15F-I). Two *in vitro* plantlets per line were delivered 400 – 500 days post transformation (dpt).

2.3.2 Arabidopsis transformation and mutant screening

Arabidopsis transformation were done by floral dip, according to (Clough and Bent, 1998) using the different pK7FWG2 or pABindGFP constructs. The Arabidopsis *fls2* mutant was transformed with *p35S::VvFLS2-GFP*, *cerk1-2* mutant was transformed with *p35S::VvCERK1-GFP, p35S::VvCERK2-GFP* or *p35S::VvCERK3-GFP* in the first set of transformations. In the second set of transformations, *GFP*-tagged *VvCERK1, 2 or 3* were introduced in the inducible pABindGFP vector. Antibiotic resistant transgenic plants were screened in T1 generation for presence of oxidative burst in leaf discs after elicitor treatment, as described previously (Zipfel *et al.*, 2006). The 3:1 segregation ratio for antibiotic resistance in T2 generation permitted the selection of single copy complemented lines. To confirm the stability of the phenotype, ROS production was measured again in T3 lines (§2.1.2). The chitin-induced oxidative burst in *cerk1-2/pLexA::VvCERK1/2/3-GFP* plants was assessed in leaf discs pretreated with 10 or 20µM β-estradiol or water for 20 h prior to elicitation. The presence of GFP fused proteins was detected by Western blotting as described elsewhere (Li *et al.*, 2009). These experiments were performed using facilities of the transformation services of the John Innes Centre (BRACT, Norwich, UK, collaboration C. Zipfel).

2.4 Histochemical GUS detection in Arabidopsis *pPR1::GUS* seedlings

Ten to 15 seeds were dispensed into each well of a 12-well tissue culture plate with 1 ml of MS medium supplemented with 0.5 g l^{-1} MES, pH 5.7. Plates were sealed with Parafilm to prevent evaporation of the medium. On the eighth day, the media were replaced with 1 ml of fresh media. Ten-day old seedlings were treated with elicitors by adding them directly to the medium at the indicated concentrations. GUS enzyme activity of *pPR1::GUS* Arabidopsis seedlings (NASC_N6357) was determined histo-chemically. Seedlings were quick wash with sodium phosphate buffer (50 mM sodium phosphate, pH 7), then incubated with 2 ml of 50 mM sodium phosphate (pH 7), 0.1% Triton X-100 and 1 mM 5-bromo-4-chloro-3-indolyl-b-D-glucuronic acid (Duchefa X1406) for 8 h at 37°C. The samples were then fixed with acetic acid/ethanol 1/3 (v/v) and chlorophyll was entirely removed by several washes in 70% ethanol. Seedlings were mounted in 100% lactic acid.

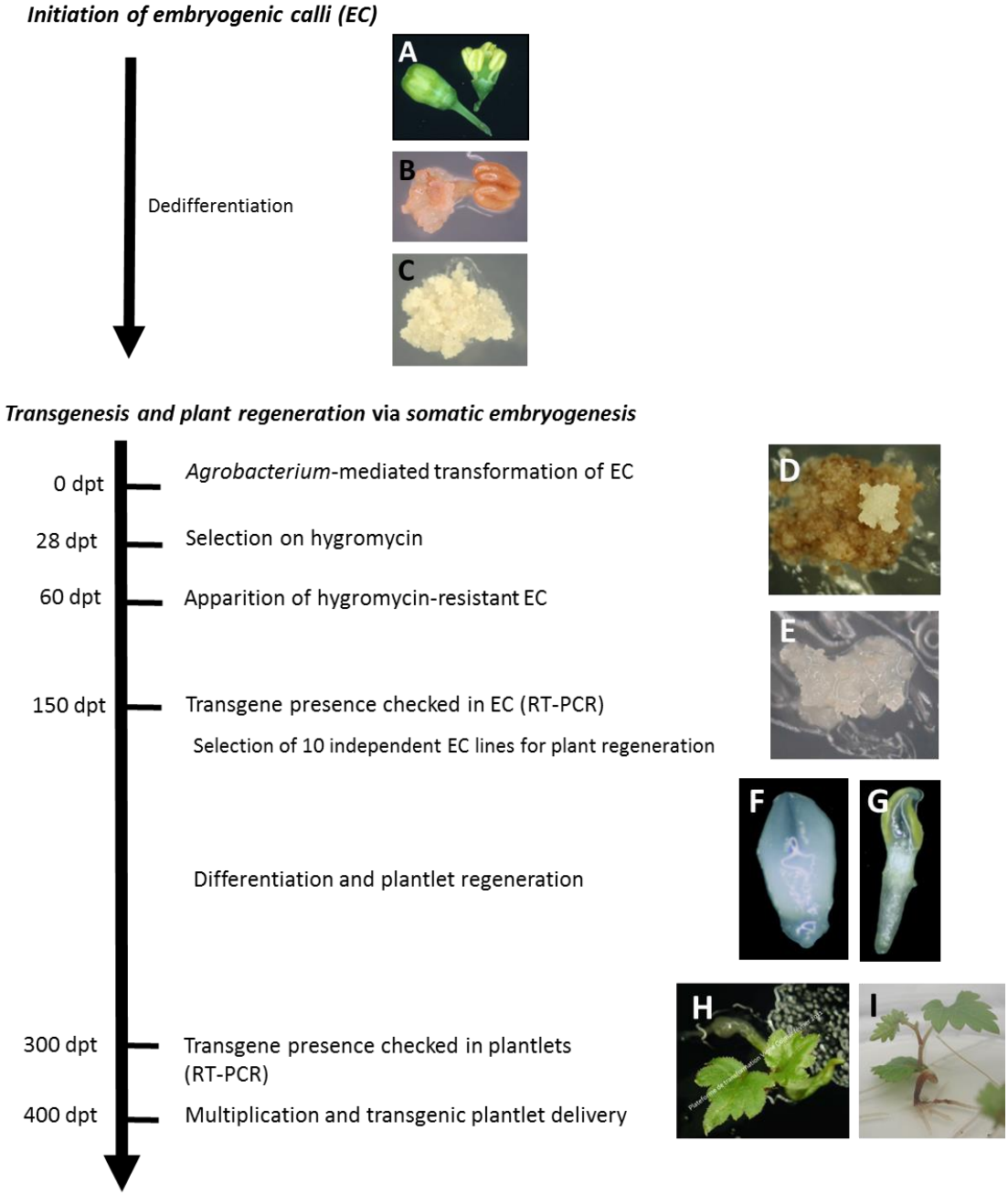

Figure 15. Different stages of transgenic grapevine transformation and plant regeneration.
Embryogenic calli (EC) are initiated from stamens of immature inflorescences that possess high embryogenic capacity. Flowers are uncapped (**A.**) and anther filaments (0.3 mm in size) are dedifferentiated to give EC (**B.**). The obtained EC (**C.**) can be transformed. **D.-I.** Timescale overview of transgenese and somatic embryogenesis. *Agrobacterium*-mediated transformation with a binary vector pH2WG7 led to hygromycin-resistant EC (**D.)** that were further subcultured on hygromycin 25 mg l^{-1} over several cycles. At 150 days post-transformation (dpt), 10 independent lines of EC, with verified presence of transgene, were selected for plantlet regeneration (**E.)**. First, differentiation led through the somatic embryo at the stage of torpedo (**F.**) and cotyledon (**G.**) until the conversion into plantlet (**H., I**.). *Images were kindly provided by Mireille Perrin and Jean Masson (INRA, Colmar).*

2.5 Flg22- triggered growth inhibition assays on Arabidopsis and grapevine

For Arabidopsis, seeds of the different genotypes (Col-0, *fls2* and *fls2/p35S::VvFLS2-GFP)* were first germinated on solid half MS medium then transferred individually into 24-well culture plates containing liquid half MS medium supplemented with the different flg22 peptides at 1 µM concentration.

For *V. vinifera* (cv Chardonnay), 2-weeks old *in vitro* plantlets were transferred from 25-mm glass tubes to Magenta boxes containing 20 ml of liquid modified MS medium supplemented with the different flg22 peptides at 1 µM.

Fresh weight of 15 individual plants was measured after 1 and 2 weeks for Arabidopsis and grapevine, respectively.

2.6 Protection assays on grapevine leaf discs

Leaf discs from the second and third adult top leaves of at least 12 grapevine plants were cut and floated on elicitor solution in 0.1% surfactant or on surfactant alone (control) for 24 h with the lower (*P. viticola*) or upper (*B. cinerea*) leaf surface facing the liquid. Discs were then washed in ultrapure water and transferred on a wet Whatman paper for additional 24 h with the treated surface upward.

For *P. viticola* infection, 35 discs (1 cm diameter) were inoculated with a 20 µl-droplet of a freshly prepared suspension at 10^4 sporangia ml^{-1} and maintained in 100% humidity in a plastic box placed in a controlled growth chamber under a 11/13 h day/night cycle at 20/17°C with a light intensity of 150 µmol m^{-2} s^{-1} provided by fluorescent tubes. Infection intensity was assessed at 7 dpi. The number of sporangia per leaf disc surface was estimated by counting sporangia using a Malassez haemocytometer on 2 sets of 5 randomly chosen discs that were placed in 50% ethanol and shaked to liberate entirely spores into ethanol. Each set was counted at least three times.

For *B. cinerea* infection, 30 discs (1.5 cm diameter) were inoculated with 5000 conidia in a 6 µl-droplet in potato dextrose broth (PDB) ¼ diluted. Inoculated discs were maintained in 100% humidity in a plastic box placed in a controlled growth chamber as described for *P. viticola* infections. Infection intensity was assessed 3 dpi by measuring the macerated lesion diameter.

2.7 Grapevine infection with *B. phytofirmans*

Roots of 2-week-old grapevine plantlets (*V. vinifera* cv Chardonnay) grown *in vitro* were immersed in bacterial inoculum of *B. phytofirmans* (3×10^8 CFU ml^{-1}) or PBS (control) for 10 s. After inoculation, plantlets were grown for one week in liquid modified MS medium before bacterial counting in root and aerial part according to (Compant *et al.*, 2005b).

2.8 Confocal microscopy

Confocal microscopy was performed using a Leica TCS SP2-AOBS confocal laser scanning microscope with 40X oil-immersion objective (numerical aperture: 1.25). Pieces of leaves were mounted in distilled water or in 1 M NaCl solution for plasmolysis experiments. For FM4-64 staining, samples were incubated in 8 µM FM4-64 solution in water during 10 min prior observation. Fluorescent markers were visualized by excitation with an argon laser at 488 nm. GFP and FM4-64 emissions were band-pass filtered between 500-525 nm and 616-694 nm, respectively. Image analysis and background corrections were carried out with the software Volocity 6.2.1 and ImageJ 1.43m. Experiments were performed using facilities of the Centre de Microscopie INRA Dijon/Université de Bourgogne, Plateforme DImaCell.

MAMP					MAMP-induced early signaling events			
Name	**Chemical nature**	**Origin**	**Species**	**References**	**Tested concentration range [1])**	**ROS production**	**Variations in $[Ca^{2+}]_{cyt}$**	**MAPK activation**
flg22	peptide (22 aa)	flagellin	*Pseudomonas aeruginosa*	Felix *et al.*, 1999	1 nM - 10 µM	+	+	+
elf18	peptide (18 aa)	elongation factor Tu	*Escherichia coli*	Kunze *et al.*, 2004	1 nM - 10 µM	-	-	-
pep13	peptide (13 aa)	cell wall transglutaminase	*Phytophthora sojae*	Brunner *et al.*, 2002	1 nM - 10 µM	-	-	-
chitin	ß-1,4-GlcNAc polymer (DP ?)	fungal cell wall / crustacean cuticle	ND	Lloyd *et al.*, 2014	1 mg l^{-1} – 10 g l^{-1}	-	+	+
chitosan	ß-1,4-GlcNAc polymer (DA<25%, DP>500)	deacetylated chitin	---	---	10 µg l^{-1} – 50 mg l^{-1}	-	+	+
Lam	ß-1,3-glucan polymer (DP~25-30)	storage carbohydrate	*Laminaria digitata*	Klarzynski *et al.*, 2000	1 mg l^{-1} – 1 g l^{-1}	+	+	+

Table 9. Screening of MAMP responsiveness in grapevine cells.
Early signaling events were tested after treatment with bacterial MAMPs (flg22, elf18), fungal MAMPs (chitin, chitosan), oomycetal MAMPs (pep13, laminarin). ROS burst was measured by chemiluminescence of luminol at 15 min post treatment with elicitor. $[Ca^{2+}]_{cyt}$ spiking after elicitor treatment was measured using apoaequorin-expressing grapevine cells. MAPK activation was detected by Western blot using an anti-phosphorylated pERK1/2 antibody. [1]) Concentration range for dose-response assays on ROS burst and free cytosolic calcium $[Ca^{2+}]_{cyt}$ spiking. Within this range, a serie of 10-fold dilutions was performed. Concentrations used for MAPK activation assays were 1 g l^{-1} for laminarin and chitin, 1 µM for flg22, elf18 and pep13 and 25 mg l^{-1} chitosan. The table summarizes data from at least two experiments per condition/concentration.

RESULTS AND DISCUSSION

I. Screening of MAMP responsiveness in grapevine

MAMPs are conserved molecules recognized by a broad variety of plant species eliciting defense responses. To discover the elicitor repertoire perceived by *V. vinifera*, the activity of MAMPs recognized in other plant species (flg22, elf18, pep-13, chitin and chitosan) was assessed in grapevine cells. The effect was compared to the β-1,3-glucan laminarin, a MAMP which is recognized by grapevine and triggers early defense signaling and immune responses (Aziz *et al.*, 2003). Following the MAMP treatment of grapevine cells, signaling events were analyzed with different concentrations of each MAMP. The oxidative burst was measured by chemiluminescence of luminol, the variation in free cytosolic calcium concentrations ($[Ca^{2+}]_{cyt}$) was measured using apoaequorin-expressing cells, and the MAPK activation was assessed by Western blot detecting the phosphorylated form of MAPKs.

According to our results (Table 9), flg22, chitin and chitosan are recognized by *V. vinifera* as they trigger signaling events, previously described for other active elicitors such as laminarin, OG or BcPG1 (Aziz *et al.*, 2003; Poinssot *et al.*, 2003; Dubreuil-Maurizi *et al.*, 2010). On the contrary, the peptides elf18 (Kunze *et al.*, 2004) and pep-13 (Brunner *et al.*, 2002) were inactive in the concentration range of 0.001 – 10 µM (Table 9).

For further work, we focused on the characterization of perception systems for flagellin (Part II) and chito-oligosaccharides (Part III) in *V. vinifera*.

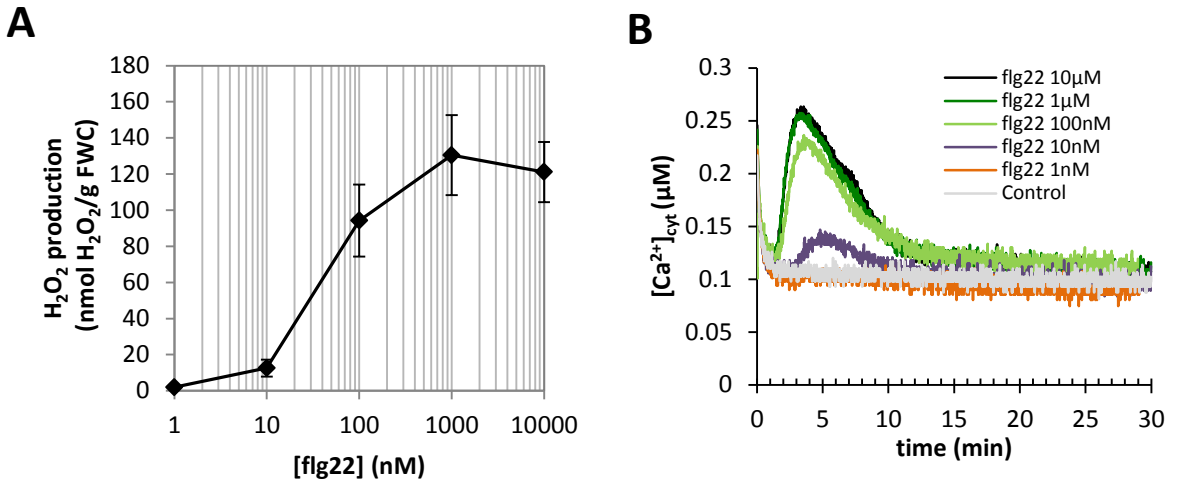

Figure 16. flg22 triggers a dose-dependent oxidative burst and variations in free cytosolic calcium concentrations ($[Ca^{2+}]_{cyt}$) in grapevine cells

A. Oxidative burst at 15 min post treatment with flg22 measured by chemiluminescence of luminol. Values are means ± SD of three independent experiments. FWC: fresh weight of cells **B.** Variations in $[Ca^{2+}]_{cyt}$ after flg22 treatment measured with apoaequorin-expressing grapevine cells. Data are from one representative experiment out of three.

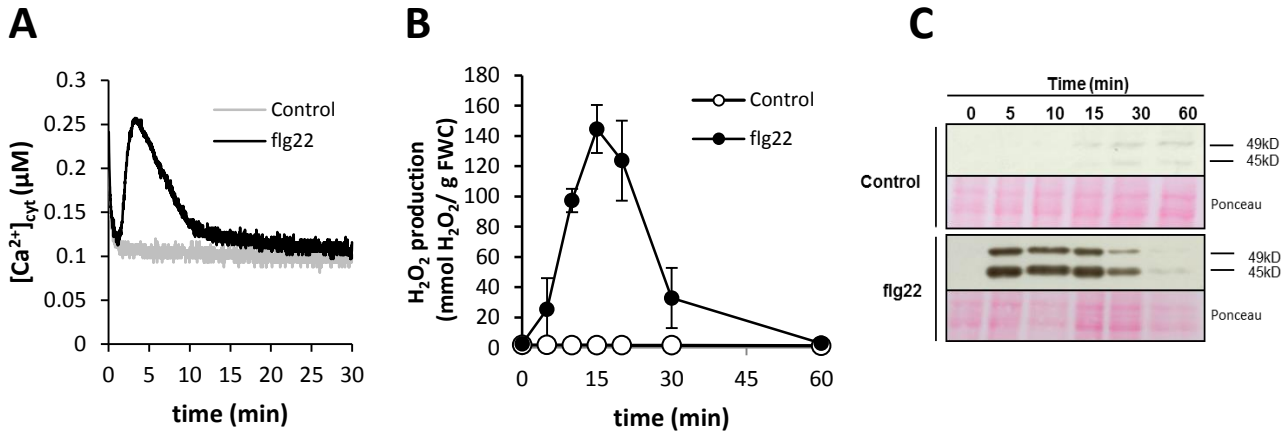

Figure 17. Kinetics of flg22-induced early signaling events in grapevine cells.

A. Free cytosolic calcium variations measured with apoaequorin-expressing grapevine cells. **B.** Oxidative burst detected by chemiluminescence of luminol. Values are means ± SD from three independent experiments. FWC: fresh weight of cells. **C.** Activation kinetics of two mitogen-activated protein kinases (MAPK) detected by Western blot with an anti-phosphorylated pERK1/2 antibody. Homogeneous loading was checked by Ponceau Red staining. **A.** and **C.** show one representative experiment out of three. Cells were treated with 1 µM flg22 or water (control).

II. Flagellin perception system in grapevine

Results

1 Flg22 induces immune responses and resistance against *Botrytis cinerea* in grapevine

To determine whether flagellin perception by grapevine triggers the responses commonly observed in Arabidopsis, tomato or tobacco (Felix *et al.*, 1999; Gomez-Gomez and Boller, 2000; Hann and Rathjen, 2007), we first characterized early signaling events and defense gene expression induced by flg22 (from *P. aeruginosa*) in *V. vinifera* cell suspensions. Flg22 treatment induced a dose-dependent oxidative burst and variations in free cytosolic Ca^{2+} (Fig. 16A, B). The saturating flg22 concentration of 1 µM was then used to study the defense-related events in grapevine cells.

Treatment with 1 µM flg22 induced a transient increase in free $[Ca^{2+}]_{cyt}$ that peaked after 4 min (Fig. 17A) and an oxidative burst with the maximal H_2O_2 production detected at 15 min (Fig. 17B). From 5 to 30 min, flg22 induced rapid and transient phosphorylation of two MAPKs with relative molecular masses of 45 and 49 kDa, which was not observed in control cells (Fig. 17C). The expression of defense marker genes activated by different elicitors (Aziz *et al.*, 2003; Aziz *et al.*, 2007; Bordiec *et al.*, 2011) was then monitored by qPCR. Flg22 induced the expression of early genes encoding a 1-aminocyclopropane-1-carboxylate synthase (*ACCS*), a respiratory burst oxidase homolog D (*RbohD*) and a 9-lipoxygenase (*LOXC*) (Fig. 18A, B, C) and genes participating in the biosynthesis pathway of stilbene phytoalexins: a stilbene synthase (*STS1-2,* Fig. 18D) and a phenylalanine ammonia lyase (*PAL,* Fig. 18E). Genes *STS1-2* and *PAL* are induced with the same expression profile, showing a peak of transcription at 1h post elicitation. From later genes, flg22 induced pathogenesis-related (*PR*) genes encoding enzymes such as an acidic chitinase (*PR3-4c*), a protease inhibitor (*PR6*) or a marker of the SA pathway *PR1-2* (Fig. 18F, G, H). In general, a battery of defense genes was induced as early as 30 min post treatment with the strongest induction detected around 1 hour post treatment (hpt). Twenty four h after flg22 treatment (1 µM), no significant cell death was observed on grapevine cell suspensions (Fig. 18I).

We further investigated the efficiency of flg22-triggered immunity on *V. vinifera* leaf discs challenged with the necrotrophic fungus *B. cinerea* or with the biotrophic oomycete *P. viticola*, the causal agents of gray mold and downy mildew, respectively.

Flg22 treatment applied 48 h before pathogen inoculation significantly reduced the *B. cinerea* lesion diameter, compared with control leaf discs (Fig. 19A). Results were comparable with those obtained by pretreatment with the β-1,3 glucan laminarin, described to trigger

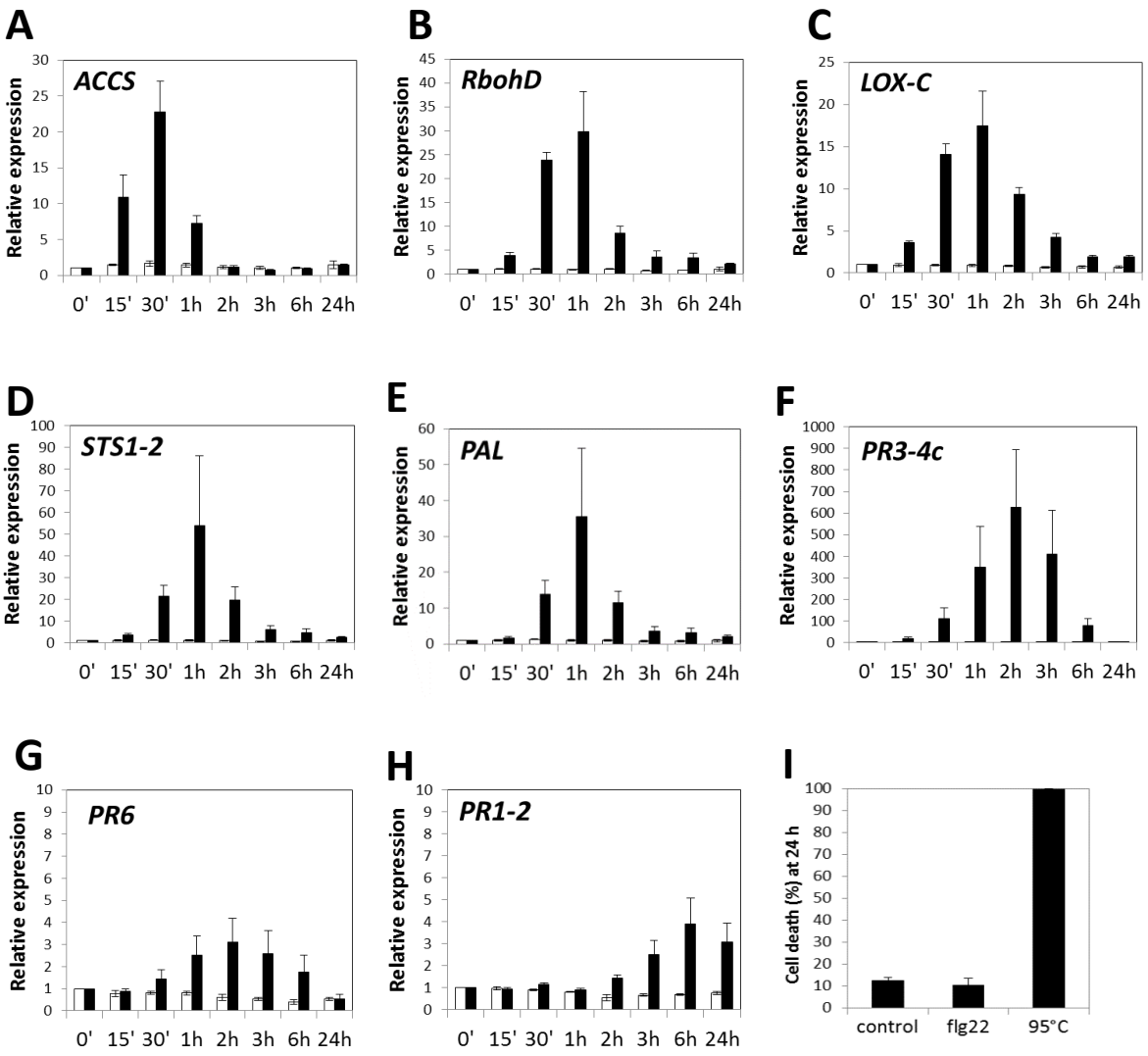

Figure 18. Kinetics of flg22-induced defense gene expression and cell death in grapevine cells.
Relative expression of defence genes encoding **A.** a 1-aminocyclopropane-1-carboxylate synthase (*ACCS*), **B.** a respiratory burst oxidase homolog D (*RbohD*), **C.** a 9-lipoxygenase (*LOX-C*), **D.** a stilbene synthase (*STS1-2*), **E.** a phenylalanine ammonia lyase (*PAL*), **F.** an acidic chitinase (*PR3-4c*), **G.** a proteinase inhibitor (*PR6*) and **H.** *PR1-2*, induced by 1 µM flg22 (black bars) or water (white bars). The relative expression was measured by qPCR, normalized by the housekeeping genes elongation factor α and γ (EF1α, γ) and reported to time 0, set as 1. Data are means ± SE from 3 experiments (n=3) **I.** Cell viability was quantified by neutral red staining 24 h after treatment with water (control) or 1 µM flg22 or after incubation at 95°C for 3 min (positive control of cell death). Values are means ± SD of two independent experiments.

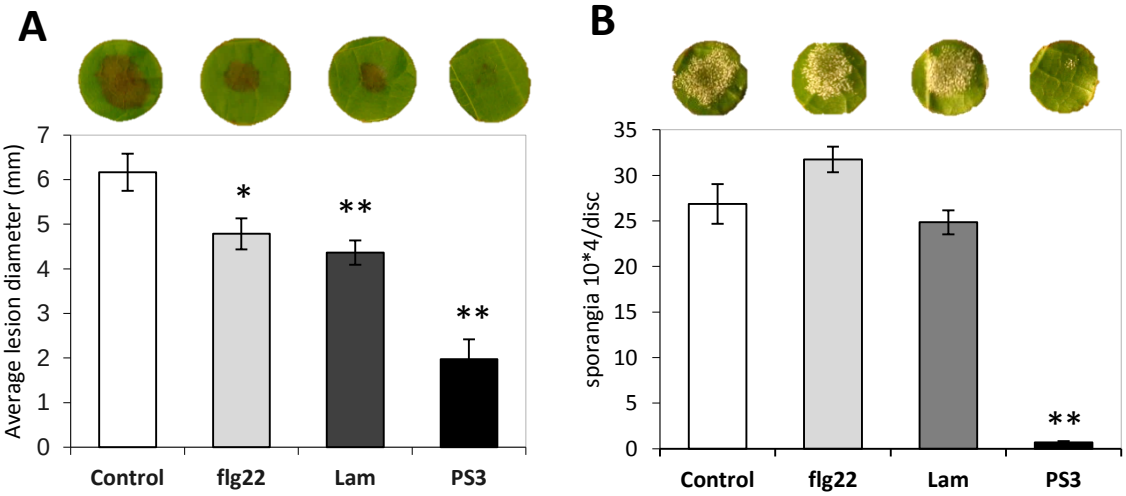

Figure 19. Flg22 enhances the resistance against *Botrytis cinerea* but not *Plasmopara viticola*. *(Find the legend on the next page).*

protection against *B. cinerea* in grapevine (Aziz *et al.*, 2003). However, the partial protection provided by flg22 pretreatment was weaker than protection induced by the sulfated laminarin (PS3), previously described to highly protect grapevine against *P. viticola* (Trouvelot *et al.*, 2008; Gauthier *et al.*, 2014). In a similar experimental setup, we have not observed any significant effect of the flg22 pretreatment on severity of disease symptoms caused by *P. viticola*. Both the mean number of sporangia per leaf disc and the sporulating area estimated visually (data not shown) remained statistically not significant, while the PS3 treatment *quasi* abolished the *P. viticola* sporulation (Fig. 19B).

2 *In silico* characterization of the predicted grapevine FLAGELLIN SENSING 2 receptor: VvFLS2

As grapevine responds to flg22 treatment, we aimed to identify the corresponding flagellin receptor. A phylogenetic analysis indicates that the grapevine genome carries a unique predicted gene encoding the putative ortholog of AtFLS2, hereby designated as VvFLS2 (CAN78669.1/ XP_002272319.2), which is clearly distinct from other grapevine LRR-RLKs (Fig. 20A). Alignment with AtFLS2 (Annex 2) permitted the identification of an upstream sequence encoding the 26 amino acids of the VvFLS2 signal peptide that was unpredicted by the NCBI. The full length *VvFLS2* gene (KF562727) consists of an open-reading frame of 3516 bp and contains a small 105-bp intron at position 1050, a location conserved amongst Arabidopsis *AtFLS2*, tomato *LeFLS2* and rice *OsFLS2* (Fig. 20B). Therefore, *FLS2* homologs exhibit a highly conserved gene structure.

The predicted encoded protein of 1171 amino acids, called VvFLS2, contains a signal peptide, a LRR ectodomain, a single transmembrane domain and a non-RD-type intracellular kinase domain also found in other FLS2 proteins (Fig. 20C, Annex 2; Boller and Felix, 2009). The LRR domain of VvFLS2 consists of 28 tandem repeats, similarly to AtFLS2 and LeFLS2, which is one repeat more than OsFLS2. The VvFLS2 protein sequence exhibits 72% similarity with AtFLS2, 77% with LeFLS2 and 66% with OsFLS2 (Table 10). LRR domains of VvFLS2 and LeFLS2 share 64% amino acid identity compared to 56% sequence identity found between VvFLS2 and AtFLS2 LRR domains (Table 10). Since LeFLS2 and OsFLS2 showed the highest homology to AtFLS2 and were identified as functional flagellin receptors in their respective species (Robatzek *et al.*, 2007; Takai *et al.*, 2008), VvFLS2 was a promising candidate to function as flagellin receptor in grapevine.

Under non-elicited conditions, *VvFLS2* gene is weakly expressed in grapevine cells. Indeed, the amount of *VvFLS2* transcripts is 100-fold lower than the transcripts level of the housekeeping gene *VvEF1γ*, and 5-fold lower than the *VvRbohD* transcripts, encoding another plasma membrane-associated protein (Fig. 21A). The expression of *VvFLS2* was monitored after

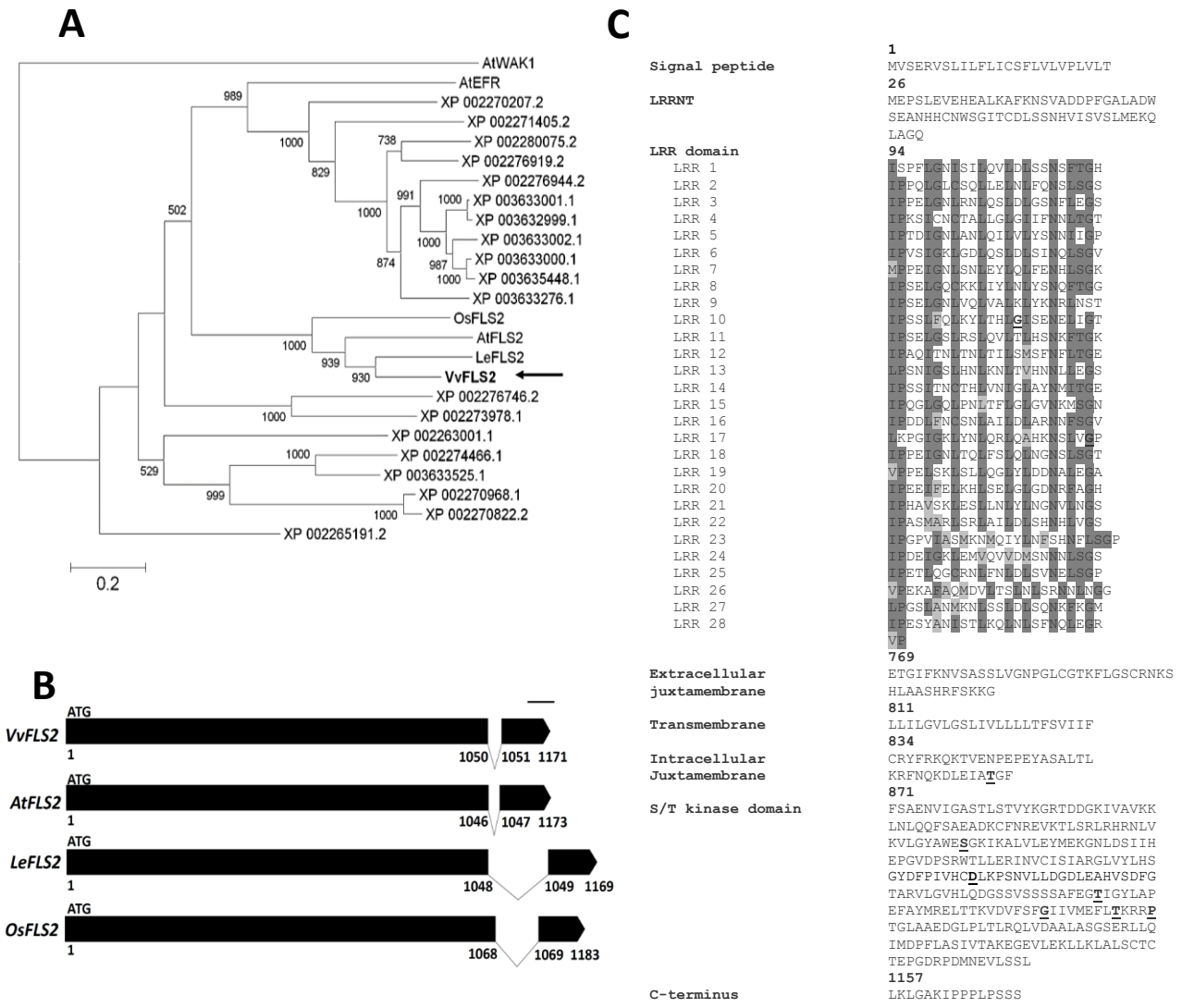

Figure 20. ***In silico*** **characterization of the putative grapevine VvFLS2 ortholog.**
A. Maximum-likelihood phylogenetic tree showing the relationship between the protein sequences (GenBank) of the Arabidopsis FLAGELLIN SENSING2 (AtFLS2), its identified orthologs in tomato (LeFLS2), rice (OsFLS2) and the most similar protein sequences of *V. vinifera*, including the predicted VvFLS2. Only bootstraps higher than 500 (from 1000) are presented. **B.** Exon-intron architecture of coding regions of VvFLS2 and FLS2 orthologs. Black boxes represent exons, numbers represent codons. Bar = 200 bp. **C.** Deduced amino acid sequence of the cloned *VvFLS2* cDNA with indication of predicted signal peptide, the N-terminal domain (LRRNT), the LRR domain, extracellular juxtamembrane region, the single transmembrane domain, the intracellular juxtamembrane region, the serine/threonine (S/T) kinase domain and the C-terminal tail. Amino acids matching LRR consensus $\frac{L}{I}GxLxxLxx\frac{L}{I}xL\frac{S}{T}xNxL\frac{S}{T}GxIPxx$ according to Mueller *et al.* (2012) are shaded in gray. Highlighted in bold and underlined are aminoacids affecting FLS2 signaling in Arabidopsis when mutated (Cao *et al.*, 2013; Robatzek and Wirthmueller, 2012).

Figure 19. Flg22 enhances the resistance against *Botrytis cinerea* but not *Plasmopara viticola*.
Leaf discs were pre-treated with flg22 (10 µM), laminarin (2.5 g l^{-1}) or sulfated laminarin (PS3; 2.5 g l^{-1}) in a surfactant or with surfactant alone (control) 48h before infection. **A.** Disease progression caused by *B. cinerea* at 3 days post inoculation (dpi). Values represent the means of lesion diameters ± SE (n≥30 lesions per experiment) from one experiments out of three. **B.** Infection symptoms caused by *P. viticola* at 7 dpi. Sporulation intensity was evaluated by counting sporangia on two sets of 5 randomly pooled discs, each set was counted at least 4 times with a haemocytometer and expressed as a number of sporangia per leaf disc. Values represent the mean ± SE (n≥8) from two experiments. Asterisks indicate statistically significant difference between control and elicitor treatment (t-test, *: p<0,05, **: p<0,01). A representative leaf disc for each treatment is shown.

treatment of grapevine cells with flg22 or other MAMPs, from 15 min to 24 h. The flg22 treatment transiently induced the expression of *VvFLS2* at 1 hpt (Fig. 21B). This induction was specific to the flg22 treatment, as no modification of *VvFLS2* gene expression was observed with chitin or laminarin treatment, at any studied time-point (Fig. 21C; data are only shown for 1 hpt).

The upregulation of *VvFLS2* expression after the flg22 treatment supports the choice of this gene as a good candidate for flagellin receptor. Further functional genomics studies were needed to confirm its involvement in flagellin perception.

3 VvFLS2 functionally complements the Arabidopsis *fls2* mutant and is localized at the plasma membrane

To investigate whether VvFLS2 is the true ortholog of AtFLS2, the functional complementation of the Arabidopsis *fls2* mutant (Zipfel *et al.*, 2004) was undertaken in collaboration with Drs Cyril Zipfel and Freddy Boutrot (The Sainsbury Laboratory, Norwich, UK), who carried out the Arabidopsis transformation, screened the mutant complemented lines before providing us the T3 generation of the most interesting lines.

The full-length *VvFLS2* cDNA was cloned into the binary expression vector pK7FWG2 (Fig. 14C), which was used to obtain stable Arabidopsis transgenic lines expressing *p35S::VvFLS2-GFP*. Expression of *VvFLS2* in the *fls2* mutant restored the ROS production after flg22 treatment in 17 of the 24 independent kanamycin-resistant transgenic T1 lines tested (Fig. 22A). This ROS production was correlated with VvFLS2-GFP accumulation detected by Western blotting using an anti-GFP antibody (Fig. 22A). For further characterization, the stable homozygous T3 lines #3 and #15 carrying a single *VvFLS2* transgene were selected. These lines were responsive to flg22 as assayed by measurement of ROS production and seedling growth inhibition triggered by 1 µM flg22, while the *fls2* mutant was unresponsive (Fig. 22B, C).

In addition, in agreement with the presence of a predicted signal peptide and a transmembrane domain (Fig. 20C), VvFLS2-GFP was localized to the cell periphery on confocal microscopy analysis of leaves from *fls2/p35S::VvFLS2-GFP* #3 plants (Fig. 22D). The green fluorescence of VvFLS2-GFP followed the plasma membrane shrinking during plasmolysis triggered by 1 M NaCl (Fig. 23A), and co-localized with the red fluorescence of the plasma membrane probe FM4-64 (Fig. 23B). These data demonstrate that VvFLS2 is localized at the plasma membrane. Together, these results show that VvFLS2 is a functional flg22 receptor capable of complementing the loss of FLS2 in Arabidopsis.

4 Recognition specificities of flagellin perception in grapevine

Following data were obtained in collaboration with Drs Stéphan Dorey and Olivier Fernandez (Université de Reims, FR).

	whole protein sequence		LRR domain (LRR1-LRR28)	
	Identity	Similarity	Identity	Similarity
LeFLS2 vs AtFLS2	54%	70%	54%	70%
OsFLS2 vs AtFLS2	45%	63%	45%	63%
VvFLS2 vs AtFLS2	56%	72%	56%	72%
VvFLS2 vs LeFLS2	64%	77%	64%	77%
VvFLS2 vs OsFLS2	51%	66%	52%	68%
LeFLS2 vs OsFLS2	49%	65%	50%	66%

Table 10. Percentage of amino acid identity or similarity between AtFLS2, LeFLS2, OsFLS2 and VvFLS2. Results were obtained with the NCBI BLAST program on the whole protein or the LRR domain of AtFLS2, LeFLS2, OsFLS2 and VvFLS2.

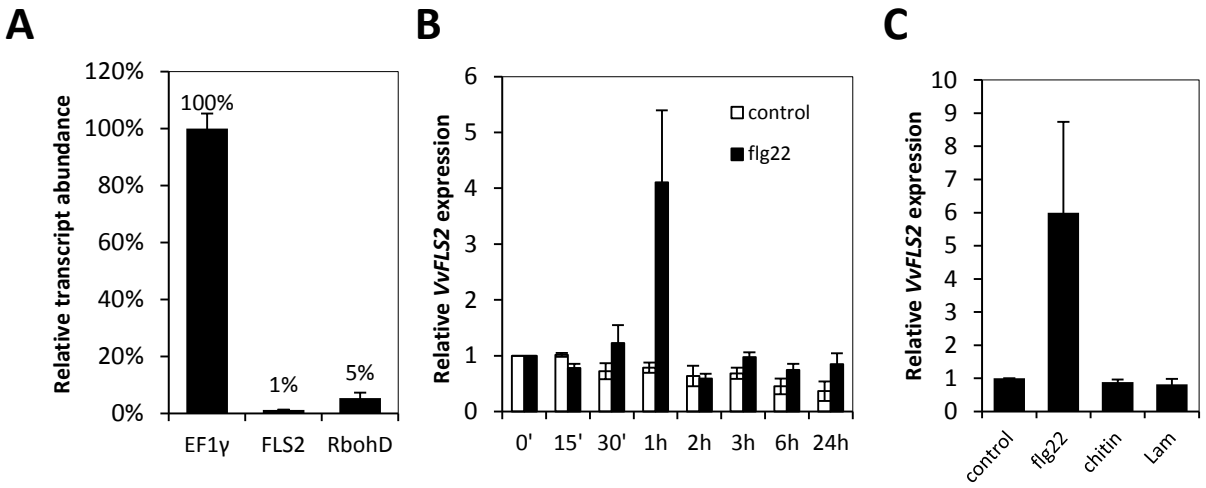

Figure 21. VvFLS2 is a low abundant transcript but transiently induced by flg22.
The transcript level of *VvFLS2*, *RbohD* genes and the housekeeping gene *EF1γ* was assessed by qPCR in MAMP- or mock-elicited grapevine cells and quantified with a LinReg program (Ruijter *et al.*, 2009). **A.** The transcript abundance in mock-treated samples were expressed as means ± SE from 3 experiments and reported to the amount of *EF1γ* transcripts, set as 100%. **B.** Kinetics of *VvFLS2* gene expression induced by 1µM flg22 (black bars) or water (white bars) and reported to time 0, set as 1. **C.** Fold-change of *VvFLS2* expression at 1 hour post treatment with flg22 (1µM), chitin (1 g l^{-1}), or laminarin (Lam, 1 g l^{-1}). For **B.** and **C.**, the relative expression of *VvFSL2* is expressed as means ± SE from three experiments (n=3).

4.1 Perception of *B. phytofirmans*-derived flg22 induces weaker defense responses in grapevine than do *X. campestris*- or *P. aeruginosa*-derived flg22

Burkholderia phytofirmans is a PGPR well adapted to grapevine, and promotes a very marked plant growth (Ait Barka *et al.*, 2000; Compant *et al.*, 2005b; Lo Piccolo *et al.*, 2010). Compared with *P. syringae* pv *pisi*, the perception of *B. phytofirmans* triggers weak defense responses in grapevine (Bordiec *et al.*, 2011) whereas a marked *PR1* gene expression was observed in Arabidopsis *pPR1::GUS* seedlings (Fig. 24A). In grapevine, the elicitation of two defense genes by a boiled crude extract from *B. phytofirmans* was greatly affected by proteinase K treatment (Fig. 24B). Moreover, purified flagellin from *B. phytofirmans* was sufficient to elicit Arabidopsis *PR1* gene expression (Fig. 24C, D). All these results suggest that flagellin might be an active MAMP of *B. phytofirmans*.

To investigate whether and how grapevine perceives flagellin from its associated PGPR, the eliciting activity of the flg22 peptide, based on the flagellin sequence from *B. phytofirmans* strain PsJN (Bp flg22), was tested in grapevine cells and compared to flg22 from *P. aeruginosa* strain PAK (Pa flg22), *X. campestris* pv *campestris* strain 305 (Xc flg22) and *A. tumefaciens* strain C58C1 (At flg22). *P. aeruginosa* PAK and *X. campestris* 305 have been previously described as plant pathogenic bacteria in lettuce and Arabidopsis, respectively (Rahme *et al.*, 1997; Sun *et al.*, 2006). Compared with the classical Pa flg22 sequence, Xc flg22 and At flg22 have 4 and 12 amino acid substitutions, respectively (Fig. 25A). Interestingly, the Bp flg22 epitope possesses 6 amino acid substitutions compared to the Pa flg22 sequence but only 3 with Xc flg22 (underlined Q1T, L7K and K13A; Fig. 25A).

Measured in apoaequorin-expressing grapevine cells, Bp flg22 reproducibly induced a lower variation in free $[Ca^{2+}]_{cyt}$ than Pa flg22 and Xc flg22 whereas At flg22 remained unable to induce any $[Ca^{2+}]_{cyt}$ variation (Fig. 25B) .

Dose-response oxidative burst assays revealed that Bp flg22 triggered production of H_2O_2 in grapevine, but to a lesser extent than Pa flg22 or Xc flg22 (Fig. 25C). The determination of the half-maximal response (EC_{50}) revealed that Xc flg22 was the most active epitope with an EC_{50} = ~80 nM compared to EC_{50} = ~300 nM for Pa flg22. The low activity of Bp flg22 is illustrated by an EC_{50} estimated at ~ 8 µM if higher concentrations reached the same plateau. Indeed, at the maximal concentration tested (10 µM), Bp flg22 was still less active than either Pa flg22 or Xc flg22 at 500 nM. Finally, At flg22 seems to be inactive in grapevine as no H_2O_2 production nor calcium variation could be detected even at a concentration of 10 µM.

The expression of typical grapevine defense marker genes (Aziz *et al.*, 2003; Bordiec *et al.*, 2011) was followed at 1, 6, 9 and 24 hpt, using 1 µM of each flg22 peptide. On the whole, maximal inductions were observed at 6 hpt. At this time point, Pa flg22 and Xc flg22 induced a high accumulation of the 4 defense gene transcripts encoding a β-1,3 glucanase (*Gluc*), *PR1.2*, a proteinase inhibitor (*PR6*) and an acidic chitinase (*Chit4c*) (Fig. 25D). By contrast, Bp flg22

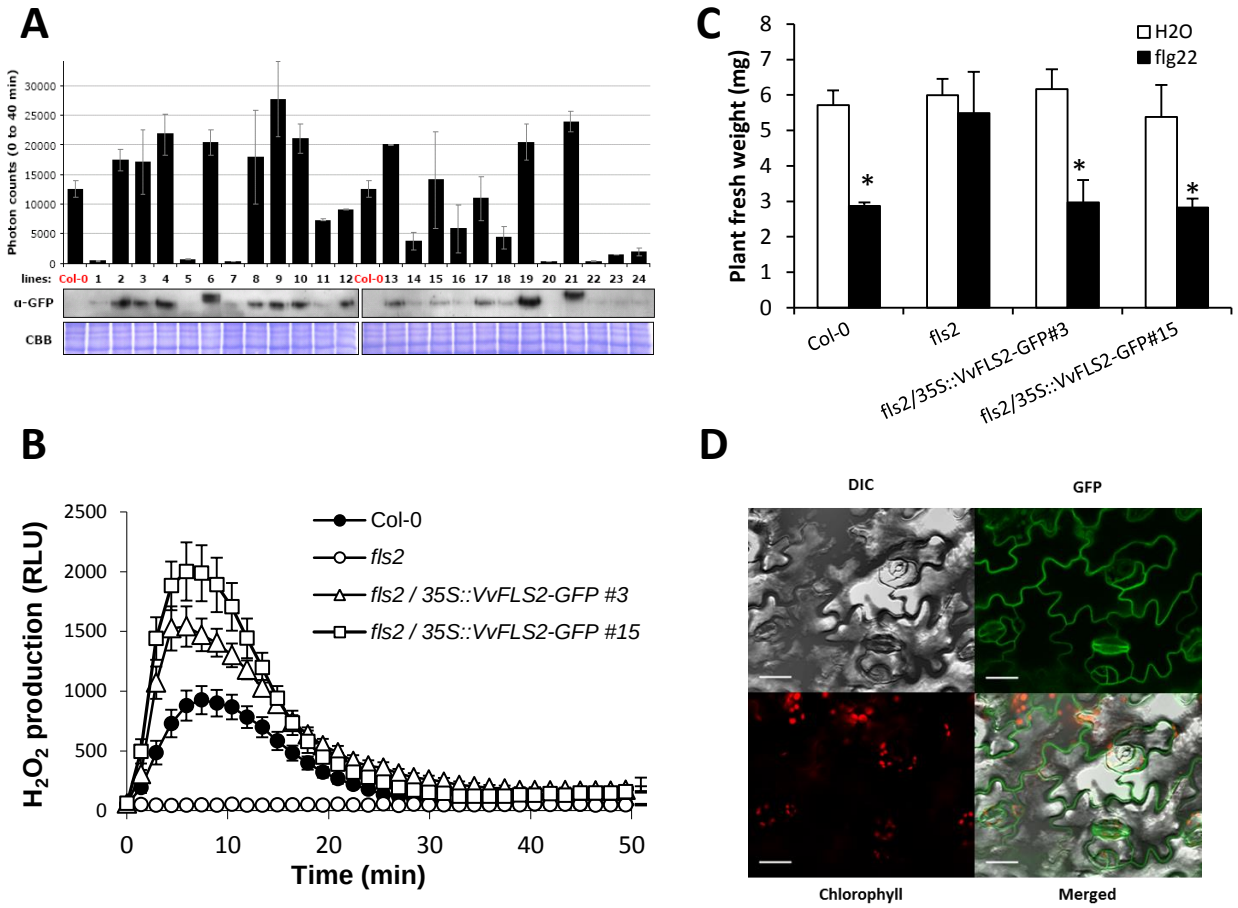

Figure 22. VvFLS2 complements the Arabidopsis *fls2* mutant and is localized at the plasma membrane.
A. Correlation between H_2O_2 production after flg22 treatment (100 nM) and VvFLS2-GFP protein amount detected by α-GFP immunoblot in different T1 lines *fls2/p35S::VvFLS2-GFP*. Equal loading was checked by Coomassie brilliant blue (CBB) staining. (*Fig. A from F. Boutrot*) **B.** H_2O_2 production after flg22 treatment (1 µM) in leaf discs of homozygous single copy T3 complemented lines #3 and #15. Data represent means ± SE in at least 16 leaf discs from 8 plants of two independent experiments. For **A.** and **B.**, ROS production was measured using chemiluminescence of luminol and photon counts were expressed as relative luminescence units (RLU). **C.** Flg22-induced growth inhibition is restored in the complemented mutant *fls2/p35S::VvFLS2-GFP* (lines #3 and #5), when compared with Col-0 (WT) and the *fls2* mutant. Data represent means ± SD (n=15). Asterisks indicate statistically significant difference between control and flg22 treatment (t-test; $p<0.05$). Similar results were obtained in three independent experiments. **D.** Subcellular localization of VvFLS2-GFP visualized by confocal microscopy in leaves of Arabidopsis *fls2* mutant transformed with *p35S::VvFLS2-GFP* line #3. DIC: differential interference contrast. Bars = 20 µm.

induced only a weak expression of *Gluc*, *PR1.2* and *PR6* (Fig. 25D, E) whereas an intermediate upregulation of *Chit4c* was detected (Fig. 25D, F). However, the Bp flg22-triggered *Chit4c* gene expression was very transient compared with the long-lasting effect of Xc flg22 and Pa flg22 treatments (Fig. 25F). In addition, the *17.3* gene, which is a SA marker in grapevine (Bordiec *et al.*, 2011), was strongly induced at 1 hpt by Xc flg22 and Pa flg22, but not by Bp flg22 (Fig. 25G). On the whole, our results show that Bp flg22 elicits only weak defense responses in grapevine. The treatment with At flg22 was totally unable to elicit defense gene expression (Fig. 25D-G).

4.2 AtFLS2 and VvFLS2 have different recognition specificities

B. phytofirmans is able to colonize Arabidopsis and to stimulate its growth in laboratory conditions (Poupin *et al.*, 2013; Zuniga *et al.*, 2013). However, both effects are less pronounced than in grapevine (Compant *et al.*, 2005b; Zuniga *et al.*, 2013), suggesting potential differences in the perception of this bacterium between grapevine and Arabidopsis. Previous studies have reported different perception specificities between FLS2 from tomato and Arabidopsis (Felix *et al.*, 1999; Bauer *et al.*, 2001; Sun *et al.*, 2006; Robatzek *et al.*, 2007; Mueller *et al.*, 2012). We therefore characterized the eliciting activity of Bp flg22 in Arabidopsis. In Arabidopsis cells, Bp flg22 triggered an oxidative burst comparable with that triggered by Pa flg22 and Xc flg22 (Fig. 26A). As a significant correlation has been observed between flg22 eliciting activity and seedling growth inhibition (Vetter *et al.*, 2012), we carried out seedling growth inhibition assays in Arabidopsis. On WT Col-0, we have shown that the level of reduction in seedling weight after treatment with Bp flg22 was comparable with the growth inhibition caused by Pa flg22 and Xc flg22 (Fig. 26C). The seedling growth inhibition induced by the three active flg22 epitopes was not observed in the *fls2* mutant, indicating that their perception was strictly FLS2 dependent (Fig. 22C and data not shown). The growth inhibition activity of flg22 peptides correlated with their ability to induce comparable *PR1* expression as revealed using *pPR1::GUS* expressing plants (Fig. 27A). As published previously (Felix *et al.*, 1999; Bauer *et al.*, 2001), At flg22 did not elicit any biological response (Fig. 26A, C, 27A).

In contrast with its strong eliciting activity in Arabidopsis, we found that Bp flg22 is a weak elicitor in grapevine. In addition to activating only a weak oxidative burst (Fig. 26B) and defense gene induction (Fig. 25D-G), Bp flg22 did not significantly inhibit grapevine plantlet growth, in contrast to what was observed on Xc flg22 treatment (Fig. 26D, 27B). Indeed, Xc flg22 was highly active in grapevine inducing strongly both defense gene expression and growth inhibition (Fig. 25D-G, 26D, 27B). In addition, grapevine plants challenged with Xc flg22 displayed a root darkening phenotype that was not observed on treatments with other flg22 peptides (Fig. 27B), or in Arabidopsis (data not shown).

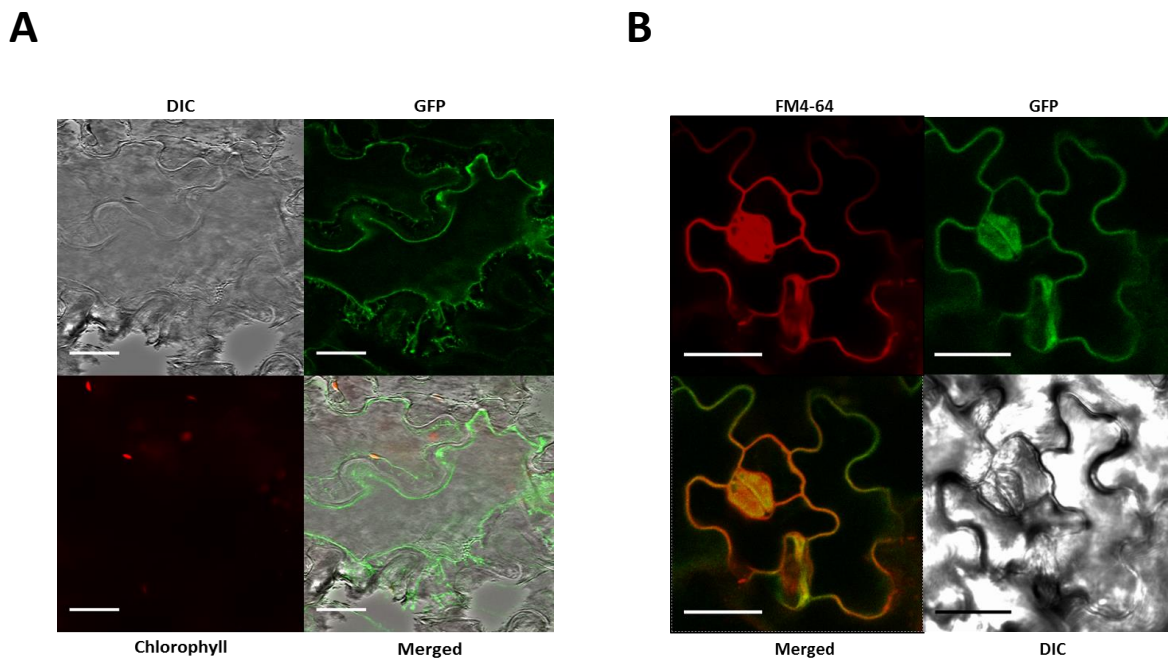

Figure 23. Confirmation of the plasma membrane localization of VvFLS2.
A. VvFLS2-GFP follows the plasma membrane shrinking during plasmolysis induced by 1M NaCl. **B.** The green fluorescence of VvFLS2-GFP colocalizes with the red fluorescence of the plasma membrane probe FM4-64. Pieces of leaves were mounted in distilled water or in 1M NaCl solution for plasmolysis experiments. For FM4-64 staining, samples were incubated in 8 µM FM4-64 in water during 10 min before observation. DIC: differential interference contrast. Bars = 20 µm.

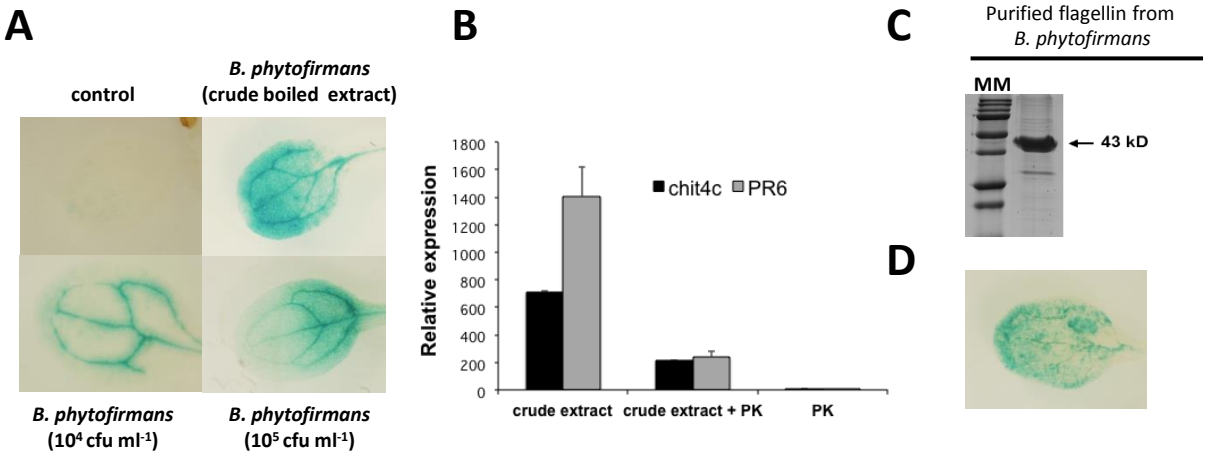

Figure 24. *Burkholderia phytofirmans* living bacteria, crude extract or purified flagellin trigger grapevine and Arabidopsis immunity.
A. Arabidopsis *pPR1::GUS* seedlings were incubated with living *B. phytofirmans* bacteria at the indicated densities or with their boiled extract for 24 hours. **B.** Expression of the grapevine defense genes *Chit4c* and *PR6*, 24 h after challenge with *B. phytofirmans* crude extract in presence or absence of proteinase K (PK). **C.** SDS-PAGE analysis of the 43 kD purified flagellin (arrow) from *B. phytofirmans* following the purification protocol described by Felix *et al.* (1999). MM: molecular weight marker. **D.** Arabidopsis *pPR1::GUS* seedlings were treated with purified flagellin from *B. phytofirmans*. For **A.** and **D.**, *PR1* expression was revealed by GUS staining at 24 hours post-challenge. (*Fig. A.-D. from S. Dorey, O. Fernandez*)

Given the polymorphism existing between AtFLS2 and VvFLS2 (Table 10), we tested if FLS2 was responsible for the observed species-specific differences in flg22 perception using growth inhibition assays on *fls2/p35S::VvFLS2* Arabidopsis seedlings. While in WT Col-0, all three flg22 epitopes exhibited similar biological activities (Fig. 28A; Table 11), Xc flg22-challenged *fls2/p35S::VvFLS2* plants were consistently and significantly smaller than Bp flg22-challenged plants (Fig. 28B; Table 11). Therefore, the expression of *VvFLS2* in *fls2* background conferred differential flg22 responses characteristic for grapevine (compare Fig. 26D and 28B). These results suggest that VvFLS2 has evolved to distinguish flagellin originating from the grapevine-associated PGPR *B. phytofirmans*.

4.3 *B. phytofirmans* overcomes Xc flg22-induced MTI to colonize grapevine plants

We hypothesized that *B. phytofirmans* flagellin partially evades strong recognition to enable successful plant colonization. As a corollary, we investigated whether the activation of MTI by fully active flagellin-derived peptide would reduce the PGPR colonization. Roots of grapevine plantlets grown *in vitro* were exposed to 1 µM Xc flg22, which displayed the strongest eliciting activity in grapevine, for either 1 minute (co-treatment) or 24 h prior to the inoculation with living *B. phytofirmans* bacteria. Surprisingly, we observed that treatment with Xc flg22 did not affect the colonization of grapevine leaves or roots (Fig. 29). These results suggest that *B. phytofirmans* might overcome flg22-induced MTI to colonize grapevine plants.

5 Silencing of VvFLS2 in grapevine induced defects in flg22 immune signaling

5.1 Generation of antisense VvFLS2 lines

In parallel to the complementation assays in Arabidopsis, we aimed to posttranscritionally silence the *VvFLS2* gene in grapevine using an antisense construct (Gateway binary expression vector pH2WG7, Fig. 14E; Karimi *et al.*, 2002). Indeed, plants silenced in *VvFLS2* would be a perfect tool to investigate the involvement of flagellin-triggered immunity in grapevine, notably during its interactions with bacteria.

The antisense fragment of 210 bp was designed to target the region 1602-1811 bp within the LRR ectodomain of VvFLS2 (Fig. 30). This fragment confers specificity for the *VvFLS2* silencing, according to BLAST programs on Genoscope 12x and NCBI databases.

Transgenic *in vitro* plantlets overexpressing the *VvFLS2* fragment in the antisense orientation (*αsVvFLS2*) were generated from *Vitis vinifera* cv Pinot Noir PN40024 by the grapevine transformation platform (Jean Masson, Mireille Perrin, Carine Schmitt, INRA, Colmar, FR). The *Agrobacterium*-mediated transformation of PN40024 embryogenic calli with pH2WG7 *p35S::αsVvFLS2* (Fig. 15) resulted in 68 hygromycin-resistant calli issued from independent

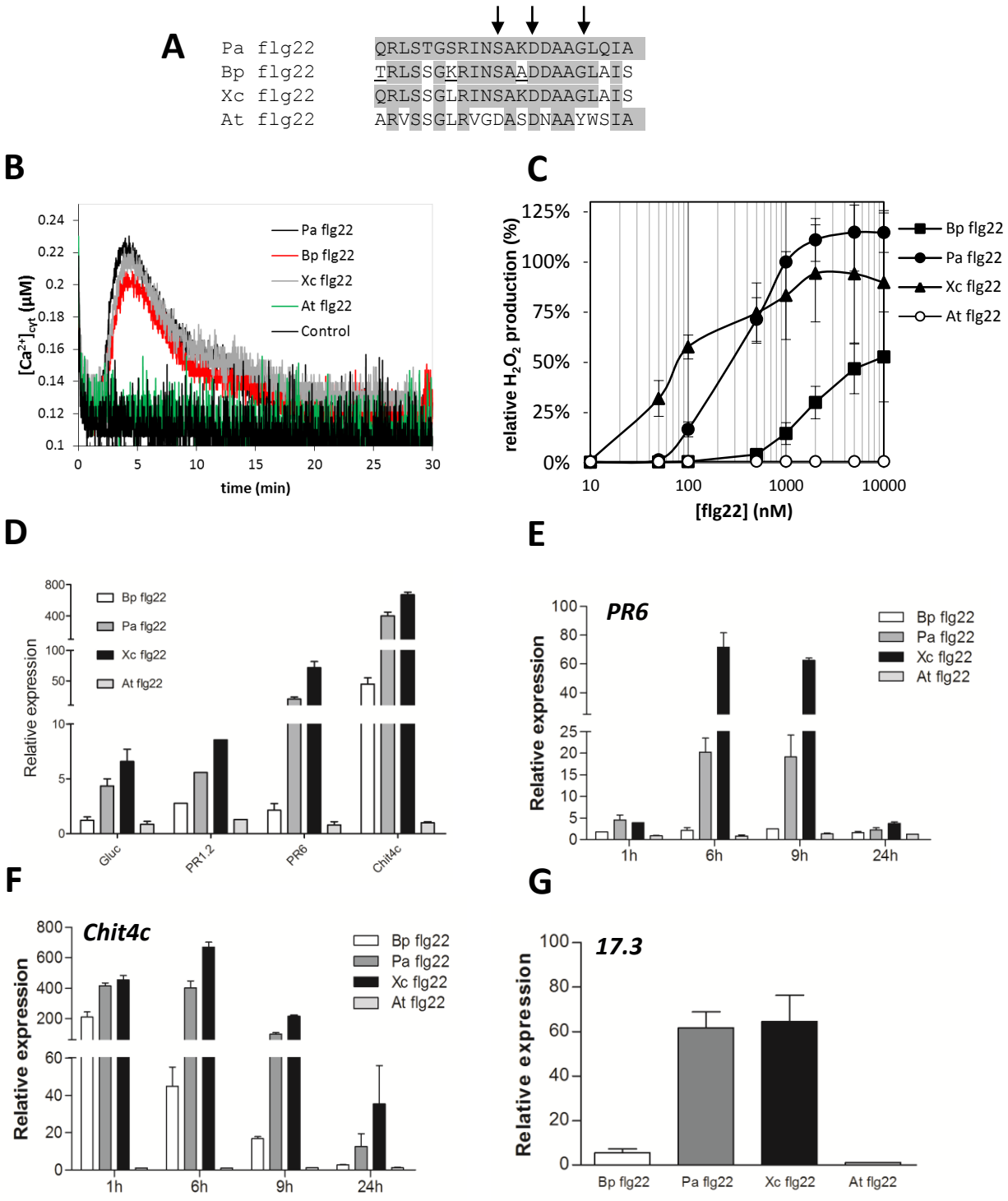

Figure 25. flg22 from the plant growth-promoting rhizobacterium (PGPR) *Burkholderia phytofirmans* triggers weaker signaling and defenses in grapevine cells than flg22 from *Pseudomonas aeruginosa* or *Xanthomonas campestris*.

A. Alignment of flg22 from bacteria *P. aeruginosa* (Pa), *B. phytofirmans* (Bp), *X. campestris* (Xc), and *A. tumefaciens* (At). Arrows indicate key amino acids for flg22 eliciting activity in tomato cells (Felix *et al.*, 1999). Underlined amino acids differ between Bp flg22 and Xc flg22. **B.** Variation in free $[Ca^{2+}]_{cyt}$ in apoaequorin expressing cells. **C.** Dose-response of flg22-induced H_2O_2 production 15 min post treatment, measured by luminol chemiluminescence. Data are expressed as percentage of response induced by 1 µM Pa flg22 and graphics show means ± SD of three independent experiments. **D.-G.** Flg22-induced expression of defense genes quantified by qPCR. Means of triplicate data were normalized by housekeeping genes *EF1a* and *60SRP* and compared to water treated control, set as 1. **D.** Expression of genes encoding a β-1,3 glucanase (*Gluc*), a PR1 protein (*PR1.2*), a proteinase inhibitor (*PR6)* and an acidic chitinase (*Chit4c)* at 6 hpt. **E., F.** Kinetics of *PR6* (**E.**) and *Chit4c* (**F.**) defense gene induction. **G.** *17.3* gene expression at 1hpt. Cells were treated with 1µM of Bp flg22 (white bars), Pa flg22 (dark gray bars), Xc flg22 (black bars) or At flg22 (light gray bars).

transformation events. Using primers matching the 3' end of the *p35S* promoter and the 5'end of the antisense fragment (Fig. 30), the RT-PCR transgene detection permitted the selection of 10 *asVvFLS2*-expressing calli, hereafter referred as lines #2-2 up to #2-22, for *in vitro* plantlet regeneration *via* somatic embryogenesis (Fig. 15). At the beginning, the root system was poorly developed and plantlets growth was very low, probably due to stresses accumulated during the *Agrobacterium*-mediated transformation and the somatic embryogenesis. By optimizing the culture conditions (Material and Methods, §1.1.2), 9 of the 10 independent transgenic lines finally possessed a similar developmental phenotype compared with the mock-transformed wild-type plants (*Vitis vinifera* PN40024) issued from a parallel somatic embryogenesis (seWT). The line #2-10 was an exception with a dwarf phenotype. These 10 independent *asVvFLS2* lines were then screened for the expression levels of *VvFLS2* transcript and the loss of flg22 responsiveness in leaves of regenerated *in vitro* plantlets. The flg22-responsive phenotype was compared with seWT.

5.2 Screening of *asVvFLS2* lines for *VvFLS2* transcript amounts and flg22 responsiveness

In at least two independent biological experiments, the amounts of *VvFLS2* transcripts were quantified by qPCR with *VvFLS2* specific primers matching the 5' end of the transcript (Fig. 30). Fig. 31A indicates that *VvFLS2* transcription was not silenced in most of the lines and some lines such as #2-13 possessed even more *VvFLS2* transcripts than seWT. However, the lines #2-11, #2-16 and #2-22 showed a lower *VvFLS2* transcript amount reaching 75%, 63% and 46% of the *VvFLS2* transcripts level in seWT, respectively (Fig. 31A).

A toolbox was developed to follow flg22 responsiveness in leaves of plantlets grown *in vitro* (Material and Methods, § 2.1.2, 2.1.4, 2.1.5). As a first overall screening, the flg22-induced MAPK phosphorylation was detected by Western blotting. Chitin treatment served as a control of a VvFLS2-independent immune signaling pathway. By contrast to the seWT and other transgenic lines which responded strongly to both elicitors, the antisense line #2-22 was the only one displaying a reduced flg22-induced MAPK phosphorylation while the chitin response was not altered (Fig. 31B). No defect in MAPK signaling was observed in lines #2-11 or #2-16 (Fig. 31B). Our preliminary results showed that silencing was partly successful only in the line #2-22.

5.3 The line #2-22 is affected in flg22 signaling

In four independent experiments, the MAPK activation triggered by flg22 was significantly reduced compared with that triggered by chitin (Fig. 32A). In addition to MAPK signaling, other defense responses were tested in the line #2-22. The flg22-triggered oxidative burst was quantified in parallel to the elicitation induced by oligogalacturonides (OG), used as a FLS2-independent immune signaling pathway. Indeed, chitin could not be used for this purpose as it does not elicit ROS production in grapevine (Part III, Results §1). The relative flg22-induced

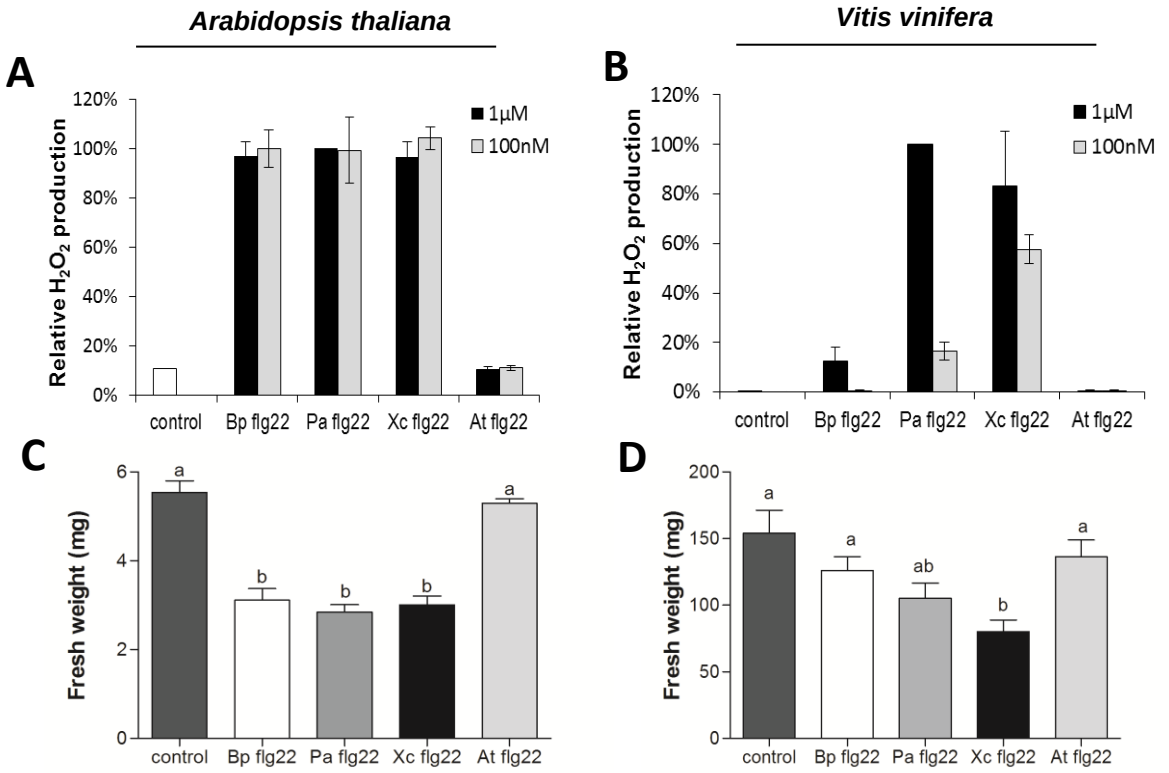

Figure 26. Species-specific differences in flg22 perception between Arabidopsis and grapevine revealed by ROS production and plant growth inhibition.
A., B. ROS production was measured at 15 min by chemiluminescence of luminol on *A. thaliana* (**A**) or *V. vinifera* (**B**) cell suspension cultures after treatment with Bp flg22, Pa flg22, Xc flg22, At flg22 peptides or water control. Data are means ± SD of three independent experiments and are expressed as percentage of response induced by 1 µM Pa flg22. **C., D.** Arabidopsis (**C**) and grapevine (**D**) growth inhibition on *in vitro* plants triggered by 1 µM Bp flg22, Pa flg22, Xc flg22, At flg22 and compared to water control (n=30). Different letters indicated significant differences (one way ANOVA test followed by a Tukey-Kramer test; $p<0.05$). Similar results were obtained in three independent experiments. *(Fig. C,D from O. Fernandez)*

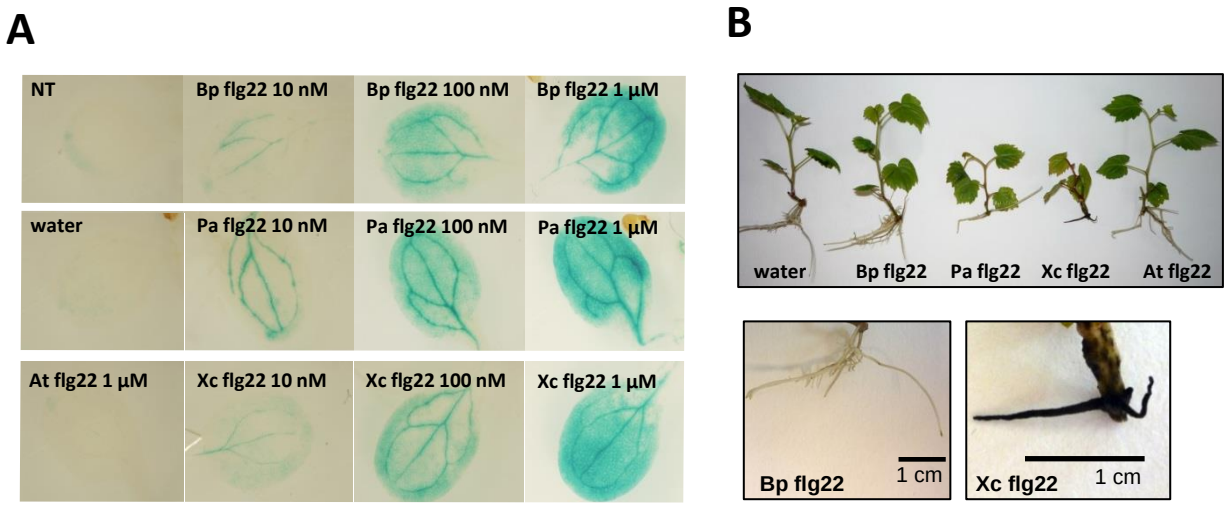

Figure 27. Bp flg22, Pa flg22 and Xc flg22 induce similar responses in Arabidopsis but not in grapevine.
A. flg22-induced expression of *PR1* defence gene was assayed in Arabidopsis *pPR1::GUS* reporter line. Seedlings were treated with Bp flg22, Pa flg22, Xc flg22, At flg22 at the indicated concentrations or with water or non-treated (NT). *PR1* activation was revealed by GUS staining at 24 hours post-challenge. **B.** Representative pictures of growth inhibition in grapevine *in vitro* plantlets triggered by different flg22 peptides (1µM) and compared to water control (n=30). On the right: enlargement of the root system from grapevine plantlets challenged by Bp flg22 and Xc flg2. Similar results were obtained in at least three independent experiments. (*Results O. Fernandez*)

ROS production of the line #2-22 represented only 40% of the oxidative burst observed in the control seWT (Fig. 32B). Similarly, the elicited *PR6* transcript amount in line #2-22 represented only 43% of the level quantified by qPCR in the seWT (Fig. 32C).

To sum up, we have characterized the line #2-22, which is partly silenced in *VvFLS2* gene expression. In this line, the decrease of the *VvFLS2* transcripts (46 % of the seWT) correlates with a lower intensity of three distinct immune responses (MAPK activation, oxidative burst and *PR6* gene expression) specifically triggered by flg22. These data show that VvFLS2 is involved in the flg22 perception in grapevine.

5.4 VvFLS2 protein detection

We also aimed to quantify the *VvFLS2* silencing efficiency at the protein level using an antibody raised against VvFLS2. According to previous works, antibodies developed against the Arabidopsis and rice proteins AtFLS2 or OsFLS2 were directed against the very C_{ter} end. These sequences are highly specific and are neither shared by other LRR-RLKs of the same family nor by FLS2 orthologs of other species (Takai *et al.*, 2008; Boutrot *et al.*, 2010, Fig. 33A). However, the BLASTp analysis indicated that the C_{ter} region of VvFLS2 (IPPPLPSSS) was not specific to a unique protein encoded by the grapevine genome. Consequently, we have chosen a specific hydrophilic epitope (KTVENPEPEYASALT) localized in the inner juxtamembrane region of VvFLS2 (Fig. 33A).

ELISA tests carried out by the antibody manufacturer (Proteogenix) and our dot blot experiments revealed that the polyclonal antibody successfully detected the Cys-KTVENPEPEYASALT antigen (C16) and did not detect a non-specific peptide, such as flg22 (Fig. 33B). Thereafter, the capacity to detect VvFLS2 protein was firstly investigated on protein extracts from Arabidopsis *fls2/p35S::VvFLS2-GFP #3* plants.

Western blots with an anti-GFP antibody detected a specific signal for the VvFLS2-GFP fused protein at the molecular mass of ~ 200 kDa (Fig. 33C) that was better visible in samples enriched in membrane fractions (C2 samples) than in total proteins (C1 samples). The theoretical molecular mass of the non-glycosylated fused protein is ~ 157 kDa. As expected, no signal was detected in *fls2* or wild-type (WT) Arabidopsis plants (Fig. 33C). However, Western blots with the anti-VvFLS2 antibody in *p35S::VvFLS2-GFP* samples did not detect any specific signal in the range 150 – 250 kDa (Fig. 33C). These results indicate that the polyclonal antibody α-VvFLS2 failed to immuno-detect the VvFLS2 protein whereas the fused protein is present, as revealed by the α-GFP antibody.

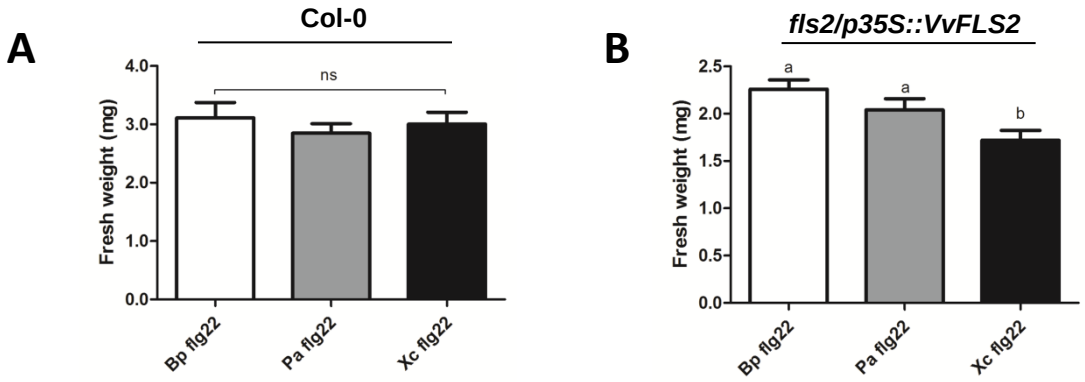

Figure 28. FLS2 is responsible for recognition specificities between grapevine and Arabidopsis.
Arabidopsis growth on 1 µM Bp flg22, Pa flg22 and Xc flg22 in **A.** wild-type Col-0 plants (n=30) or in **B.** the complemented mutant *fls2/p35S::VvFLS2* line #3 (n=30). Different letters indicated significant differences and ns=non significant differences (one way ANOVA test followed by a Tukey-Kramer test; P<0.05). Similar results were obtained in at least three independent experiments. (*Results O. Fernandez*)

	A. thaliana		***V. vinifera***
	Col-0 (WT)	*fls2/p35S::VvFLS2*	Chardonnay (WT)
Control	0 %	0 %	0 %
Bp flg22	43.8 % ± 4.7	40.9 % ± 2.5	18.2 % ± 8.0
Pa flg22	48.5 % ± 2.9	46.7 % ± 3.1	31.8 % ± 10.9
Xc flg22	45.7 % ± 3.6	55.0 % ± 2.7	47.9 % ± 10.8

Table 11. flg22-triggered growth inhibition in Arabidopsis and grapevine
Comparison between *A. thaliana* (wild type (WT) Col-0 and the complemented line *fls2/p35S::VvFLS2* #3) and *V. vinifera* (WT; cv Chardonnay) *in vitro* plantlets grown on 1 µM Bp flg22, Pa flg22, Xc flg22 or water control. Data represent growth inhibition means ± SE (n=30) relative to control, set as 0% of growth inhibition.

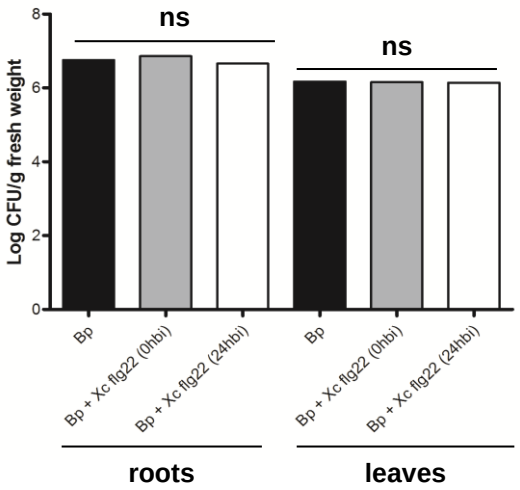

Figure 29. ***Burkholderia phytofirmans*** **overcomes Xc flg22-induced MTI to colonize grapevine plants.**
Grapevine *in vitro* plantlets were challenged at the root level with Xc flg22 (1µM), at the same time or 24 h before inoculation (hbi) with *B. phytofirmans* (Bp). Bacterial counting was performed 4 days later in the roots and the leaves. Data are from one representative experiment (n=8). Similar results were obtained in three independent experiments (ns=non significant according to one way ANOVA test followed by a Tukey-Kramer test; p<0.05). (*Results O. Fernandez*)

6 FLS2-like gene in grapevine

VvFLS2 (CAN78669) is the closest predicted ortholog of AtFLS2, located on the minus strand of the chromosome 10. According to protein BLAST against grapevine genome with AtFLS2 or VvFLS2, CAN78669 is a unique non-duplicated protein prediction. However, a BLAST with the nucleotide sequence of *VvFLS2* revealed that a highly similar sequence (~3.5 kb long) is present on a neighbor locus, hereafter referred as *VvFLS2-like* (Fig. 34). The gene predictions available for this locus, such as GSVIVT01021409001 (Genoscope), cover only partially the hypothetical *VvFLS2-like* coding sequence (CDS). The CDS of *VvFLS2* and the nucleotide sequence of *VvFLS2-like* display 86% of identity with the highest conservation over the encoded kinase domain. At the CRIBI and Genoscope websites, no read for the *VvFLS2-like* transcript has been detected by different RNA sequencing technologies (454, Illumina and Solid) in different tissues from distinct grapevine cultivars (Fig. 34 and data not shown). Moreover, frequent transposable elements exist in a distant promoter (Fig. 34). All these results suggest that *VvFLS2-like* gene might be a pseudogene.

However, we tested if *VvFLS2-like* gene was transcribed. Using specific primers matching the beginning and the end of the hypothetical *VvFLS2-like* CDS (Table 6), no amplification was achieved with cDNA from *V. vinifera* cv Pinot Noir 40024, Gamay nor Chardonnay. Surprisingly, a ~ 3,5 kb-long amplicon was obtained from leaves of cv Marselan (Fig. 35A). Its partial sequencing confirmed the identity of the *VvFLS2-like* transcript, distinct from the *VvFLS2* transcript, and permitted to precise its splicing sites (Fig. 35B). The predicted VvFLS2-like protein sequence displays 81% identity with VvFLS2 and contains a signal peptide, 27 LRR repeats in the ectodomain, a single transmembrane domain and a kinase domain truncated in the last 22 amino acids (Annex 3).

This sequencing also enabled the design of a specific pair of primers that can distinguish *VvFLS2-like* from *VvFLS2* by PCR (Fig. 35C, Table 5). A non-quantitative PCR with these specific primers confirmed that *VvFLS2-like* transcripts are absent in control grapevine tissue from cv Pinot Noir and Gamay (Fig 35D). *VvFLS2-like* expression was not induced by flg22, unlike *VvFLS2* gene that was upregulated by flg22 treatment (Fig. 21B,C, 35D). Even 40 cycles of qPCR were unable to reveal any *VvFLS2-like* amplification from basal or flg22-elicited tissue of cv Pinot Noir and Gamay (data not shown).

We further aimed to determine whether the *VvFLS2-like* gene product from cv Marselan could participate in flagellin perception by performing a complementation assay in Arabidopsis *fls2* mutant. This could be interesting for structure-function studies, as ectodomains of VvFLS2 and VvFLS2-like differ at several residues (Annex 3). However, the preparation of the pK7FWG2 *p35S::VvFLS2-like-GFP* constructs have repeatedly failed. Both 5' and 3' parts of the sequence

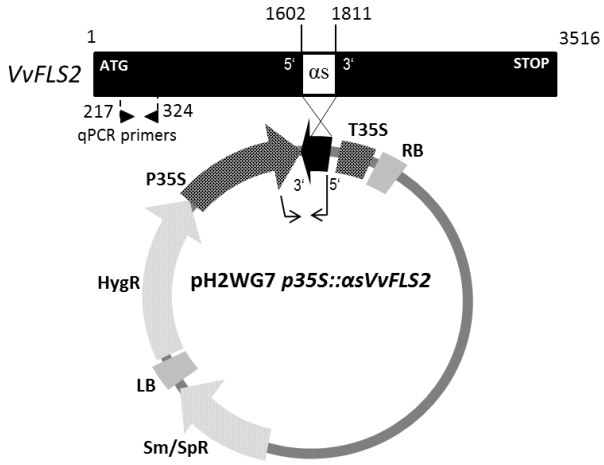

Figure 30. Antisense construct for *VvFLS2* silencing.
Position of the *VvFLS2* antisense fragment (αs) in the *VvFLS2* coding sequence and map of the pH2WG7 *p35S::αsVvFLS2* vector. Nucleotide (nt) 1 indicates the start of VvFLS2 translation. The fragment (nt 1602 – 1811) was PCR-amplified using specific primers and inserted in the antisense orientation into the pH2WG7 vector. pH2WG7 *p35S::αsVvFLS2* was used for the transformation of grapevine embryogenic calli *via Agrobacterium tumefaciens*. Arrows indicate primers used to verify the presence of transgene in transgenic calli and plantlets. Black triangles indicate primers used for *VvFLS2* quantification by qPCR.

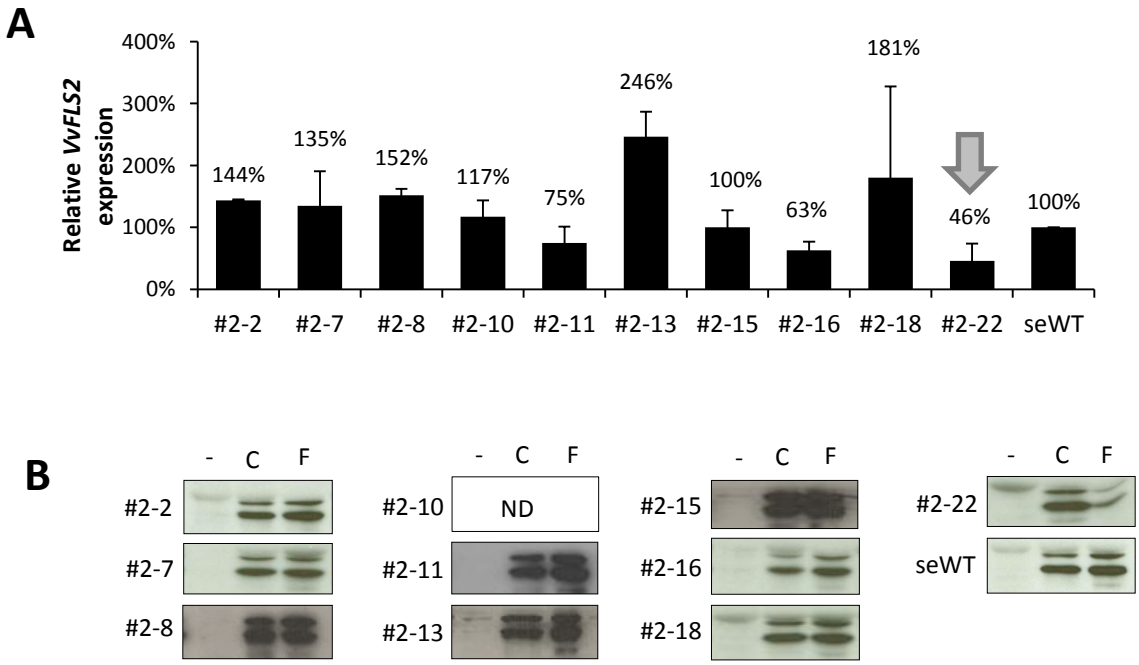

Figure 31. Quantification of VvFLS2 transcript amount and flg22 responsiveness in 10 grapevine transgenic lines expressing *p35S::αsVvFLS2* (#2-2 - #2-22).
VvFLS2 expression and flg22 responsiveness were evaluated in leaves of *in vitro* plantlets expressing *p35S::αsVvFLS2* or in wild-type plants issued from a parallel somatic embryogenesis (seWT). **A.** Relative *VvFLS2* expression was measured by qPCR, normalized to the housekeeping genes *EF1α* and *EF1γ* and reported to seWT, set as 100 %. Data are means ± SD of at least two independent experiments. **B.** Phosphorylation of two MAPKs (45 and 49 kDa) detected by anti-pERK1/2 Western blots at 15 min post treatment with water control (-), 1 g l^{-1} chitin (C) or 500 nM flg22 (F). Homogeneous loading was checked by Coomassie Brilliant Blue (CBB) staining of a parallel gel (not shown). Experiment was repeated twice with similar results. Data from one representative experiment out of two is shown. ND=not determined.

were missing in the final construct which therefore lacked the signal peptide and presented a premature STOP codon in the GFP sequence.

All over, the bioinformatics analyses together with these data suggest that the *VvFLS2-like* locus might be a pseudogene in *V. vinifera* cv Pinot Noir and Gamay while it is transcribed in cv Marselan. Due to the fail of the *VvFLS2-like* cloning, we cannot definitely confirm or exclude the putative involvement of the VvFLS2-like protein in flagellin perception.

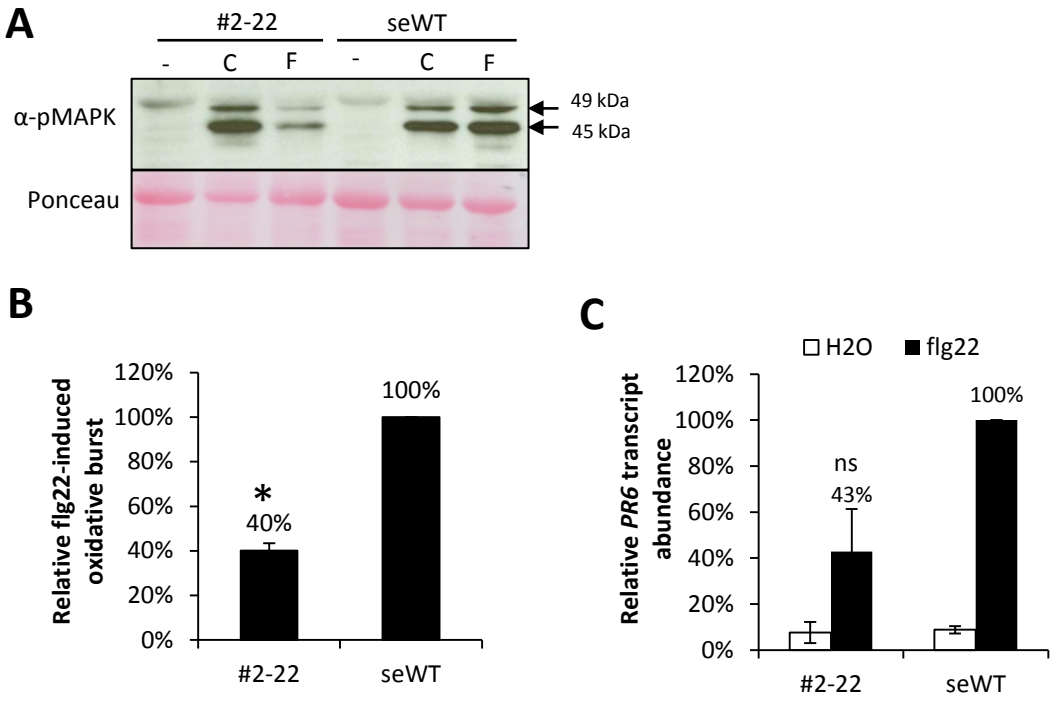

Figure 32. Grapevine *p35S::αs-VvFLS2 in vitro* plantlets are affected in flg22 signaling.
Defense responses in leaves of *p35S::αs-VvFLS2* line #2-22 and control (seWT) plants treated with flg22. **A.** Phosphorylation of two MAPKs detected by α-pERK1/2 Western blots at 15 min post treatment with chitin (C), flg22 (F), or water control (-). Homogenous loading was checked by Ponceau Red staining. Experiment was repeated four times with similar results. **B.** Oxidative burst measured by luminol method in grapevine leaf discs (n≥6) treated with flg22, oligogalacturonides (OG) or water. The total relative luminescence (rlu) was counted over 45 min. The ratio between the flg22- and OG-induced oxidative bursts was calculated and reported to seWT, set as 100%. Data are means ± SE of three independent experiments. **C.** Relative transcript abundance of the defense gene encoding a proteinase inhibitor (*PR6*) 6 hours post treatment with flg22 or water. Expression was measured by qPCR, normalized by the housekeeping genes *EF1α* and *EF1γ* and reported to seWT treated with flg22, set as 100 %. Data are means ± SE from three experiments. In **A.**, **B.**, **C.**, leaves were treated with 500nM flg22, 1 g l^{-1} chitin or 500 mg l^{-1} OG. Asterisk indicates statistically significant difference between seWT and the #2-22 line (heteroscedastic t-test, $p<0.05$, ns=non significant).

Discussion

1 The FLS2/flg22 perception system is conserved in grapevine and triggers a typical MTI

The flagellin-derived flg22 peptide spans the highly conserved N-terminal region and is an active elicitor in many plant species. Immune responses elicited by flg22 of *P. aeruginosa* have been characterized in detail in multiple studies, including Arabidopsis and tomato (Boller and Felix, 2009). Flg22 triggers a Ca^{2+}-associated membrane depolarization, pH alkalinization, oxidative burst, MAPK cascade activation, transcriptional reprogramming, ethylene production, callose deposition, and seedling growth inhibition (Gomez-Gomez *et al.*, 1999; Asai *et al.*, 2002; Zipfel *et al.*, 2004; Jeworutzki *et al.*, 2010). Not much is known about flagellin perception in grapevine (*V. vinifera*). Here, we show that flg22 elicits grapevine immune responses, such as $[Ca^{2+}]_{cyt}$ variations, an oxidative burst, phosphorylation of two MAPKs (Fig. 17), defense gene expression (Fig. 18) and growth inhibition (Fig. 26D, 27B). Our results are in accordance and complement the recent study of Chang & Nick (Chang and Nick, 2012) who reported flg22-triggered medium alkalinization, oxidative burst, induction of several defense genes, but not cell death, in *V. vinifera* and the north-American species *V. rupestris*. In cell cultures from *V. vinifera* cv Pinot Noir, the EC_{50} of apoplastic alkalinization was estimated at 877 nM (Chang and Nick, 2012) whereas our data indicated that *V. vinifera* cv Gamay cells are around 3 times more sensitive to flg22 (EC_{50} = ~300 nM; Fig. 25C). Moreover, *V. rupestris*, a species considered as naturally more resistant to different diseases, is more sensitive to flg22 perception with an estimated EC_{50} = ~5 nM (Chang and Nick, 2012). These differences may be caused by different species or cultivar responsiveness in the *Vitaceae* family, as observed previously in *Brassicaceae* where variation in flg22 perception mostly results from changes in FLS2 protein abundance (Vetter *et al.*, 2012). However, an EC_{50} value should not be considered as absolute, as we have noticed that the estimated EC_{50} could vary from ~30 nM to ~300 nM depending on when the grapevine cell suspensions have been used (compare Fig. 16A and 25C).

We have also shown that flg22 induces resistance against the fungal pathogen *B. cinerea*. In grapevine, flg22 perception triggers the expression of some *PR* genes (Fig. 18F-H, 25D-F) and the activation of the phytoalexin pathway leading to stilbene biosynthesis (Fig. 18D, E; Chang and Nick, 2012), two mechanisms known to delay *B. cinerea* spreading (Coutos-Thevenot *et al.*, 2001; Aziz *et al.*, 2007). Our data are in agreement with previous work showing that flg22 induces resistance to *B. cinerea* also in Arabidopsis (Ferrari *et al.*, 2007) and supports the concept that MTI confers broad-spectrum disease resistance regardless of the origin of the MAMP perceived. Thus, our results indicate that flg22-triggered immune responses are shared between *V. vinifera* and *A. thaliana*.

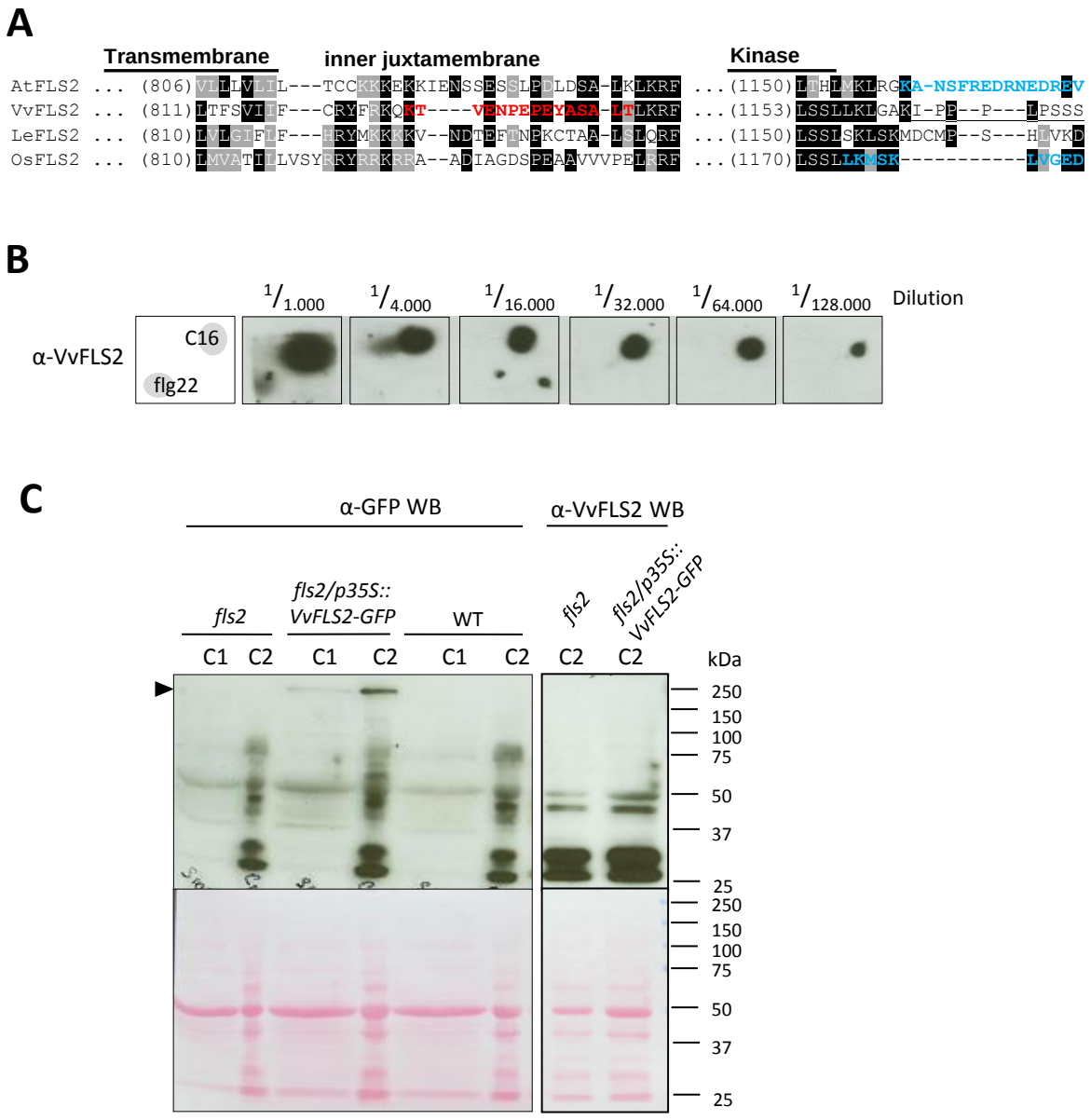

Figure 33. The rabbit anti-VvFLS2 polyclonal antibody directed against a specific epitope of VvFLS2 does not detect the VvFLS2 protein.

A. Alignment of the inner juxtamembrane regions and the C_{ter} end of the FLS2 orthologous proteins. Fifteen residues KTVENPEPEYASALT used as an epitope for generation of a polyclonal α-VvFLS2 antibody are highlighted in red. Residues used as epitopes for generation of α-AtFLS2 (Chinchilla *et al.*, 2006) and α-OsFLS2 (Takai *et al.*, 2008) antibodies are highlighted in blue. Underlined is a non-specific sequence (IPPPLPSSS) matching other gene products in grapevine. **B.** Test of the α-VvFLS2 antibody specificity by dot blot. Immunogenic antigen C16 (Cys- KTVENPEPEYASALT) and flg22 peptide (control for the non-specific detection) were spotted on each membrane piece that was further immuno-marked with different titers of the primary α-VvFLS2 antibody. **D.** Western blotting detection of VvFLS2-GFP protein with anti-GFP or anti-VvFLS2 antibody in leaves of Arabidopsis *fls2*, *fls2/p35S::VvFLS2-GFP #3* or wild-type (WT; Col-0) plants. Samples were prepared by a two-step centrifugation. C1: supernatant after the 1st centrifugation (10 000 g), C2: pellet after the 2nd centrifugation (100 000 g). Black arrow indicates the position of the immunodetected protein: ~ 200 kDa. Homogenous loading was checked by Ponceau Red staining. The α-GFP and α-VvFLS2 antibodies were used at 1/10 000 and 1/5 000, respectively.

Broad varieties of plant species are highly sensitive to flg22 and carry a functional FLS2 receptor in their genomes (Boller and Felix, 2009). The successful complementation of the Arabidopsis mutant *fls2* with the closest grapevine FLS2 ortholog, *VvFLS2,* demonstrates its function as a grapevine flagellin receptor (Fig. 22). The signaling pathways downstream of the flg22-FLS2 perception system are highly conserved between species as demonstrated by heterologous expression of VvFLS2, OsFLS2 or LeFLS2 in Arabidopsis (our results; Takai *et al.*, 2008; Mueller *et al.*, 2012). In concordance, the overall organization of the *FLS2* gene is conserved between the four functionally characterized flagellin receptors, with a unique intron in the 3' end (Fig. 20B). The structure of VvFLS2 is similar to the Arabidopsis FLS2, as VvFLS2 contains an ectodomain comprising 28 LRRs arranged in tandem and a typical non-RD kinase intracellular domain (Fig. 20C). The predicted signal peptide and the transmembrane domain of VvFLS2 targeted the protein to the plasma membrane (Fig. 20C, 22D, 23), as demonstrated previously in Arabidopsis (Robatzek *et al.*, 2006; Beck *et al.*, 2012). Lastly, the N-terminal cysteine pair (C61/C68) required for normal processing, stability and function of AtFLS2 (Sun *et al.*, 2012) as well as residues G318, G493, T867, S938, D997, T1040, G1064, T1072 and P1076, identified to affect AtFLS2 function when mutated (Robatzek and Wirthmueller, 2012; Cao *et al.*, 2013), are strictly conserved in VvFLS2 (Fig. 20C, Annex 2). Based on its observed electrophoretic mobility (Fig. 33C), VvFLS2 is a post-translationally modified protein, similarly to Arabidopsis or tomato FLS2 orthologs (Chinchilla *et al.*, 2006; Robatzek *et al.*, 2007) or other LRR-RLKs (Bleckmann *et al.*, 2010).

To sum up, our study indicates that the flg22/FLS2 perception system is conserved in *V. vinifera* as in most of higher plants, thus supporting a concept of an ancient origin of flagellin perception in plants (Boller and Felix, 2009).

2 The reduction in *VvFLS2* transcript levels affects the flg22 signaling in grapevine

We have generated and characterized the transgenic line *p35S::αs-VvFLS2* #2-22, in which the expression of *VvFLS2* gene was decreased by ~ 55% (Fig. 31A). Compared with seWT, this line #2-22 also displayed attenuated oxidative burst, MAPK phosphorylation and defense gene expression, specifically after flg22 treatment (Fig. 32A-C). Therefore, our results confirm the involvement of VvFLS2 in the grapevine perception of flg22. Together with the functional complementation of the Arabidopsis *fls2* mutant, these results indicate that VvFLS2 functions as a flagellin receptor in grapevine. Our data from the line #2-22 (Fig. 32) also indicate that the flg22 perception is finely tuned by the amount of *VvFLS2* transcripts. This is in agreement with previous studies in Arabidopsis showing that the level of *AtFLS2* transcripts directly impacts on the intensity of the flg22-triggered immune responses (Gomez-Gomez and Boller, 2000; Boutrot *et al.*, 2010; Vetter *et al.*, 2012).

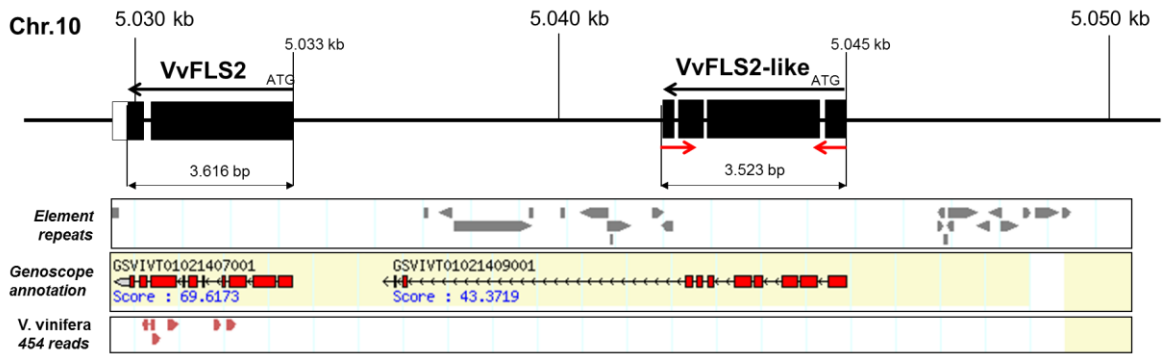

Figure 34. Genomic organization and gene structure of the *VvFLS2-like* locus in the proximity of the *VvFLS2* locus on chromosome 10.
Genomic organisation of the *VvFLS2-like* locus. Black boxes represent a gene prediction based on a partial sequencing of a full-length *VvFLS2-like* coding sequence (CDS) amplified from cDNA (cv Marselan) with specific primers illustrated by red arrows. ATG represents the beginning of translation. Gene annotations for these loci together with the existence of 454 reads and transposable element repeats are shown (*Source Genoscope Vitis 12x*).

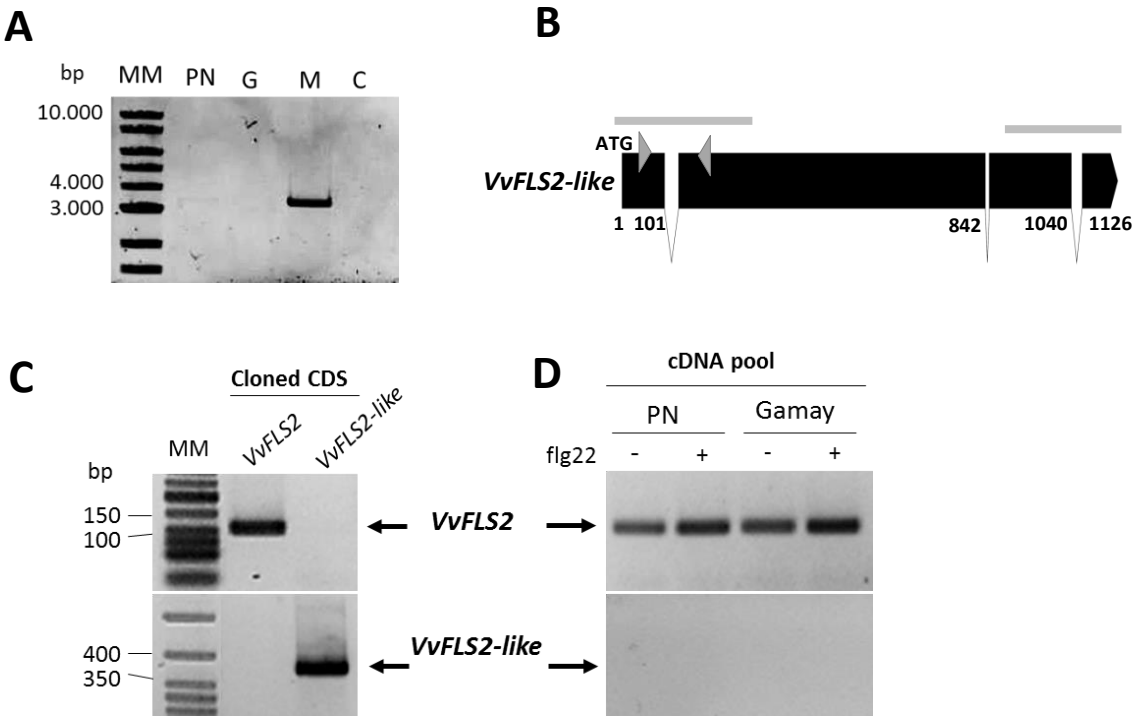

Figure 35. Expression of *VvFLS2-like* in different *V. vinifera* cultivars.
A. Amplification of full-length coding sequence of *VvFLS2-like* from cDNA of different *V. vinifera* cultivars Pinot Noir (PN), Gamay (G), Marselan (M) and Chardonnay (C). The expected size of fragment was around 3.500 bp. The annealing temperature was 62°C. **B.** Exon-intron architecture of *VvFLS2-like* gene based on sequenced CDS. Numbers represent the position of codons. Gray arrows represent the position of primers spanning an exon1/exon2 boundary used for qPCR. Gray bars represent the sequenced region. The presence of the 2nd intron (following codon 842) is not confirmed by sequencing. **C.** Specificity of *VvFLS2* and *VvFLS2-like* qPCR primers tested by PCR on cloned coding sequences (CDS) of *VvFLS2* and *VvFLS2-like*. **D.** Amplification of *VvFLS2* and *VvFLS2-like* transcripts from grapevine cDNA from leaves of cv. Pinot Noir or cells of cv. Gamay treated with water (-) or flg22 (+) for 6 hours. PCR was run for 28 cycles. The expected amplicon sizes are 108 bp for *VvFLS2* and 394 bp for *VvFLS2-like*. MM: Molecular marker.

Unfortunately, we could not correlate the level of *VvFLS2* transcripts to the level of protein, as the VvFLS2-GFP immuno-detection by the α-VvFLS2 polyclonal antibody failed whereas it could be detected by the α-GFP antibody (Fig. 33B, C). These results indicate that the failed immuno-detection by the α-VvFLS2 antibody is not due to the absence of VvFLS2 in protein extracts but rather to the epitope inaccessibility inside the protein. Indeed, an epitope within the inner juxtamembrane region might be sterically hindered by the compact kinase domain or the membrane proximity, unlike the C-terminal regions chosen as immune epitopes for detection of the other FLS2 orthologs (Takai *et al.*, 2008; Boutrot *et al.*, 2010).

As indicated previously, the silencing in the line #2-22 was not complete, leading to residual flg22-triggered immune responses. Grapevine genome possesses a highly close *VvFLS2* paralog, designated as *VvFLS2-like*. As the *VvFLS2-like* transcripts were never detected by qPCR in mock- or flg22-treated leaves of cv Pinot Noir (seWT or any antisense line), we assume that the encoded protein could not substitute the VvFLS2 function. So, in the line #2-22, the remaining immune responses triggered by flg22 are rather due to the partial silencing of *VvFLS2* than to a putative functional redundancy which might have been associated with the *VvFLS2-like* locus. These remaining immune responses of the antisense line #2-22 might become an obstacle for evaluating the involvement of VvFLS2 during grapevine interactions with microorganisms, such as *B. phytofirmans*.

Taken together, our results indicate that VvFLS2 seems to be the unique receptor for the flg22 detection in grapevine, similarly to Arabidopsis where the *fls2* mutant is flg22 non-responsive (Zipfel *et al.*, 2004).

3 Weak eliciting activity of Bp flg22 in grapevine

We observed that flg22 peptides derived from different bacteria had distinct eliciting activities in grapevine. Bp flg22 derived from the non-pathogenic endophytic bacterium *B. phytofirmans* exhibited reduced oxidative burst and defense gene expression compared with the same epitope derived from the plant pathogenic bacteria *P. aeruginosa* or *X. campestris* (Fig. 25C-G). The calcium signature and oxidative burst triggered by Bp flg22 were lower compared with the one triggered by Pa flg22 or Xc flg22 (Fig. 25B, C). Similarly the expression of some defense genes, such as *Chit4c*, was only transiently induced by Bp flg22 (Fig. 25F). Moreover, other genes were not significantly activated by Bp flg22 (*e.g. PR6* and *17.3*; Fig. 25D, E, G). Accordingly, Bp flg22 did not trigger a significant growth inhibition of grapevine plantlets (Fig. 26D, 27B). Thus, Bp flg22 is a weak elicitor in grapevine that triggers only partly and transiently flg22-responsive events. Indeed, the gene *17.3*, which is exclusively regulated by SA in grapevine (Bordiec *et al.*, 2011), was activated by Xc flg22 and Pa flg22, but not by Bp flg22 (Fig. 25G). These results suggest that the SA signaling pathway might not be activated by Bp flg22, but only by the two

other epitopes. Moreover, the kinetics of genes induction was very distinct. Although the three epitopes induced *Chit4c* expression at similar level in early time point (1h), the induction of expression of this gene was very transient after Bp flg22 treatment (Fig. 25F).

By contrast, *X. campestris*-derived flg22 displayed a strong eliciting activity in grapevine as demonstrated by low EC_{50} value in oxidative burst assays, a strong induction of defense genes and a marked growth inhibition (Fig. 25, 26B, D, 27B).

Key amino acids described as crucial for flg22 eliciting activity (Felix *et al.*, 1999; Bauer *et al.*, 2001; Sun *et al.*, 2006) are unchanged in Bp flg22 (Fig. 25A). However, the 3 amino acid substitutions between the most active peptide in grapevine Xc flg22 and Bp flg22 (Q1T, L7K and K13A) are sufficient to strongly increase its EC_{50} from ~80 nM to ~8 µM, a 100-fold difference in sensitivity (Fig. 25C). In tomato, deletion of the first seven N-terminal amino residues of flg22 did not strongly affect the biological activity, as the flg15 sequence remained fully active (Felix *et al.*, 1999). However, *fls2* protoplasts expressing *AtFLS2* are 1000-fold more sensitive to flg22, relative to flg15 (Mueller *et al.*, 2012). Interestingly, mutation of K13A in flg22 has been reported previously to decrease its biological activity to 60% in tomato (Felix *et al.*, 1999), whereas the mutation K13S had a minimal effect on flg22-eliciting activity in Arabidopsis (Sun *et al.*, 2006). Very recently, a solved crystal structure of the Arabidopsis FLS2-flg22-BAK1 complex led to the identification of the mutually interacting flg22 and FLS2 residues (Sun *et al.*, 2013). It was shown that K13 of flg22 binds directly to Y272 and Y296 residues in LRR8 and 9 of FLS2 and contributes to the interacting interface (Sun *et al.*, 2013). However the side chain of K13 is not involved in these interactions (Sun *et al.*, 2013), explaining why mutations in this residue had low impact on flg22 activity. The corresponding amino acids in LRR 8 and 9 of VvFLS2 are unchanged (Annex 2). It seems therefore probable that the N-terminal part of flg22 is important for flg22 perception in grapevine, similarly to Arabidopsis, but unlike in tomato. It would be interesting to perform substitutions of these distinct amino acids in Bp flg22 in order to identify their role in VvFLS2 perception, as previously performed for perception of pathovar variants of Xc flg22 in Arabidopsis (Sun *et al.*, 2006).

Certain pathogenic or symbiotic bacteria, such as *R. solanacearum*, *A. tumefaciens, Azoarcus sp.* or S. *meliloti* have specific flg22 sequences that are not recognized by FLS2 (Felix *et al.*, 1999; Pfund *et al.*, 2004; Buschart *et al.*, 2012; Lopez-Gomez *et al.*, 2012). In agreement, grapevine did not perceive flg22 peptide derived from *A. tumefaciens* (Fig. 25, 26 B, D, 27 B). Other bacteria are able to reduce or increase their flagellum content depending on the stages of colonization (Achouak *et al.*, 2004; Bardoel *et al.*, 2011; Bardoel *et al.*, 2012). Another evasion strategy is flagellin glycosylation that masks its perception (Taguchi *et al.*, 2009; Hirai *et al.*, 2011). Weak recognition of their MAMPs, such as flagellin, or even their loss can facilitate host tissue colonization by plant-associated bacteria. Our data suggest that alterations in Bp flg22

sequence might be a successful adaptation of *B. phytofirmans* to avoid recognition by the host VvFLS2.

4 AtFLS2 and VvFLS2 have different recognition specificities

Our results clearly show that *V. vinifera* and *A. thaliana* display species-specific differences in flg22 perception (Fig. 26, 27). In wild-type Arabidopsis, Pa flg22, Xc flg22 and Bp flg22 induced immune responses of a similar intensity (Fig. 26A, C, 27A, 28A). Thus differences in MAMP recognition exist between VvFLS2 and AtFLS2. We have further shown that the expression of VvFLS2 in the Arabidopsis *fls2* mutant conferred a flagellin responsiveness profile characteristic to grapevine (Fig. 28B). These results clearly suggest that the differences observed between Arabidopsis and grapevine are caused, at least in part, by the different FLS2 proteins.

As flg22 binding is mediated by the FLS2 LRR ectodomain (Dunning *et al.*, 2007; Robatzek and Wirthmueller, 2012), it is interesting to note that the LRR domains of AtFLS2 and VvFLS2 only share 56% of amino acid identity (Table 10, Annex 2). Similarly, the LRR ectodomain of AtFLS2 shares only 54% identity with the LRR ectodomain of LeFLS2, which possesses species-specific traits for flg22 recognition (Robatzek *et al.*, 2007; Mueller *et al.*, 2012; Robatzek and Wirthmueller, 2012). Comparing the LRRs of eight FLS2 orthologs, Boller & Felix (2009) identified conserved amino acid of β-strands only in LRR 1 and LRR 22-28. Interestingly, domain swap experiments between AtFLS2 and LeFLS2 narrowed down the potential Pa flg22 binding domain to LRRs 7-10 for the RINSAKDD core sequence (Mueller *et al.*, 2012). Mutational scanning of LRR domains has also indicated that LRRs 9-15 play an important role for FLS2 function (Dunning *et al.*, 2007). Recently, a crystallographic study confirmed that LRRs 8-11 bind the flg22 core sequence (Sun *et al.*, 2013). The interacting residues in these LRRs are conserved in grapevine, with the exception of R294 (Annex 2). The LRRs 3 and 6, and LRRs 13-17 involved in the recognition of the N- and C-terminus of flg22 (Sun *et al.*, 2013) are less conserved between species and differ between grapevine and Arabidopsis (Annex 2). This lower conservation could potentially explain the different sensitivities of *A. thaliana* and *V. vinifera* towards flg22 treatment. Interestingly, OsFLS2 is only weakly conserved in the key residues recognizing flg22 (Annex 2), which might be a reason for lower sensitivity to flg22 reported in rice cells (Felix *et al.*, 1999; Takai *et al.*, 2008). Future work should reveal which polymorphisms underlie the different perception specificities of AtFLS2 and VvFLS2.

5 *B. phytofirmans* overcomes MTI in Arabidopsis and grapevine to colonize plants

The eliciting activity of *B. phytofirmans* was mainly conserved in the boiled extract and proteinase K treatment greatly affected the eliciting activity, indicating that it is mostly proteinaceous compounds that are responsible for the elicitation (Fig. 24A, B). Moreover, the

purified flagellin from *B. phytofirmans* and Bp flg22 are strongly active in Arabidopsis (Fig. 24D, 26A, B, 27A). Thus flagellin seems to be a main MAMP of *B. phytofirmans*, even if we cannot exclude that other elicitors, such as LPS, might participate to the elicitation process (Erbs and Newman, 2012). The eliciting properties of flagellins from endophytic bacteria have been studied in a few plant systems. For instance, flagellins from *P. putida* or *P. fluorescens* induced different early defense responses in tobacco cells depending on their origin (van Loon *et al.*, 2008). Similarly, boiled extracts from different strains of endophytic PGPRs *P. fluorescens* and *P. putida* differentially stimulated H_2O_2 and phytoalexin production in grapevine cell suspensions (Verhagen *et al.*, 2010). Unfortunately, flagellin sequences from these bacteria are not known, and it is therefore difficult to make a structure-activity correlation.

B. phytofirmans is a PGPR naturally associated with grapevine (Ait Barka *et al.*, 2000; Lo Piccolo *et al.*, 2010). Although this bacterium is not known to be associated with Arabidopsis in nature, it is able to colonize this plant under laboratory conditions (Poupin *et al.*, 2013; Zuniga *et al.*, 2013). Our data show that, although Bp flg22 has a weak elicitor activity in grapevine, it is strongly active in Arabidopsis. These results suggest that VvFLS2 and/or flagellin from *B. phytofirmans* may have undergone evolutionally changes allowing the adapted endophytic bacterium to colonize its natural host plants without inducing a strong MTI.

However, the addition of the strongly-eliciting Xc flg22 during the first stages of bacterialization did not interfere with the colonization process in grapevine (Fig. 29). Moreover, in Arabidopsis, Bp flg22 triggers a strong growth inhibition which contrasts with the described PGPR effect (Poupin *et al.*, 2013; Zuniga *et al.*, 2013). On the basis of these data, it seems that *B. phytofirmans* may ultimately neutralize plant immunity induced by flg22 or other MAMPs using a strong evasion process that could be related to ETS (Jones and Dangl, 2006) to successfully colonize plants. Therefore, the bacterium may inhibit MTI by injecting effectors.

Interestingly, no potential secreted effectors have been identified in its sequenced genome (Sessitsch *et al.*, 2005; Weilharter *et al.*, 2011; Mitter *et al.*, 2013). Moreover, although *B. phytofirmans* possesses all relevant TTSS genes, the gene encoding the needle-forming protein is absent, suggesting that this TTSS apparatus is not functional (Mitter *et al.*, 2013). Furthermore, a cell culture filtrate of *B. phytofirmans* did not suppress flg22-induced Arabidopsis defense responses (S. Dorey, unpublished data), in contrast with that shown previously for *P. fluorescens* and *Bacillus subtilis* (Millet *et al.*, 2010; Lakshmanan *et al.*, 2012). Another hypothesis is that bacteria might regulate MAMP responses by lowering ethylene production. Indeed, *B. phytofirmans* is known to reduce the level of ethylene in plants *via* its 1-aminocyclopropane-1-carboxylate deaminase activity (Onofre-Lemus *et al.*, 2009; Sun *et al.*, 2009) and endogenous ethylene is known to control *FLS2* expression (Boutrot *et al.*, 2010; Tintor *et al.*, 2013). Further experiments will be needed to investigate the mechanisms underlying the multi-layered evasion of plant immunity by the PGPR *B. phytofirmans.*

6 *VvFLS2-like* gene in grapevine

We reported that a close paralog of *VvFLS2*, which we designated as *VvFLS2-like*, exists in an adjacent locus to *VvFLS2* on chromosome 10. In basal conditions or after flg22 treatment, the *VvFLS2-like* transcript has never been detected by qPCR in *V. vinifera* cv Pinot Noir, Gamay nor Chardonnay (Fig. 35A, D). Moreover, the SOLID and Illumina's RNAseq signal for the *VvFLS2-like* transcript is ~0 at the CRIBI website (http://genomes.cribi.unipd.it) and no 454 read has been found at the genoscope website (Fig. 34). Finally, the *VvFLS2-like* transcript has been amplified only once from leaves of the *V. vinifera* cv Marselan (Fig. 35A). All over, these results suggest that the basal level of the *VvFLS2-like* transcripts is very low or not transcribed in most of the conditions.

As attempts to functionally characterize this gene have failed, we cannot definitely conclude about the putative role of VvFLS2-like in the flagellin perception. In the tomato genome (*Solanum lycopersicum*), a close paralog, named *LeFLS2.2*, has also been reported (Clarke *et al.*, 2013). The *LeFLS2.2* gene shares 89% identity with *LeFLS2* and is actively transcribed. In Arabidopsis, no AtFLS2 paralog sequence exists (BLASTn results). However recent data suggest that *LeFLS2.2* does not contribute to the perception of the second flagellin epitope active in tomato, named flgII-28 (Clarke *et al.*, 2013). Actually, the function of these paralogs in grapevine and tomato is still unknown.

Perspectives

We report here the identification of VvFLS2, the *V. vinifera* receptor of bacterial flagellin *via* the flg22 epitope. We have demonstrated by complementation assays in Arabidopsis and a partial silencing in grapevine that VvFLS2 is the functional ortholog of AtFLS2. VvFLS2 exhibits distinct recognition specificities than AtFLS2. Our data show that flagellin from the beneficial PGPR *B. phytofirmans* is a weak elicitor in grapevine and might have evolved to evade this grapevine immune recognition system.

Our findings raise several novel questions:

i) Is the evasion of flg22 recognition a general adaptation of *B. phytofirmans* to its hosts? Thus, it would be interesting to compare the perception of Bp flg22 in tomato, potato or other natural host plants that also benefit from *B. phytofirmans* colonization and growth-promoting effect (Mitter *et al.*, 2013).

ii) What is the role of VvFLS2-mediated flagellin perception during the colonization of grapevine with *B. phytofirmans*? It would be interesting to obtain Δ*fliC* mutants of *B. phytofirmans* and Δ*fliC* complemented with a highly eliciting FliC, such as FliC from *X. campestris* and test whether colonization of grapevine plants would be impaired after recognition of these mutants. Infection assays with *B. phytofirmans* Δ*fliC* would also answer a question whether *B. phytofirmans* requires flagellin for colonization. Furthermore, *B. phytofirmans* may also lower the ethylene levels in host plants (Onofre-Lemus *et al.*, 2009; Sun *et al.*, 2009), which can control FLS2 amounts (Boutrot *et al.,* 2010). Thus, the expression of VvFLS2 in colonized tissues might be tested on the protein and transcript level in parallel with the ET quantification. Similarly, it could be possible to quantify the *B. phytofirmans* growth on *V. vinifer*a plants treated with ET inhibitors.

The VvFLS2 RNAi plants may be tested for colonization with different flagellin-expressing mutants of *B. phytofirmans*. It could be also interesting to express different chimeric FLS2 receptors in grapevine, combining the ectodomains of VvFLS2, LeFLS2 or AtFLS2 with the transmembrane and kinase domain of a strong kinase such as XA21 and assess the efficiency of colonization.

iii) What is the role of VvFLS2-mediated flagellin perception in the disease resistance against pathogenic bacteria? Again, the VvFLS2 RNAi plants may be tested in various pathoassays.

iv) Is the flg22 region the main flagellin epitope for grapevine or can it also recognize extra epitopes outside the flg22 region? A number of solanaceous species, including tomato, can sense an extra peptide of flagellin, named flgII-28 (Cai *et al.*, 2011; Clarke *et al.*, 2013). The activity of flgII-28 could be assessed in grapevine cells and compared to flg22. The eliciting

activity of full-length flagellins of *P. aeruginosa*, *B. phytofirmans or P. syringae* pv *pisi* might be also tested using VvFLS2 RNAi grapevine.

v) Does VvFLS2-like participate in the flagellin recognition? It might be interesting to obtain the Arabidopsis *fls2* mutant complemented with *VvFLS2-like* and the grapevine lines silenced in the *VvFLS2-like* gene. These mutants might be tested for the immune responses after elicitation with flg22 or full-length flagellins purified from different bacteria.

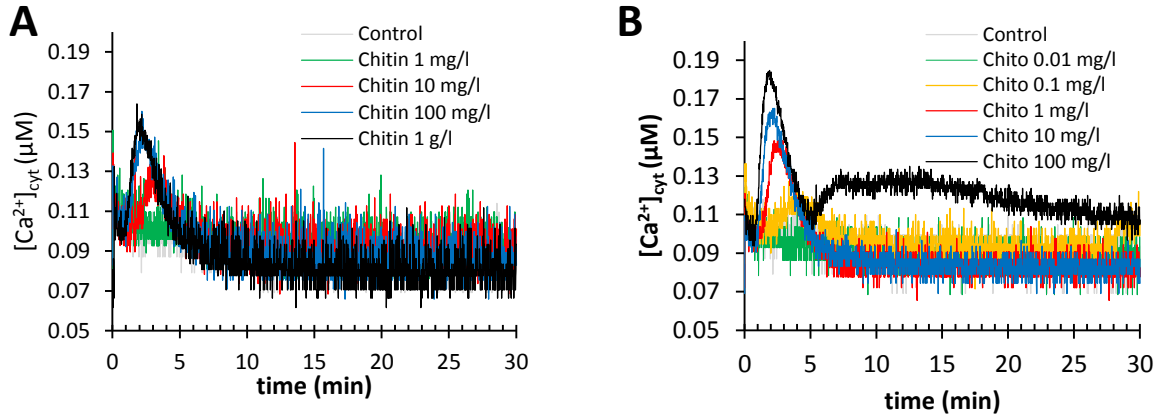

Figure 36. Chitin and chitosan trigger a dose-dependent variation in free cytosolic calcium $[Ca^{2+}]_{cyt}$ in grapevine cells.
Dose-response curves of free $[Ca^{2+}]_{cyt}$ variations after chitin (A) or chitosan (B) treatment measured with apoaequorin-expressing grapevine cells. Data are from one representative experiment out of two.

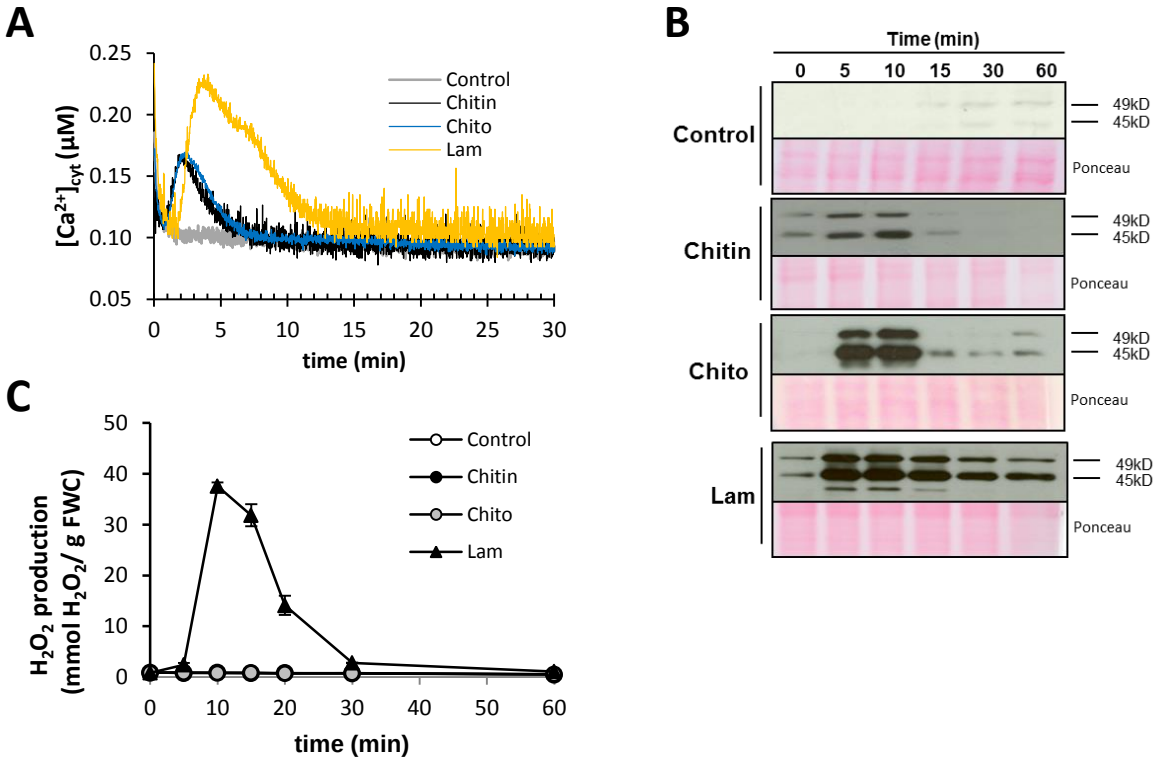

Figure 37. Chitin and chitosan induce early signaling events in grapevine cells.
A. Free $[Ca^{2+}]_{cyt}$ variations measured with apoaequorin-expressing grapevine cells. Values are means from two independent experiments. **B.** Activation kinetics of two mitogen-activated protein kinases (MAPK) detected by Western blot α-pERK1/2. Homogeneous loading was checked by Ponceau Red staining. Data are from one representative experiment out of three. **C.** Time course of ROS production detected by luminescence of luminol. Values are means ± SD from three independent experiments. FWC: fresh weight of cells. Cells were treated with 1 g l^{-1} chitin, 25 mg l^{-1} chitosan, 1 g l^{-1} laminarin or water (control).

Figure 39. Chitosan but not chitin enhances the resistance to *Botrytis cinerea* and *Plasmopara viticola*.
Leaf discs were pre-treated with chitin (1 g l^{-1}), chitosan (150 mg l^{-1}) or sulfated laminarin (PS3; 2.5 g l^{-1}) in a surfactant or with surfactant alone (control) 48h before infection. **A.** Disease progression caused by *B. cinerea* at 3 dpi. Values represent the means of lesion diameters ± SE (n≥20 discs from 10 different plants) from one experiment out of three. **B.** Infection symptoms caused by *P. viticola* at 7 dpi on grapevine leaf discs (30 discs). Sporulation intensity was evaluated by counting sporangia on two sets of randomly pooled 5 discs, each set was counted at least 4 times with a haemocytometer and expressed as a number of sporangia per leaf disc. Values represent the mean ± SE (n=8) from one experiment out of three. Asterisk(s) indicate a statistically significant difference between control and the elicitor treatment (t-test, *: p<0,05, **: p<0,01). A representative leaf disc for each treatment is shown.

III. Chitin perception system in grapevine

Results

1 Chitin and chitosan induce defense responses in grapevine

Chitin and chitosan, its partially deacetylated derivative, are active MAMPs in grapevine (Table 9). We therefore aimed to characterize chitin and chitosan responsiveness in grapevine.

In apoequorin-expressing grapevine cells, both chitin and chitosan (Chito) induced a dose-dependent variation in free cytosolic Ca^{2+} (Fig. 36). The chitin and chitosan responsiveness were detected from 10 mg l^{-1} and 0.1 mg l^{-1} concentrations, respectively. In this bioassay, chitin responses became saturated at 1 g l^{-1}, concentration used for further experiments. For chitosan, the saturating concentration was not reached due to its low solubility, but for further studies 25 mg l^{-1} chitosan was applied.

After chitin or chitosan treatment, variations in $[Ca^{2+}]_{cyt}$ displayed a similar profile: $[Ca^{2+}]_{cyt}$ started to increase at 1 min, peaked at 3 min and decreased to the basal level within the next 7 min (Fig. 37A). These $[Ca^{2+}]_{cyt}$ variations were weaker and more transient than those triggered by laminarin. Chitin also induced rapid phosphorylation of two MAP kinases (Fig. 37B), with relative molecular masses of 45 and 49 kDa. Phosphorylation was detected after 5 and 10 min of chitin treatment and almost decreased to the basal level already at 15 min post treatment. Chitosan induced a similar kinetics of MAPK phosphorylation and both of them were more transient than laminarin-induced MAPK phosphorylation. Using a luminol-based bioassay, neither chitin nor chitosan induced a detectable oxidative burst throughout the 60 min of experiment (Fig. 37C). The H_2O_2 production was undetectable at any concentration tested in the range 0.001-10 g l^{-1} for chitin or 0.01-50 mg l^{-1} for chitosan (data not shown).

The expression of defense marker genes (Aziz *et al.*, 2003; Aziz *et al.*, 2007; Bordiec *et al.*, 2011) was monitored by qPCR in grapevine cells treated with chitin (Fig. 38). Chitin only weakly and transiently upregulated the expression of defense genes encoding a 1-aminocyclopropane-1-carboxylate synthase (*ACCS*, Fig. 38A), a 9-lipoxygenase (*LOX-C*, Fig. 38C) or genes participating in the stilbene pathway: a stilbene synthase (*STS1-2,* Fig. 38D) and a phenylalanine ammonia lyase (*PAL,* Fig. 38E). Nevertheless, the *PR3-4c* gene, encoding the acidic chitinase Chit4c, was more strongly upregulated by chitin (Fig. 38F). Surprisingly, the gene *RbohD,* encoding the corresponding NADPH-oxidase responsible for the oxidative burst in grapevine cells (B. Poinssot, unpublished data), was transiently induced by chitin (Fig 38B), whereas no H_2O_2 production has been detected. Chitin treatment did not induce the expression of

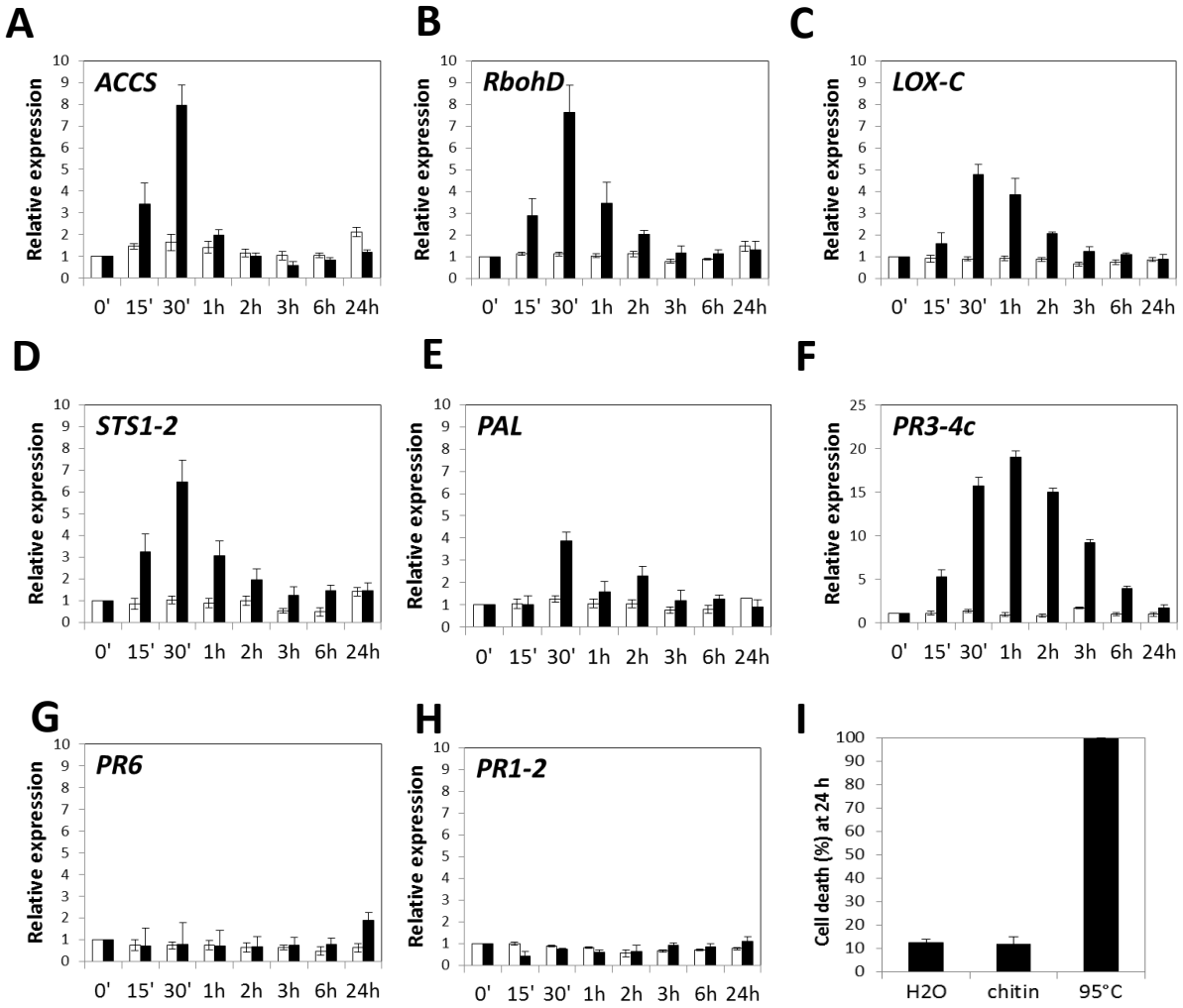

Figure 38. Kinetics of chitin-induced defence gene expression and cell death in grapevine cells.
A.-H. Relative expression of defence genes encoding **A.** a 1-aminocyclopropane-1-carboxylate synthase (*ACCS*), **B.** a respiratory burst oxidase homolog D (*RbohD*) and **C.** a 9-lipoxygenase (*LOX-C*), **D.** a stilbene synthase (*STS1-2*), **E.** a phenylalanine ammonia lyase (PAL), **F.** an acidic chitinase (*PR3-4c*), **G.** a proteinase inhibitor (*PR6*), and **H.** PR1-2 induced by chitin (1g l^{-1}) (black bars) or water (white bars) was measured by qPCR, normalized to housekeeping genes elongation factor α and γ (EF1α, γ) and reported to time 0, set as 1. Data are means ± SE from 3 experiments. **I.** Cell viability was quantified by neutral red staining 24 h after treatment with water or chitin (1 g l^{-1}) or after cell incubation at 95°C for 3 min (positive control of cell death). Values are means ± SD of two independent experiments.

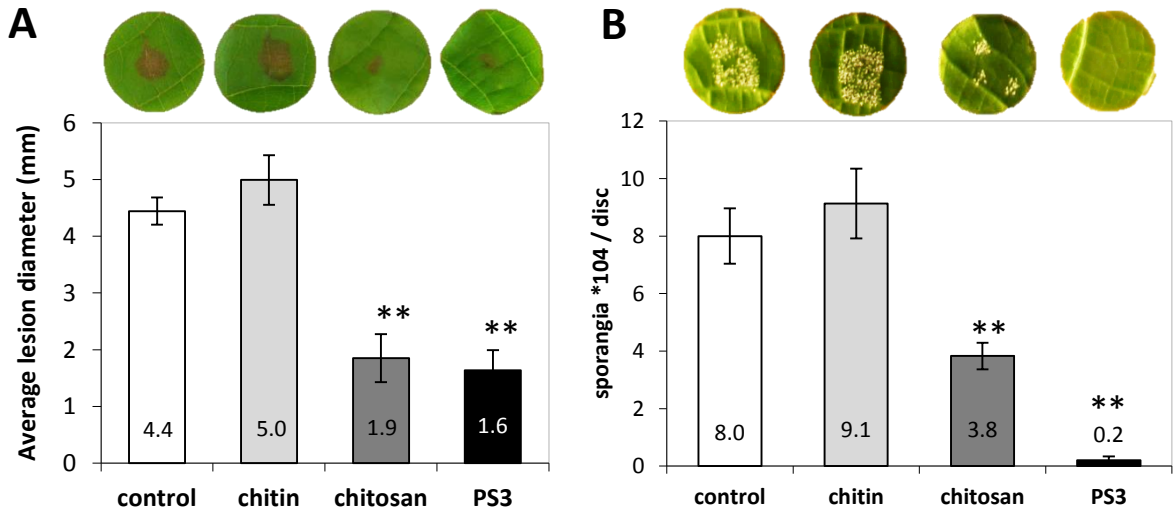

Figure 39. Chitosan but not chitin enhances the resistance to *Botrytis cinerea* and *Plasmopara viticola*.
(Find the legend on the previous page).

two *PR* genes encoding a protease inhibitor (*PR6,* Fig. 38G) and *PR1-2* (Fig. 38H). No cell death was observed on grapevine cell suspensions treated for 24 h with chitin (Fig. 38I).

We further investigated the effectiveness of chitin- and chitosan-induced immunity on *V. vinifera* leaf discs challenged with the necrotrophic fungus *B. cinerea* or with the biotrophic oomycete *P. viticola*, the causal agents of gray mold and downy mildew, respectively. Chitin pretreatment did not induce any significant resistance against these pathogens (Fig. 39A, B). On the other hand, chitosan treatment applied 48 h before pathogen inoculation strongly reduced the *B. cinerea* lesion diameter, compared to control leaf discs (Fig. 39A). The observed necrosis reduction was comparable to the reduction obtained by pretreatment with the sulfated laminarin (PS3). Chitosan treatment was also strongly effective to reduce the *P. viticola* sporulation (Fig. 39B).

To sum up, chitin and chitosan induce typical grapevine immune responses with different kinetics and intensity compared to those triggered by laminarin or flg22 (compare Fig. 37, 38 and Fig. 17,18, Part II §1). While chitin pretreatment does not impact resistance against *B. cinerea* and *P. viticola*, chitosan is highly effective to protect grapevine against these pathogens.

2 LysM-RLKs (LYKs) in grapevine and identification of putative AtCERK1 orthologs in grapevine

2.1 *In silico* characterization of the predicted grapevine CHITIN ELICITOR RECEPTOR KINASE 1 orthologs: VvCERK1, 2 and 3

We aimed to identify the corresponding chitin/chitosan receptor in grapevine. In Arabidopsis, the LysM-containing RLK (LYK) CERK1 is involved in chitin perception by direct binding (Miya *et al.*, 2007; Wan *et al.*, 2008; Petutschnig *et al.*, 2010).

Grapevine genome encodes 12 LYK proteins (VvLYK1 – VvLYK 12, Table 12). BLASTp results (E-value = 0) and phylogenetic analysis indicated that the three predicted RLKs VvLYK1/VvCERK1 (XP_002270987), VvLYK2/VvCERK2 (XP_002264327) and VvLYK3/VvCERK3 (XP_002264288) display the highest degree of homology with AtCERK1 and OsCERK1 and are clearly distinct from other grapevine or Arabidopsis LysM-RLKs (Fig. 40, Table 12). The encoded VvCERK proteins contain a signal peptide, 3 LysM motifs in the extracellular part, a single transmembrane domain and a RD-type intracellular kinase domain (Annex 5). VvCERKs exhibit 69-73% similarity with ACERK1 and their LysM ectodomains share 65-68% of amino acid similarity between grapevine and Arabidopsis (Annex 4A). The kinase domains of VvCERKs are particularly conserved and share 80-87% similarity with orthologs in Arabidopsis or rice (Annex 4A, 5). Compared to VvCERK2 and 3, VvCERK1 shares the highest degree of conservation with AtCERK1, OsCERK1 and LeCERK1, the closest predicted ortholog in tomato. Compared to AtCERK1, the VvCERK3 protein carries the most identical LysM

Grapevine protein			*The closest Arabidopsis ortholog*		
Name	**Protein ID (GenBank)**	**Length (aa)**	**ID (TAIR)**	**Name**	**E-value (blastp)**
VvLYK1/VvCERK1	XP_002270987	614	AT3G21630	AtCERK1	0
VvLYK2/VvCERK2	XP_002264327	625			0
VvLYK3/VvCERK3	XP_002264288	622			0
VvLYK4	XP_002282620	593	AT1G51940	AtLYK3	2e-89
VvLYK5	XP_002272814	605			e-105
VvLYK6	XP_002283628	666			0
VvLYK7	XP_002277331	665	AT2G33580	AtLYK5	e-166
VvLYK8	VIT_18s0122g00240*	586			e-135
VvLYK9	XP_002280070	622	AT2G23770	AtLYK4	5e-62
VvLYK10	XP_002269408	638			e-137
VvLYK11	XP_002263070	675	AT3G01840	AtLYK2	e-124
VvLYK12	XP_002269472	608	AT2G33580	AtLYK5	6e-65

Table 12. List of LysM-containing receptor-like kinases (LYKs) in *Vitis vinifera*.
Protein sequences (GenBank prediction) were identified by BLASTp with AtCERK1, AtLYKs and LjNRFs. The presence of predicted LysM domains (PF01476), trans-membrane region and kinase domain (SM000221) was verified by SMART (http://smart.embl-heidelberg.de). The closest ortholog of each VvLYK in Arabidopsis was searched with BLASTp (TAIR http://www.arabidopsis.org/Blast).
*) Protein sequence retrieved from CRIBI.

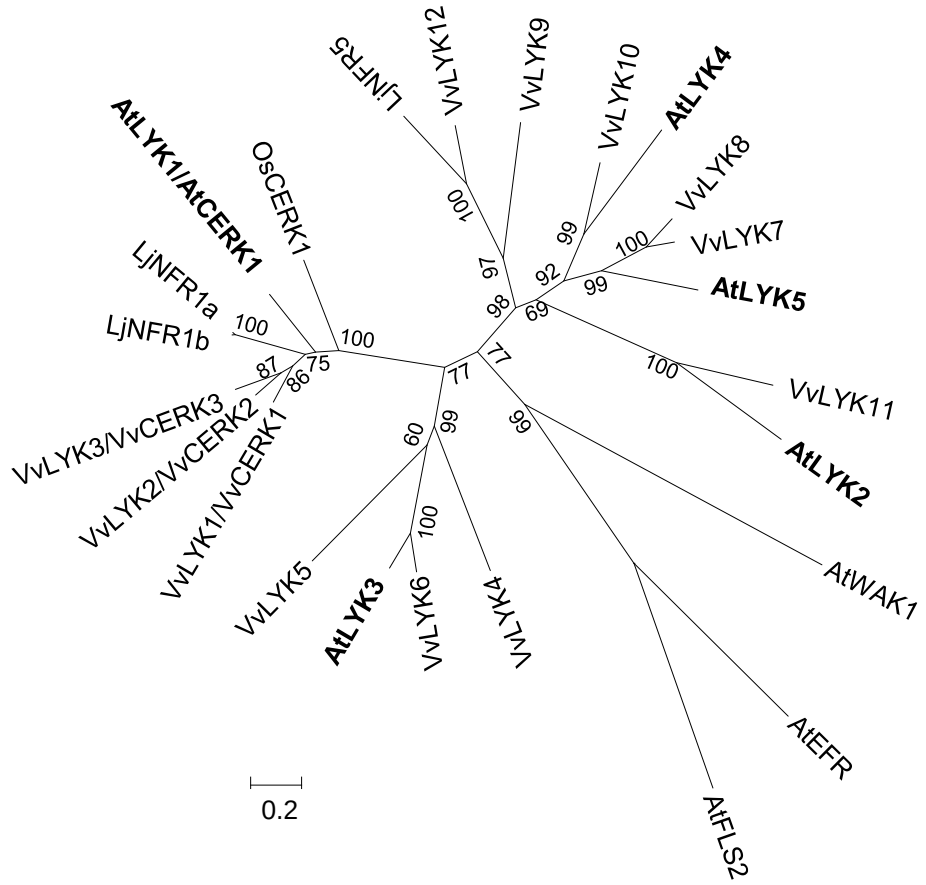

Figure 40. *In silico* characterization of the LysM-RLK (LYK) family.
A. Maximum-likelihood phylogenetic tree (500 bootstraps) showing the relationship between the protein sequences (GenBank) of the Arabidopsis AtLYK1/AtCERK1 (AT3G21630), AtLYK2 (AT3G01840), AtLYK3 (AT1G51940), AtLYK4 (AT2G23770) and AtLYK5 (AT2G33580), the rice ortholog OsCERK1 (D7UPN3), Nod factor receptors of *Lotus japonicus* LjNFR1a (CAE02591), LjNFR1b (CAE02592), LjNFR5 (CAE02598) and the LYK protein sequences VvLYK1-12 of *V. vinifera*. Percentage of bootstraps are presented, only values higher than 50% are shown.

domain, reaching 51% of identity (Annex 4A). When aligned, all three VvCERK protein sequences share together a high degree of identity (Annex 4B, 5). At the gene level, *VvCERK1* is located on chromosome 12, whereas *VvCERK2* and *VvCERK3* lie in neighboring loci on the chromosome 10.

The full-length coding sequences (CDS) of *VvCERK1*, *VvCERK2* and *VvCERK3* were amplified from cDNA of *V. vinifera* cv Gamay leading to one major PCR product of the expected size for each gene. Sequencing of the cloned CDSs revealed that genes *VvCERK1, 2* or *3* consist of open-reading frames of 1845, 1878 and 1869 bp, respectively. Their transcripts contain 11 exons for *VvCERK1* and 12 exons for *VvCERK2* and *VvCERK3* (Fig. 41), similarly to *AtCERK1*, which also contains 12 exons. Sequencing revealed the presence of nucleotide substitutions present in alleles of *VvCERK2* and *VvCERK3* (cv Gamay). Some of SNPs present in *VvCERK3* led to changes in amino acid residues (Annex 4C). Some splicing sites between the predicted and the sequenced *VvCERK*s were also different (Annex 4C).

Based on the sequence conservation, VvCERK1 seems to be the best candidate ortholog of AtCERK1, however VvCERK3 displays more conserved LysM ectodomain and the exon-intron gene architecture. Concerning other grapevine LysM-RLKs, VvLYK11 appears to be the ortholog of AtLYK2, VvLYK6 the ortholog of AtLYK3, VvLYK10 the ortholog of AtLYK4 and VvLYK7/8 the orthologs of AtLYK5 (Fig. 40). Clear orthologous sequences of VvCERK9 and VvCERK12 are missing in Arabidopsis. These sequences share a high similarity with LjNFR5 (BLASTp E-value 2e-117, 0.0 and sequence similarity 56% and 68%, respectively).

All three VvCERKs are candidates to function as chitin receptor in grapevine. As AtCERK1 expression was weakly induced by chitin (Wan *et al.*, 2008), the expression of each VvCERK gene in grapevine cells after chitin treatment was monitored by qPCR. Under non-elicited conditions, *VvCERK1* and *VvCERK3* transcript amounts account for ~9% of the transcript level of the housekeeping gene *EF1γ,* whereas *VvCERK2* transcripts are the less abundant with ~3% of *EF1γ* expression (Fig. 42A). From 15 min up to 24 hours, chitin treatment did not induce the expression of any of the *VvCERK*s at any studied time-point (Fig. 42B).

Functional genomics studies were needed to investigate the function of each VvCERK in chitin perception. We have undertaken two parallel strategies: i) the functional complementation of the Arabidopsis *cerk1-2* mutant, and ii) a silencing strategy of each of *VvCERK* genes in grapevine, by using expression vectors and the Gateway technology (Karimi *et al.*, 2002).

2.2 Functional complementation of the Arabidopsis *cerk1-2* mutant with grapevine *VvCERK*s

The functional complementation of the Arabidopsis *cerk1-2* mutant (Gimenez-Ibanez *et al.*, 2009) was undertaken in collaboration with Cyril Zipfel, Freddy Boutrot and Lena Stransfeld

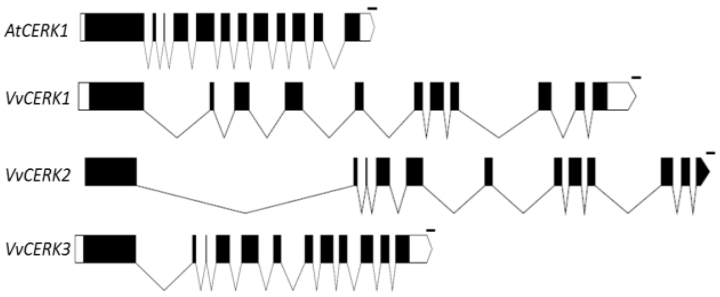

Figure 41. Exon-intron architecture of spliced *AtCERK1* and *VvCERK* transcripts.
Black and white boxes represent exons and UTR regions, respectively. Bar = 100 bp.

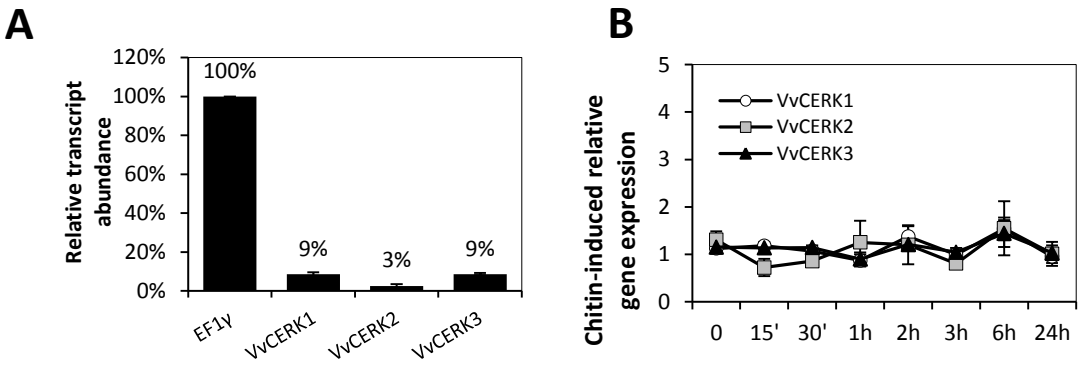

Figure 42. The basal transcript abundance and gene expression of *VvCERK*s following chitin treatment in grapevine cells.
The transcript abundance of the genes *VvCERK1*, *VvCERK2*, *VvCERK3* and the housekeeping gene *EF1γ* were determined by qPCR in chitin- or mock-elicited grapevine cells and quantified with a LinReg program (Ruijter *et al.*, 2009). **A.** The transcript abundance in mock-treated samples expressed as means ± SE from 3 experiments, relative to the amount of *EF1γ* transcripts, set as 100%. **B.** Kinetics of *VvCERK* gene expression induced by chitin 1g l^{-1}. Expression of *VvCERKs* was normalized to housekeeping genes *EF1α* and *EF1γ* and data are expressed as means ± SE from three experiments (n=3) relative to water treated control.

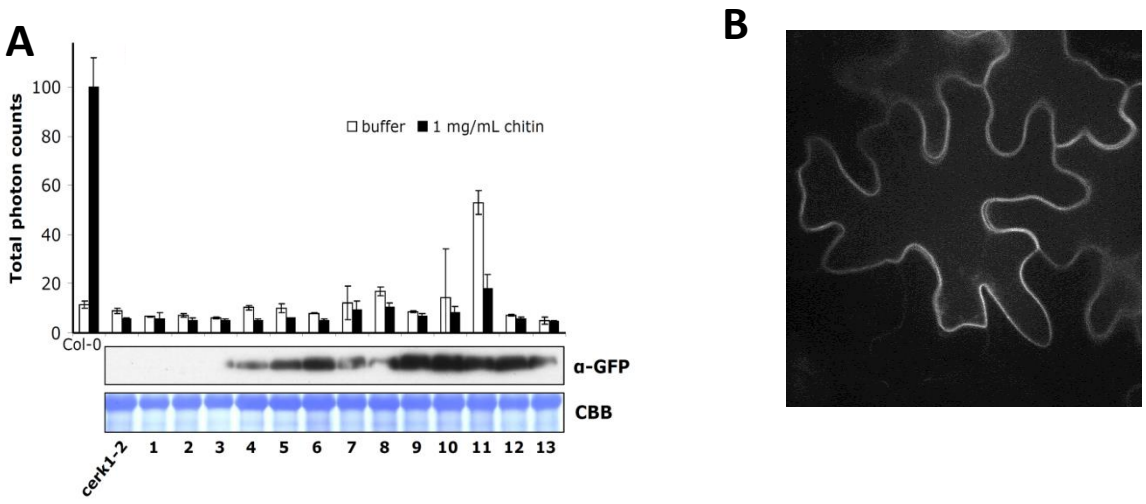

Figure 43. *VvCERK1* does not complement the chitin-induced ROS production in the Arabidopsis mutant *cerk1-2*. A. Correlation between H_2O_2 production after chitin treatment (1 g l^{-1}) and VvCERK1-GFP protein amount detected by α-GFP immunoblot in different kanamycin resistant T3 lines *cerk1-2/p35S::VvCERK1-GFP*. Equal loading was checked by Coomassie brilliant blue (CBB) staining. ROS production was measured in leaf discs using chemiluminescence of luminol. (*Fig. A from F. Boutrot*) **B.** Subcellular localization of VvCERK1-GFP visualized by confocal microscopy in leaves of *N. benthamiana* transiently transformed with *p35S::VvCERK1-GFP*. Fluorescence was observed 2 days post Agrobacterium-mediated transformation (*Fig. B from J. Collemare*).

(The Sainsbury Laboratory, Norwich, UK), who carried out the Arabidopsis transformation and screened the mutant complemented lines.

At first, the constitutive overexpression of each of *VvCERK*s in the *cerk1-2* background was tested. The full-length CDS of *VvCERK1, VvCERK2* or *VvCERK3* was cloned into the binary vector pK7FWG2 (Kanamycin resistance) and then used to obtain Arabidopsis *cerk1-2* transgenic lines expressing *p35S::VvCERK1-GFP*, *p35S::VvCERK2-GFP* or *p35S::VvCERK3-GFP*.

2.2.1 Constitutive overexpression of *VvCERK1* does not complement *cerk1-2*

Transformation of *cerk1-2* with *p35S::VvCERK1-GFP* resulted in 28 independent T1 kanamycin-resistant lines. For all of these T1 plants, responsiveness was not clear: no or only one leaf disc out of two was slightly responsive (data not shown). Thirteen stable homozygous T3 lines carrying a single transgene (3:1 antibiotic resistance segregation in progeny) were generated. None of them gave a ROS burst in response to 1 g l^{-1} chitin even though the VvCERK1-GFP fusion protein accumulated in some lines, as shown by the Western blot detection (Fig. 43A).

In agreement with the presence of a predicted signal peptide and a predicted transmembrane domain (Predotar), confocal microscopy analysis of *N. benthamiana* leaves transiently transformed with *p35S::VvCERK1- GFP* indicated that the corresponding protein seems to be targeted to the plasma membrane (Fig. 43B).

All together, our data showed that *VvCERK1* did not restore chitin-triggered ROS responsiveness in at least seven independent stable T3 lines of *cerk1-2 p35S::VvCERK1-GFP* plants, although the fused protein was immuno-detected (Table 13).

2.2.2 Constitutive overexpression of *VvCERK2* or *VvCERK3* leads to cell death

While the transformation with *p35S::VvCERK1-GFP* was successful, repeated transformations with *p35S::VvCERK2-GFP* and *p35S::VvCERK3-GFP* resulted in only two kanamycin-resistant T1 lines. A hundred of resistant T1 lines are usually obtained. Moreover, T2 progenies of these lines were sensitive to kanamycin. Thus, no stable *cerk1-2* lines constitutively expressing *p35S::VvCERK2* and *p35S::VvCERK3* could be obtained.

In agreement with this, microscopic analyses of the *N. benthamiana* leaves transiently transformed with *p35S::VvCERK2-GFP* and *p35S::VvCERK3-GFP* led to a tissue collapse suggesting cell death (Jérôme Collemare, Wageningen University, NL, personal communication). This correlates with the failed Arabidopsis transformation with *p35S::VvCERK2/3* constructs.

To sum up, the constitutive overexpression of *VvCERK2* and *VvCERK3* in Arabidopsis failed to generate stable transgenic lines possibly due to an induced lethality (Table 13).

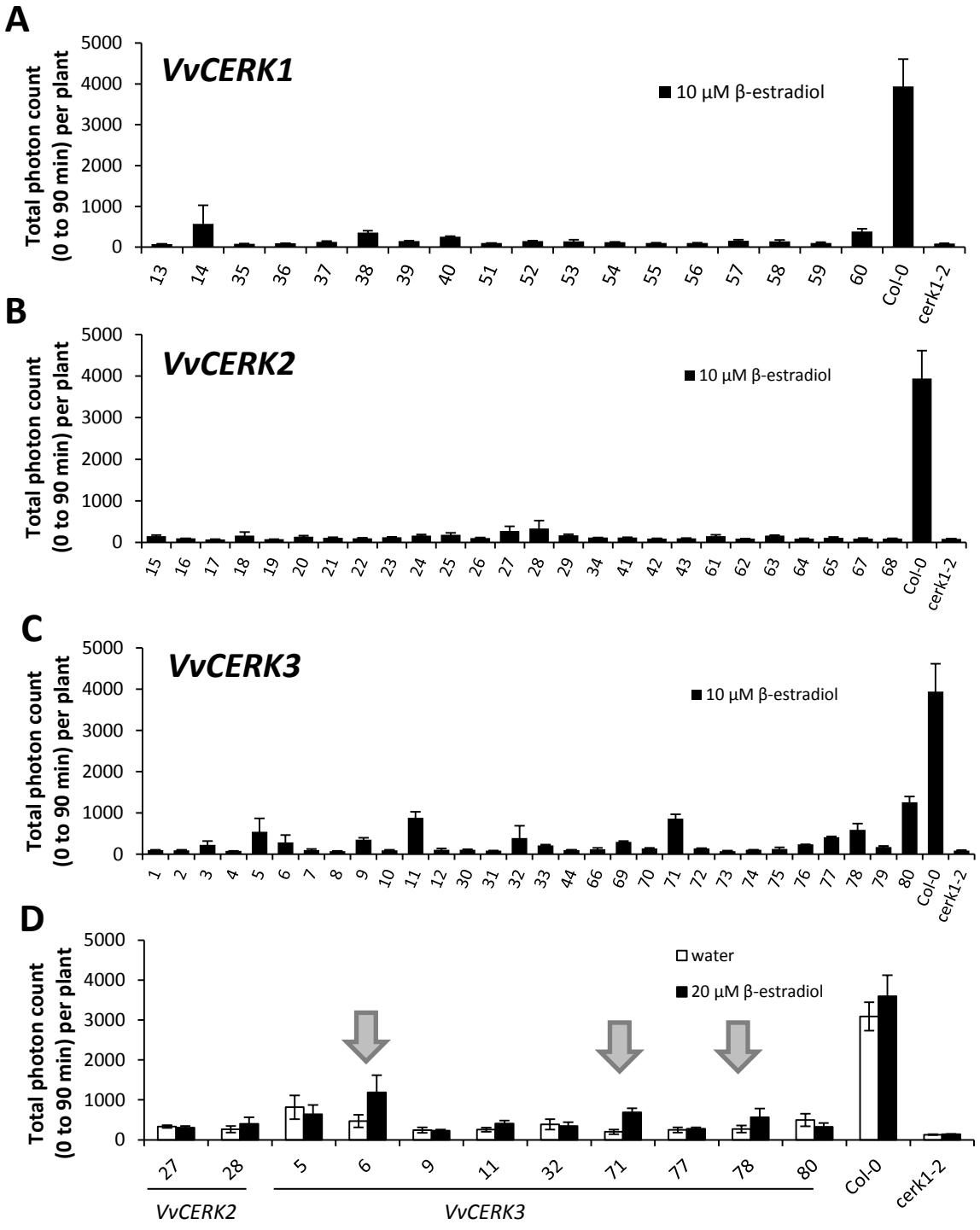

Figure 44. β-estradiol inducible expression of *VvCERK2* or *VvCERK3* partly complements the chitin-induced ROS production in the Arabidopsis mutant *cerk1-2*.

Oxidative burst after chitin treatment (100 mg l^{-1}) was analyzed by luminol-based method. **A.-C.** Screening of chitin-induced oxidative burst in T1 (**A.-C.**) and T2 (**D.**) generation of *cerk1-2* plants with estradiol-inducible expression of *pLexA::VvCERK1* (**A.),** *pLexA::VvCERK2* (**B.**), *pLexA::VvCERK3* (**C.**). Two discs from one plant per line were pre-treated with 10µM β-estradiol for 20 h, then treated with chitin. **D.** Chitin induced oxidative burst in T2 progeny of the most responsive T1 lines. For each line, twelve discs were pre-treated with 20µM β-estradiol (black bars) or with water (white bars) for 20 h, prior to elicitation with chitin. ROS production is compared to wild-type (Col-0) and *cerk1-2* plants. (*Data L. Stransfeld*).

2.2.3 Inducible expression of *VvCERK*s in *cerk1-2* background

Given the lethality of the constitutive overexpression of *VvCERK2/3*, new assays were launched with the expression of *VvCERK1, 2* and *3* driven by an inducible promoter, using the pABindGFP vector (Bleckmann *et al.*, 2010). This vector permits the expression of a C_{ter} tagged GFP-VvCERK regulated by the β-estradiol inducible *pLexA* promoter.

For each transformation, 18-30 hygromycin-resistant T1 lines were obtained. The *VvCERK* expression was induced by β-estradiol, then 20 h later the chitin-induced oxidative burst was measured. Estradiol treatment did not affect chitin-induced ROS production in wild-type Col-0 (Fig. 44D). This first rapid screening showed that a number of T1 lines seemed to partially complement *cerk1-2* mutant (Fig. 44 A, B, C). Most of these chitin responsive lines were obtained with the *VvCERK3* construct (Fig. 44C). The most responsive lines of *VvCERK2* and *VvCERK3* were checked again in T2 generation (Fig. 44D). In fact, many of these lines were revealed as false positives. However, in lines *pLexA::VvCERK3-GFP* #6, #71 and #78, but not in *cerk1-2*, the detected chitin-induced ROS production was enhanced in estradiol pretreated leaf discs compared to water-treated leaf discs (Fig. 44D). These data suggest that VvCERK3 complements the chitin-induced ROS burst in *cerk1-2* and therefore indicate that VvCERK3 might function as a chitin receptor. However, the complementation was only partial. As *VvCERK1* did not complement *cerk1-2* in different stable T3 lines of *cerk1-2/p35S::VvCERK1-GFP* (Fig. 43A), the inducible T2 progeny was not tested. For *VvCERK2*, we did not obtain clear data whether VvCERK2 can complement Arabidopsis as the chitin-induced ROS burst observed in *cerk1-2*/*pLexA::VvCERK2* plants was unstable between T1 and T2 generations (Fig. 44B, Table 13). Further experiments are needed to confirm these preliminary results and to better characterize each of VvCERKs.

2.3 Silencing of *VvCERK*s in grapevine

In parallel to complementation assays in Arabidopsis, we aimed to silence the *VvCERK1, 2* and *VvCERK3* genes in grapevine using antisense constructs pH2WG7 (Fig. 14E; Karimi *et al.*, 2002) using the service of the grapevine transformation platform (Jean Masson, Mireille Perrin, Carine Schmitt, INRA, Colmar, FR). Indeed, plants silenced in *VvCERK1, VvCERK2* or *VvCERK3* would be a perfect tool to investigate the involvement of each VvCERK in chitin perception and during the grapevine interactions with fungi.

The antisense fragments of 235-684 bp were designed to target the ectodomain of a given *VvCERK* (Table 6, Materials and Methods). Their specificity was verified with the BLASTn program implemented in Genoscope and NCBI databases. *Agrobacterium*-mediated transformation was successful only with the *p35::αsVvCERK3* construct (Fig. 45), while no hygromycin-resistant calli could be obtained in repeated transformations with *p35S::αsVvCERK1* and *p35S:: αsVvCERK2* constructs (Fig. 46A, Table 13)

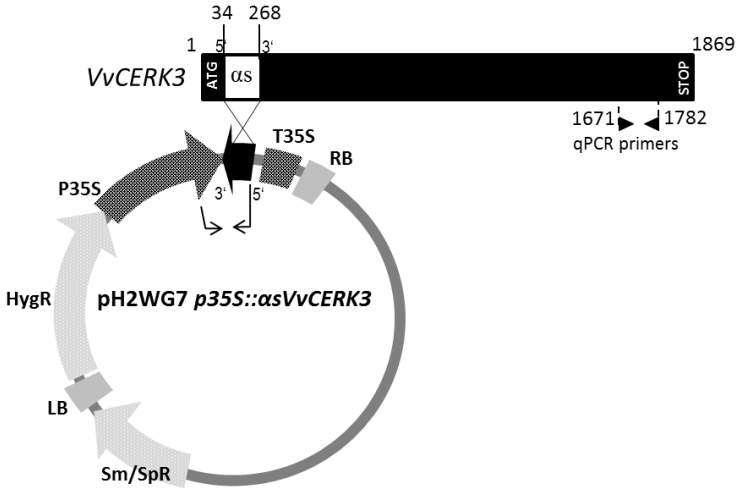

Figure 45. Antisense construct for VvCERK3 silencing.
Position of the *VvCERK3* antisense fragment (αs) in the *VvCERK3* coding sequence and pH2WG7 *p35S::αsVvCERK3* vector map. Nucleotide (nt) 1 indicates the start of translation. The fragment (nt 34 – 268) was PCR-amplified using specific primers and inserted in the antisense orientation into pH2WG7 vector. The plasmid pH2WG7 *p35S::αsVvCERK3* was used for the transformation of grapevine embryogenic calli *via Agrobacterium tumefaciens*. Arrows indicate primers used to verify transgene presence. Black triangles indicate qPCR primers used for *VvCERK3* quantification.

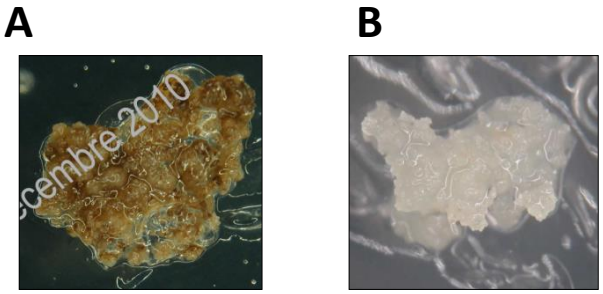

Figure 46. Expression of *αsVvCERK1* and *αsVvCERK2* , unlike *αsVvCERK3* causes lethality in grapevine embryogenic calli.
Selection of embryogenic calli (cv. Pinot Noir PN40024) transformed with *p35S::αsVvCERK1* (**A.**) or *p35S::αsVvCERK3* (**B.**) on hygromycin 25 mg l^{-1}. Lethality was also caused by *p35S::αsVvCERK2* (figure not shown).

The transformation with *p35S::αsVvCERK3* construct enabling the expression of a specific VvCERK3 fragment (Annex 6A) resulted in 45 hygromycin-resistant calli issued from independent transformation events (Fig. 46B). Using primers matching the 3' end of the *p35S* promoter and the 5'end of the antisense fragment (Fig. 45), the RT-PCR transgene detection permitted the selection of 10 *αsVvCERK3*-expressing calli, hereafter referred as lines #6-2 up to #6-28, for *in vitro* plantlet regeneration *via* somatic embryogenesis. Nine independent lines of *p35S::αsVvCERK3* plants possessed a similar developmental phenotype compared to the mock-transformed WT plants issued from a parallel somatic embryogenesis (seWT), whereas one line (#6-11) possessed a low growth rate and has been stopped. Lines were then screened for the *VvCERK3* expression and the loss of chitin responsiveness.

The *VvCERK3* expression was quantified in all lines by qPCR with *VvCERK3* specific primers matching the 3' end of the transcript (Fig. 45, Table 5). The *VvCERK3* transcript amounts were not reduced in most of the lines reaching in average 98 ± 21 % of levels in seWT (Fig. 47A), except in the line #6-2, where *VvCERK3* transcripts were significantly reduced to 48% (t-test, $p<0.05$; Fig. 47B). Knowing that the *VvCERK3* fragment used in our silencing construct has one and two stretches of at least 11 nucleotides with perfect identity to *VvCERK2* and *VvCERK1*, respectively (Annex 6A), transcripts of *VvCERK1/2* were also quantified. Compared to the seWT levels (set as 100%), silencing did not significantly affect the level of *VvCERK1* and *VvCERK2* expression in the line #6-2 (t-test, $p>0.05$; Fig. 47B).

Chitin responsiveness in the independent *p35S::αsVvCERK3* plant lines was verified by MAPK phosphorylation assays (Fig. 47C). Leaves of all lines showed a strong MAPK phosphorylation, both after chitin and flg22 treatment. Also the line #6-2 exhibited a similar response to chitin compared to leaves of seWT or the other *p35S::αsVvCERK3* lines.

To sum up, our effort to silence *VvCERK3* in grapevine led to only one interesting transgenic line *p35S::αsVvCERK3* (#6-2) where *VvCERK3* transcripts were silenced to 48% of the seWT. Nevertheless, no decrease in chitin responsiveness was observed in this line or any other line based on detection of the chitin-induced MAPK phosphorylation. Given these results, the role of VvCERK3 in grapevine chitin perception remains unclear. Silencing of *VvCERK1* and *VvCERK2* probably led to the embryogenic callus lethality as transformation assays repeatedly failed whereas parallel control transformations with *p35S::GFP* were successful (Table 13).

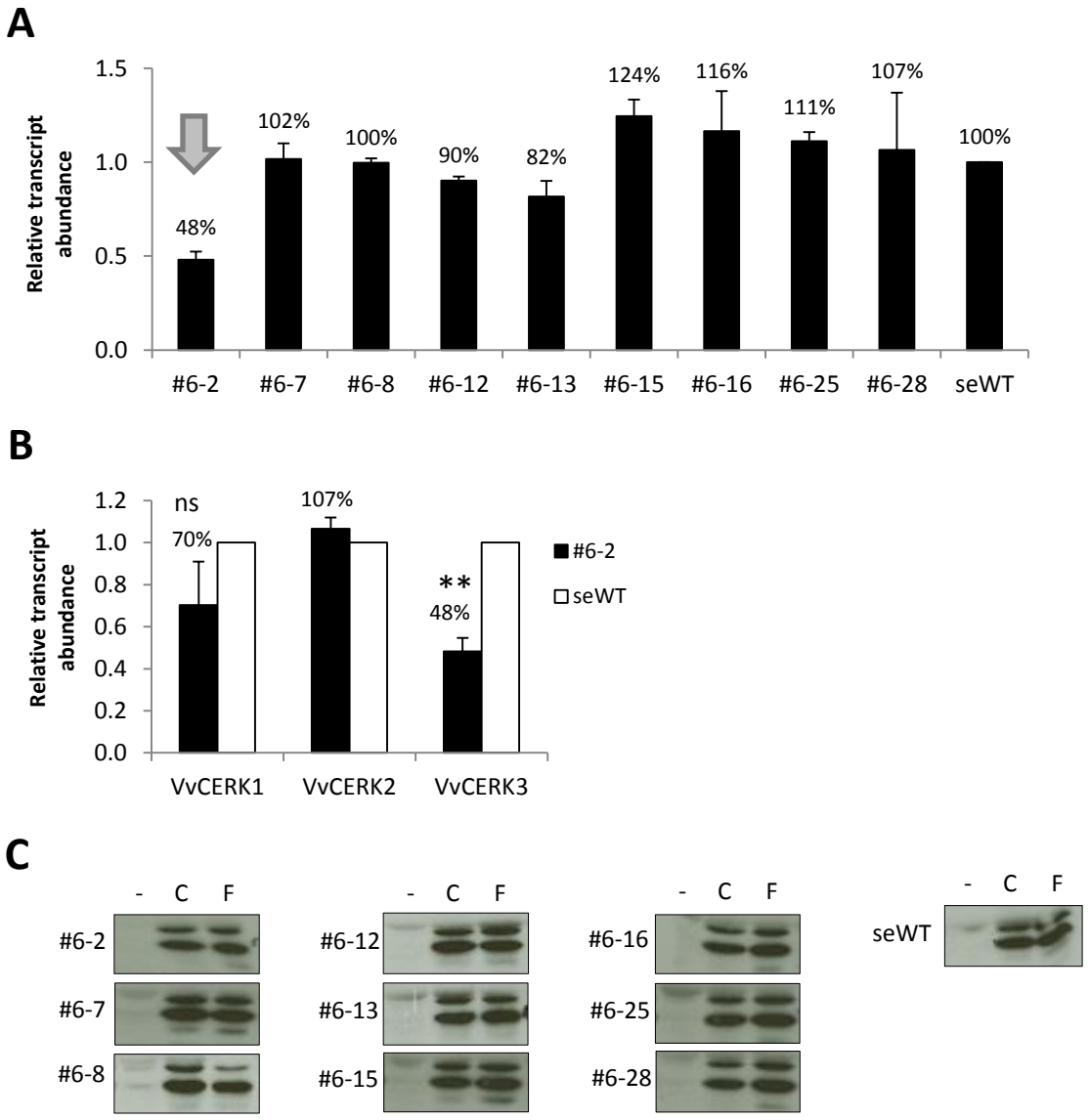

Figure 47. Quantification of *VvCERK3* transcript amount and chitin responsiveness in grapevine transgenic lines expressing *p35S::αsVvCERK3*.

The expression of *VvCERK3* and chitin responsiveness were evaluated in leaves of different *in-vitro* plantlets expressing *p35S::αsVvCERK3* or in wild-type *in-vitro* plantlets issued from a parallel somatic embryogenesis (seWT). **A., B.** Relative transcript abundance of *VvCERK3* (**A.**) or of *VvCERK*s (**B.**) in different lines (A.) or the *p35S::αsVvCERK3* line #6-2 was measured by qPCR, normalized to housekeeping genes EF1α and EF1γ and reported to seWT, set as 100 %. For **A.**, data are means ± SE from at least two independent experiments, for **B.,** data are means ± SD from three independent experiments, ** indicates statistical significance (t-test, $p<0.01$), ns: non-significant. **B.** Phosphorylation of two mitogen-activated protein kinases (MAPK) detected by α-pERK1/2 Western blots at 15 min post treatment with water control (-), chitin (C) or flg22 (F). Homogeneous loading was checked by Coomassie Brilliant Blue (CBB) staining of a parallel gel (not shown). Experiment was repeated at least twice with similar results. Data from one representative experiment are shown. Treatments were performed with 1 g l^{-1} chitin and 500 nM flg22.

3 LysM-RLPs (LYPs) family and identification of putative OsCEBiP ortholog in grapevine (VvCEBiP)

3.1 *In silico* characterization of the predicted grapevine CHITIN ELICITOR BINDING PROTEIN orthologs

Beside identification of the AtCERK1 ortholog, the OsCEBiP ortholog was also searched in the grapevine genome. Indeed, the LYP OsCEBiP is the major chitin receptor in rice (Kaku *et al.*, 2006). Moreoever, orthologs of CEBiP seems to be implicated in chitin perception in barley and wheat (Lee *et al.*, 2014 and Henk-Jan Schoonbeek, John Innes Centre, Norwich, UK, personal communication;).

The grapevine genome encodes a total of 4 LysM-RLPs (LYPs, VvLYP1-VvLYP4, Table 14). A phylogenetic analysis indicates that the two predicted LysM-RLPs VvLYP1 (XP_002278760) and VvLYP2 (XP_002278742) display the highest degree of homology to OsCEBiP (Fig. 48) and are clearly distinct from other grapevine or Arabidopsis LYPs. Hereafter, they are referred to as VvCEBiP1 and VvCEBiP2, respectively. VvCEBiP1 exhibits slightly higher BLASTp hits to OsCEBiP (2e-68) and to the closest Arabidopsis ortholog, AtLYM2 (e-99), than VvCEBiP2 (E-values 7e-65 and e-76 for the homology to OsCEBiP and AtLYM2, respectively; Table 14). The phylogenetic tree also indicates that VvLYP3 (XP_002285848) and VvLYP4 (XP_002276124) might be the homologs of AtLYM1/AtLYM3 and OsLYP4/OsLYP6, which are involved in the peptidoglycan (PGN) binding and perception (Fig. 48; Willmann *et al.*, 2011; Liu *et al.*, 2012a).

VvCEBiP1 and *VvCEBiP2* are located in close loci on chromosome 3 and share a high degree of identity both at the protein (78% identity) and the nucleotide level (88% identity). The gene predictions of *VvCEBiP1* and *VvCEBiP2* in the genome of *V. vinifera* cv Pinot Noir consist of open-reading frames of 1056 and 1074 bp containing 3 and 4 exons, respectively. *VvCEBiP1* possesses a clear predicted 5'UTR in contrast to *VvCEBiP2* (Fig. 49).

The predicted encoded proteins of 353 and 357 amino acids contain each a signal peptide, and two predicted LysM domains (LysM1 and LysM2), while the prediction of the N-terminal LysM0 domain was not clear (Annex 7). VvCEBiP2 has a predicted transmembrane region at the C_{ter} extremity, unlike VvCEBiP1 (Annex 7). The VvCEBiP1 protein sequence exhibits 58% amino acid similarity with OsCEBiP.

Under non-elicited conditions, amounts of *VvCEBiP1* transcript are ~three times more expressed than those of *VvCEBiP2*, accounting for ~12% of the transcript level of housekeeping gene *EF1γ* (Fig. 50A). In grapevine cells, *VvCEBiP1* gene expression was upregulated between 2 – 6 h after chitin treatment (Fig. 50B). *VvCEBiP2* gene expression was not regulated by chitin treatment during the whole kinetics (Fig. 50B). *VvCEBiP1* seems therefore to be the best candidate for functional characterization.

Targeted Vv*PRR*s	Silencing antisense (αs) constructions (*V. vinifera*)	Complementation in *cerk1-2 (A. thaliana)*	
		p35S::VvPRR-GFP	***pLexA::VvPRR-GFP***
Vv*CERK1*	xxx (lethal)	Fused protein expression No complementation	? Fused protein ? complementation (T1:+, T2: ND)
Vv*CERK2*	xxx (lethal)	xxx (lethal)	? Fused protein Partial complementation (T1: +, T2: -)
Vv*CERK3*	Silencing (50%), Fully responsive to chitin	xxx (lethal)	? Fused protein Partial complementation (T1: ++, T2:+)

Table 13. The summary of the *VvCERK* genetic characterization.
Endogenous transcript silencing was evaluated by qPCR with primers specific to the targeted *VvCERK*s. Chitin responsiveness in *V. vinifera* was evaluated by MAPK phosphorylation assays. In Arabidopsis, complementation was evaluated by ROS burst assays in T1 and T2 generation of *cerk1-2* overexpressing constitutively (*p35S*) or after oestradiol induction (*pLexA*) *VvCERK*s. -/+/++ indicate the intensity of complementation. The presence of fused protein was verified by the anti-GFP Western Blots or the confocal microscopy. ND: Not determined, xxx: fail in the transformant regeneration.

Grapevine protein			***The closest Arabidopsis ortholog***		
Name	**Protein ID (GenBank)**	**Length (aa)**	**ID (TAIR)**	**Name**	**E-value (blastp)**
VvLYP1/VvCEBiP1	XP_002278760	353	AT2G17120	AtLYM2	e-99
VvLYP2/VvCEBiP2	XP_002278742	357			e-76
VvLYP3	XP_002285848	357	AT1G21880	AtLYM1	e-156
VvLYP4	XP_002276124	408			3e-68

Table 14. List of LysM-containing receptor-like proteins (LYPs) in *Vitis Vinifera*.
Protein sequences (GenBank prediction) were identified by BLASTp with OsCEBiP and AtLYPs. The presence of predicted LysM domains (PF01476) was verified by SMART (http://smart.embl-heidelberg.de). The closest ortholog of each VvLYP in Arabidopsis was searched with BLASTp (TAIR http://www.arabidopsis.org/Blast).

3.2 Silencing of *VvCEBiP1* in grapevine

To investigate the function of VvCEBiP1, a silencing strategy was undertaken using the Gateway vector pH2WG7 for antisense expression. In order to limit the non-specific matches with *VvCEBiP2*, the antisense fragment (317 bp) was designed to partly target the 5'UTR of the *VvCEBiP1* transcript (Fig. 51; Table 6, Materials and Methods). However, two stretches of 30 and 32 nucleotides with perfect identity between *VvCEBiP1* and *VvCEBiP2* were present within the *αs-VvCEBiP1* fragment (Annex 6B).

Transgenic grapevine lines expressing *p35S::αsVvCEBiP1* were generated. From the 61 hygromycin-resistant calli that were obtained, ten were selected based on the transgene detection by PCR (data not shown). These lines, referred as #3-1 up to #3-24, were kept for *in vitro* plantlet regeneration *via* somatic embryogenesis. The obtained transgenic *αsVvCEBiP1* lines were then screened for the expression levels of *VvCEBiP1* by qPCR with specific primers (Fig. 51, Table 5) and for the loss of chitin responsiveness.

Compared with seWT, all lines except the line #3-18 contained lower amounts of *VvCEBiP1* transcripts, ranging from 21% to 84% (Fig. 52A). Six lines exhibited a silencing efficiency higher than 50%, including the best-silenced lines #3-4 and #3-24 presenting only 21% and 25% of *VvCEBiP1* transcripts, respectively. Compared to seWT, the amount of *VvCEBiP2* transcripts was not significantly reduced in lines #3-4 and #3-24 but its expression might be affected in other lines (Fig. 52B). Unfortunately, MAPK phosphorylation assays did not reveal any decrease in chitin responsiveness in lines #3-4 and #3-24 or in any of the other lines (Fig. 52C)

Therefore, no correlation between the level of *VvCEBiP1* transcript and chitin responsiveness could be deduced. Our preliminary results seem to indicate that VvCEBiP1 does not play a major role in chitin perception in *V. vinifera*, even if some *VvCEBiP1* transcripts remained.

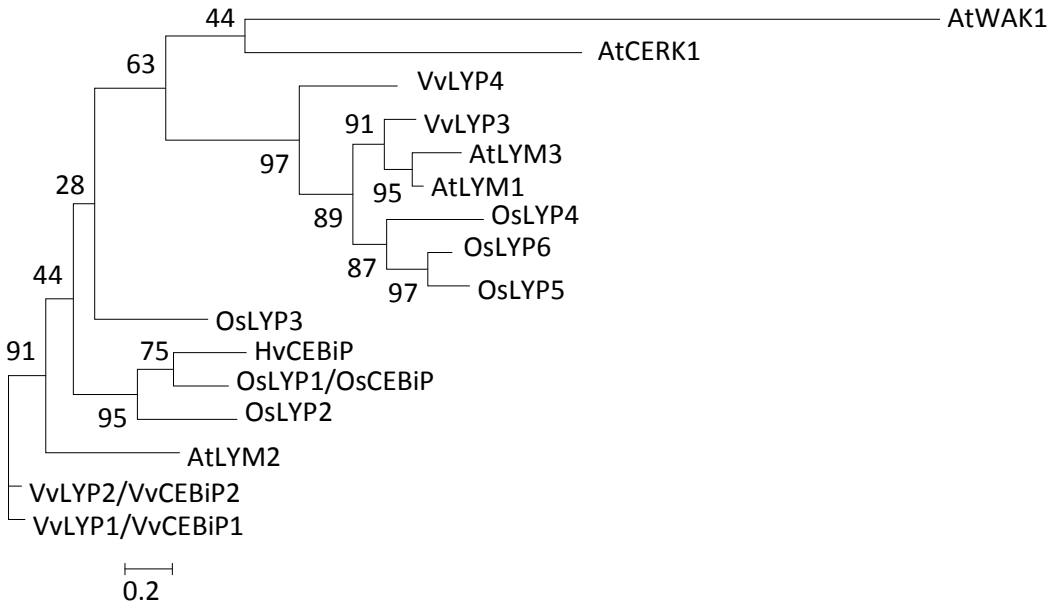

Figure 48. ***In silico*** **characterization of the LysM-RLP (LYP) family and OsCEBiP ortholog in** ***Vitis vinifera*****.**
A. Maximum-likelihood phylogenetic tree (500 boostraps) showing the relationship between the full-length protein sequences (GenBank) of the rice OsCEBiP (NP_001048875), other LYPs of rice (OsLYP2:ABA94116, OsLYP3:NP_001063853, OsLYP4:NP_001063335, OsLYP5:NP_001048242, OsLYP6:BAD35901), LYPs of Arabidopsis (AtLYM1:AT1G21880, AtLYM2:AT2G17120, AtLYM3:AT1G77630) and the VvLYPs (VvLYP1-4) of *V. vinifera*. Percentage of bootstraps are presented.

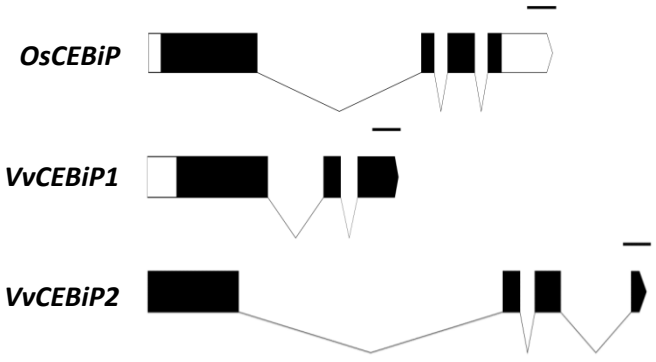

Figure 49. Exon-intron architecture of spliced ***OsCEBiP*** **and** ***VvCEBiP1, 2*** **transcripts.**
Black and white boxes represent exons and UTR regions, respectively. Bar = 200 bp.

Discussion

1 Chitin is a weak elicitor in grapevine

Chitin elicits defense responses in various plant species, but not much is known about its effect in grapevine. We show that chitin elicited defense responses in grapevine, including variations in free $[Ca^{2+}]_{cyt}$, phosphorylation of two MAPKs and the expression of defense genes including *PR3-4c*, *ACCS*, *STS1-2* and *PAL* (Fig. 37, 38). Upregulation of genes encoding chitinases and PAL was also observed in Arabidopsis and rice (Kaku *et al.*, 2006; Miya *et al.*, 2007). The *PR3-4c* gene expression was the most strongly upregulated by chitin, yet its induction was 30 times lower than that triggered by flg22 (Fig. 38F, Fig. 18F; Trda *et al.*, 2014) or the β-1,3-glucan laminarin (Aziz *et al.*, 2003). In the same way, both the chitin-induced MAPK activation and the $[Ca^{2+}]_{cyt}$ variations were triggered more transiently compared with laminarin or flg22 (Fig. 37 A, B).

It is curious that chitin did not trigger any detectable H_2O_2 production in grapevine (*V. vinifera* cv Gamay, Fig. 37 C), unlike in Arabidopsis (Miya *et al.*, 2007), *Brassica napus* (Lloyd *et al.*, 2014), *N. benthamiana* (Segonzac *et al.*, 2011) or rice (Hayafune *et al.*, 2014). We found that chitin upregulated the expression of the grapevine gene *RbohD* (Fig. 38B), which is also upregulated by OGs (Dubreuil-Maurizi *et al.*, 2010) and flg22 (Fig. 3). AtRbohD and NbRbohD are responsible for the flg22-induced ROS production in Arabidopsis and *N. benthamiana*, respectively (Zhang *et al.*, 2007; Segonzac *et al.*, 2011). Similarly, chitin induced a rather weak oxidative burst in *N. benthamiana* and Arabidopsis (Nekrasov *et al.*, 2009; Segonzac *et al.*, 2011). Studies in *N. benthamiana* show that flg22- or chitin-induced ROS burst is not required for MAPK activation (Segonzac *et al.*, 2011). In grapevine, these two events induced by BcPG1 also lie on independent signaling branches (Vandelle *et al.*, 2006). According to our data, chitin/chitosan signaling in grapevine seems to lack the ROS pathway. However, we cannot exclude that using a more sensitive method (such as enhanced luminol L-012), the chitin-induced H_2O_2 production could have been detected or that another reactive oxygen species is produced but not detected by luminol-based method.

In grapevine, chitosan induced early MAPK phosphorylation and $[Ca^{2+}]_{cyt}$ variations with a similar amplitude and duration as the chitin treatment (Fig. 37A, B). Additionally, the chitosan-induced H_2O_2 production was not detected in grapevine (Fig. 37C), even though it has been reported in tobacco or rice (Iriti and Faoro, 2009). These data suggest that chitin and chitosan might be perceived by the same mechanism in *V. vinifera*. In Arabidopsis, the totally deacetylated chitosan penta- to octamers were unable to bind AtCERK1, whereas chitin oligomers of the same length possessed affinity to AtCERK1 (Petutschnig *et al.*, 2010). Both binding competitions and solved crystal structure show that the acetylation is required for binding to AtCERK1 (Petutschnig

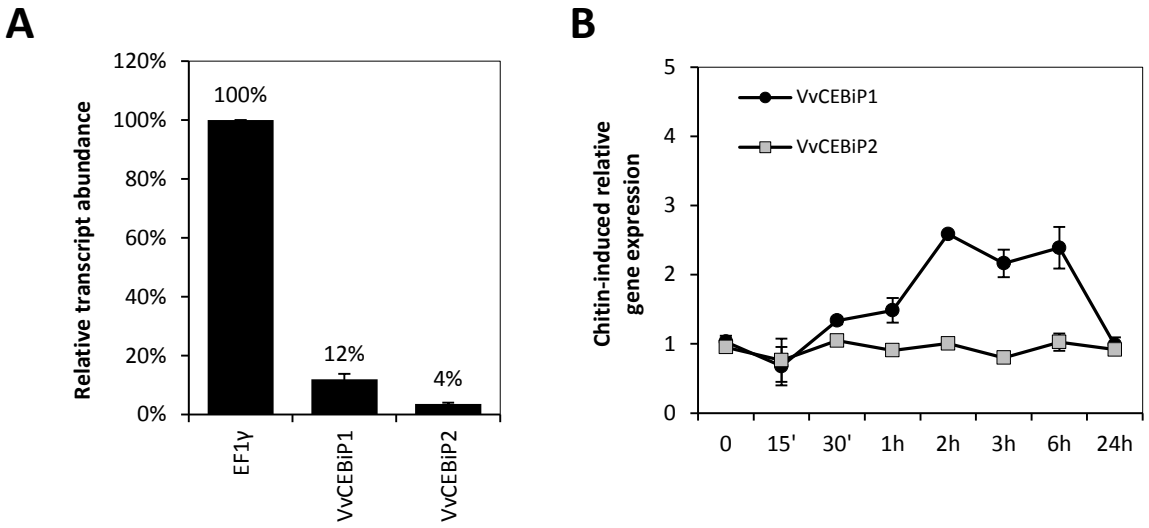

Figure 50. The basal transcript abundance and gene expression of *VvCEBiP*s following chitin treatment in grapevine cells.

The transcript abundance of genes *VvCEBiP1, VvCEBiP2* and housekeeping gene *EF1γ* was assessed by qPCR in chitin- or mock-elicited grapevine cells and quantified with a LinReg program (Ruijter *et al.*, 2009). **A.** Transcript abundances in mock-treated samples are expressed as means ± SE from 3 experiments, relative to the amount of *EF1γ* transcripts set as 100%. **B.** Kinetics of *VvCEBiP* gene expression induced by 1g l^{-1} chitin. Relative expression was normalized to housekeeping genes *EF1α* and *EF1γ* and data are expressed as means ± SE from three experiments (n=3) relative to water treated control.

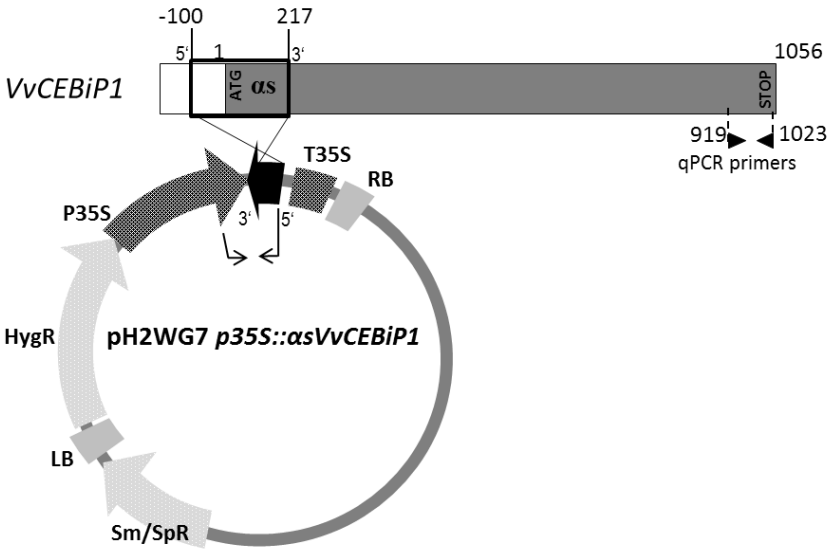

Figure 51. Antisense construct for *VvCEBiP1* silencing.

Position of the *VvCEBiP1* antisense fragment (αs) in the coding sequence (gray band) and 5'UTR (white band) and pH2WG7 *p35S::αsVvCEBiP1* vector map. Nucleotide (nt) 1 indicates the start of translation. The fragment (nt -100 to + 217) was PCR-amplified using specific primers and inserted in the antisense orientation into pH2WG7 vector. pH2WG7 *p35S::αsVvCEBiP1* was used for the transformation of grapevine embryogenic calli via *Agrobacterium tumefaciens*. Arrows indicate primers used to verify transgene presence. Black triangles indicate qPCR primers used for *VvCEBiP1* quantification.

et al., 2010; Liu *et al.*, 2012b). As the chitosan we used was not fully deacetylated (DA<25%), the -$(GlcNAc)_n$- residues might be key for its biological activity as previously shown (Iriti and Faoro, 2009; Petutschnig *et al.*, 2010).

We have also shown that chitin did not enhance the resistance of grapevine leaves to the necrotrophic fungus *B. cinerea* or to the obligate biotrophic oomycete *P. viticola* (Fig. 39). Parallel pretreatment with flg22, laminarin or PS3 partly inhibited the infection with *B. cinerea* (Fig. 19A), suggesting that chitin-induced responses might not be sufficiently strong. Especially the weak chitin-induced expression of *PAL* and *STS1-2* genes (Fig. 38 D, E) suggests a low activation of the phenylpropanoid pathway responsible for stilbene, lignin or flavonoid production. These metabolites were identified as active compounds against both pathogens (Coutos-Thevenot *et al.*, 2001; Polesani *et al.*, 2010). In rice, $(GlcNAc)_8$ induced local and systemic resistance against the rice blast fungus *M. oryzae* (Tanabe *et al.*, 2006). In Arabidopsis, chitooligomers also enhanced resistance to *A. brassicicola* (Wan *et al.*, 2008).

Previous works reported a chitosan-induced resistance in different plant species (Benhamou *et al.*, 1994; El Ghaouth *et al.*, 1994; Trotel-Aziz *et al.*, 2006). In our experiments, chitosan reduced the development of *B. cinerea* and *P. viticola* by approximately 50 and 70%, respectively (Fig. 39). Although chitosan we used was polymeric, these data are consistent with the activity of smaller chitosan oligomers (1.5 kDa, DA~20%) conferring a similar rate of protection against both pathogens (Aziz *et al.*, 2006; Trotel-Aziz *et al.*, 2006). Chitosan was previously shown to induce phytoalexin accumulation and activities of ß-1,3-glucanases and chitinases in grapevine leaves (Aziz *et al.*, 2006; Trotel-Aziz *et al.*, 2006). However, it also acts as an antifungal compound reducing the radial growth of *B. cinerea in vitro* and inducing cytological alteration of the pathogen and it is toxic to *P. viticola* spores as well (Benhamou *et al.*, 1994; El Ghaouth *et al.*, 1994; Trotel-Aziz *et al.*, 2006).

2 Role of VvCERK1

In Arabidopsis, AtCERK1 is the main chitin receptor (Miya *et al.*, 2007; Petutschnig *et al.*, 2010; Liu *et al.*, 2012b). Grapevine encodes three predicted orthologs of AtCERK1 (VvCERK1/2/3) that exhibit ~70% similarity to AtCERK1 (Fig. 40, Annex 4A). All VvCERKs possess a signal peptide, three LysM domains, one transmembrane region and an active kinase domain of the RD-type also found in AtCERK1 and OsCERK1 but unlike in most of the identified plant PRRs (Annex 5; Boller and Felix, 2009). Based on the similarity in amino acid sequences, VvCERK1 shares the highest degree of conservation with AtCERK1 and OsCERK1 (Annex 4A, 5) and was also identified as the closest ortholog in previous bioinformatics studies (Boller and Felix, 2009; Liu *et al.*, 2012b).

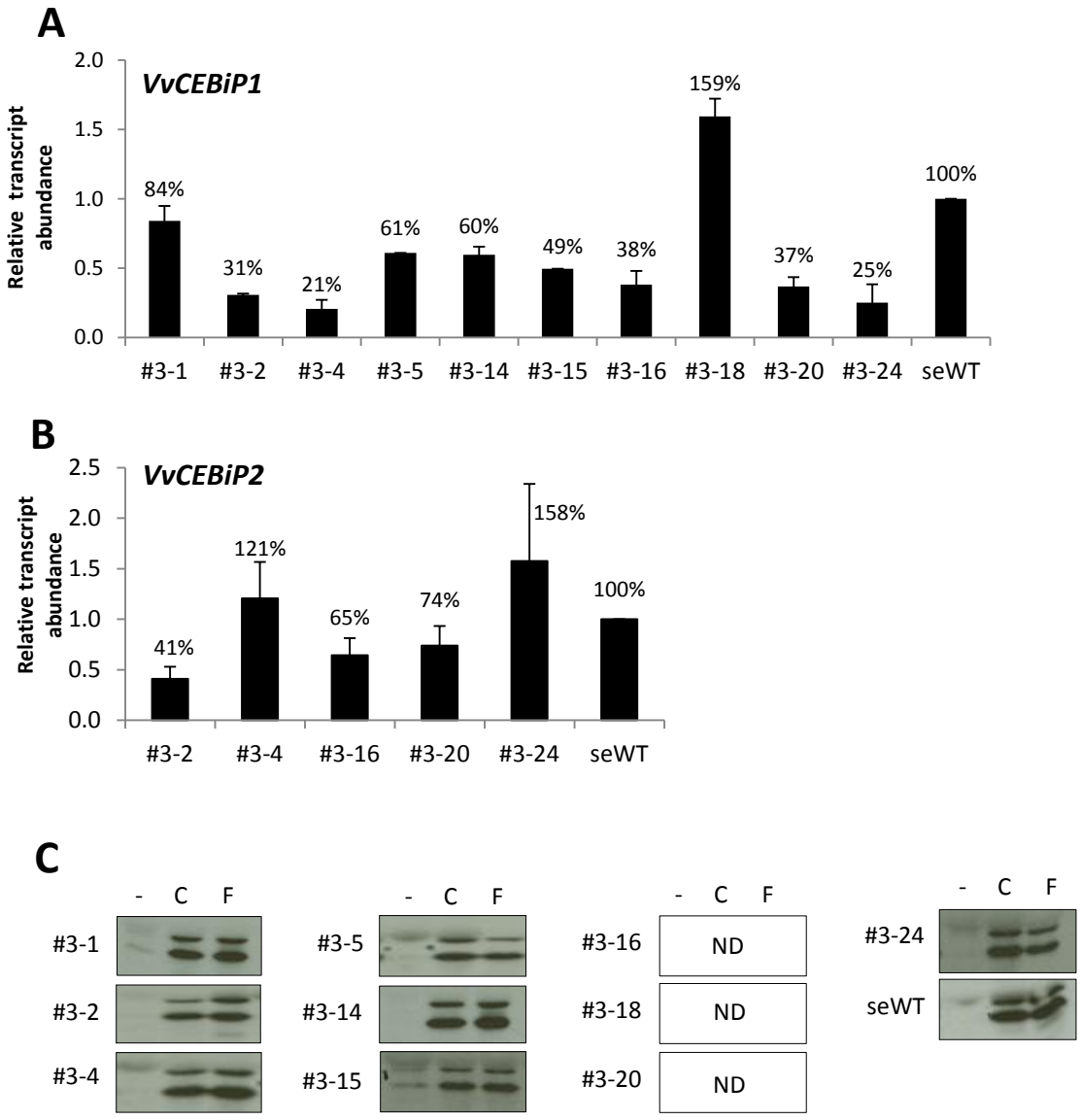

Figure 52. Quantification of *VvCEBiP1* transcript amount and chitin responsiveness in grapevine transgenic lines expressing *p35S::αsVvCEBiP1*.

The expression of *VvCEBiPs* and chitin responsiveness were evaluated in leaves of *in-vitro* plantlets expressing pH2WG7 *p35S::αsVvCEBiP1* or in wild-type *in-vitro* plantlets issued from a parallel somatic embryogenesis (seWT). **A., B.** Relative *VvCEBiP1* (**A.**) and *VvCEBiP2* (**B.**) transcript abundances were measured by qPCR, normalized to housekeeping genes EF1α and EF1γ and reported to seWT, set as 100 %. Data are means ± SE from at least two independent experiments (except from the line #3-5 and #3-15 that were measured once). **C.** Phosphorylation of two mitogen-activated protein kinases (MAPK) detected by α-pERK1/2 Western blots at 15 min post treatment with water control (-), chitin (C) and flg22 (F). Homogeneous loading was checked by Coomassie Brilliant Blue (CBB) staining of a parallel gel (not shown). Experiment was repeated at least twice with similar results. Data from one representative experiment are shown. Treatments were performed with 1 g l^{-1} chitin and 500 nM flg22. ND=Not determined.

In the transient expression assays in *N. benthamiana*, VvCERK1 fused to GFP in the C-terminal end was localized at the cell periphery (Fig. 43B). This suggests that VvCERK1 is localized to the plasma membrane as predicted by the presence of a signal peptide. According to our complementation assays in the Arabidopsis *cerk1-2* mutant, the overexpression of *p35S::VvCERK1-GFP* did not restore the chitin-induced oxidative burst, although the fused protein was accumulated in nine independent transgenic lines (Fig. 43A). These data suggest that VvCERK1 is not a functional ortholog of AtCERK1. As chitin perception in grapevine does not elicit an evident H_2O_2 production, other chitin-triggered responses should be tested to confirm these preliminary results.

3 Role of VvCERK2

Functional complementation assays in Arabidopsis show that the expression of *VvCERK2* enables the *cerk1-2* mutant to partly restore the chitin-induced ROS burst in two lines out of 26 in the T1 generation (Fig. 44B). However, the involvement of VvCERK2 in chitin perception remains unclear as the complemented phenotype of *cerk1-2*/*pLexA::VvCERK2* was unstable between T1 and T2 generation (Fig. 44D, Table 13).

4 VvCERK3 can partly complement the chitin-induced ROS burst in *Atcerk1-2*

VvCERK3 protein carries a LysM ectodomain which is the most similar to AtCERK1 reaching 51% of identity (Annex 4A). The *VvCERK3* gene also displays a gene architecture similar to *AtCERK1*, containing the similar number of exons and introns of conserved length (Fig. 41). To limit the negative impact of the receptor overexpression, *VvCERK3* was expressed in *cerk1-2* mutant controlled by an estradiol-inducible promoter. Some of the T2 lines of *cerk1-2/pLexA::VvCERK3-GFP* plants transiently expressing *VvCERK3* after estradiol induction partly restored the chitin-induced oxidative burst normally abolished in the *cerk1-2* mutant (Fig. 44C, D). According to these preliminary results, VvCERK3 might be the AtCERK1 ortholog in grapevine.

As AtCERK1 is the crucial binding and transduction factor required for chitin recognition in Arabidopsis (Miya *et al.*, 2007; Wan *et al.*, 2008; Petutschnig *et al.*, 2010), it would imply that *VvCERK3* can bind chitin by its ectodomain and induce chitin signaling. AtLYK4 is another LysM-RLK which was described to possess an auxiliary role in chitin sensing and thus might interact with AtCERK1 (Wan *et al.*, 2012). This suggests that VvCERK3 might also associate with other proteins into receptor complexes.

However, a 20µM estradiol-induced expression of *VvCERK3* led only to the partial chitin-induced ROS burst, reaching ~20% of the maximal ROS production induced by chitin in Col-0 (Fig. 44D). A parallel transformation of the Arabidopsis *fls2* mutant with a constitutive expression

of Vv*FLS2* led to a fully functional complementation, reaching similar amplitudes of flg22-induced oxidative burst in transformants as in Col-0 (Fig. 22A). However perception mechanisms and signaling in FLS2 and CERK1 pathways are different (Monaghan and Zipfel, 2012). The first requires the association with a co-receptor BAK1 (LRR-RLK), while the latter self-dimerizes to activate signaling (Chinchilla *et al.*, 2007; Liu *et al.*, 2012b). Different reasons for this low recovery of chitin response might exist: i) GFP fusion at the C_{ter} might impair the conformation of VvCERK3 protein and does not allow proper self-dimerization and/or substrate phosphorylation; ii) VvCERK3 kinase domain does not completely fit to the downstream signaling components in Arabidopsis, iii) VvCERK3 is not transiently expressed in sufficient quantities, iv) VvCERK3 possesses a lower affinity to chitin than AtCERK1. Optimizing the transgene expression by the estradiol treatment (concentration, time of pretreatment) should lead to an appropriate amount of VvCERK3-GFP. In another study, the expression of the LRR-RLK CLAVATA1-GFP protein using the *pLexA* expression system was firstly detected at the plasma membrane 3h post induction with estradiol, but after 12h, proteins started to aggregate (Bleckmann *et al.*, 2010). The inducible expression of a chimeric receptor consisting of the LysM ectodomain of VvCERK3 and the kinase domain of AtCERK1 should elegantly solve the other possible problems.

5 A partial loss of VvCERK3 in grapevine does not attenuate chitin responses

As VvCERK3 can complement the chitin-induced ROS production in Arabidopsis, we expect that it should be required for chitin sensing in grapevine. The loss of AtCERK1, OsCERK1 or CERK1 ortholog in wheat led to chitin insensitivity in those plant species (Miya *et al.*, 2007; Kishimoto *et al.*, 2010; Lee *et al.*, 2014). We generated grapevine transgenic plants partly silenced in *VvCERK3* expression. In these plants, the level of *VvCERK3* transcripts was decreased by ~50% in the best silenced transgenic line *p35S::asVvCERK3* #6-2 (Fig. 47A). However, compared with the untransformed line seWT, the line #6-2 was not affected in the chitin- induced MAPK phosphorylation in grapevine (Fig. 47B). The decrease in *VvCERK3* transcript amounts might not be sufficient to affect the VvCERK3 protein amount critical for chitin signaling. We have shown that a similar partial silencing (~50%) of *VvFLS2* transcript amounts inhibited more than half the flg22 responsiveness (Fig. 31, 32). Therefore a tight correlation between the *VvFLS2* transcript level and flg22 response exists in grapevine, as it was also described for Arabidopsis (Boutrot *et al.*, 2010; Vetter *et al.*, 2012). A similar transcriptional control of the *AtCERK1* gene is not known in Arabidopsis. In grapevine, VvCERK3 might be a relatively abundant protein as *VvCERK3* transcripts are ~10 times more abundant than those of *VvFLS2* (compare Fig. 21 and 42).

Even if our preliminary results indicate that VvCERK3 partly complements the *cerk1-2* mutation, we cannot exclude that other perception components are required for chitin sensing in

grapevine. These could assist/substitute the VvCERK3 function. Therefore, the total knockdown of each of *VvCERK*s is needed to unravel their respective role in grapevine chitin perception.

6 VvCERK-associated cell death phenotype

Our data showed that the complementation of Arabidopsis *cerk1-2* with *VvCERK2* and *VvCERK3* under the control of a strong constitutive promoter caused lethality of transformants. Similarly, *N. benthamiana* leaves transformed with Vv*CERK2* or Vv*CERK3* exhibited a cell death-associated phenotype (J. Collemare, personal communication). Based on these data, it seems that it is not possible to constitutively overexpress Vv*CERK2* or Vv*CERK3* neither in Arabidopsis nor in *N. benthamiana.* The overexpression of At*CERK1* in *N. benthamiana* also caused cell death (Andrea Gust, Tübingen University, D, personal communication). Thus, it seems that the expression of AtCERK1 is strongly controlled. AtCERK1 has an important role in mediating crosstalk between chitin and PGN sensing in Arabidopsis (Willmann *et al.*, 2011). Mechanisms by which this lethality could be triggered are unknown. Similarly, the overexpression of other receptors such as WAK1, the receptor for OG, led to lethality (Brutus *et al.*, 2010). Interestingly, no lethality or cell death phenotype was observed when *VvCERK1* was constitutively overexpressed in Arabidopsis or *N. benthamiana*, suggesting that its function might be different from those of VvCERK2, VvCERK3 and AtCERK1. This also suggests that VvCERK3 and/or VvCERK2 may function as chitin receptors. Of note, the Arabidopsis *cerk1-2/p35S::VvCERK1* plants show twisted leaves suggesting that VvCERK1 might be involved in plant leaf development (data not shown).

7 Lethality of antisense *VvCERK1* and *VvCERK2* calli

In parallel, the grapevine transformation assays with *p35S::αsVvCERK1* and *p35S::αsVvCERK2* to silence *VvCERK1* or *VvCERK2* did not succeed in generating hygromycin-resistant calli whereas transformed calli expressing *αsVvCERK3* or the *GFP* controls were successfully obtained in the same experiments. These results suggest a probable lethal effect of these two antisense constructions. Thus perturbation in *VvCERK1* and *VvCERK2* expression might interfere with the embryo development or the susceptibility to the *Agrobacterium* spreading during the transformation event. The development of an inducible silencing strategy (in grapevine) could be suitable to study the role of VvCERKs. This method was recently developed in the moss *Physcomitrella patens* (Nakaoka *et al.*, 2012).

8 The role of the closest grapevine ortholog of OsCEBiP in chitin perception

CEBiP is the main chitin-binding receptor in rice (Kaku *et al.*, 2006) and the *CEBiP* silencing abolished chitin sensing in rice or wheat (Kaku *et al.*, 2006; Lee *et al.*, 2014). In Arabidopsis, none of the three closest OsCEBiP-like proteins (AtLYM1, AtLYM2, AtLYM3) is critical for chitin signaling (Wan *et al.*, 2012). Even the triple *lym1/2/3* mutant was not affected in chitin responses (Wan *et al.*, 2012). Thus, it seems that CEBiP might play an important role for chitin perception in monocots but not in dicots.

The grapevine genome encodes four LysM proteins (VvLYPs; Table 14). Two of them (VvCEBiP1 and VvCEBiP2) share the highest homology to OsCEBiP. The transcription of *VvCEBiP1,* but not *VvCEBiP2*, was upregulated following chitin treatment (Fig. 50B) as it was shown for *CEBiP* in rice (Kaku *et al.*, 2006) and barley (H.-J. Schoonbeek, personal communication).

Two silenced lines have been obtained, where the amounts of *VvCEBiP1* transcripts were reduced by more than 75% (Fig. 52A). In these two lines (#3-4 and #3-24), such a decrease in the *VvCEBiP1* expression did not lead to a loss of chitin responsiveness, such as MAPK activation (Fig. 52C). As the expression of the close paralog *VvCEBiP2* is not affected by silencing in these lines (Fig. 52B) and is not upregulated by chitin treatment in grapevine cells (Fig. 50B), it seems improbable that VvCEBiP2 would substitute the effect of VvCEBiP1. These data suggest that grapevine does not require VvCEBiP1 for chitin sensing. However this knockdown must be confirmed at the protein level to validate these preliminary results.

Perspectives

We have shown that chitin is a weak elicitor leading to a low induction of defense genes, notably involved in the phenylpropanoid pathway. Chitin pretreatment did not led to an enhanced resistance against *P. viticola* and *B. cinerea*, suggesting that chitin-triggered immunity might not be so effective to stop or delay these diseases in grapevine. The profile and timing of chitosan-induced early signaling events was similar to those triggered by chitin. Our preliminary results suggest that VvCERK3, but not VvCERK1, might recognize chitin. The role of the third candidate, VvCERK2, remains unclear. It also seems that chitin sensing in grapevine does not rely on VvCEBiP1, suggesting that the grapevine chitin perception system is rather similar to that of dicots.

All over, the preliminary work concerning chitin perception in grapevine is still partial and raises many questions:

i) What is the involvement of VvCERKs in chitin perception? As chitin does not induce an evident oxidative burst in grapevine, the role of each VvCERK in the complemented *cerk1-2* lines should be better characterized by testing other immune responses such as MAPK activation and defense gene expression.

As soon as a functional ortholog of AtCERK1 will be confirmed, complementary studies should be performed to investigate:

ii) What is the involvement of each VvCERK in chitosan and PGN recognition? First, the perception of PGN and defined chitin and fully deacetylated chitosan oligomers of the same length (hexaose – octaose) should be compared in grapevine cells. Then, the Arabidopsis lines complemented with each grapevine VvCERK should be tested for PGN and chitosan oligomer response. In parallel, the direct binding of these GlcNAc-containing ligands to distinct grapevine VvCERKs might be tested with expressed recombinant VvCERK ectodomains or with chitin-magnetic beads on soluble and microsomal protein fractions (Petutschnig *et al.*, 2010). Concerning PGN sensing, At CERK1 interacts with LYM1 and LYM3 for PGN binding in Arabidopsis (Willmann *et al.*, 2011). Thus, the interaction between AtCERK1 and the grapevine LYM1 and LYM3 orthologs (VvLYP3 and VvLYP4) might be investigated.

iii) What is the involvement of chitin perception in immune responses against fungal infections? Chitin-induced immunity was shown to be important for resistance against fungal pathogens. Of note, the involvement of chitin perception during fungal infections was rather reported against low pathogenic strains or pathogens causing incompatible interaction on hosts (Miya *et al.*, 2007; Wan *et al.*, 2008; Kishimoto *et al.*, 2010; Lee *et al.*, 2014). In fact, diverse pathogens are known to secrete different effectors or toxins to block MTI and fungi can inhibit chitin-mediated immunity upon infections (van Esse *et al.*, 2007; de Jonge *et al.*, 2010; Mentlak *et*

al., 2012; Lee *et al.*, 2014). Grapevine plants knocked-down in the grapevine AtCERK1 ortholog shoud be tested in fungal infection assays (*B. cinerea*; *E. necator*). As the *cerk1-2* mutant is affected in disease resistance (*A. brassicicola*, *Erysiphe cichoracearum*; Miya *et al.*, 2007; Wan *et al.*, 2008), VvCERKs might be tested for the restoration of these resistances. Interestingly, the *cerk1-2* mutant is susceptible to an adapted strain of *Erysiphe necator*, the causal agent of powdery mildew on grapevine (Ian Dry, CSIRO, AUS, personal communication). A collaboration has been established with this research group to test our *cerk1-2/VvCERKs* transformed lines for complementation of the *E. necator* resistance level normally found in the non-host resistant WT Col-0.

It is important to keep in mind the complexity of the receptor complexes, as it was particularly revealed for the GlcNAc-sensing multipartite receptor systems. The PRRs that are not involved in chitin sensing may be involved in chitosan or PGN sensing. Optimally, studies proposed above could be performed on the whole with all VvCERKs/VvCEBiPs. It would be also interesting to investigate the role of VvLYK12 and VvLYK9, the closest orthologs of the LjNFR5, which is required for nodulation in *Lotus japonicus* (Gust *et al.,* 2012).

Taken together, all these results should improve our knowledge to better understand how grapevine can specifically perceive different GlcNAc-containing ligands *via* complex receptors.

GENERAL DISCUSSION

1 Conservation of MTI signaling between species

The tested MAMPs flg22 and chitin induced typical defense responses as described in Arabidopsis or other plant species. The only exception was a lack of chitin/chitosan-induced oxidative burst. Different studies show that strong flg22-induced MTI is rather a hallmark of dicotyledons (Felix *et al.*, 1999; Sun *et al.*, 2006), while it is a weak elicitor in rice and monocots in general (Felix *et al.*, 1999; Takai *et al.*, 2008). On the other hand, chitin appears to be a more powerful MAMP in rice than in dicots, inducing a strong oxidative burst and defense gene expression that lead to stronger fungal disease resistance (Che *et al.*, 2000; Tanabe *et al.*, 2006; Nekrasov *et al.*, 2009; Segonzac *et al.*, 2011). Grapevine induced much stronger MTI in response to flagellin than chitin, showing similarity with other dicots. These differences might be based on different PRR architecture or different perception systems. It seems that the downstream cell signaling components are highly conserved between species and enables heterologous PRR expression (Zipfel *et al.*, 2006; Robatzek *et al.*, 2007; Takai *et al.*, 2008; Lacombe *et al.*, 2010; Fradin *et al.*, 2011). We also show that the grapevine VvFLS2 and possibly VvCERK3 receptors could mediate MAMP signaling in Arabidopsis.

From our orthology-based approach it seems evident that for one functional gene in Arabidopsis, grapevine possesses often at least two paralogs, occurring on the adjacent loci. Protein families searched in grapevine are much bigger than in Arabidopsis, as was shown for the LysM-RLKs (LYKs; 12 grapevine LYKs versus 5 Arabidopsis LYKs). From the phylogenetic analyses and sequence homology of candidate PRRs (VvFLS2 and VvCERK1-3), we also noticed that grapevine is evolutionary closer to tomato compared to Arabidopsis. Therefore differences in perception are likely to exist between grapevine and Arabidopsis. Indeed, we have shown that differences in flagellin-derived flg22 epitopes exist between VvFLS2 and AtFLS2 receptors, as it was described for the tomato receptor LeFLS2.

2 Antisense strategy for use in gene silencing

The phenomenon of RNA interference (RNAi) is exploited in the RNA post-transcriptional silencing as a powerful tool for gene function studies. Gene silencing is especially required for species where wide mutant collections are not available. In the RNAi, plants detect a double-stranded RNA (dsRNAs) that are cleaved into smaller RNAs, called small-interfering RNAs (siRNAs). After activation by unwinding, the latter bind to complementary mRNAs resulting in their cleavage or inhibition of translation depending whether the base pairing is complete or not. In this study, we used an antisense (αs) strategy for gene silencing. It consists in

the expression of a gene fragment in the antisense orientation which should lead to transcript degradation.

According to our results, the efficiency of silencing observed with the Gateway vector (pH2WG7) was very low and no line with complete silencing was obtained. For each of *αsVvFLS2* and *αsVvCERK3* constructs, the expression of the targeted gene was reduced below 50% only in one line out of ten. The best silencing efficiency was achieved in the *αsVvCEBiP* transgenic plants, where 2 lines out of 10 contained less than 30 % of the amount of the targeted mRNA. Although the antisense strategy can be efficient (Simon-Plas *et al.*, 2002), our data clearly show, that it frequently failed to silence our target genes. As a consequence, using this vector would require screening of more antibiotic resistant calli and test them for the efficient silencing before the plant regeneration.

Nevertheless, it was shown in other plant species that more efficient silencing was achieved with inverted repeat constructs (hairpin, hp), where a fragment from target gene is expressed in sense and antisense orientations separated by a spacer (Waterhouse *et al.*, 1998). Most of reverse genetics studies currently use hpRNAs. Silencing of OsCEBiP and OsCERK1 receptors in rice was achieved with this type of vector (pANDA) and led to marked decrease of targeted mRNA quantity reaching ~3% and ~20% of the amount found in untransformed cells (Kaku *et al.*, 2006; Shimizu *et al.*, 2010). The efficiency of silencing was shown to depend on the size of dsRNA and most studies use a 300-700 bp fragment. However, even shorter dsRNA can lead to sufficient silencing and fragments of only 23 nucleotides in length could silence a target gene (reviewed in Eamens *et al.*, 2008).

Silencing can be also mediated by artificial miRNA (amiRNA)-mediated silencing. miRNAs are ~21-nucleotide-long endogenous RNAs generated from hairpin-like transcribed precursors (pre-mi RNA). amiRNAs can be obtained by replacing the miRNA sequence with a short ~21 nucleotide-long sequence specific for targeting a given gene. The engineered pre-mi RNAs of Arabidopsis are correctly spliced and leads to silencing in different plants including grapevine, as recently reported (Jelly *et al.*, 2012).

The transgenesis *via* somatic embryogenesis is without any doubt the key method to obtain stable transgenic plants. However, it is time consuming and technically complex. Interestingly, several previous studies reported a successful *Agrobacterium*-mediated transformation of grapevine cells (Baribault *et al.*, 1989), or a transient expression in grapevine leaves (Santos-Rosa *et al.*, 2008). Developing these technologies in our laboratory would permit to obtain the first rapid insight into the function of candidate genes.

3 PRRs for engineering disease resistance

The identification of novel PRRs in a given crop species is important to make an inventory of the defense equipment the plant disposes with. In Arabidopsis, the screening of vast mutant collections and naturally occurring ecotypes, as well as the forward genetics approach, is highly facilitated and several studies led to the successful identification of novel PRRs. In crops, analyzing genomic variations within different cultivars but also the "wild" relative species and their introgression lines allows to map the Quantitative Trait Loci (QTLs) related to disease resistance. Although QTLs will mostly carry *R*-genes, they may also contain *PRR* genes (encoding RLKs or RLPs). Indeed, a gene encoding the PRR XA21 (*XA21* was initially classified as *R*-gene) was isolated as an introgressed trait for the bacterial blight resistance (Wang *et al.*, 1996).

During the last years, a lot of progress has been done in the understanding of the MAMP perception and signaling and the role of plant PRRs. So, can we apply this knowledge in agriculture?

Different studies reveal that the simple overexpression of PRR in plants did not lead to increased resistance, even if PRRs are key for plant immunity (Takai *et al.*, 2008; Kishimoto *et al.*, 2010). However, it was shown that PRRs can be successfully transferred from one plant species to another, even between dicots and monocots. A very effective demonstration was achieved in tomato (from the *Solanaceae* family), where the transfer of the EFR receptor led to important resistance against a wide range of different agriculturally important bacterial pathogens (Lacombe *et al.,* 2010). This high efficacy results from the fact that tomato pathogens did not evolve with the EFR receptor (from the *Brassicaceae* family) and thus lack means to inhibit EFR-mediated immunity. Therefore, the transfer of EFR seems promising to cure bacterial diseases in non-*Brassicaceae* plants. In practice, an interesting project tests whether EFR-mediated resistance can work even in other crops such as cereals, bananas, apples or cassava, for which bacterial infections are destructive (C. Zipfel, personal communication).

Also transfer of other LRR-RLK receptors, XA21 and Ve1, led to a robust resistance, even though the latter was restricted to one microbial genus or a group of species, respectively. Up to now, successful transfer was shown only with LRR-RLK receptors. Different studies showed that the ectodomain and kinase domains from distinct PRR can be combined leading to chimera receptors with preserved signal transduction determined by the kinase domain. Such a chimeric receptor build from the chitin-binding ectodomain of OsCEBiP and the kinase domain of XA21 highly improved resistance to fungus *M. oryzae*, when expressed in rice (Kishimoto *et al.*, 2010). Thus XA21 receptor and its strong kinase capable to initiate HR in rice (Kishimoto *et al.*, 2010) represents an interest for practical use in disease resistance engineering. The potential of chimeric receptors is wide: they can i) enhance immune response especially for MAMPs that are only weakly abundant during the plant-pathogen interaction or are manipulated by pathogens during the

interaction, or ii) improve receptor affinity or kinase activity. Indeed, the latter two are among the first factors to impact the amplitude of the host immune responses.

Analysis of the polymorphism occurring in plant PRRs in different cultivars or species may lead to the identification of more efficient PRR variants. As an alternative to the transgenic approach, conventional breeding can be assisted by the use of molecular markers that assist to deliver the desired *PRR* gene into the crop, and pyramid it with other genes important for the resistance genes such as R-genes.

All over, the PRR-based breeding, the PRR transfer and creation of novel chimeric PRRs might be applicable "one day" as an alternative in agriculture disease and pest management, as a "tailored PRR therapy" and might provide more durable and broader resistance than *R*-genes.

CONCLUSION

Recognition of microbial patterns (MAMPs) by host recognition receptors (PRRs) is important for the activation of plant immune system. This work focused on the perception of two widely-distributed MAMPs in grapevine: flagellin-derived flg22 epitope and chitin, signatures of bacterial and fungal presence, respectively. Immune responses triggered by these MAMPs were characterized. As perception systems for these MAMPs were described in other species, mostly Arabidopsis, we further aimed to identify the cognate receptors by an orthology based approach.

The flg22 peptide is an active MAMP in grapevine and triggers early signaling events, expression of a set of defense genes and plant growth inhibition in grapevine. Flg22-induced immunity is also effective against the necrotrophic fungus *B. cinerea*. We report here the identification of VvFLS2, the *V. vinifera* flg22 receptor, which is the closest ortholog of FLS2 of Arabidopsis. The functionality of VvFLS2 was demonstrated by complementing the lack of flg22 responsiveness in an Arabidopsis null *fls2* mutant. Also the partial silencing of VvFLS2 by RNAi in grapevine led to impaired flg22 signaling and defense gene expression confirming its requirement for flg22 responses in grapevine. We further compared the recognition specificities of VvFLS2 and AtFLS2 in relation to their capability to perceive flagellin-derived immunogenic epitopes from endophytic and pathogenic bacteria. We provide evidence that grapevine immune responses triggered by flg22 from the endophytic bacteria *B. phytofirmans* were lower than those triggered by the pathogen-derived flg22 peptides from *P. aeruginosa* or *X. campestris*. Interestingly, these differences were not observed in wild-type (WT) Arabidopsis but were gained upon expression of *VvFLS2* in the Arabidopsis *fls2* mutant, suggesting that FLS2 itself underlies the differences observed in FLS2-mediated responses in these species. To our knowledge, VvFLS2 is the first characterized receptor that differentially recognizes flg22 epitopes from pathogenic or endophytic bacteria. In addition, our work provides the first description of an active PRR/MAMP pair functioning in grapevine.

We further show that chitin and chitosan, two carbohydrate polymers, act as MAMPs for grapevine immunity, inducing typical signaling and defense gene expression. We show that chitin act as a weak MAMP in grapevine as it elicits only transient signaling and weak defense gene expression. This chitin-triggered immunity turned out to be insufficient to protect grapevine against *B. cinerea* or *P. viticola*, though effective immunity could be achieved by other MAMPs, such as sulfated β-1,3 glucan or chitosan. We have initiated the work to identify the chitin receptor/s. Our preliminary results suggest that VvCERK3, homologous to the main Arabidopsis chitin receptor AtCERK1, might recognize chitin. VvCERK3, but not VvCERK1, partially restored the chitin perception when expressed in the *cerk1-2* Arabidopsis mutant. Role of the two other candidates, VvCERK1 and 2, remain unclear. It also seems that grapevine chitin sensing

does not rely on a grapevine homolog of CEBiP, the main rice chitin receptor. From these findings we suggest that the grapevine chitin perception system is rather similar to other dicots than monocots. Further data are needed to expand our knowledge on the function of these candidate receptors and the grapevine chitin perception system in general.

The complementation assays in Arabidopsis enabled to assess the functionality of putative grapevine PRRs. The receptors and the downstream signaling components for flg22, and possibly also chitin, are conserved between grapevine and Arabidopsis. We also aimed to evaluate the biological significance of these VvPRRs by the means of grapevine transgenic plants post-transcriptionally silenced in each of the candidate genes. However, the antisense strategy for gene knockdown led to only partial silencing. Therefore other silencing methods should be tested to achieve efficient gene invalidation.

We could identify grapevine orthologs of FLS2, and possibly CERK1, as functional PRRs of grapevine. This opens a space for questions: What is the contribution of these PRRs for MAMP sensing in grapevine? Are they the major receptors? Are they specific receptors or provide recognition of structurally similar ligands? Is the grapevine CERK1 ortholog involved in both chitin and peptidoglycan sensing? Do they play an important role in disease resistance, *i.e.* will the lines silenced in VvFLS2 and VvCERK1, 2, 3 or VvCEBiP exhibit decreased susceptibility to bacterial or fungal infections?

Finally, this work only started the journey for better understanding how grapevine perceives microbial motifs and the oncoming pathogen attack. Expanding the knowledge on grapevine immune mechanisms is essential to develop alternative strategies in viticulture.

Annexes

	Nitsch-Nitsch
Macroelements	
$CaCl_2 \cdot 2H_2O$	166
KH_2PO_4	68
KNO_3	950
$MgSO_4 \cdot 7H_2O$	185
NH_4NO_3	720
Microelements	
$CoCl_2 \cdot 6H_2O$	0.025
$CuSO_4 \cdot 5H_2O$	0.025
H_3BO_3	10
KI	0.83
$MnSO_4 \cdot 2H_2O$	19.5
$Na_2MoO_4 \cdot 2H_2O$	0.25
$ZnSO_4 \cdot 7H_2O$	10
Fe-EDTA	
$FeSO_4 \cdot 7H_2O$	27.85
Na_2-EDTA	37.25
Fe-EDTA	6.9
Vitamins and amino acids	
Folic acid	0.5
Nicotinic acid	5
Biotin	0.05
Glycine	2
Myo-inositol	100
Calcium pantothenate	3
Pyridoxine HCl	0.5
Thiamine HCl	0.5
casein hydrolysate	1 g l^{-1}
pH before autoclaving	5.5
autoclaving 120°C, 20min	

Annex 1. Composition of the Nitsch-Nitsch medium used for cultivation of grapevine cells. Concentrations are indicated in mg l^{-1}, if not mentioned otherwise.

Annex 2. Alignment of AtFLS2 and its orthologs in grapevine (VvFLS2), tomato (LeFLS2) and rice (OsFLS2). *(continues on the next page)*

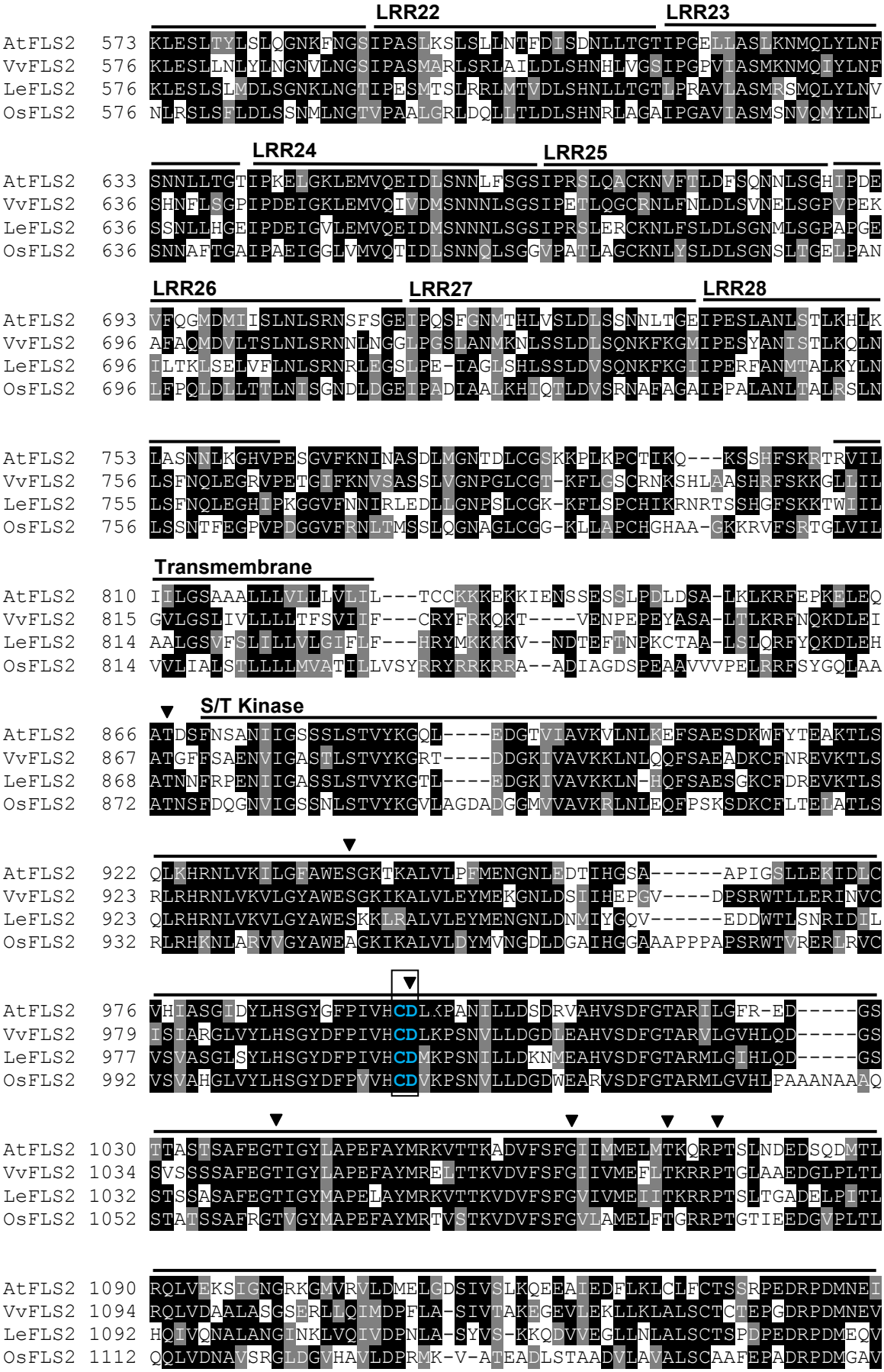

Annex 2. Alignment of AtFLS2 and its orthologs in grapevine (VvFLS2), tomato (LeFLS2) and rice (OsFLS2). *(continues on the next page)*

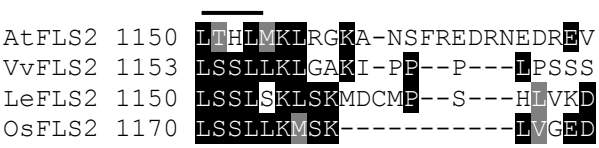

Annex 2. Alignment of AtFLS2 and its orthologs in grapevine (VvFLS2), tomato (LeFLS2) and rice (OsFLS2).
Protein sequences were aligned with T-Coffee. Black and gray shading representing identical and positive amino acids, respectively, was visualized with Boxshade. The predicted signal peptide, the N-terminal domain (LRRNT), the leucine-rich repeats (LRRs), the transmembrane region and the serine/threonine (S/T) kinase are shown. Arrows indicate residues crucial for FLS2 function: the cysteine pair C61/C68 (Sun *et al.*, 2013), residues G318 (*fls2-24*; Gomez-Gomez and Boller, 2000), G493 (stor; Vetter *et al.*, 2012) in the LRR ectodomain, S938 (Cao *et al.*, 2013), residues T867, T1040, T1072 in the phosphorylation sites (Robatzek *et al.*, 2006), the PEST like motif P1076 (Robatzek *et al.*, 2006) and the residues G1064 (*fls2-17*; Gomez-Gomez and Boller, 2000) and D997 (Sun *et al.*, 2006) required for the kinase catalytic activity. The non-RD kinase motif is highlighted in blue. Asterisks indicate residues involved in the interaction with flg22 (Sun *et al.*, 2013), including Y272, R294, Y296 and H316 (highlighted in red) binding the core flg22 sequence (K13 and D14). A: Ala, C:Cys, D:Asp, E:Glu, F:Phe, G:Gly, H:His, I:Ile, K:Lys, L:Leu, M:Met, N:Asn, P:Pro, Q:Gln, R:Arg, S:Ser, T:Thr, V:Val, W:Trp, Y:Tyr.

(on the next page)

Annex 3. Alignment of deduced protein sequences of VvFLS2 and VvFLS2-like. Protein sequences were aligned with T-Coffee and visualized with Boxshade. Black and gray shading represent identical and positive amino acids, respectively. The predicted signal peptide, the LRR ectodomain containing 27 LRRs, the transmembrane region and the serine/threonine (S/T) kinase are indicated (SMART http://smart.embl-heidelberg.de/).

.

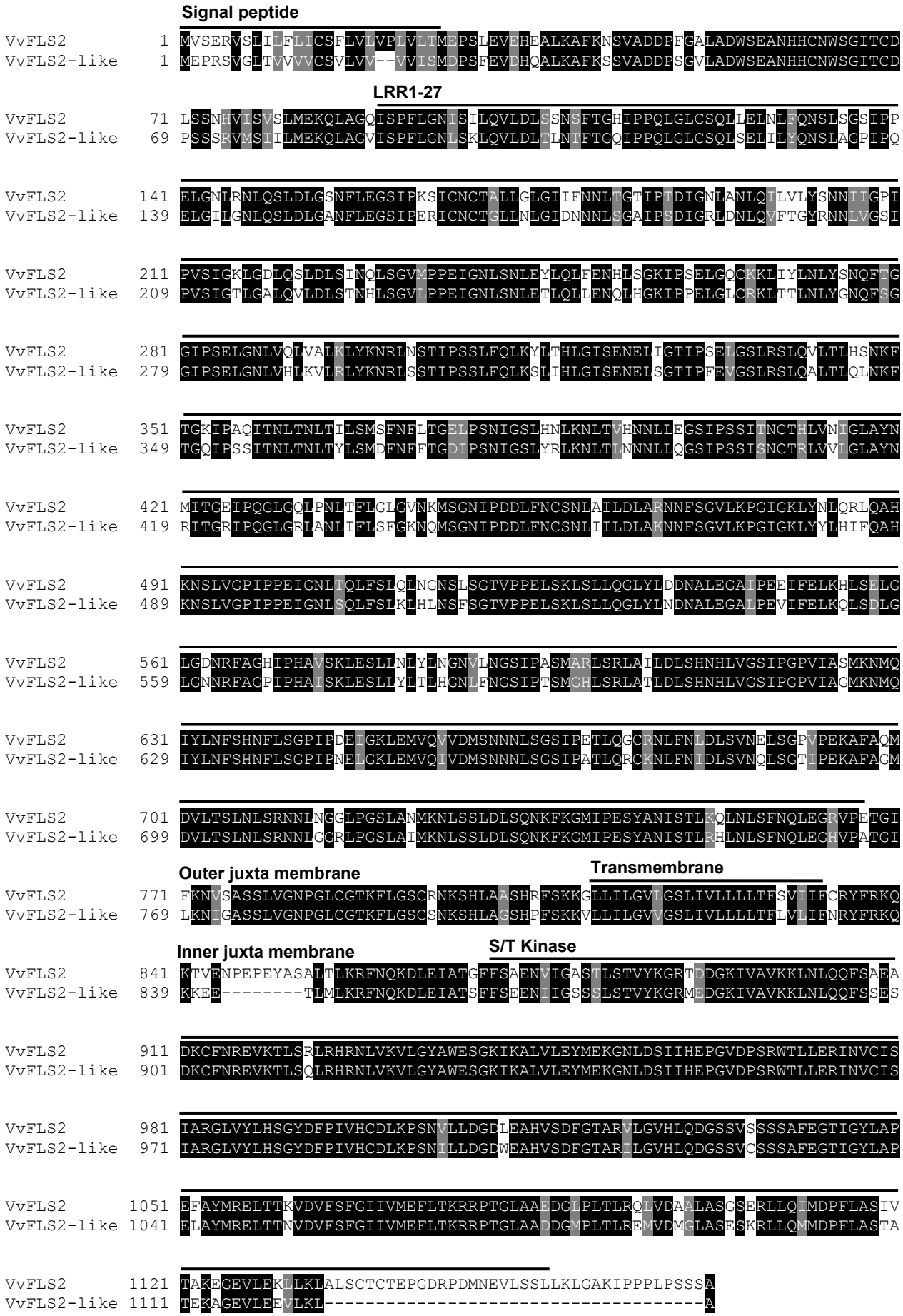

Annex 3. Alignment of deduced protein sequences of VvFLS2 and VvFLS2-like. *(Find the legend on the previous page).*

	Protein alignment (id. % / pos. %)								
	AtCERK1			**OsCERK1**			**LeCERK1**		
	Total	LysM	Kin	Total	LysM	Kin	Total	LysM	Kin
VvCERK1	60 / 73	46 / 68	77 / 85	54 / 69	42 / 55	73 / 87	**71 / 83**	**56 / 75**	**89 / 95**
VvCERK2	57 / 71	44 / 65	74 / 84	55 / 68	47 / 59	73 / 85	65 / 78	53 / 73	84 / 92
VvCERK3	56 / 69	**51 / 68**	70 / 80	52 / 66	42 / 57	69 / 81	62 / 77	47 / 71	78 / 90
AtCERK1	-	-	-	49 / 63	40 / 56	67 / 79	57 / 73	47 / 67	76 / 86

Annex 4A. Percentage of amino acid identity or similarity between VvCERKs, AtCERK1, OsCERK1 and predicted ortholog in tomato (LeCERK1).
Two sequences of the total protein (Total), the LysM ectodomain (LysM) or kinase domain (Kin) were aligned each time with pBLAST (NCBI). OsCERK1 (D7UPN3), LeCERK1 (NP_001233773), AtCERK1 (NP_566689). Lys Motifs (LysM, PF01476) and Kinase domain (PF07714) were annotated with SMART. The signal peptide and the outer juxtamembrane region were not included in each of LysM domains. The highest homologies are highlighted in red. Alignments were based on sequenced *VvCERK* coding sequences.

	Protein (id. % / pos. %)			Nucleotide
	Total	LysM	Kin	id. % (cover %)
VvCERK1 vs. VvCERK2	69 / 81	57 / 73	**88 / 93**	83% (cover 52%)
VvCERK1 vs. VvCERK3	67 / 80	57 / 75	81 / 90	80% (cover 51%)
VvCERK2 vs. VvCERK3	70 / 81	56 / 72	82 / 91	83% (cover **67%**)

Annex 4B. Homology in protein and nucleotide sequence between VvCERK1, 2 and 3.
Two sequences of the total protein, the LysM ectodomain (LysM) or the kinase domain (Kin) or the total nucleotide sequences were aligned each time with pBLAST or nBLAST (NCBI), respectively. Lys Motifs (LysM, PF01476) and Kinase domain (PF07714) were annotated with SMART.

Gene name	**mRNA ID (GenBank)**	**CDS Length * (pb)**	**SNPs**	**intron splicing**
VvCERK1	XM_002270951	1845	---	Missing predicted exon (30 bp) after bp 657
VvCERK2	XM_002264291	1878	825(G→A:x), 1212(C→T:x)	Different splicing between 355-633 (Exon1) Missing a part (42 bp) of predicted exon after bp 680 (Exon3)
VvCERK3	XM_002264252	1869	81(T→C:x),306(T→A:x), 752(T→C:Val→Ala), **1481(C→A:Ala→Glu)**, 1552(A→G:Ile→Val), **1733(A→T:Gln→Leu)**	Contains extra codon (671-673, Exon4)

Annex 4C. Sequencing of *VvCERK*s reveals SNPs and different intron splicing.
The nucleotide sequences of cloned full-length grapevine CDS of *VvCERK*s (cv. Gamay) and the corresponding transcript predictions based on genome sequencing (cv. Pinot Noir PN40024) available on NCBI (Vitis 8x) were aligned. The resulting SNPs and differences in splicing are indicated, relative to PN40024 prediction. In bold are SNPs changing the amino acid character. *) Length in bp is indicated for sequenced CDS. x: no amino acid modification.

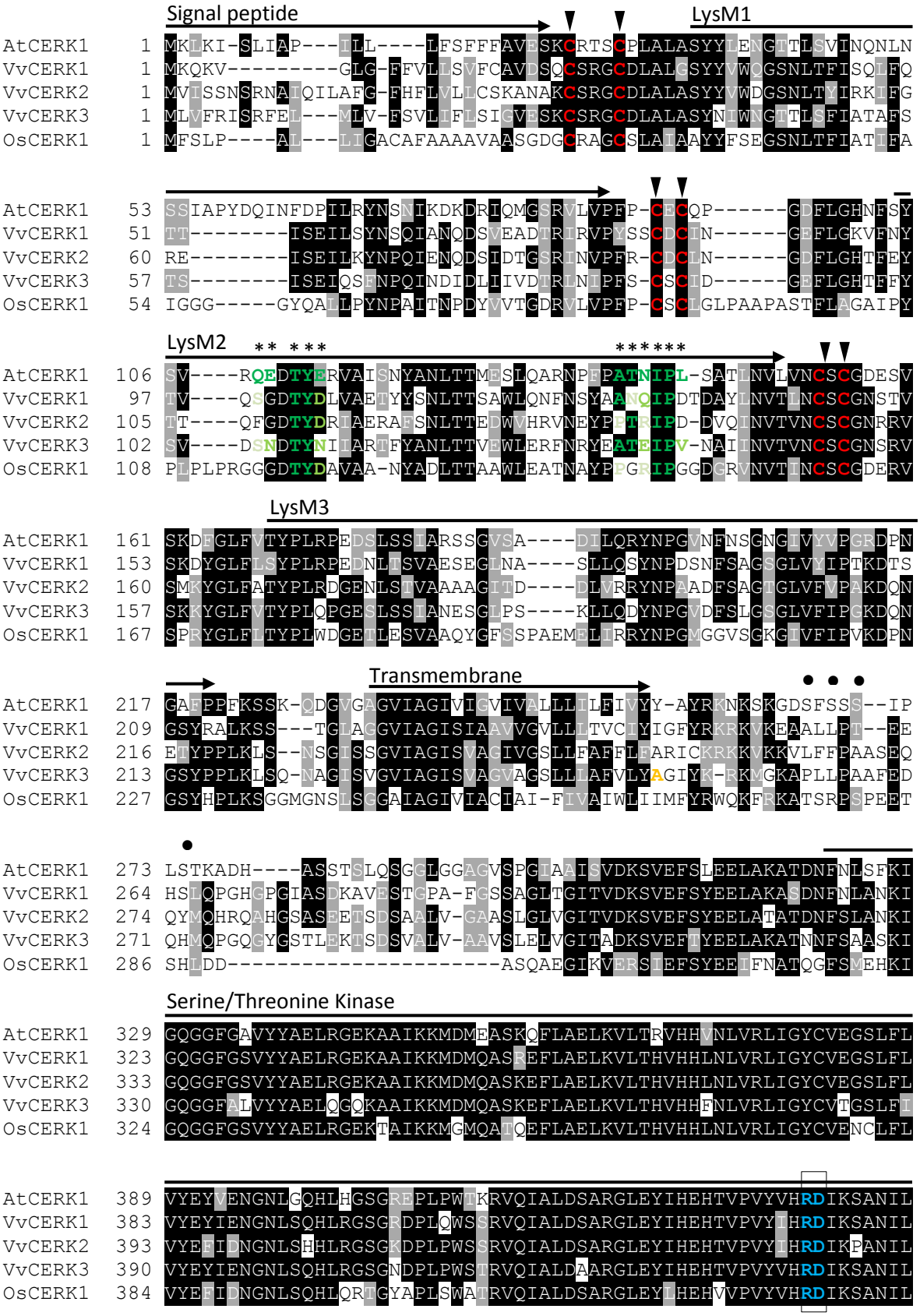

Annex 4. Alignment of AtCERK1 and its putative orthologs in grapevine (VvCERK1, 2, 3) and in rice (OsCERK1). *(continues on the next page)*

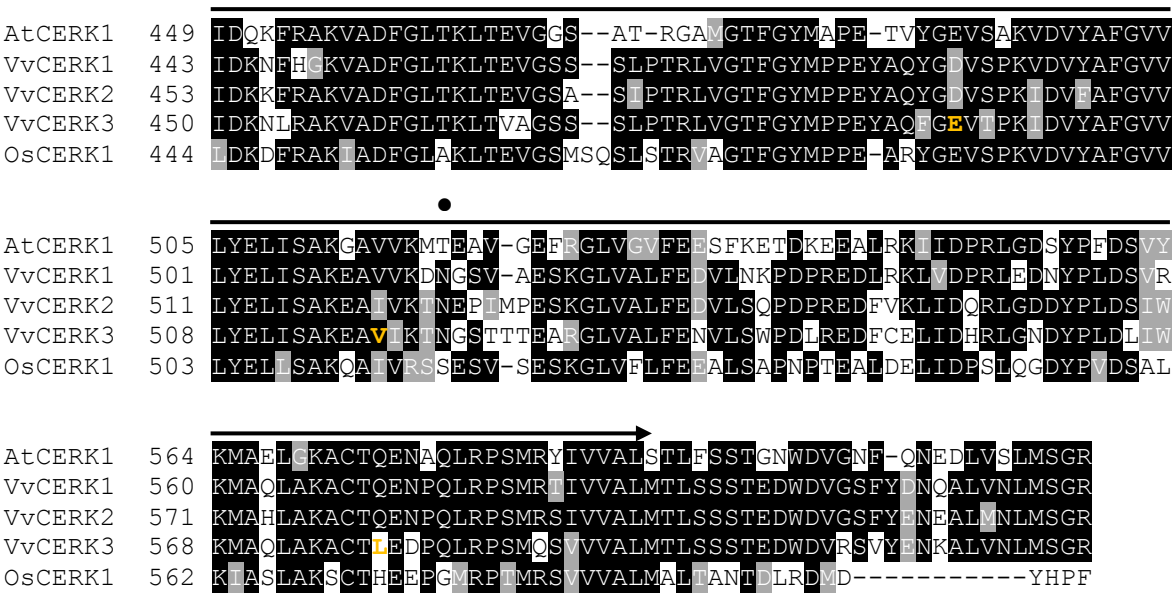

Annex 5. Alignment of AtCERK1 and its putative orthologs in grapevine (VvCERK1, 2, 3) and in rice (OsCERK1).

Protein sequences were aligned with T-Coffee. Black and gray shading representing identical and positive amino acids, respectively, was visualized with Boxshade. The predicted signal peptide, the lysin motifs (LysM), the transmembrane region and the serine/threonine (S/T) kinase are shown. The residues of the chitin-binding site in AtCERK1-LysM2 are indicated by asterisks and their conservation is highlighted in the grades of green. The residues E110, E114 and I141 bind to N-acetyl moieties of $(GlcNAc)_5$, while Q109, T112, Y113, A138, T139, N140, P142 and L143 interact with hydroxyl and hydroxymethyl groups of glucose part (Liu *et al.*, 2012b). Conserved Cys residues (in red) form disulfide bridges (indicated by arrows). The RD type of kinase is highlighted in blue. SNPs A251, E494, V518 and L578 found in *VvCERK3* (cv Gamay) are highlighted in orange. Residues S266, S268, S270, S274 and T519 (indicated by ●) were found to be phosphorylated in AtCERK1 after chitin treatment (Petutschnig *et al.*, 2010). A: Ala, C:Cys, D:Asp, E:Glu, F:Phe, G:Gly, H:His, I:Ile, K:Lys, L:Leu, M:Met, N:Asn, P:Pro, Q:Gln, R:Arg, S:Ser, T:Thr, V:Val, W:Trp, Y:Tyr.

```
VvCERK3      1 ATGTTAGTGTTTTCTGTGTTGATATTTCTCAGTATTGGAGTAGAATCCAAGTGTAGCAGA
VvCERK1      1 GGTTTAGGGTTTTTTGTACTGCTCTCCGTTTTCTGTGCAGTTGATTCGCAGTGCAGTCGC
VvCERK2      1 GCCTTTGGATTTCACTTTCTCGTTCTCCTCTGTTCCAAGGCCAATGCCAAGTGCTCCCGC

VvCERK3     61 GGCTGTGATCTTGCTTTAGCTTCATACAATATATGGAATGGTACAACTCTCAGTTTTATA
VvCERK1     61 GGCTGTGATCTTGCTCTGGGCTCATACTATGTCTGGCAAGGTTCCAACCTCACTTTTATC
VvCERK2     61 GGCTGTGATCTCGCCCTGGCTTCATACTACGTGTGGGATGGCTCAAACCTCACCTACATT

VvCERK3    121 GCCA-CCGCCTTCTCCACTTCTATTTCTGAAATTCAAAGCTTCAATCCTCAAATAAATGA
VvCERK1    121 TCTC-AGCTATTCCAGACAACGATTTCTGAAATTCTCAGCTACAACTCACAAATCGCTAA
VvCERK2    121 AGAAAAATCTTTGGCCGC-GAAATCTCGGAAATTCTCAAGTACAATCCCCAAATCGAAAA

VvCERK3    180 TATAGATTTGATCATAGTTGATACAAGATTGAATATCCCCTTC---TCCTGCAGTTGCA
VvCERK1    180 TCAAGATAGTGTTGAAGCCGATACCAGAATCCGCGTGCCTTACTCCTCATGTGATTGCA
VvCERK2    180 CCAAGACAGCATCGACACTGGCTCCAGAATCAACGTGCCGTTC---CGGTGCGATTGCC
```

Annex 6A. The specificity of αs*VvCERK3* fragment used for silencing in grapevine.
Comparison of similarity between the 235 bp fragment used for *VvCERK3* silencing and the closest grapevine sequences *VvCERK1* and *VvCERK2* in grapevine.

```
VvCEBiP1     1 ATGGGTTCTGCTACGCTGCTTCTCGCCCTATCCTTCCTCTCGGTGCTCATCACTGCGCCG
VvCEBiP2     1 ATGGGTTCTGCTACTCTGCTTCTCGCCCTATTCTTCCTCTCCGTGCTCACCACTGTGCCC

VvCEBiP1    61 AGAGCTCAGGCCAGCTTCAAATGCAGCTCCG-------GC--CCCACCTGTAACGCTCTC
VvCEBiP2    61 AAAGTTCAGGCAGCCTTCACCTGTAACTCCACCACCAGGTCCACCACCTGCAGCGCTCTC

VvCEBiP1   112 GTCGGCTACGTCTCCCCCAACACCACCACTCTATCCGCCATCCAGACTCTCTTCGGCGTC
VvCEBiP2   121 ATCGACTACGTCTCCCCCAACACCACCACTCTATCTGCCATCCAGACTCTCTTCGACGTC

VvCEBiP1   172 AAAAACTTTCGAACTCTACTCGGCGCCAACTCCCTCCCGGCCTCGA
VvCEBiP2   181 AAAAACCTTCGAACTCTACTCGGCGCCAACTCCCTCCCGACCTCGA
```

Annex 6B. The specificity of *αsVvCEBiP1* fragment used for silencing in grapevine.
Comparison of similarity between the last 217 bp of the DNA fragment, used for *VvCEBiP1* silencing, and the closest grapevine sequence *VvCEBiP2*. The first 100 bp of the *αsVvCEBiP1* fragment are in 5'UTR of *VvCEBiP1* and are missing in *VvCEBiP2*. Highlighted in red are stretches of nucleotides identical to *αsVvCEBiP1* that are longer than 21 nucleotides.

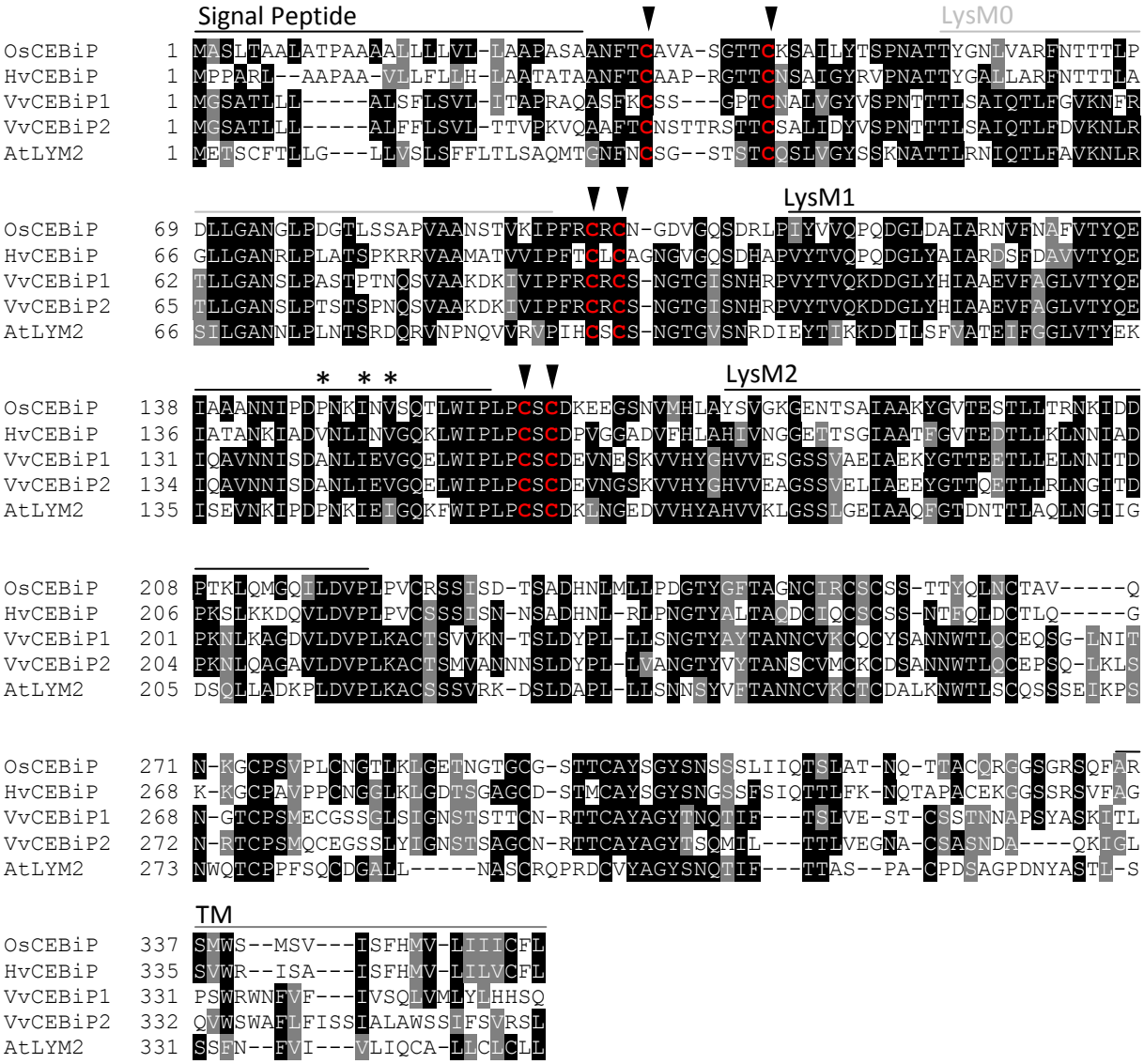

Annex 7. Alignment of OsCEBiP and its orthologs in barley (HvCEBiP), Arabidopsis (AtLYM2) and the putative orthologs in grapevine (VvCEBiP1, 2). Protein sequences were aligned with T-Coffee and shading was visualized with Boxshade. Lys motifs (LysM) and transmembrane region (TM) are indicated. Conserved Cys residues (in red) form disulfide bridges (indicated by arrows). The residues P119, I122 and V124 (counted without the signal peptide) involved in the interaction of LysM1-OsCEBiP with the $(GlcNAc)_8$ ligand (Hayafune *et al.*, 2014) are indicated with asterisks. A: Ala, C:Cys, D:Asp, E:Glu, F:Phe, G:Gly, H:His, I:Ile, K:Lys, L:Leu, M:Met, N:Asn, P:Pro, Q:Gln, R:Arg, S:Ser, T:Thr, V:Val, W:Trp, Y:Tyr.

References

Achouak W, Conrod S, Cohen V and Heulin T (**2004**) Phenotypic variation of *Pseudomonas brassicacearum* as a plant root-colonization strategy. *Mol Plant Microbe Interact* **17**: 872-879

Adrian M, Trouvelot S, Gamm M, Poinssot B, Heloir MC and Daire X (**2012**) Activation of grapevine defense mechanisms: Theoretical and applied approaches. *In*: Merillon JM and Ramawat KG (eds) Plant defence: Biological control. *Springer Science + Business Media B.V.*

Agrios G (**2005**) Plant Pathology, Ed 5th edition. *Elsevier Academic Press*

Ait Barka E, Belarbi A, Hachet C, Nowak J and Audran J (**2000**) Enhancement of *in vitro* growth and resistance to gray mould of *Vitis vinifera* co-cultured with plant growth-promoting rhizobacteria. *FEMS Microbiol Lett* **186**: 91-95

Ait Barka E, Nowak J and Clement C (**2006**) Enhancement of chilling resistance of inoculated grapevine plantlets with a plant growth-promoting rhizobacterium, *Burkholderia phytofirmans* strain PsJN. *Appl Environ Microbiol* **72**: 7246-7252

Akamatsu A, Wong HL, Fujiwara M, Okuda J, Nishide K, Uno K, Imai K, Umemura K, Kawasaki T, Kawano Y and Shimamoto K (**2013**) An OsCEBiP/OsCERK1-OsRacGEF1-OsRac1 module is an essential early component of chitin-induced rice immunity. *Cell Host Microbe* **13**: 465-476

Albert M, Jehle AK, Mueller K, Eisele C, Lipschis M and Felix G (**2010**) Arabidopsis thaliana pattern recognition receptors for bacterial elongation factor Tu and flagellin can be combined to form functional chimeric receptors. *J Biol Chem* **285**: 19035-19042

Albrecht C, Boutrot F, Segonzac C, Schwessinger B, Gimenez-Ibanez S, Chinchilla D, Rathjen JP, de Vries SC and Zipfel C (**2012**) Brassinosteroids inhibit pathogen-associated molecular pattern-triggered immune signaling independent of the receptor kinase BAK1. *Proc Natl Acad Sci U S A* **109**: 303-308

Ames P and Bergman K (**1981**) Competitive advantage provided by bacterial motility in the formation of nodules by *Rhizobium meliloti*. *J Bacteriol* **148**: 728-908 p

Andersen-Nissen E, Smith KD, Strobe KL, Barrett SL, Cookson BT, Logan SM and Aderem A (**2005**) Evasion of Toll-like receptor 5 by flagellated bacteria. *Proc Natl Acad Sci U S A* **102**: 9247-9252

Arkhipov A, Freddolino PL, Imada K, Namba K and Schulten K (**2006**) Coarse-grained molecular dynamics simulations of a rotating bacterial flagellum. *Biophys J* **91**: 4589-4597

Asai T, Tena G, Plotnikova J, Willmann MR, Chiu WL, Gomez-Gomez L, Boller T, Ausubel FM and Sheen J (**2002**) MAP kinase signalling cascade in Arabidopsis innate immunity. *Nature* **415**: 977-983

Aziz A, Gauthier A, Bezler A, Poinssot B, Joubert J, Pugin A, Heyraud A and Baillieul F (**2007**) Elicitor and resistance-inducing activities of beta-1,4 cellodextrins in grapevine, comparison with beta-1,3 glucans and alpha-1,4 oligogalacturonides. *J Exp Bot* **58**: 1463-1472

Aziz A, Poinssot B, Daire X, Adrian M, Bezier A, Lambert B, Joubert J and Pugin A (**2003**) Laminarin elicits defense responses in grapevine and induces protection against *Botrytis cinerea* and *Plasmopara viticola*. *Mol Plant Microbe Interact* **16**: 1118-1128

Aziz A, Trotel-Aziz P, Dhuicq L, Jeandet P, Couderchet M and Vernet G (**2006**) Chitosan oligomers and copper sulfate induce grapevine defense reactions and resistance to gray mold and downy mildew. *Phytopathology* **96**: 1188-1194

Bardoel B, van der Ent S, Pel M, Tommassen J, Pieterse C, van Kessel K and van Strijp J (**2011**) Pseudomonas evades immune recognition of flagellin in both mammals and plants. *PLoS Pathog* **7**: e1002206

Bardoel B, van Kessel K, van Strijp J and Milder F (**2012**) Inhibition of *Pseudomonas aeruginosa* virulence: characterization of the AprA-AprI interface and species selectivity. *J Mol Biol* **415**: 573-583

Baribault TJ, Skene KG and Steele Scott N (1989) Genetic transformation of grapevine cells. *Plant Cell Rep* **8**: 137-140

Bauer Z, Gomez-Gomez L, Boller T and Felix G (2001) Sensitivity of different ecotypes and mutants of *Arabidopsis thaliana* toward the bacterial elicitor flagellin correlates with the presence of receptor-binding sites. *J Biol Chem* **276**: 45669-45676

Beck M, Zhou J, Faulkner C, MacLean D and Robatzek S (2012) Spatio-temporal cellular dynamics of the Arabidopsis flagellin receptor reveal activation status-dependent endosomal sorting. *Plant Cell* **24**: 4205-4219

Bellin D, Peressotti E, Merdinoglu D, Wiedemann-Merdinoglu S, Adam-Blondon AF, Cipriani G, Morgante M, Testolin R and Di Gaspero G (2009) Resistance to *Plasmopara viticola* in grapevine 'Bianca' is controlled by a major dominant gene causing localised necrosis at the infection site. *Theor Appl Genet* **120**: 163-176

Benhamou N, Lafontaine PJ and Nicole M (1994) Induction of systemic resistance to fusarium crown and root rot in tomato plants by seed treatment with chitosan. *Phytopathology* **84**: 1432-1444

Bhaskara M, Arul J, Barka E, Richard C, Angers P and Castaigne F (1998) Effect of chitosan on growth and toxin production by *A. alternata* f. sp. *lycopersici. Biocontrol Sci Technol* **8**: 33-43

Bleckmann A, Weidtkamp-Peters S, Seidel CA and Simon R (2010) Stem cell signaling in Arabidopsis requires CRN to localize CLV2 to the plasma membrane. *Plant Physiol* **152**: 166-176

Boller T and Felix G (2009) A renaissance of elicitors: Perception of microbe-associated molecular patterns and danger signals by pattern-recognition receptors. *Annu Rev Plant Biol* **60**: 379-406

Bordiec S, Paquis S, Lacroix H, Dhondt S, Ait Barka E, Kauffmann S, Jeandet P, Mazeyrat-Gourbeyre F, Clement C, Baillieul F and Dorey S (2011) Comparative analysis of defence responses induced by the endophytic plant growth-promoting rhizobacterium *Burkholderia phytofirmans* strain PsJN and the non-host bacterium *Pseudomonas syringae* pv. *pisi* in grapevine cell suspensions. *J Exp Bot* **62**: 595-603

Boudsocq M, Willmann MR, McCormack M, Lee H, Shan L, He P, Bush J, Cheng SH and Sheen J (2010) Differential innate immune signalling *via* $Ca^{(2+)}$ sensor protein kinases. *Nature* **464**: 418-422

Boutrot F, Segonzac C, Chang K, Qiao H, Ecker J, Zipfel C and Rathjen J (2010) Direct transcriptional control of the Arabidopsis immune receptor FLS2 by the ethylene-dependent transcription factors EIN3 and EIL1. *Proc Natl Acad Sci U S A* **107**: 14502-14507

Bradford MM (1976) A rapid and sensitive method for the quantitation of microgram quantities of protein utilizing the principle of protein-dye binding. *Anal Biochem* **72**: 248-254

Brunner F, Rosahl S, Lee J, Rudd JJ, Geiler C, Kauppinen S, Rasmussen G, Scheel D and Nurnberger T (2002) Pep-13, a plant defense-inducing pathogen-associated pattern from *Phytophthora* transglutaminases. *EMBO J* **21**: 6681-6688

Brutus A, Sicilia F, Macone A, Cervone F and De Lorenzo G (2010) A domain swap approach reveals a role of the plant wall-associated kinase 1 (WAK1) as a receptor of oligogalacturonides. *Proc Natl Acad Sci U S A* **107**: 9452-9457

Bueter CL, Specht CA and Levitz SM (2013) Innate sensing of chitin and chitosan. *PLoS Pathog* **9**: e1003080

Burr TJ and Otten L (1999) CROWN GALL OF GRAPE: Biology and disease management. *Annu Rev Phytopathol* **37**: 53-80

Busam G, Kassemeyer HH and Matern U (1997) Differential expression of chitinases in *Vitis vinifera* L. responding to systemic acquired resistance activators or fungal challenge. *Plant Physiol* **115**: 1029-1038

Buschart A, Sachs S, Chen X, Herglotz J, Krause A and Reinhold-Hurek B (2012) Flagella mediate endophytic competence rather than act as MAMPS in rice-*Azoarcus* sp. strain BH72 interactions. *Mol Plant Microbe Interact* **25**: 191-199

Cai R, Lewis J, Yan S, Liu H, Clarke CR, Campanile F, Almeida NF, Studholme DJ, Lindeberg M, Schneider D, Zaccardelli M, Setubal JC, Morales-Lizcano NP, Bernal A, Coaker G, Baker C, Bender CL, Leman S and Vinatzer BA (2011) The plant pathogen *Pseudomonas syringae* pv. *tomato* is genetically monomorphic and under strong selection to evade tomato immunity. *PLoS Pathog* **7**: e1002130

Cao Y, Aceti D, Sabat G, Song J, Makino S, Fox B and Bent A (**2013**) Mutations in FLS2 Ser-938 dissect signaling activation in FLS2-mediated Arabidopsis immunity. *PLoS Pathog* **9**: e1003313

Chang X and Nick P (**2012**) Defence signalling triggered by flg22 and harpin is integrated into a different stilbene output in *Vitis* cells. *Plos ONE* **7**: e40446

Che FS, Nakajima Y, Tanaka N, Iwano M, Yoshida T, Takayama S, Kadota I and Isogai A (**2000**) Flagellin from an incompatible strain of *Pseudomonas avenae* induces a resistance response in cultured rice cells. *J Biol Chem* **275**: 32347-32356

Chinchilla D, Bauer Z, Regenass M, Boller T and Felix G (**2006**) The Arabidopsis receptor kinase FLS2 binds flg22 and determines the specificity of flagellin perception. *Plant Cell* **18**: 465-476

Chinchilla D, Zipfel C, Robatzek S, Kemmerling B, Nurnberger T, Jones JD, Felix G and Boller T (**2007**) A flagellin-induced complex of the receptor FLS2 and BAK1 initiates plant defence. *Nature* **448**: 497-500

Clarke CR, Chinchilla D, Hind SR, Taguchi F, Miki R, Ichinose Y, Martin GB, Leman S, Felix G and Vinatzer BA (**2013**) Allelic variation in two distinct *Pseudomonas syringae* flagellin epitopes modulates the strength of plant immune responses but not bacterial motility. *New Phytol* **200**:847-860

Clay NK, Adio AM, Denoux C, Jander G and Ausubel FM (**2009**) Glucosinolate metabolites required for an Arabidopsis innate immune response. *Science* **323**: 95-101

Clough S and Bent A (**1998**) Floral dip: a simplified method for *Agrobacterium*-mediated transformation of *Arabidopsis thaliana*. *Plant J* **16**: 735-743

Compant S, Duffy B, Nowak J, Clement C and Ait Barka E (**2005a**) Use of plant growth-promoting bacteria for biocontrol of plant diseases: Principles, mechanisms of action, and future prospects. *Appl Environ Microbiol* **71**: 4951-4959

Compant S, Reiter B, Sessitsch A, Nowak J, Clement C and Ait Barka E (**2005b**) Endophytic colonization of *Vitis vinifera* L. by plant growth promoting bacterium *Burkholderia* sp strain PsJN. *Appl Environ Microbiol* **71**: 1685-1693

Coutos-Thevenot P, Poinssot B, Bonomelli A, Yean H, Breda C, Buffard D, Esnault R, Hain R and Boulay M (**2001**) *In vitro* tolerance to *Botrytis cinerea* of grapevine 41B rootstock in transgenic plants expressing the stilbene synthase *Vst1* gene under the control of a pathogen-inducible *PR 10* promoter. *J Exp Bot* **52**: 901-910

Dardick C and Ronald P (**2006**) Plant and animal pathogen recognition receptors signal through non-RD kinases. *PLoS Pathog* **2**: e2

de Jonge R, van Esse HP, Kombrink A, Shinya T, Desaki Y, Bours R, van der Krol S, Shibuya N, Joosten MH and Thomma BP (**2010**) Conserved fungal LysM effector Ecp6 prevents chitin-triggered immunity in plants. *Science* **329**: 953-955

de Jonge R, van Esse HP, Maruthachalam K, Bolton MD, Santhanam P, Saber MK, Zhang Z, Usami T, Lievens B, Subbarao KV and Thomma BP (**2012**) Tomato immune receptor Ve1 recognizes effector of multiple fungal pathogens uncovered by genome and RNA sequencing. *Proc Natl Acad Sci U S A* **109**: 5110-5115

Delaunois B, Farace G, Jeandet P, Clement C, Baillieul F, Dorey S and Cordelier S (**2014**) Elicitors as alternative strategy to pesticides in grapevine? Current knowledge on their mode of action from controlled conditions to vineyard. *Environ Sci Pollut Res Int* **21**: 4837-4846

Dereeper A, Guignon V, Blanc G, Audic S, Buffet S, Chevenet F, Dufayard JF, Guindon S, Lefort V, Lescot M, Claverie JM and Gascuel O (**2008**) Phylogeny.fr: robust phylogenetic analysis for the non-specialist. *Nucleic acids research* **36**: W465-469

Derkel J, Baillieul F, Manteau S, Audran J, Haye B, Lambert B and Legendre L (**1999**) Differential induction of grapevine defenses by two strains of *Botrytis cinerea*. *Phytopathology* **89**: 197-203

Dodds P and Rathjen J (**2010**) Plant immunity: towards an integrated view of plant-pathogen interactions. *Nat Rev Genet* **11**: 539-548

Drake D and Montie TC (**1988**) Flagella, motility, and invasive virulence of *Pseudomonas aeruginosa*. *J Gen Microbiol* **134**: 43-52

Dubreuil-Maurizi C, Trouvelot S, Frettinger P, Pugin A, Wendehenne D and Poinssot B (**2010**) beta-aminobutyric acid primes an NADPH oxidase-dependent reactive oxygen species production during grapevine-triggered immunity. *Mol Plant Microbe Interact* **23**: 1012-1021

Dufour MC, Lambert C, Bouscaut J, Mérillon JM and Corio-Costet MF (**2013**) Benzothiadiazole-primed defence responses and enhanced differential expression of defence genes in Vitis vinifera infected with biotrophic pathogens Erysiphe necator and *Plasmopara viticola*. *Plant Pathol* **62**: 370-382

Dunning F, Sun W, Jansen K, Helft L and Bent A (**2007**) Identification and mutational analysis of Arabidopsis FLS2 leucine-rich repeat domain residues that contribute to flagellin perception. *Plant Cell* **19**: 3297-3313

Eamens A, Wang MB, Smith NA and Waterhouse PM (**2008**) RNA silencing in plants: yesterday, today, and tomorrow. *Plant Physiol* **147**: 456-468

El Ghaouth A, Arul J, Wilson C and Benhamou N (**1994**) Ultrastructural and cytochemical aspects of the effect of chitosan on decay of bell pepper fruit. *Physiological and Molecular Plant Pathology* **44**: 417-432

Elmer P and Michailides T (**2007**) Epidemiology of *Botrytis cinerea* in orchard and vine crops. *In*: Elad Y, Williamson B, Tudzynski P and Delen N (eds) Botrytis: Biology, pathology and Control. *Springer*, The Netherlands, pp 243-272

Erbs G and Newman M (**2012**) The role of lipopolysaccharide and peptidoglycan, two glycosylated bacterial microbe-associated molecular patterns (MAMPs), in plant innate immunity. *Mol Plant Pathol* **13**: 95-104

Faulkner C, Petutschnig E, Benitez-Alfonso Y, Beck M, Robatzek S, Lipka V and Maule AJ (**2013**) LYM2-dependent chitin perception limits molecular flux *via* plasmodesmata. *Proc Natl Acad Sci U S A* **110**: 9166-9170

Felix G, Duran JD, Volko S and Boller T (**1999**) Plants have a sensitive perception system for the most conserved domain of bacterial flagellin. *Plant J* **18**: 265-276

Fernandez O, Theocharis A, Bordiec S, Feil R, Jacquens L, Clement C, Fontaine F and Ait Barka E (**2012**) *Burkholderia phytofirmans* PsJN acclimates grapevine to cold by modulating carbohydrate metabolism. *Mol Plant Microbe Interact* **25**: 496-504

Ferrari S, Galletti R, Denoux C, De Lorenzo G, Ausubel FM and Dewdney J (**2007**) Resistance to *Botrytis cinere*a induced in Arabidopsis by elicitors is independent of salicylic acid, ethylene, or jasmonate signaling but requires PHYTOALEXIN DEFICIENT3. *Plant Physiol* **144**: 367-379

Fradin EF, Abd-El-Haliem A, Masini L, van den Berg GC, Joosten MH and Thomma BP (**2011**) Interfamily transfer of tomato Ve1 mediates *Verticillium* resistance in Arabidopsis. *Plant Physiol* **156**: 2255-2265

Fujikawa T, Sakaguchi A, Nishizawa Y, Kouzai Y, Minami E, Yano S, Koga H, Meshi T and Nishimura M (**2012**) Surface alpha-1,3-glucan facilitates fungal stealth infection by interfering with innate immunity in plants. *PLoS Pathog* **8**: e1002882

Gamm M (**2011**) Impact de *Plasmopara viticola* sur le métabolisme de l'amidon et le fonctionnement stomatique chez la vigne. *Thesis.* Université de Bourgogne, Dijon, France

Gamm M, Heloir MC, Kelloniemi J, Poinssot B, Wendehenne D and Adrian M (**2011**) Identification of reference genes suitable for qRT-PCR in grapevine and application for the study of the expression of genes involved in pterostilbene synthesis. *Mol Genet Genomics* **285**: 273-285

Garcia-Brugger A, Lamotte O, Vandelle E, Bourque S, Lecourieux D, Poinssot B, Wendehenne D and Pugin A (**2006**) Early signaling events induced by elicitors of plant defenses. *Mol Plant Microbe Interact* **19**: 711-724

Gauthier A (**2009**) Comparaison de différent éliciteurs des réactions de défense de la vigne. Etude du mode d'action de la laminarine sulfatée, un inducteur de résistance à *P. viticola*. *Thesis*. Université de Bourgogne, Dijon, France

Gauthier A, Trouvelot S, Kelloniemi J, Frettinger P, Wendehenne D, Daire X, Joubert JM, Ferrarini A, Delledonne M, Flors V and Poinssot B (**2014**) The sulfated laminarin triggers a stress transcriptome before priming the SA- and ROS-dependent defenses during grapevine's induced resistance against *Plasmopara viticola*. *Plos ONE* **9**: e88145

Gessler C, Pertot I and Perazzolli M (**2011**) *Plasmopara viticola*: a review of knowledge on downy mildew of grapevine and effective disease management. *Phytopathol mediterr* **50**: 3-44

Geurts R, Fedorova E and Bisseling T (**2005**) Nod factor signaling genes and their function in the early stages of *Rhizobium* infection. *Curr Opin Plant Biol* **8**: 346-352

Gimenez-Ibanez S, Hann DR, Ntoukakis V, Petutschnig E, Lipka V and Rathjen JP (**2009**) AvrPtoB targets the LysM receptor kinase CERK1 to promote bacterial virulence on plants. *Curr Biol* **19**: 423-429

Glazebrook J (**2005**) Contrasting mechanisms of defense against biotrophic and necrotrophic pathogens. *Annu Rev Phytopathol* **43**: 205-227

Gohre V, Spallek T, Haweker H, Mersmann S, Mentzel T, Boller T, de Torres M, Mansfield JW and Robatzek S (**2008**) Plant pattern-recognition receptor FLS2 is directed for degradation by the bacterial ubiquitin ligase AvrPtoB. *Curr Biol* **18**: 1824-1832

Gomez-Gomez L, Bauer Z and Boller T (**2001**) Both the extracellular leucine-rich repeat domain and the kinase activity of FSL2 are required for flagellin binding and signaling in Arabidopsis. *Plant Cell* **13**: 1155-1163

Gomez-Gomez L and Boller T (**2000**) FLS2: An LRR receptor-like kinase involved in the perception of the bacterial elicitor flagellin in Arabidopsis. *Mol Cell* **5**: 1003-1011

Gomez-Gomez L, Felix G and Boller T (**1999**) A single locus determines sensitivity to bacterial flagellin in *Arabidopsis thaliana*. *Plant J* **18**: 277-284

Gouy M, Guindon S and Gascuel O (**2010**) SeaView version 4: A multiplatform graphical user interface for sequence alignment and phylogenetic tree building. *Mol Biol Evol* **27**: 221-224

Gust AA, Willmann R, Desaki Y, Grabherr HM and Nurnberger T (**2012**) Plant LysM proteins: modules mediating symbiosis and immunity. *Trends Plant Sci* **17**: 495-502

Hamel LP and Beaudoin N (**2010**) Chitooligosaccharide sensing and downstream signaling: contrasted outcomes in pathogenic and beneficial plant-microbe interactions. *Planta* **232**: 787-806

Hann D and Rathjen J (**2007**) Early events in the pathogenicity of *Pseudomonas syringae* on *Nicotiana benthamiana*. *Plant J* **49**: 607-618

Hann DR, Dominguez-Ferreras A, Motyka V, Dobrev PI, Schornack S, Jehle A, Felix G, Chinchilla D, Rathjen JP and Boller T (**2013**) The Pseudomonas type III effector HopQ1 activates cytokinin signaling and interferes with plant innate immunity. *New Phytol* doi: 10.1111/nph.12544

Hartl L, Zach S and Seidl-Seiboth V (**2012**) Fungal chitinases: diversity, mechanistic properties and biotechnological potential. *Appl Microbiol Biotechnol* **93**: 533-543

Hatterman DR and Ries SM (**1989**) Motility of *Pseudomonas syringae* pv. *glycinea* and its role in infection. *Phytopathology* **79**: 284-289

Haweker H, Rips S, Koiwa H, Salomon S, Saijo Y, Chinchilla D, Robatzek S and von Schaewen A (**2010**) Pattern recognition receptors require N-glycosylation to mediate plant immunity. *J Biol Chem* **285**: 4629-4636

Hawn TR, Verbon A, Lettinga KD, Zhao LP, Li SS, Laws RJ, Skerrett SJ, Beutler B, Schroeder L, Nachman A, Ozinsky A, Smith KD and Aderem A (**2003**) A common dominant TLR5 stop codon polymorphism abolishes flagellin signaling and is associated with susceptibility to legionnaires' disease. *J Exp Med* **198**: 1563-1572

Hayafune M, Berisio R, Marchetti R, Silipo A, Kayama M, Desaki Y, Arima S, Squeglia F, Ruggiero A, Tokuyasu K, Molinaro A, Kaku H and Shibuya N (**2014**) Chitin-induced activation of immune signaling by the rice receptor CEBiP relies on a unique sandwich-type dimerization. *Proc Natl Acad Sci U S A* **111**: E404-413

Hayashi F, Smith KD, Ozinsky A, Hawn TR, Yi EC, Goodlett DR, Eng JK, Akira S, Underhill DM and Aderem A (**2001**) The innate immune response to bacterial flagellin is mediated by Toll-like receptor 5. *Nature* **410**: 1099-1103

He Z, Wang ZY, Li J, Zhu Q, Lamb C, Ronald P and Chory J (**2000**) Perception of brassinosteroids by the extracellular domain of the receptor kinase BRI1. *Science* **288**: 2360-2363

Heese A, Hann DR, Gimenez-Ibanez S, Jones AM, He K, Li J, Schroeder JI, Peck SC and Rathjen JP (**2007**) The receptor-like kinase SERK3/BAK1 is a central regulator of innate immunity in plants. *Proc Natl Acad Sci U S A* **104**: 12217-12222

Hirai H, Takai R, Iwano M, Nakai M, Kondo M, Takayama S, Isogai A and Che F (**2011**) Glycosylation regulates specific induction of rice immune responses by *Acidovorax avenae* flagellin. *J Biol Chem* **286**: 25519-25530

Ichimura K, Casais C, Peck SC, Shinozaki K and Shirasu K (**2006**) MEKK1 is required for MPK4 activation and regulates tissue-specific and temperature-dependent cell death in Arabidopsis. *J Biol Chem* **281**: 36969-36976

Iizasa E, Mitsutomi M and Nagano Y (**2010**) Direct binding of a plant LysM receptor-like kinase, LysM RLK1/CERK1, to chitin *in vitro*. *J Biol Chem* **285**: 2996-3004

Ikeda JS, Schmitt CK, Darnell SC, Watson PR, Bispham J, Wallis TS, Weinstein DL, Metcalf ES, Adams P, O'Connor CD and O'Brien AD (**2001**) Flagellar phase variation of *Salmonella enterica* serovar *Typhimurium* contributes to virulence in the murine typhoid infection model but does not influence *Salmonella*-induced enteropathogenesis. *Infect Immun* **69**: 3021-3030

Iriti M and Faoro F (**2009**) Chitosan as a MAMP, searching for a PRR. *Plant Signal Behav* **4**: 66-68

Jacobs AK, Dry I and Robinson S (**1999**) Induction of different pathogenesis-related cDNAs in grapevine infected with powdery mildew and treated with ethephon. *Plant Pathology* **48**: 325-336

Jaillon O, Aury JM, Noel B, Policriti A, Clepet C, Casagrande A, Choisne N, Aubourg S, Vitulo N, Jubin C, Vezzi A, Legeai F, Hugueney P, Dasilva C, Horner D, Mica E, Jublot D, Poulain J, Bruyere C, Billault A, Segurens B, Gouyvenoux M, Ugarte E, Cattonaro F, Anthouard V, Vico V, Del Fabbro C, Alaux M, Di Gaspero G, Dumas V, Felice N, Paillard S, Juman I, Moroldo M, Scalabrin S, Canaguier A, Le Clainche I, Malacrida G, Durand E, Pesole G, Laucou V, Chatelet P, Merdinoglu D, Delledonne M, Pezzotti M, Lecharny A, Scarpelli C, Artiguenave F, Pe ME, Valle G, Morgante M, Caboche M, Adam-Blondon AF, Weissenbach J, Quetier F and Wincker P (**2007**) The grapevine genome sequence suggests ancestral hexaploidization in major angiosperm phyla. *Nature* **449**: 463-467

Jeandet P, Douillet-Breuil AC, Bessis R, Debord S, Sbaghi M and Adrian M (**2002**) Phytoalexins from the Vitaceae: biosynthesis, phytoalexin gene expression in transgenic plants, antifungal activity, and metabolism. *J Agric Food Chem* **50**: 2731-2741

Jelly NS, Schellenbaum P, Walter B and Maillot P (**2012**) Transient expression of artificial microRNAs targeting Grapevine fanleaf virus and evidence for RNA silencing in grapevine somatic embryos. *Transgenic Res* **21**: 1319-1327

Jeworutzki E, Roelfsema M, Anschutz U, Krol E, Elzenga J, Felix G, Boller T, Hedrich R and Becker D (**2010**) Early signaling through the Arabidopsis pattern recognition receptors FLS2 and EFR involves Ca^{2+}-associated opening of plasma membrane anion channels. *Plant J* **62**: 367-378

Jones JD and Dangl JL (**2006**) The plant immune system. *Nature* **444**: 323-329

Kaku H, Nishizawa Y, Ishii-Minami N, Akimoto-Tomiyama C, Dohmae N, Takio K, Minami E and Shibuya N (**2006**) Plant cells recognize chitin fragments for defense signaling through a plasma membrane receptor. *Proc Natl Acad Sci U S A* **103**: 11086-11091

Karimi M, Inze D and Depicker A (**2002**) GATEWAY vectors for Agrobacterium-mediated plant transformation. *Trends Plant Sci* **7**: 193-195

Kawano Y and Shimamoto K (**2013**) Early signaling network in rice PRR-mediated and R-mediated immunity. *Curr Opin Plant Biol* **16**: 496-504

Kishi-Kaboshi M, Okada K, Kurimoto L, Murakami S, Umezawa T, Shibuya N, Yamane H, Miyao A, Takatsuji H, Takahashi A and Hirochika H (**2010**) A rice fungal MAMP-responsive MAPK cascade regulates metabolic flow to antimicrobial metabolite synthesis. *Plant J* **63**: 599-612

Kishimoto K, Kouzai Y, Kaku H, Shibuya N, Minami E and Nishizawa Y (**2010**) Perception of the chitin oligosaccharides contributes to disease resistance to blast fungus *Magnaporthe oryzae* in rice. *Plant J* **64**: 343-354

Klarzynski O, Plesse B, Joubert JM, Yvin JC, Kopp M, Kloareg B and Fritig B (**2000**) Linear beta-1,3 glucans are elicitors of defense responses in tobacco. *Plant Physiol* **124**: 1027-1038

Koller B, Muller-Wiefel AS, Rupec R, Korting HC and Ruzicka T (2011) Chitin modulates innate immune responses of keratinocytes. *Plos ONE* **6**: e16594

Kortekamp A (2006) Expression analysis of defence-related genes in grapevine leaves after inoculation with a host and a non-host pathogen. *Plant Physiol Biochem* **44**: 58-67

Kouzai Y, Nakajima K, Hayafune M, Ozawa K, Kaku H, Shibuya N, Minami E and Nishizawa Y (2014) CEBiP is the major chitin oligomer-binding protein in rice and plays a main role in the perception of chitin oligomers. *Plant Mol Biol* **84**: 519-528

Krol E, Mentzel T, Chinchilla D, Boller T, Felix G, Kemmerling B, Postel S, Arents M, Jeworutzki E, Al-Rasheid KA, Becker D and Hedrich R (2010) Perception of the Arabidopsis danger signal peptide 1 involves the pattern recognition receptor AtPEPR1 and its close homologue AtPEPR2. *J Biol Chem* **285**: 13471-13479

Kunze G, Zipfel C, Robatzek S, Niehaus K, Boller T and Felix G (2004) The N terminus of bacterial elongation factor Tu elicits innate immunity in Arabidopsis plants. *Plant Cell* **16**: 3496-3507

Kvitko BH, Park DH, Velasquez AC, Wei CF, Russell AB, Martin GB, Schneider DJ and Collmer A (2009) Deletions in the repertoire of *Pseudomonas syringae* pv. *tomato* DC3000 type III secretion effector genes reveal functional overlap among effectors. *PLoS Pathog* **5**: e1000388

Lacombe S, Rougon-Cardoso A, Sherwood E, Peeters N, Dahlbeck D, van Esse HP, Smoker M, Rallapalli G, Thomma BP, Staskawicz B, Jones JD and Zipfel C (2010) Interfamily transfer of a plant pattern-recognition receptor confers broad-spectrum bacterial resistance. *Nat Biotechnol* **28**: 365-369

Laemmli UK (1970) Cleavage of structural proteins during the assembly of the head of bacteriophage T4. *Nature* **227**: 680-685

Lakshmanan V, Kitto S, Caplan J, Hsueh Y, Kearns D, Wu Y and Bais H (2012) Microbe-associated molecular patterns-triggered root responses mediate beneficial rhizobacterial recruitment in Arabidopsis. *Plant Physiol* **160**: 1642-1661

Lamotte O, Courtois C, Dobrowolska G, Besson A, Pugin A and Wendehenne D (2006) Mechanisms of nitric-oxide-induced increase of free cytosolic Ca^{2+} concentration in *Nicotiana plumbaginifolia* cells. *Free Radic Biol Med* **40**: 1369-1376

Lee CG, Da Silva CA, Lee JY, Hartl D and Elias JA (2008) Chitin regulation of immune responses: an old molecule with new roles. *Curr Opin Immunol* **20**: 684-689

Lee SW, Han SW, Sririyanum M, Park CJ, Seo YS and Ronald PC (2009) A type I-secreted, sulfated peptide triggers XA21-mediated innate immunity. *Science* **326**: 850-853

Lee WS, Rudd JJ, Hammond-Kosack KE and Kanyuka K (2014) *Mycosphaerella graminicola* LysM effector-mediated stealth pathogenesis subverts recognition through both CERK1 and CEBiP homologues in wheat. *Mol Plant Microbe Interact* **27**: 236-243

Li J, Wen J, Lease KA, Doke JT, Tax FE and Walker JC (2002) BAK1, an Arabidopsis LRR receptor-like protein kinase, interacts with BRI1 and modulates brassinosteroid signaling. *Cell* **110**: 213-222

Li J, Zhao-Hui C, Batoux M, Nekrasov V, Roux M, Chinchilla D, Zipfel C and Jones JD (2009) Specific ER quality control components required for biogenesis of the plant innate immune receptor EFR. *Proc Natl Acad Sci U S A* **106**: 15973-15978

Lin W, Lu D, Gao X, Jiang S, Ma X, Wang Z, Mengiste T, He P and Shan L (2013) Inverse modulation of plant immune and brassinosteroid signaling pathways by the receptor-like cytoplasmic kinase BIK1. *Proc Natl Acad Sci U S A* **110**: 12114-12119

Liu B, Li JF, Ao Y, Qu J, Li Z, Su J, Zhang Y, Liu J, Feng D, Qi K, He Y, Wang J and Wang HB (2012a) Lysin motif-containing proteins LYP4 and LYP6 play dual roles in peptidoglycan and chitin perception in rice innate immunity. *Plant Cell* **24**: 3406-3419

Liu T, Liu Z, Song C, Hu Y, Han Z, She J, Fan F, Wang J, Jin C, Chang J, Zhou JM and Chai J (2012b) Chitin-induced dimerization activates a plant immune receptor. *Science* **336**: 1160-1164

Livak KJ and Schmittgen TD (2001) Analysis of relative gene expression data using real-time quantitative PCR and the 2(-ΔΔ C(t)) Method. *Methods* **25**: 402-408

Lloyd SR, Schoonbeek HJ, Trick M, Zipfel C and Ridout CJ (2014) Methods to Study PAMP-Triggered Immunity in Brassica Species. *Mol Plant Microbe Interact* **27**: 286-295

Lo Piccolo S, Ferraro V, Alfonzo A, Settanni L, Ercolini D, Burruano S and Moschetti G (2010) Presence of endophytic bacteria in *Vitis vinifera* leaves as detected by fluorescence in situ hybridization. *Ann Microbiol* **60**: 161-167

Lopez-Gomez M, Sandal N, Stougaard J and Boller T (2012) Interplay of flg22-induced defence responses and nodulation in Lotus japonicus. *J Exp Bot* **63**: 393-401

Lu D, Lin W, Gao X, Wu S, Cheng C, Avila J, Heese A, Devarenne TP, He P and Shan L (2011) Direct ubiquitination of pattern recognition receptor FLS2 attenuates plant innate immunity. *Science* **332**: 1439-1442

Lu D, Wu S, Gao X, Zhang Y, Shan L and He P (2010) A receptor-like cytoplasmic kinase, BIK1, associates with a flagellin receptor complex to initiate plant innate immunity. *Proc Natl Acad Sci U S A* **107**: 496-501

Lu J and Sun PD (2012) The structure of the TLR5-flagellin complex: a new mode of pathogen detection, conserved receptor dimerization for signaling. *Sci signal* **5**: pe11

Lugtenberg B and Kamilova F (2009) Plant-Growth-Promoting Rhizobacteria. *Annu Rev Microbiol* **63**: 541-556

Macnab RM (1999) The bacterial flagellum: reversible rotary propellor and type III export apparatus. *J Bacteriol* **181**: 7149-7153

Macnab RM (2003) How bacteria assemble flagella. *Annu Rev Microbiol* **57**: 77-100

McCann HC, Nahal H, Thakur S and Guttman DS (2012) Identification of innate immunity elicitors using molecular signatures of natural selection. *Proc Natl Acad Sci U S A* **109**: 4215-4220

Meindl T, Boller T and Felix G (2000) The bacterial elicitor flagellin activates its receptor in tomato cells according to the address-message concept. *Plant Cell* **12**: 1783-1794

Melotto M, Underwood W, Koczan J, Nomura K and He SY (2006) Plant stomata function in innate immunity against bacterial invasion. *Cell* **126**: 969-980

Menard R, Alban S, de Ruffray P, Jamois F, Franz G, Fritig B, Yvin JC and Kauffmann S (2004) Beta-1,3 glucan sulfate, but not beta-1,3 glucan, induces the salicylic acid signaling pathway in tobacco and Arabidopsis. *Plant Cell* **16**: 3020-3032

Mendes BMJ, Cardoso SC, Boscariol-Camargo RL, Cruz RB, Mourão Filho FAA and Bergamin Filho A (2010) Reduction in susceptibility to *Xanthomonas axonopodis* pv. *citri* in transgenic *Citrus sinensis* expressing the rice *Xa21* gene. *Plant Pathol* **59**: 68-75

Mentlak TA, Kombrink A, Shinya T, Ryder LS, Otomo I, Saitoh H, Terauchi R, Nishizawa Y, Shibuya N, Thomma BP and Talbot NJ (2012) Effector-mediated suppression of chitin-triggered immunity by *Magnaporthe oryza*e is necessary for rice blast disease. *Plant Cell* **24**: 322-335

Merzendorfer H (2011) The cellular basis of chitin synthesis in fungi and insects: common principles and differences. *Eur J Cell Biol* **90**: 759-769

Millet Y, Danna C, Clay N, Songnuan W, Simon M, Werck-Reichhart D and Ausubel F (2010) Innate immune responses activated in Arabidopsis roots by microbe-associated molecular patterns. *Plant Cell* **22**: 973-990

Mitter B, Petric A, Shin MW, Chain PS, Hauberg-Lotte L, Reinhold-Hurek B, Nowak J and Sessitsch A (2013) Comparative genome analysis of *Burkholderia phytofirmans* PsJN reveals a wide spectrum of endophytic lifestyles based on interaction strategies with host plants. *Front Plant Sci* **4**: 120

Miya A, Albert P, Shinya T, Desaki Y, Ichimura K, Shirasu K, Narusaka Y, Kawakami N, Kaku H and Shibuya N (2007) CERK1, a LysM receptor kinase, is essential for chitin elicitor signaling in Arabidopsis. *Proc Natl Acad Sci U S A* **104**: 19613-19618

Monaghan J and Zipfel C (2012) Plant pattern recognition receptor complexes at the plasma membrane. *Curr Opin Plant Biol* **15**: 349-357

Mueller K, Bittel P, Chinchilla D, Jehle A, Albert M, Boller T and Felix G (**2012**) Chimeric FLS2 receptors reveal the basis for differential flagellin perception in Arabidopsis and tomato. *Plant Cell* **24**: 2213-2224

Nakaoka Y, Miki T, Fujioka R, Uehara R, Tomioka A, Obuse C, Kubo M, Hiwatashi Y and Goshima G (**2012**) An inducible RNA interference system in Physcomitrella patens reveals a dominant role of augmin in phragmoplast microtubule generation. *Plant Cell* **24**: 1478-1493

Naton B, Hahlbrock K and Schmelzer E (**1996**) Correlation of rapid cell death with metabolic changes in fungus-infected, cultured parsley cells. *Plant Physiol* **112**: 433-444

Nekrasov V, Li J, Batoux M, Roux M, Chu ZH, Lacombe S, *et al.* (**2009**) Control of the pattern-recognition receptor EFR by an ER protein complex in plant immunity. *EMBO J* **28**: 3428-3438

Newman MA, Sundelin T, Nielsen JT and Erbs G (**2013**) MAMP (microbe-associated molecular pattern) triggered immunity in plants. *Front Plant Sci* **4**: 139

Nitsch J and Nitsch C (**1969**) Haploid plants from pollen grains. *Science* **163**: 85-87

Nunney L, Yuan X, Bromley R, Hartung J, Montero-Astua M, Moreira L, Ortiz B and Stouthamer R (**2010**) Population genomic analysis of a bacterial plant pathogen: novel insight into the origin of Pierce's disease of grapevine in the U.S. *Plos ONE* **5**: e15488

Ono E, Wong HL, Kawasaki T, Hasegawa M, Kodama O and Shimamoto K (**2001**) Essential role of the small GTPase Rac in disease resistance of rice. *Proc Natl Acad Sci U S A* **98**: 759-764

Onofre-Lemus J, Hernandez-Lucas I, Girard L and Caballero-Mellado J (**2009**) ACC (1-aminocyclopropane-1-carboxylate) deaminase activity, a widespread trait in *Burkholderia* Species, and its growth-promoting effect on tomato plants. *Appl Environ Microbiol* **75**: 6581-6590

Paparella C, Savatin DV, Marti L, De Lorenzo G and Ferrari S (**2014**) The *Arabidopsis thaliana* LYSM-CONTAINING RECEPTOR-LIKE KINASE 3 regulates the cross talk between immunity and abscisic acid responses. *Plant Physiol* doi:10.1104/pp.113.233759

Park CJ, Caddell DF and Ronald PC (**2013**) Protein phosphorylation in plant immunity: insights into the regulation of pattern recognition receptor-mediated signaling. *In*: Jones AME, Monaghan J and Ntoukakis V (eds) Mechanisms regulating immunity in plants. *Frontiers*, pp 36-44

Park CJ and Ronald PC (**2012**) Cleavage and nuclear localization of the rice XA21 immune receptor. *Nat commun* **3**: 920

Pasare C and Medzhitov R (**2004**) Toll-like receptors: linking innate and adaptive immunity. *Microbes Infect* **6**: 1382-1387

Perrin M, Gertz C and Masson JE (**2004**) High efficiency initiation of regenerable embryogenic callus from anther filaments of 19 grapevine genotypes grown worldwide. *Plant Science* **167**: 1343-1349

Perrin M, Martin D, Joly D, Demangeat G, This P and Masson JE (**2001**) Medium-dependent response of grapevine somatic embryogenic cells. *Plant Sci* **161**: 107-116

Petutschnig EK, Jones AM, Serazetdinova L, Lipka U and Lipka V (**2010**) The lysin motif receptor-like kinase (LysM-RLK) CERK1 is a major chitin-binding protein in *Arabidopsis thaliana* and subject to chitin-induced phosphorylation. *J Biol Chem* **285**: 28902-28911

Pezet R, Gindro K, Viret O and Spring J (**2004**) Glycosylation and oxidative dimerization of resveratrol are respectively associated to sensitivity and resistance of grapevine cultivars to downy mildew. *Physiol Mol Plant Pathol* **65**: 297-303

Pfund C, Tans-Kersten J, Dunning F, Alonso J, Ecker J, Allen C and Bent A (**2004**) Flagellin is not a major defense elicitor in *Ralstonia solanacearum* cells or extracts applied to *Arabidopsis thaliana*. *Mol Plant Microbe Interact* **17**: 696-706

Poinssot B, Vandelle E, Bentejac M, Adrian M, Levis C, Brygoo Y, Garin J, Sicilia F, Coutos-Thevenot P and Pugin A (**2003**) The endopolygalacturonase 1 from *Botrytis cinerea* activates grapevine defense reactions unrelated to its enzymatic activity. *Mol Plant Microbe Interact* **16**: 553-564

Polesani M, Bortesi L, Ferrarini A, Zamboni A, Fasoli M, Zadra C, Lovato A, Pezzotti M, Delledonne M and Polverari A (**2010**) General and species-specific transcriptional responses to downy mildew

infection in a susceptible (*Vitis vinifera*) and a resistant (*V. riparia*) grapevine species. *BMC Genomics* **11**: 117

Postel S and Kemmerling B (**2009**) Plant systems for recognition of pathogen-associated molecular patterns. *Semin Cell Dev Biol* **20**: 1025-1031

Poupin MJ, Timmermann T, Vega A, Zuniga A and Gonzalez B (**2013**) Effects of the plant growth-promoting bacterium *Burkholderia phytofirmans* PsJN throughout the life cycle of *Arabidopsis thaliana*. *Plos ONE* **8**: e69435

Povero G, Loreti E, Pucciariello C, Santaniello A, Di Tommaso D, Di Tommaso G, Kapetis D, Zolezzi F, Piaggesi A and Perata P (**2011**) Transcript profiling of chitosan-treated Arabidopsis seedlings. *J Plant Res* **124**: 619-629

Radutoiu S, Madsen LH, Madsen EB, Felle HH, Umehara Y, Gronlund M, Sato S, Nakamura Y, Tabata S, Sandal N and Stougaard J (**2003**) Plant recognition of symbiotic bacteria requires two LysM receptor-like kinases. *Nature* **425**: 585-592

Rahme LG, Tan MW, Le L, Wong SM, Tompkins RG, Calderwood SB and Ausubel FM (**1997**) Use of model plant hosts to identify *Pseudomonas aeruginosa* virulence factors. *Proc Natl Acad Sci U S A* **94**: 13245-13250

Ramos HC, Rumbo M and Sirard JC (**2004**) Bacterial flagellins: mediators of pathogenicity and host immune responses in mucosa. *Trends Microbiol* **12**: 509-517

Ranf S, Wunnenberg P, Lee J, Becker D, Dunkel M, Hedrich R, Scheel D and Dietrich P (**2008**) Loss of the vacuolar cation channel, AtTPC1, does not impair Ca^{2+} signals induced by abiotic and biotic stresses. *Plant J* **53**: 287-299

Rentel MC and Knight MR (**2004**) Oxidative stress-induced calcium signaling in Arabidopsis. *Plant Physiol* **135**: 1471-1479

Robatzek S, Bittel P, Chinchilla D, Kochner P, Felix G, Shiu SH and Boller T (**2007**) Molecular identification and characterization of the tomato flagellin receptor LeFLS2, an orthologue of Arabidopsis FLS2 exhibiting characteristically different perception specificities. *Plant Mol Biol* **64**: 539-547

Robatzek S, Chinchilla D and Boller T (**2006**) Ligand-induced endocytosis of the pattern recognition receptor FLS2 in Arabidopsis. *Genes Dev* **20**: 537-542

Robatzek S and Wirthmueller L (**2012**) Mapping FLS2 function to structure: LRRs, kinase and its working bits. *Protoplasma* **250**: 671-681

Robert-Seilaniantz A, Grant M and Jones JD (**2011**) Hormone crosstalk in plant disease and defense: more than just jasmonate-salicylate antagonism. *Annu Rev Phytopathol* **49**: 317-343

Ron M and Avni A (**2004**) The receptor for the fungal elicitor ethylene-inducing xylanase is a member of a resistance-like gene family in tomato. *Plant Cell* **16**: 1604-1615

Ross A, Yamada K, Hiruma K, Yamashita-Yamada M, Lu X, Takano Y, Tsuda K and Saijo Y (**2014**) The Arabidopsis PEPR pathway couples local and systemic plant immunity. *EMBO J* **33**: 62-75

Roux M, Schwessinger B, Albrecht C, Chinchilla D, Jones A, Holton N, Malinovsky FG, Tor M, de Vries S and Zipfel C (**2011**) The Arabidopsis leucine-rich repeat receptor-like kinases BAK1/SERK3 and BKK1/SERK4 are required for innate immunity to hemibiotrophic and biotrophic pathogens. *Plant Cell* **23**: 2440-2455

Ruijter JM, Ramakers C, Hoogaars WM, Karlen Y, Bakker O, van den Hoff MJ and Moorman AF (**2009**) Amplification efficiency: linking baseline and bias in the analysis of quantitative PCR data. *Nucleic Acids Res* **37**: e45

Santos-Rosa M, Poutaraud A, Merdinoglu D and Mestre P (**2008**) Development of a transient expression system in grapevine *via* agro-infiltration. *Plant Cell Rep* **27**: 1053-1063

Schwessinger B, Roux M, Kadota Y, Ntoukakis V, Sklenar J, Jones A and Zipfel C (**2011**) Phosphorylation-dependent differential regulation of plant growth, cell death, and innate immunity by the regulatory receptor-like kinase BAK1. *PLoS Genet* **7**: e1002046

Segonzac C, Feike D, Gimenez-Ibanez S, Hann DR, Zipfel C and Rathjen JP (**2011**) Hierarchy and roles of pathogen-associated molecular pattern-induced responses in *Nicotiana benthamiana*. *Plant Physiol* **156**: 687-699

Segonzac C and Zipfel C (**2011**) Activation of plant pattern-recognition receptors by bacteria. *Curr Opin Microbiol* **14**: 54-61

Sessitsch A, Coenye T, Sturz A, Vandamme P, Barka E, Salles J, Van Elsas J, Faure D, Reiter B, Glick B, Wang-Pruski G and Nowak J (**2005**) Burkholderia phytofirmans sp. nov., a novel plant-associated bacterium with plant-beneficial properties. *Int J Syst Evol Microbiol* **55**: 1187-1192

Shan L, He P, Li J, Heese A, Peck SC, Nurnberger T, Martin GB and Sheen J (**2008**) Bacterial effectors target the common signaling partner BAK1 to disrupt multiple MAMP receptor-signaling complexes and impede plant immunity. *Cell Host Microbe* **4**: 17-27

She J, Han Z, Kim TW, Wang J, Cheng W, Chang J, Shi S, Yang M, Wang ZY and Chai J (**2011**) Structural insight into brassinosteroid perception by BRI1. *Nature* **474**: 472-476

Shimizu T, Nakano T, Takamizawa D, Desaki Y, Ishii-Minami N, Nishizawa Y, Minami E, Okada K, Yamane H, Kaku H and Shibuya N (**2010**) Two LysM receptor molecules, CEBiP and OsCERK1, cooperatively regulate chitin elicitor signaling in rice. *Plant J* **64**: 204-214

Shinya T, Motoyama N, Ikeda A, Wada M, Kamiya K, Hayafune M, Kaku H and Shibuya N (**2012**) Functional characterization of CEBiP and CERK1 homologs in arabidopsis and rice reveals the presence of different chitin receptor systems in plants. *Plant Cell Physiol* **53**: 1696-1706

Shiu SH and Bleecker AB (**2003**) Expansion of the receptor-like kinase/Pelle gene family and receptor-like proteins in Arabidopsis. *Plant Physiol* **132**: 530-543

Simon-Plas F, Elmayan T and Blein JP (**2002**) The plasma membrane oxidase NtrbohD is responsible for AOS production in elicited tobacco cells. *Plant J* **31**: 137-147

Smith MF, Jr., Mitchell A, Li G, Ding S, Fitzmaurice AM, Ryan K, Crowe S and Goldberg JB (**2003**) Toll-like receptor (TLR) 2 and TLR5, but not TLR4, are required for *Helicobacter pylori*-induced NF-kappa B activation and chemokine expression by epithelial cells. *J Biol Chem* **278**: 32552-32560

Stergiopoulos I, van den Burg HA, Okmen B, Beenen HG, van Liere S, Kema GH and de Wit PJ (**2010**) Tomato Cf resistance proteins mediate recognition of cognate homologous effectors from fungi pathogenic on dicots and monocots. *Proc Natl Acad Sci U S A* **107**: 7610-7615

Suharsono U, Fujisawa Y, Kawasaki T, Iwasaki Y, Satoh H and Shimamoto K (**2002**) The heterotrimeric G protein alpha subunit acts upstream of the small GTPase Rac in disease resistance of rice. *Proc Natl Acad Sci U S A* **99**: 13307-13312

Sun W, Cao Y, Labby K, Bittel P, Boller T and Bent A (**2012**) Probing the Arabidopsis flagellin receptor: FLS2-FLS2 association and the contributions of specific domains to signaling function. *Plant Cell* **24**: 1096-1113

Sun Y, Cheng Z and Glick B (**2009**) The presence of a 1-aminocyclopropane-1-carboxylate (ACC) deaminase deletion mutation alters the physiology of the endophytic plant growth-promoting bacterium *Burkholderia phytofirmans* PsJN. *FEMS Microbiol Lett* **296**: 131-136

Sun W, Dunning F, Pfund C, Weingarten R and Bent A (**2006**) Within-species flagellin polymorphism in *Xanthomonas campestris* pv *campestris* and its impact on elicitation of Arabidopsis FLAGELLIN SENSING2-dependent defenses. *Plant Cell* **18**: 764-779

Sun Y, Li L, Macho AP, Han Z, Hu Z, Zipfel C, Zhou JM and Chai J (**2013**) Structural basis for flg22-induced activation of the Arabidopsis FLS2-BAK1 immune complex. *Science* **342**: 624-628

Szegedi E, Bottka S, Mikulas J, Otten L and Sule S (**2005**) Characterization of *Agrobacterium tumefaciens* strains isolated from grapevine. *Vitis* **44**: 49-54

Taguchi F, Shibata S, Suzuki T, Ogawa Y, Aizawa S, Takeuchi K and Ichinose Y (**2008**) Effects of glycosylation on swimming ability and flagellar polymorphic transformation in *Pseudomonas syringae* pv. *tabaci* 6605. *J Bacteriol* **190**: 764-768

Taguchi F, Shimizu R, Inagaki Y, Toyoda K, Shiraishi T and Ichinose Y (**2003**) Post-translational modification of flagellin determines the specificity of HR induction. *Plant Cell Physiol* **44**: 342-349

Taguchi F, Suzuki T, Takeuchi K, Inagaki Y, Toyoda K, Shiraishi T and Ichinose Y (**2009**) Glycosylation of flagellin from *Pseudomonas syringae* pv. *tabaci* 6605 contributes to evasion of host tobacco plant surveillance system. *Physiol Mol Plant Pathol* **74**: 11-17

Takai R, Isogai A, Takayama S and Che F (**2008**) Analysis of Flagellin Perception Mediated by flg22 Receptor OsFLS2 in Rice. *Mol Plant Microbe Interact* **21**: 1635-1642

Takeuchi K, Taguchi F, Inagaki Y, Toyoda K, Shiraishi T and Ichinose Y (**2003**) Flagellin glycosylation island in *Pseudomonas syringae* pv. *glycinea* and its role in host specificity. *J Bacteriol* **185**: 6658-6665

Tamura K, Peterson D, Peterson N, Stecher G, Nei M and Kumar S (**2011**) MEGA5: molecular evolutionary genetics analysis using maximum likelihood, evolutionary distance, and maximum parsimony methods. *Mol Biol Evol* **28**: 2731-2739

Tanabe S, Okada M, Jikumaru Y, Yamane H, Kaku H, Shibuya N and Minami E (**2006**) Induction of resistance against rice blast fungus in rice plants treated with a potent elicitor, N-acetylchitooligosaccharide. *Biosci Biotechnol Biochem* **70**: 1599-1605

Tanaka S, Ichikawa A, Yamada K, Tsuji G, Nishiuchi T, Mori M, Koga H, Nishizawa Y, O'Connell R and Kubo Y (**2010**) HvCEBiP, a gene homologous to rice chitin receptor CEBiP, contributes to basal resistance of barley to *Magnaporthe oryzae*. *BMC Plant Biol* **10**: 288

Tanner DE, Ma W, Chen Z and Schulten K (**2011**) Theoretical and computational investigation of flagellin translocation and bacterial flagellum growth. *Biophys J* **100**: 2548-2556

Theocharis A, Bordiec S, Fernandez O, Paquis S, Dhondt-Cordelier S, Baillieul F, Clement C and Ait Barka E (**2012**) *Burkholderia phytofirmans* PsJN primes *Vitis vinifera* L. and confers a better tolerance to low nonfreezing temperatures. *Mol Plant Microbe Interact* **25**: 241-249

Thomma BP, Nurnberger T and Joosten MH (**2011**) Of PAMPs and effectors: the blurred PTI-ETI dichotomy. *Plant Cell* **23**: 4-15

Tintor N, Ross A, Kanehara K, Yamada K, Fan L, Kemmerling B, Nurnberger T, Tsuda K and Saijo Y (**2013**) Layered pattern receptor signaling *via* ethylene and endogenous elicitor peptides during Arabidopsis immunity to bacterial infection. *Proc Natl Acad Sci U S A* **110**: 6211-6216

Trda L, Fernandez O, Boutrot F, Heloir MC, Kelloniemi J, Daire X, Adrian M, Clement C, Zipfel C, Dorey S and Poinssot B (**2014**) The grapevine flagellin receptor VvFLS2 differentially recognizes flagellin-derived epitopes from the endophytic growth-promoting bacterium *Burkholderia phytofirmans* and plant pathogenic bacteria. *New phytol* **201**: 1371-1384

Trotel-Aziz P, Couderchet M, Vernet G and Aziz A (**2006**) Chitosan stimulates defense reactions in grapevine leaves and inhibits development of *Botrytis cinerea*. *Eur J Plant Pathol* **114**: 405-413

Trouvelot S, Varnier AL, Allegre M, Mercier L, Baillieul F, Arnould C, Gianinazzi-Pearson V, Klarzynski O, Joubert JM, Pugin A and Daire X (**2008**) A beta-1,3 glucan sulfate induces resistance in grapevine against *Plasmopara viticola* through priming of defense responses, including HR-like cell death. *Mol Plant Microbe Interact* **21**: 232-243

Tsuda K and Katagiri F (**2010**) Comparing signaling mechanisms engaged in pattern-triggered and effector-triggered immunity. *Curr Opin Plant Biol* **13**: 459-465

Tsuda K, Sato M, Stoddard T, Glazebrook J and Katagiri F (**2009**) Network properties of robust immunity in plants. *PLoS Genet* **5**: e1000772

van der Hoorn RA, Wulff BB, Rivas S, Durrant MC, van der Ploeg A, de Wit PJ and Jones JD (**2005**) Structure-function analysis of cf-9, a receptor-like protein with extracytoplasmic leucine-rich repeats. *Plant Cell* **17**: 1000-1015

van Esse HP, Bolton MD, Stergiopoulos I, de Wit PJ and Thomma BP (**2007**) The chitin-binding *Cladosporium fulvum* effector protein Avr4 is a virulence factor. *Mol Plant Microbe Interact* **20**: 1092-1101

van Loon L, Bakker P, van der Heijdt W, Wendehenne D and Pugin A (**2008**) Early responses of tobacco suspension cells to rhizobacterial elicitors of induced systemic resistance. *Mol Plant Microbe Interact* **21**: 1609-1621

Vandelle E, Poinssot B, Wendehenne D, Bentejac M and Pugin A (**2006**) Integrated signaling network involving calcium, nitric oxide, and active oxygen species but not mitogen-activated protein kin in BcPG1-elicited grapevine defenses. *Mol Plant Microbe Interact* **19**: 429-440

Velasco R, Zharkikh A, Troggio M, Cartwright DA, Cestaro A, Pruss D, Pindo M, Fitzgerald LM, Vezzulli S, Reid J, Malacarne G, Iliev D, Coppola G, Wardell B, Micheletti D, Macalma T, Facci M, Mitchell JT, Perazzolli M, Eldredge G, Gatto P, Oyzerski R, Moretto M, Gutin N, Stefanini M, Chen Y, Segala C, Davenport C, Dematte L, Mraz A, Battilana J, Stormo K, Costa F, Tao Q, Si-Ammour A, Harkins T, Lackey A, Perbost C, Taillon B, Stella A, Solovyev V, Fawcett JA, Sterck L, Vandepoele K, Grando SM, Toppo S, Moser C, Lanchbury J, Bogden R, Skolnick M, Sgaramella V, Bhatnagar SK, Fontana P, Gutin A, Van de Peer Y, Salamini F and Viola R (**2007**) A high quality draft consensus sequence of the genome of a heterozygous grapevine variety. *Plos ONE* **2**: e1326

Verhagen B, Trotel-Aziz P, Couderchet M, Hofte M and Aziz A (**2010**) *Pseudomonas* spp.-induced systemic resistance to *Botrytis cinerea* is associated with induction and priming of defence responses in grapevine. *J Exp Bot* **61**: 249-260

Vetter M, Kronholm I, He F, Haweker H, Reymond M, Bergelson J, Robatzek S and de Meaux J (**2012**) Flagellin perception varies quantitatively in *Arabidopsis thaliana* and its relatives. *Mol Biol Evol* **29**: 1655-1667

Wan J, Tanaka K, Zhang XC, Son GH, Brechenmacher L, Nguyen TH and Stacey G (**2012**) LYK4, a lysin motif receptor-like kinase, is important for chitin signaling and plant innate immunity in Arabidopsis. *Plant Physiol* **160**: 396-406

Wan J, Zhang XC, Neece D, Ramonell KM, Clough S, Kim SY, Stacey MG and Stacey G (**2008**) A LysM receptor-like kinase plays a critical role in chitin signaling and fungal resistance in Arabidopsis. *Plant Cell* **20**: 471-481

Wang GL, Song WY, Ruan DL, Sideris S and Ronald PC (**1996**) The cloned gene, Xa21, confers resistance to multiple *Xanthomonas oryzae* pv. *oryzae* isolates in transgenic plants. *Mol Plant Microbe Interact* **9**: 850-855

Waterhouse PM, Graham MW and Wang MB (**1998**) Virus resistance and gene silencing in plants can be induced by simultaneous expression of sense and antisense RNA. *Proc Natl Acad Sci U S A* **95**: 13959-13964

Weilharter A, Mitter B, Shin M, Chain P, Nowak J and Sessitsch A (**2011**) Complete genome sequence of the plant growth-promoting endophyte *Burkholderia phytofirmans* strain PsJN. *J Bacteriol* **193**: 3383-3384

West ER, Cother EJ, Steel CC and Ash GJ (**2010**) The characterization and diversity of bacterial endophytes of grapevine. *Can J Microbiol* **56**: 209-216

Willmann R, Lajunen HM, Erbs G, Newman MA, Kolb D, Tsuda K, *et al.* (**2011**) Arabidopsis lysin-motif proteins LYM1 LYM3 CERK1 mediate bacterial peptidoglycan sensing and immunity to bacterial infection. *Proc Natl Acad Sci U S A* **108**: 19824-19829

Xiang T, Zong N, Zou Y, Wu Y, Zhang J, Xing W, Li Y, Tang X, Zhu L, Chai J and Zhou JM (**2008**) *Pseudomonas syringae* effector AvrPto blocks innate immunity by targeting receptor kinases. *Curr Biol* **18**: 74-80

Xin DW, Liao S, Xie ZP, Hann DR, Steinle L, Boller T and Staehelin C (**2012**) Functional analysis of NopM, a novel E3 ubiquitin ligase (NEL) domain effector of *Rhizobium* sp. strain NGR234. *PLoS Pathog* **8**: e1002707

Yamaguchi K, Yamada K, Ishikawa K, Yoshimura S, Hayashi N, Uchihashi K, *et al.* (**2013**) A receptor-like cytoplasmic kinase targeted by a plant pathogen effector is directly phosphorylated by the chitin receptor and mediates rice immunity. *Cell Host Microbe* **13**: 347-357

Yamaguchi Y, Pearce G and Ryan CA (**2006**) The cell surface leucine-rich repeat receptor for AtPep1, an endogenous peptide elicitor in Arabidopsis, is functional in transgenic tobacco cells. *Proc Natl Acad Sci U S A* **103**: 10104-10109

Yonekura K, Maki-Yonekura S and Namba K (**2003**) Complete atomic model of the bacterial flagellar filament by electron cryomicroscopy. *Nature* **424**: 643-650

Yoon SI, Kurnasov O, Natarajan V, Hong M, Gudkov AV, Osterman AL and Wilson IA (**2012**) Structural basis of TLR5-flagellin recognition and signaling. *Science* **335**: 859-864

Zamioudis C and Pieterse C (**2012**) Modulation of host immunity by beneficial microbes. *Mol Plant Microbe Interact* **25**: 139-150

Zeng H, Carlson AQ, Guo Y, Yu Y, Collier-Hyams LS, Madara JL, Gewirtz AT and Neish AS (**2003**) Flagellin is the major proinflammatory determinant of enteropathogenic *Salmonella*. *J Immunol* **171**: 3668-3674

Zeng W and He S (**2010**) A prominent role of the flagellin receptor FLAGELLIN-SENSING2 in mediating stomatal response to *Pseudomonas syringae* pv *tomato* DC3000 in Arabidopsis. *Plant Physiol* **153**: 1188-1198

Zhang J, Li W, Xiang T, Liu Z, Laluk K, Ding X, Zou Y, Gao M, Zhang X, Chen S, Mengiste T, Zhang Y and Zhou JM (**2010**) Receptor-like cytoplasmic kinases integrate signaling from multiple plant immune receptors and are targeted by a *Pseudomonas syringae* effector. *Cell Host Microbe* **7**: 290-301

Zhang J, Shao F, Li Y, Cui H, Chen L, Li H, Zou Y, Long C, Lan L, Chai J, Chen S, Tang X and Zhou JM (**2007**) A *Pseudomonas syringae* effector inactivates MAPKs to suppress PAMP-induced immunity in plants. *Cell Host Microbe* **1**: 175-185

Zhang L, Kars I, Essenstam B, Liebrand TW, Wagemakers L, Elberse J, Tagkalaki P, Tjoitang D, van den Ackerveken G and van Kan JA (**2014**) Fungal endopolygalacturonases are recognized as microbe-associated molecular patterns by the arabidopsis receptor-like protein RESPONSIVENESS TO BOTRYTIS POLYGALACTURONASES1. *Plant Physiol* **164**: 352-364

Zhang W, Fraiture M, Kolb D, Loffelhardt B, Desaki Y, Boutrot FF, Tor M, Zipfel C, Gust AA and Brunner F (**2013**) Arabidopsis receptor-like protein30 and receptor-like kinase suppressor of BIR1-1/EVERSHED mediate innate immunity to necrotrophic fungi. *Plant Cell* **25**: 4227-4241

Zhao Y, Yang J, Shi J, Gong YN, Lu Q, Xu H, Liu L and Shao F (**2011**) The NLRC4 inflammasome receptors for bacterial flagellin and type III secretion apparatus. *Nature* **477**: 596-600

Zipfel C, Kunze G, Chinchilla D, Caniard A, Jones JDG, Boller T and Felix G (**2006**) Perception of the bacterial PAMP EF-Tu by the receptor EFR restricts *Agrobacterium*-mediated transformation. *Cell* **125**: 749-760

Zipfel C, Robatzek S, Navarro L, Oakeley EJ, Jones JDG, Felix G and Boller T (**2004**) Bacterial disease resistance in Arabidopsis through flagellin perception. *Nature* **428**: 764-767

Zuniga A, Poupin M, Donoso R, Ledger T, Guiliani N, Gutierrez R and Gonzalez B (**2013**) Quorum sensing and indole-3-acetic acid degradation play a role in colonization and plant growth promotion of *Arabidopsis thaliana* by *Burkholderia phytofirmans* PsJN. *Mol Plant Microbe Interact* **26**: 546-553

List of publications and presentations

Publications:

The grapevine flagellin receptor VvFLS2 differentially recognizes flagellin-derived epitopes from the endophytic growth-promoting bacterium *Burkholderia phytofirmans* and plant pathogenic bacteria.
Trdá L, Fernandez O, Boutrot F, Heloir MC, Kelloniemi J, Daire X, Adrian M, Clement C, Zipfel C, Dorey S and Poinssot B (2014) *The New phytologist* **201**: 1371-1384

New Phytologist

Research

The grapevine flagellin receptor VvFLS2 differentially recognizes flagellin-derived epitopes from the endophytic growth-promoting bacterium *Burkholderia phytofirmans* and plant pathogenic bacteria

Lucie Trdá[1]*, Olivier Fernandez[2]*, Freddy Boutrot[3], Marie-Claire Héloir[1], Jani Kelloniemi[1], Xavier Daire[4], Marielle Adrian[1], Christophe Clément[2], Cyril Zipfel[3], Stéphan Dorey[2]* and Benoit Poinssot[1]*

[1]Université de Bourgogne, UMR 1347 Agroécologie, Pôle Interactions Plantes Micro-organismes – ERL CNRS 6300, 17 rue Sully, 21000 Dijon, France; [2]Laboratoire Stress, Défenses et Reproduction des Plantes, URVVC EA 4707, Université de Reims Champagne-Ardenne, Campus Moulin de la Housse Chemin des Rouliers, 51687 Reims, France; [3]The Sainsbury Laboratory, Norwich Research Park, Norwich, NR4 7UH, UK; [4]INRA, UMR 1347 Agroécologie, Pôle Interactions Plantes Micro-organismes – ERL CNRS 6300, 17 rue Sully, 21000 Dijon, France

Authors for correspondence:
Benoit Poinssot
Tel: +33 380 693 458
Email: benoit.poinssot@dijon.inra.fr

Stéphan Dorey
Tel: +33 326 918 587
Email: stephan.dorey@univ-reims.fr

Received: *5 August 2013*
Accepted: *6 October 2013*

New Phytologist (2013)
doi: 10.1111/nph.12592

Key words: *Burkholderia phytofirmans*, flagellin sensing, flg22, microbe-associated molecular pattern (MAMP), pattern recognition receptor (PRR), PGPR, *Vitis vinifera*.

Summary

• The role of flagellin perception in the context of plant beneficial bacteria still remains unclear. Here, we characterized the flagellin sensing system flg22–FLAGELLIN SENSING 2 (FLS2) in grapevine, and analyzed the flagellin perception in the interaction with the endophytic plant growth-promoting rhizobacterium (PGPR) *Burkholderia phytofirmans*.

• The functionality of the grapevine FLS2 receptor, VvFLS2, was demonstrated by complementation assays in the *Arabidopsis thaliana fls2* mutant, which restored flg22-induced H_2O_2 production and growth inhibition. Using synthetic flg22 peptides from different bacterial origins, we compared recognition specificities between VvFLS2 and AtFLS2.

• In grapevine, flg22-triggered immune responses are conserved and led to partial resistance against *Botrytis cinerea*. Unlike flg22 peptides derived from *Pseudomonas aeruginosa* or *Xanthomonas campestris*, flg22 peptide derived from *B. phytofirmans* triggered only a small oxidative burst, weak and transient defense gene induction and no growth inhibition in grapevine. Although, in Arabidopsis, all the flg22 epitopes exhibited similar biological activities, the expression of *VvFLS2* into the *fls2* background conferred differential flg22 responses characteristic for grapevine.

• These results demonstrate that VvFLS2 differentially recognizes flg22 from different bacteria, and suggest that flagellin from the beneficial PGPR *B. phytofirmans* has evolved to evade this grapevine immune recognition system.

Transcriptomic analyses of interacting *Botrytis cinerea* and *Vitis vinifera* highlight fungal virulence determinants and changes in defense mechanisms during berry ripening.
J. Kelloniemi *et al.*, (in preparation)

Induced resistance in grapevine: from concept to vineyard application.
Poinssot B, Trdá L, Kelloniemi J,Steimetz E, Héloir M-C, Trouvelot S, Daire X and Adrian M. (2012) VI Brazilian Meeting on Induced Resistance in Plants against Pathogens", Viçosa Federal University, Brazil. *Book chapter*

Presentations :

Oral:

Identification of grapevine pattern recognition receptors involved in PAMP-triggered immunity against P. viticola *and* B. cinerea.
September **2011**, **IOBC workshop PR-proteins and induced resistance against pathogens and insect, Neuchatel, Swiss, *oral presentation*** (Talk award for the best student presentation)

Posters:

Identification of the VvFLS2 grapevine flagellin receptor by a functional genomics strategy.
June **2013**, **IOBC workshop induced resistance against pathogens and insect, Avignon, France, *poster*** (Award for the best student poster)

Identification of the VvFLS2 grapevine flagellin receptor by a functional genomics strategy.
June **2012**, **student conference** Journées des Doctorants du département SPE , Toulouse, France, ***poster***

Identification of grapevine pattern recognition receptors involved in PAMP-triggered immunity against P. viticola *and* B. cinerea.
June **2011**, **student conference** Forum des Jeunes chercheurs, Dijon, France, ***poster*** (Award for the best poster)

Identification of grapevine pattern recognition receptors involved in PAMP-triggered immunity against P. viticola *and* B. cinerea.
May **2011**, **student conference** Journées des Doctorants du département SPE , Dijon, France, ***poster***

Teaching at Université de Bourgogne :

Laboratory classes in Biochemistry (L2, UFR Sciences Vie Terre Environnement)

Laboratory classes in Grapevine physiology (L3, l'Institut Universitaire de la Vigne et du Vin)

120 hours in the period **2011 - 2013**

Abstract

Pattern-recognition receptors (PRRs) play a key role in plant immunity by assuring recognition of microbe-associated molecular patterns (MAMPs), signature of microbial presence. MAMP perception constitutes the first layer of pathogen detection and activates defense mechanisms that aim to block the intruder.

This study brings an insight into how grapevine (*Vitis vinifera*) perceives two MAMPs: the flagellin-derived flg22 peptide and chitin, which are conserved motifs occurring over the whole bacterial and fungal classes, respectively. This study analyzed MAMP-triggered early signaling events, defense gene expression and also the efficiency of elicited defense against gray mold and downy mildew diseases. These two MAMPs are active in grapevine suggesting that perception systems exist. So far, no PRR is known for this crop.

Given the availability of grapevine genome, we could identify *in silico* putative grapevine receptors (VvFLS2, VvCERK1-3 and VvCEBiP1-2) that might function as PRRs for flg22 and chitin, respectively. Their functional characterization was firstly achieved by complementation assays in the corresponding *A. thaliana* mutants and, secondly, by a gene silencing strategy in grapevine.

Our results permitted the identification of VvFLS2, the *V. vinifera* receptor for the bacterial flagellin. The function of VvFLS2 was demonstrated by restoring the flg22 responsiveness in the Arabidopsis *fls2* null mutant. Thus, our work provides the first description of an active grapevine PRR-MAMP pair. We further compared VvFLS2 and the Arabidopsis receptor, AtFLS2, in their capability to perceive flagellin-derived flg22 epitopes from endophytic or pathogenic bacteria. Our data clearly show that VvFLS2 differentially recognizes flg22 from different bacteria and suggest that flagellin from the beneficial plant growth-promoting rhizobacteria (PGPR) *Burkholderia phytofirmans* has evolved to evade grapevine immune recognition system. We also obtained preliminary data on chitin sensing system in grapevine and show that VvCERK3 might be a functional ortholog of AtCERK1 by partly restoring the oxidative burst triggered by chitin in the Arabidopsis *cerk1-2* mutant.

Key words: grapevine, immunity, MAMP, receptors, PRR, FLS2, flg22, CERK1, chitin, *Vitis vinifera*